INSTITUTO POLITÉCNICO NACIONAL

CENTRO INTERDISCIPLINARIO DE INVESTIGACIÓN PARA
EL DESARROLLO INTEGRAL REGIONAL
CIIDIR UNIDAD OAXACA

Doctorado en Ciencias en Conservación y Aprovechamiento de Recursos Naturales

Línea de investigación de Ingeniería

"DURABILIDAD DE COMPOSITOS A BASE DE CEMENTO PORTLAND-CENIZA DE BAGAZO DE CAÑA REFORZADOS CON ACERO GALVANIZADO"

**Durability of sugarcane bagasse ash-cement based composites
reinforced with galvanized steel**

Tesis que para obtener el grado de

Doctor en Ciencias

PRESENTA:

M en C. Marco Antonio Maldonado García

DIRECTORES DE TESIS:

Dr. Pedro Montes García

Dr. Pedro Leobardo Valdez Tamez

Santa Cruz Xoxocotlán   Diciembre de 2018

SIP-14-BIS

INSTITUTO POLITÉCNICO NACIONAL
SECRETARÍA DE INVESTIGACIÓN Y POSGRADO

ACTA DE REVISIÓN DE TESIS

En la Ciudad de ___Oaxaca___ Siendo las __11:00__ horas del día __29__ del mes de __octubre__ del __2018__ se reunieron los miembros de la Comisión Revisora de la Tesis, designada por el Colegio de Profesores de Estudios de Posgrado e Investigación de ___CIIDIR UNIDAD OAXACA___ para examinar la tesis titulada:

Durabilidad de compositos a base de cemento Portland-ceniza de bagazo de caña reforzados con acero galvanizado.

Presentada por el alumno:

Maldonado	García
Apellido paterno	Apellido materno

Nombre(s) Marco Antonio

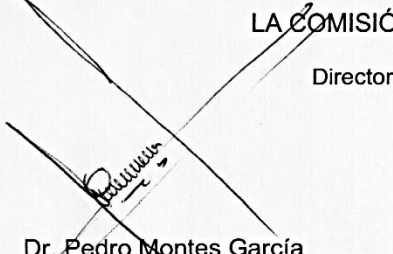Con registro: | A | 1 | 5 | 0 | 0 | 5 | 5 |

aspirante de:

Doctorado en Ciencias en Conservación y Aprovechamiento de Recursos Naturales
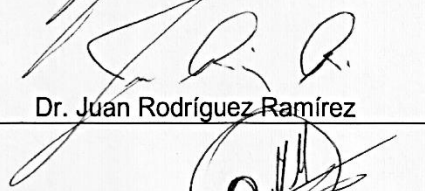
Después de intercambiar opiniones los miembros de la Comisión manifestaron **APROBAR LA TESIS**, en virtud de que satisface los requisitos señalados por las disposiciones reglamentarias vigentes.
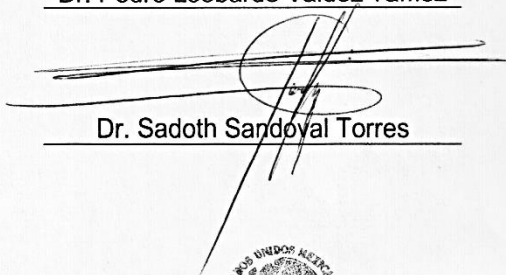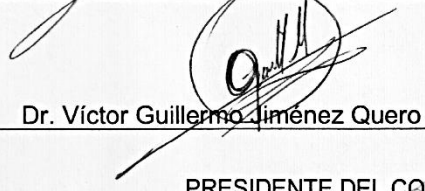
LA COMISIÓN REVISORA
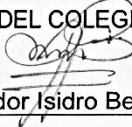
Directores de tesis

Dr. Pedro Montes García

Dr. Pedro Leobardo Valdez Tamez

Dr. Juan Rodríguez Ramírez

Dr. Sadoth Sandoval Torres

Dr. Víctor Guillermo Jiménez Quero

PRESIDENTE DEL COLEGIO DE PROFESORES

Dr. Salvador Isidro Belmonte Jiménez

CENTRO INTERDISCIPLINARIO
DE INVESTIGACIÓN PARA EL
DESARROLLO INTEGRAL REGIONAL
C.I.I.D.I.R.
UNIDAD OAXACA
I.P.N.

INSTITUTO POLITÉCNICO NACIONAL

SECRETARÍA DE INVESTIGACIÓN Y POSGRADO

CARTA CESION DE DERECHOS

En la Ciudad de __Oaxaca__ el día _3_ del mes de __diciembre__ el año ___2018_, el (la) que suscribe _Marco Antonio Maldonado García_ alumno(a) del Programa de Doctorado en Ciencias en Conservación y Aprovechamiento de Recursos Naturales con número de registro _A150055_, adscrito a Centro Interdisciplinario de Investigación para el Desarrollo Integral Regional Unidad Oaxaca, manifiesta que es autor (a) intelectual del presente trabajo de Tesis bajo la dirección de los Dres. Pedro Montes García y Pedro Leobardo Valdez Tamez y cede los derechos del trabajo intitulado **Durabilidad de compositos a base de cemento Portland-ceniza de bagazo de caña reforzados con acero galvanizado**, al Instituto Politécnico Nacional para su difusión, con fines académicos y de investigación.

Los usuarios de la información no deben reproducir el contenido textual, gráficas o datos del trabajo sin el permiso expreso del autor y/o director del trabajo. Este puede ser obtenido escribiendo a la siguiente dirección marco_mg.age@hotmail.com. Si el permiso se otorga, el usuario deberá dar el agradecimiento correspondiente y citar la fuente del mismo.

Marco Antonio Maldonado García

Nombre y firma

CENTRO INTERDISCIPLINARIO
DE INVESTIGACIÓN PARA EL
DESARROLLO INTEGRAL REGIONAL
C.I.I.D.I.R.
UNIDAD OAXACA
I.P.N.

RESUMEN

La corrosión es uno de los principales problemas de deterioro en compuestos cementantes a base de cemento Portland reforzados. Este problema puede provocar altos costos de reparación o el colapso de estructuras de ingeniería civil en casos extremos. La principal causa de corrosión en estos compuestos reforzados es el ingreso de sustancias agresivas a través de la matriz cementante, las cuales provienen del ambiente en el cual se encuentran expuestos. Una de estas sustancias son los iones cloruros presentes en ambientes marinos. Una posible solución a esta problemática es el uso de materiales cementantes suplementarios (MCS) como sustitutos parciales del cemento Portland. Lo anterior debido al potencial puzolánico que tienen estos materiales mejorando la microestructura de la matriz cementante de los compuestos a base de cemento. Sin embargo, el uso de MCS está limitado por su disponibilidad en ciertas regiones además del impacto ambiental que pueden ocasionar durante su obtención. Otra alternativa es utilizar materiales de desecho de la agroindustria como MCS al cemento Portland. Estos materiales ofrecen una solución más amigable con el medio ambiente. Uno de estos materiales de desecho es la ceniza de bagazo de caña (CBC). La CBC está compuesta principalmente por óxidos de sílice, aluminio y fierro necesarios para su potencial pozolánico. Sin embargo, la CBC requiere de un mínimo postratamiento antes de utilizarse como MCS en compuestos cementantes. Entre estos postratamientos se encuentran el re-calcinado, molido y cribado o combinación de estos métodos. El cribado puede ser la opción más viable ambientalmente debido a que requiere de una menor demanda energética. Con base en lo anterior, el objetivo de esta tesis fue evaluar el efecto de la adición de 10 y 20% de CBC sin tratamiento (CBC-st), la cual fue solamente cribada a través de la malla de 75 µm ASTM durante 5 minutos, en la durabilidad de morteros reforzados con acero galvanizado expuestos en una solución de iones cloruro. El efecto del tiempo de curado, 0, 7 y 28 días, también fué considerado durante la etapa experimental de la investigación. Los resultados mostraron que la adición de 10 y 20% de CBC-st hizo más compleja la microestructura, incrementó la resistencia a compresión y redujo la difusión de iones cloruros en morteros. La adición de 10 y 20% de CBC-st también disminuyó el riesgo de corrosión en morteros reforzados con acero galvanizado. Lo anterior debido a las reacciones puzolánicas de la CBC-st y el decremento de la difusión de iones cloruro. El incremento del tiempo de curado también fue benéfico para reducir el riesgo de corrosión en los morteros reforzados adicionados con CBC-st. Con base en los resultados de la investigación, se sugiere que el uso de 10% de CBC-st y 7 días de curado pueden ser la mejor opción para reducir la corrosión de morteros reforzados. El uso de 20% de CBC-st también reduce la corrosión de morteros reforzados en comparación con un mortero sin adición de CBC-st. Los resultados de esta investigación proporcionan las bases necesarias para el uso de la CBC-st, la cual genera problemas de contaminación ambiental debido a su actual disposición; asimismo, con el uso de la CBC-st se incrementará la durabilidad de morteros reforzados. De igual manera, los resultados de esta investigación proporcionan las bases para futuras investigaciones en concretos reforzados adicionados con CBC-st.

ABSTRACT

Corrosion is considered as one of the main deterioration problems in reinforced cement-based composites, which leads to a high repair cost or the collapse of civil engineering structures. Penetration of harmful substances from the surrounding environment through the cementitious matrix is the most common cause for corrosion in those reinforced composites. One of these substances is chloride ions from a marine environment. A possible solution against corrosion in reinforced cement-based composites is the use of supplementary cementitious materials (SCM), when they are used as a partial Portland cement replacement. SCM have pozzolanic properties which help to improve the microstructure of the cementitious matrix. However, the use of any specific SCM could be limited by its availability and environmental impact. In this context, agro-industry waste materials appear as suitable environmentally-friendly alternative. One of these materials is sugarcane bagasse ash (SCBA). SCBA contains silica, aluminum and iron oxides as main compounds necessary for pozzolanic reactions in cement-based composites. Nevertheless, SCBA needs a minimum post-treatment to enhance its pozzolanic properties such as re-calcination, grinding and long-term sieving or the combination of these methods. From this, sieving might be the best alternative because its low energy demand. Based on the previous statements, this thesis aimed the use of 10 and 20% of untreated SCBA (UtSCBA), which was only sieved through the 75 µm ASTM mesh for 5 minutes, to enhance the durability of galvanized steel mesh reinforced mortars against chloride-induced corrosion. Curing times of 0, 7 and 28 days were also considered for the experiment. Results show that the use of 10 and 20% UtSCBA as partial Portland cement replacement made more complex the microstructure, increased the compressive strength and reduced the chloride ion diffusion of mortars. The addition of 10 and 20% of UtSCBA also decreased the corrosion risk of small-scale mortar slabs reinforced with galvanized steel. This is attributed to the pozzolanic reactions of the UtSCBA and the decrement of chloride ion diffusion rate. The increase of the curing time was also beneficial. From the results, 10% of UtSCBA and 7 days of curing could be enough for proper performance of reinforced mortars against chloride-induced corrosion. Furthermore, the addition of 20% of UtSCBA also gives a proper performance against corrosion when compared to mortars without UtSCBA. Collectively, advances presented in this thesis provide a possible solution to the dispose of sugarcane bagasse ash which is causing environmental issues due to its improper disposal in developing countries; additionally, the incorporation of UtSCBA enhances the durability of reinforced mortars. Furthermore, a framework for future research on concrete durability using UtSCBA is provided.

ACKNOWLEDGEMENTS

Thank you
Marco Antonio Maldonado García

DEDICATION

To my grandparents:
Onofre Maldonado Valencia and *Felisa Nuñez Gijón*
I am exceedingly grateful for their love, time and guidance in life

To my father:
M.Eng. Marco Antonio Maldonado Nuñez
I am grateful for his knowledge and experience for academic purposes and life

To my mother:
M.Eng. Saula García Gomez[†]
Who take cares of me wherever she is

To the rest of my family…… for everything given in life

Thank you so much
Marco Antonio Maldonado García

TABLE OF CONTENT

CHAPTER ONE

General introduction

Cement-based mortars are widely used in the construction industry due to its convenient manufacturing, low cost and high mechanical strength [Dong et al. 2014]. When these mortars are reinforced could be used to repair concrete structures and sewage systems, and for the manufacturing of ferrocement and pre-cast structural elements [López-Calvo et al. 2006, Dong et al. 2014]. However, the reinforced elements could be susceptible to corrosion deterioration due to the presence of harmful substances from its surrounding environment, such as chloride ions and CO_2 [Fernández-Jiménez et al. 2010, Valencia et al. 2012, Česen et al. 2013]. As a result of this deterioration process, the durability of the reinforced mortar is compromised.

The use of some supplementary cementitious materials (SCM) as a partial Portland cement replacement could help to combat the corrosion deterioration of reinforced mortars. These materials might improve the microstructure and reduce the permeability of the mortar matrix due to pozzolanic reactions [Chusilp et al 2009, Valencia et al. 2012, Muangtong et al, 2013, Biricik and Sarier 2014]. Some of these SCM are by-products from manufacturing (such as fly ash) and agro-industry (such as sugarcane bagasse ash). Fly ash has been successfully used in cement-based composites; however, its use concerns the construction industry because of its uncertain availability and high cost of production as compared to other by-products [Gastaldini et al 2010].

The sugarcane bagasse ash (SCBA) is a by-product from sugar mills. The annual production of sugarcane is estimated to be about 1.5 billion tons around the world. From this amount, approximately 375 and 15 million tons of bagasse and bagasse ash are generated, respectively; which can cause environmental pollution. [Frias and Sánchez 2013]. Considering the above, researchers have focused on the use of SCBA as a partial Portland cement replacement for the manufacturing of ecological cement-based composites, such as mortars and concretes [Ganesan et al. 2007, Morales et al. 2009, Cordeiro et al. 2010, Noor-Ul 2011, Valencia et al. 2012, Montakartiwong et al. 2013, Muangtong et al, 2013, Cordeiro et al. 2018]. Those researchers affirm that the SCBA does not negatively affect the mechanical properties of mortars and concretes when the ash is post-treated; however, there is a need to evaluate the durability of these mortars and concretes.

In this thesis, an untreated sugarcane bagasse ash (UtSCBA), which refers to the used of practically "as received" sugarcane bagasse from sugar mills, is used as a partial Portland cement replacement to prevent corrosion and enhance the durability of reinforced cement-based composites. The thesis is presented as a series of discrete manuscripts (chapters 2 to 7).

Chapter 2 provides a literature review about the use of SCBA subjected to different post-treatments to prepare cement-based composites. The effect of the loss on ignition of SCBA in these composites is also addressed in this chapter. Chapter 3 focused on the

pozzolanic enhancement of SCBA in mortars. From this a SCBA sieved through the 75 µm ASTM mesh for five minutes was chosen as research matter. The microstructure and mechanical properties of mortars added with 10 and 20% of UtSCBA as cement replacement is also reported in this chapter.

Chapters 4 to 6 aims the corrosion risk/damage in reinforced small-scale mortar slabs, added with 10 and 20% of UtSCBA, which were exposed to wetting-drying cycles of 12 hours each in a 3% NaCl solution for 75 months. The effect of 0, 7 and 28 days of curing time in the reinforced slabs was also evaluated. Chapter 4 establishes the initiation periods of uncured reinforced mortar slabs. Chapter 5 discuss the chloride diffusion coefficients in mortars and the corrosion risk (monitored by electrochemical methods) of uncured/cured reinforced mortar slabs after a long-term exposure to wetting-drying cycles. Autopsy results of the slabs is also reported and correlated with the electrochemical results in this chapter. In chapter 6, the evaluation of corrosion in the reinforced mortar slabs, after the exposure to the wetting-drying cycles, is reported by corrosion and current density mapping and using ultrasonic guided waves.

Chapter 7 is focused on the effect of 10 and 20% of UtSCBA on the evaluation of the steel/mortar interface of reinforced mortar slabs after the exposure to the wetting-drying cycles. The effect of the addition of UtSCBA in the corrosion mechanism in the reinforced mortar slabs was also elucidated in this chapter.

Finally, chapter 8 provides a general discussion of the results from the research.

Problem statement

Corrosion of steel reinforcement affects negatively the durability of reinforced cement-based composites. This problem is attributed to the presence of harmful substances to which the composites are subjected, for example, chloride ions and CO_2. Chlorides penetrate through the cementitious matrix of the composites reaching a maximum chloride threshold value triggering corrosion [Angs et al. 2009]. A possible solution to prevent corrosion in those composites is the use of some SCM as a partial Portland cement replacement. These SCMs improve the microstructure of the cementitious matrix [Aprianti et al. 2015]. One of these materials, which is nowadays under investigation, is the SCBA. This ash is a by-product from sugar mills and its inadequate disposal causes diverse environmental issues [Akram et al. 2009, Montakarntiwong et al. 2013, Aprianti et al. 2015]. Some research results indicate that when SCBA is post-treated can be used as a partial Portland cement replacement without adverse effects on the microstructural and mechanical properties of mortars and concretes [Ganesan et al. 2007, Morales et al. 2009, Frías et al. 2011, Valencia et al. 2012, Bahurudeen et al. 2015]. Addititonal studies suggest that when SCBA is used "practically as received", named untreated sugarcane bagasse ash (UtSCBA),

the microstructural and mechanical properties of mortars and concretes are not negatively affected [Hernández 2010, Maldonado 2012, Arenas-Piedrahita et al. 2016, Ríos-Parada et al. 2017]. However, presently there is not enough research about durability of those composites containing UtSCBA.

Justification

This research is justified for generating scientific knowledge about the effect of the addition of UtSCBA on the corrosion and durability of reinforced mortars. This knowledge could improve existing construction materials. Furthermore, this research promotes the manufacturing of ecological mortars using a waste material such as the UtSCBA as partial substitution of Portland cement (which contributes to the generation of approximately 0.7 tons of CO_2 per ton of produced cement). The use of this waste material might contribute to regional and social development.

Contextual overview

The use of supplementary cementitious materials in cement-based composites

Portland cement is the most used material in cement-based composites for civil infrastructure around the world [Aprianti et al. 2015]. However, cement production is a high energy demanding process which generates approximately 0.8 to 1.0 ton of CO^2/ ton cement into the atmosphere [Hendriks 2004, Josa et al. 2007]. To combat pollution from cement production researchers have been using waste supplementary cementitious materials (SCM) from different industrial sectors, as partial cement replacement in composites [Lothenbach et al. 2011, Arianti et al. 2015]. It has been found that these waste materials could enhance durability of cement-based composites [Siddique and Khan 2011, Aprianti et al. 2015].

The use of SCM as a prevention method for reinforced steel corrosion

Several studies confirm that a denser cementitious matrix (CM) can decrease the chloride ingress in RC; in consequence, the time in which the maximum chloride threshold value is reached at the steel´s surface in RC can increases accordingly [Song et al. 2008, Angs et al. 2009]. A denser CM could be obtained using SCM as a partial Portland cement replacement. These supplementary materials increase the amount of cementitious compounds due to pozzolanic reactions (described as a chemical process between the SiO_2, Al_2O_3 and Fe_2O_3 from the SCM, the $Ca(OH)_2$ from cement hydration and moisture) which in turn reduce the porosity and permeability of the CM [Escalante 2002, Lothenbach et al. 2011, Aprianti et al. 2015].

There are different kinds of SCM around the world used to prepare cement-based composites; some of them are by-products from manufacturing and agro-industry. An example of manufacturing by-product is fly ash (FA). FA is produced from coal combustion and has been extensively used in cement-based composites. Research results affirm that FA improves the microstructure of the CM which in turn reduces its permeability to chloride ions [Simčič et al. 2015, Liu et al. 2016]. However, the use of manufacturing by-products is mostly limited by concerns of availability and cost of production [Gastaldini et al 2010]. Furthermore, the production of manufacturing by-products could promote a greater environmental impact. Considering the above, agro-industry waste materials appear as a more suitable option for ecological cement-based composites. One of these waste materials is the SCBA.

The sugarcane bagasse ash

The SCBA is a by-product from the combustion of sugarcane bagasse in sugar mills and is mostly composed by silicon, aluminium and iron oxides. The SCBA is certainly available in developing countries such as Brazil, India and Mexico, and can cause serious disposal problems and environmental issues [Frias et al. 2013]. In Mexico, the national union of sugarcane producers (UNC 2017) reports a production of sugarcane in approximately 54 million tons between 2016 and 2017. From that production, about 15 million tons of bagasse were obtained. Approximately 0.64% of residual ash is obtained from each ton of sugarcane bagasse after calcinating according to Akram et al. 2009. This suggests that in Mexico aproximately 0.34 million tons of SCBA are annually produced. In most of the cases, this SCBA is deposited in open damps causing different environmental issues such as soil, rivers and groundwater contamination [Soares et al. 2015, Dhengare et al. 2015, Katare et al. 2017]. An alternative for alleviating the environmental problems that SCBA is causing is its use in the manufacturing of ecological cement-based composites.

The SCBA as SCM in cement-based composites

Recent investigations on the use of SCBA as a partial Portland cement replacement in cement-based composites reveal no negative effects on the physical and mechanical properties of mortars and concretes containing it [Ganesan et al. 2007, Cordeiro et al. 2009, Chusilp et al. 2009, Morales et al. 2009, Montakarntiwong et al. 2013, Bahurudeen et al. 2015, Dhengare et al. 2015, Cordeiro et al. 2018]. However, most of the studies considered SCBA subjected to different post-treatments, such as re-calcination, grinding, long-term sieving or the combination of these methods. The main goal of the post-treatments was to improve the pozzolanizity of the ash by diminishing the loss on ignition. Nevertheless, such post-treatments demand high energy consumption and generate contaminants. In conclusion, the use of a post-treatment with the minimum energy requirements is needed for the SCBA.

The use of untreated sugarcane bagasse ash as SCM in cement-based composites

The term UtSCBA was adopted from a previous research in which the SCBA was only sieved though the No 200 (75µm) ASTM mesh for four to five minutes [Arenas-Piedrahita et al. 2016]. This ash was also used in other studies [Maldonado-Garcia 2012, Jiménez-Quero et al. 2013, Ríos-Parada et al. 2017]. In general, these studies affirm that the UtSCBA could be used as a partial Portland cement replacement without having negative effects on rheological, microstructural and mechanical properties of cement-based composites. Furthermore, it has been reported that the UtSCBA increases electrical resistivity and decreases permeability of cement-based composites [Arenas-Piedrahita et al. 2016]. However, the effect of UtSCBA in durability against chloride-induced corrosion of those composites must be investigated.

Durability of cement-based composites

Durability of cement-based composites may be described as their capability to stay for a long-time without significant deterioration [PCA 2018]. This is an important issue all over the world which depends of several factors such as the environment in which the cement-based composites are exposed. From this, chloride-induced corrosion is one of the major causes of the decrease in durability of reinforced cement-based composites [Angs et al. 2009, Michel et al. 2016]. Durability of cement based-composites against corrosion might be achieved using a low water/cement ratio to diminish permeability of the cementitious matrix and inconsequence decrease the chloride ion diffusion. Furthermore, the use of SCM of Portland cement can change the cementitious matrix enhancing durability [Broomfield 1997].

The corrosion of embedded steel in cement-based composites

Corrosion may be defined as the deterioration or destruction of a material because of reactions with its environment [Fontana 1986]. For metals, practically all environments are corrosive due to the presence of air and humidity and other chemical substances. The rate in which corrosion occurs depends on temperature and humidity fluctuations but also on the concentration of the chemical substances [Smith and Hashemi 2006]. The corrosion process of metals could occur by chemical, electrochemical and electrolytical reactions depending of the environment in which the metal is subjected [ACI 116R-00].

Steel corrosion is a serious problem in reinforced cement-based composites leading to high repair costs or to the final collapse of civil structures. The corrosion in those composites is mainly attributed to the penetration of harmful chemical substances from the surrounding environment such as chloride ions and CO_2 [Liu et al. 2016, Michel et al. 2016]. In the case of chlorides, these ions penetrate through the cement-based composites pore

network allowing steel corrosion once a maximum threshold value is reached at the steel´s surface [Angs et al. 2009, Shi et al. 2012]. During that process the passive layer of the embedded steel, which is built as a result of the alkaline environment, is destroyed because the chloride ions concentration. The quantity of chloride ions which may reach the embedded steel´s surface are those dissolved in the pore solution of cement-based composites and those physically adsorbed by cementitious phases [Castellote and Andrade 2001, RILEM TC 178-TMC 2002]. The rest of chlorides are chemically bound in the cementitious matrix by cementitious compounds and by SCM with high alumina content [Lu et al. 2002, Zibara et al. 2008, Kayali et al. 2012]. Finally, the corrosion process of reinforced steel is delayed because the chloride ion diffusion coefficient of the concrete is decremented as chloride ions are bound [Thomas et al. 2012].

The corrosion process of embedded steel in cement-based composites

Different chemical reactions occur during corrosion of the embedded steel in cement-based composites and the rate in which those reactions happen depends of oxygen and moisture availability [Broomfield 1997]. The corrosion products resulting from this process reduce the durability of the RC due to physical and mechanical properties changes in the concrete matrix [Torres-Luque et al. 2014]. Figure 1 shows the corrosion mechanism of steel bars embedded in concrete. During that process anodic reactions occurs due to dissolution of Fe ions ($Fe \rightarrow Fe^2 + 2e^-$). The two negative electrons from the anodic reaction are consumed in another region of the steel to maintain electrical neutrality (cathodic reaction). From this hydroxyl ions ($2e^- + 2H_2O + 1/2O_2 \rightarrow 2OH^-$) are created due to the oxygen and moisture. The hydroxyl ions increase the alkalinity of concrete maintaining integrity of the passive film of steel. However, new corrosion stages occur while Fe^2 ions (from anodic reactions) are dissolved in the pore solution of concrete. During that stages, ferrous hydroxide ($Fe^2 + 2OH^- \rightarrow Fe(OH)_2$), ferric hydroxide ($4Fe(OH)_2 + O_2 + 2H_2O \rightarrow 4Fe(OH)_3$) and hydrated ferric oxide ($2Fe(OH)_3 \rightarrow Fe_2O_3.H_2O + 2H_2O$) are created.
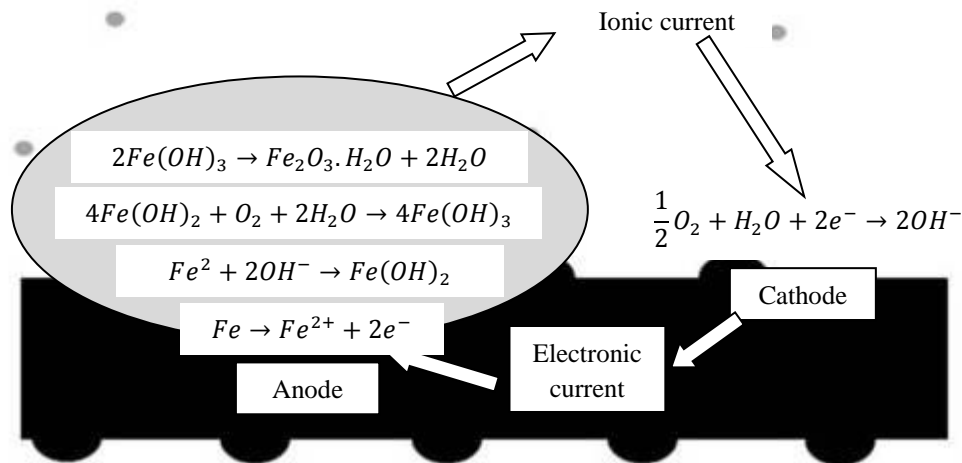
Figure 1. Schematic view of reinforced steel corrosion in concrete [Adapted from Broomfield 1997]

The effect of UtSCBA on delaying chloride-induced corrosion in cement-based composites

According to the mentioned in the last sections, it is expected that the addition of UtSCBA could delay chloride-induced corrosion in reinforced cement-based composites because of the following mechanisms. First, the pozzolanic reactions occurring between the silicon, aluminum and iron oxides from the UtSCBA and the calcium hydroxide from cement hydration and moisture. This makes a more complex cementitious matrix and might reduce the chloride ion penetration. Second, a filler effect of some crystalline particles from the UtSCBA which in turn makes more complex the cementitious matrix of the composites reducing chloride ingress. Third, an increment of chloride binding of the composites containing UtSCBA due to chemical or physical interactions with cementitious compounds and unburned matter from the ash.

Concluding remarks

The UtSCBA could be used as SCM for the manufacturing of ecological cement-based composites. This is the result of its pozzolanic potential which might improve the microstructural and mechanical properties of the composites containing it. Furthermore, the addition of UtSCBA could reduce the chloride ion diffusion through the cementitious matrix of the composites. Nevertheless, research on the effect of UtSCBA on the corrosion resistance of reinforced composites is required; in this sense, no negative effects on increasing the corrosion risk of reinforced cement-based composites are expected when using UtSCBA.

Next chapter is a literature review about the effect of different post-treatments for the SCBA. From this, sieving was selected as treatment method for the SCBA used in the present

research, and this low-energy post-treatment in fact originated the term "untreated sugarcane bagasse ash" (UtSCBA).

References

1. ACI 116R-00. 2001. Cement and concrete terminology. ACI manual of concrete practice: Part 1.
2. Akram T., Memon S.A., Obaid H. 2009. Production of low-cost self-compacting concrete using bagasse ash. *Constr. Build. Mater.,* 23(2), 703–12.
3. Angst U., Elsener B., Larsen C.K., Vennesland Ø. 2009. Critical chloride content in reinforced concrete – A review. *Cem. Concrete. Res*., 39(12), 1122 1138.
4. Arenas-Piedrahita J.C., Montes-García P., Mendoza-Rangel J.M., López-Calvo H.Z., Valdez-Tamez P.L., Martínez-Reyes J. 2016. Mechanical and durability properties of mortars prepared with untreated sugarcane bagasse ash and untreated fly ash. *Constr. Build. Mater.,* 105, 69-81.
5. Aprianti E., Shafigh P., Bahri S., and Nodeh F. J. 2015. Supplementary cementitious materials' origin from agricultural wastes – A review. *Constr. Build. Mater.*, 74, 176-187.
6. Bahurudeen A., Santhanam M. 2015. Influence of different processing methods in the pozzolanic performance of sugarcane bagasse ash. *Cem. Concrete. Comp.,* 56, 32-45.
7. Biricik H., Sarier N. 2014. Comparative study of the characteristics of nano silica, silica fume and fly ash incorporated cement mortars. *Materials Research*, 17(3), 570-582.
8. Broomfield J. P. 1997. Corrosion of steel in concrete: Understanding, investigation and repair. First edition. E & FN Spon.
9. Castellote M. Anddrade C. 2001. Round-Robin test on chloride analysis in concrete part 2: Analysis of water soluble chloride content. *Materials and Structures*. 34, 589-598.
10. Chusilp N., Jaturapitakkul C., Kiattikomol K. 2009. Effects of LOI of ground bagasse ash on the compressive strength and sulfate resistance of mortars. *Constr. Build. Mater*., 23(12), 3523-3531
11. Cordeiro, G.C., Toledo F. R.D., Fairbairn, E.M.R. 2009. Effect of calcination temperature on the pozzolanic activity of sugar cane bagasse ash. *Construct. Build. Mat*. 23[10], 3301–3303.
12. Cordeiro G. C., Toledo F. R. D., Fairbair E. M. R. 2010. Ultrafine sugarcane bagasse ash: High pozzolanic material for tropical countries. *IBRACON structures and materials journal*. 3[1], 50-67.
13. Cordeiro G. C., Paiva O. A., Toledo F. R. D., Fairbairn E. M. R., and Tavares L. M. 2018. Long-term compressive behavior of concretes with sugarcane bagasse ash as a supplementary cementitious material. *J. Test. Eval*. 46[2], 176-183.

14. Česen Aleš, Kosec Tadeja, Legat Andraž. 2013. Characterization of steel corrosión in mortar by various electrochemical and physical techniques. *Corros Sci*, 75, 47-57.

15. Dhengare S., Amrodiya S., Shelote M., Asati A., Bandwaf N., Anand K., Jichkar. 2015. Utilization of sugarcane bagasse ash as a supplementary cementitious material in concrete and mortar – a review. *International Journal of Civil Engineering and Technology*. 6 [4], 94–106.

16. Dong Biqin, Qiu Qiwen, Xiang Jaiqi, Huang Canjie, Xing Feng, Han Ningxu. 2014. Study on the carbonation behaviour of cement mortar by electrochemical impedance spectroscopy. *Revista Materials*, 7, 218-231.

17. Escalante-García J. I. 2002. Materiales alternativos al cemento Portland. *Avance y Perspectiva* 21. CINVESTAV-Saltillo.

18. Fontana M. 1986. Corrosion engineering. Third edition. Mc Graw Hill.

19. Frias R. M., Sánchez de Rojas Gómez M. I. 2013. Eco-efficient concrete. Chapter 5: Artificial pozzolans in eco-efficient concrete. Woodhead Publishing Limited.

20. Frías M., Villar E., Savastano H. 2011. Brazilian sugar cane bagasse ashes from the cogeneration industry as active pozzolans for cement manufacture, *Cem. Concrete Comp*, 33, 490-496.

21. Ganesan K., Rajagopal K., Thangavel K. 2007. Evaluation of bagasse ash as supplementary cementitious material. *Cem. Concrete Comp.,* 29(6), 515-524.

22. Gastaldini A. L. G., Isaia G. C., Saciloto A. P., Missau F., Hoppe T. F. 2010. Influence of curing time on the chloride penetration resistance of concrete containing rice husk ash: A technical and economical feasibility study. *Cem. Concrete Comp.,* 32(10), 783-793.

23. Hendriks C. A., Worrel E., de Jader D., Blok K., Riemer P. 2004. Emission reduction of greenhouse gases from the cement industry. Greenhouse gas control technologies conference paper-cement. www.ieagreen.org.uk

24. Hernández Toledo U. I. 2010, Efecto de una puzolana de desperdicio agrícola y el tiempo de curado en la corrosión del Ferrocemento", Master thesis, IPN-CIIDIR-Oaxaca, México. (In spanish).

25. Jiménez-Quero V. G., León-Martínez F. M., Montes-García P., Gaona-Tiburcio C., Chacón-Nava J.G. (2013). "Influence of sugarcane bagasse ash and fly ash on the rheological behavior of cement pastes and mortars." *Constr. Build. Mater.,* 40, 691-701.

26. Josa A., Aguado A., Cardim A., Byars E. 2007. Comparative análisis of the cycle impact assessment of available cement inventories in the EU. *Cem. Concrete Res.*, 37, 781-788.

27. Liu J., Qiu Q., Chen X., Wang X., Xing F., Han N., He Y. 2016. Degradation of fly ash concrete under the coupled effect of carbonation and chloride aerosol ingress. *Corros. Sci.,* 112, 364-372.

28. López-Calvo H. Z., Jiménez-Quero V. G., Cano-barrita P.F. 2006. Comportamiento de un muro construido con paneles prefabricados de mortero armado sometido a compresión simple y diagonal. *Revista Naturaleza y Desarrollo*, 4(1), 55-63.

29. Lothenbach B., Scrivener K., Hooton R. D. 2011. Supplementary cementitious materials. Cement and Concrete Research 41, 1244-1256.

30. Lu X. Li C. Zhang H. 2002. Relationship between the free and total chloride diffusivity in concrete. *Cem. Concrete Res.*, 32, 323-326.

31. Kayali O., Khan M. S. H., Sharfuddin Ahmed M. 2012. The role of hydrotalcite in chloride binding and corrosion protection in concretes with ground granulated blast furnace slag. *Cem. Concrete Comp.* 34, 936-945.

32. Katare V. D., and Madurwar M. V. 2017. Experimental characterization of sugarcane biomass ash – A review. *Constr. Build. Mater.,* 152, 1-15.

33. Lothenbach B., Scrivener K., Hooton R. D. 2011. Supplementary cementitious materials. *Cem. Concrete Res.,* 41(12), 1244-1256.

34. Maldonado-García M. A. 2012. Efecto de la adición de ceniza de bagazo de caña en la microestructura y durabilidad del ferrocemento, Master thesis, IPN-CIIDIR-Oaxaca, México. (In spanish).

35. Michel A., Otieno M., Stang H., Geiker M. R. 2016. Propagation of steel in concrete: Experimental and numerical investigations. *Cem. Concrete Comp.,* 70, 171-182.

36. Morales E. V., Villar-Cociña E., Frías M., Santos S. F., Savastano Jr. H. 2009. Effects of calcining conditions on the microstructure of sugarcane waste ashes (SCWA): influence in the pozzolanic activation. *Cem. Concrete Comp.,* 31(1), 22-28.

37. Montakarntiwong K., Chusilp N., Tangchirapat W., Jaturapitakkul C. 2013. Strength and heat evolution of concretes containing bagasse ash from thermal power plants in sugar industry. *Materials and Desing*. 49, 414-420.

38. Muangtong P., Sujjavanich S., Boonsalee S., Poomiapiradee S., Chaysuwan D. 2013. Effects of fine bagasse ash on the workability and compressive strenght of mortars. *Chiang Mai Journal*. 40[1], 126-134.

39. Noor-Ul A. 2011. Use of bagasse ash in concrete and its impact on the strength and chloride resistivity. *Journal of Materials in Civil Engineering*. ASCE. Technical Note.

40. Olibeira de Paula Marcos, Ferreira Tinôco Ilda de Fátima, Rodríguez Conrado de Souza, Osorio Díaz Jairo Alexander. 2010. Sugarcane bagasse ash as a partial-Portland-cement-replacement material. *Revista Dyna*, 77(163), 47-54.

41. PCA. America´s Cement Manufacturers. 2018. Durability www.cement.org/learn/concrete-technology/durability# (Viewed October 17, 2018).

42. RILEM TC 178-TCM. 2002. Testing and modelling chloride penetration in concrete – Analysis of water soluble chloride content in concrete. *Materials and Structures*. 38, 583-585.

43. Ríos-Parada V. Jiménez-Quero V. G., Valdez-Tamez P. L. Montes-García P. 2017. Characterization and use of an untreated Mexican sugarcane bagasse ash as

supplementary material for the preparation of ternary concretes. *Constr. Build. Mater.,* 157, 83-95.

44. Siddique R., Iqbal K. M. 2011. Supplementary Cementing Materials. Springer-Verlag Berlin Heidelberg.

45. Shi X., Xie N., Fortune K., Gong J. 2012. Durability of steel-reinforced concrete in chloride environments: An overview. *Constr. Build. Mater.,* 30, 125-138.

46. Simčič T., Pejovnik S., De Schutter G., Bokan B. V. 2015. Chloride ion penetration into fly ash concrete during wetting-drying cycles. *Constr. Build. Mater.,* 93, 1216-1223.

47. Smith W. Hashemi J. 2006. Fundamentos de ciencia e ingeniería de materiales. First eddition. Mc Graw Hill Interamericana.

48. Soares M. M. N. S., Poggiali F. S. J., Bezerra A. C. S. Figueiredo R. B., Aguilar M-T- P, Cetlin P. R. 2014. The effect of the calcination conditions on the physical and chemical characteristics of sugar cae bagasse ash. *R. Esc. Minas*. 67, 33-39.

49. Song H. W., Lee C. H., Ann K. Y. 2008. Factors influencing chloride transport in concrete structures exposed to marine environments. *Cem. Concrete Comp.,* 30(2), 113-121.

50. Thomas M. D. A., Hooton R. D. Scott A., Zibara H. 2012. The effect of supplementary cementitious materials on chloride binding in hardened cement paste. *Cem. Concrete Res.,* 42, 1-7.

51. Torres-Luque M., Bastidas-Arteaga E., Schoefs F., Sánchez-Silva M., Osma J. F. 2014. Non-destructive methods for measuring chloride ingress into concrete: State-of-the-art and future challenges. *Constr. Build. Mater.,* 68, 68-81.

52. UNC (Unión Nacional de Cañeros A. C. de México). 2017. www.caneros.org.mx (Viewed october 04, 2017).

53. Valencia G., Mejía de Gutiérrez R., Barrera J., Delvasto S. 2012. Estudio de la durabilidad y corrosión en morteros armados adicionados con toba volcánica y ceniza de bagazo de caña de azúcar. *Revista de la Construcción*. 12, 112-122.

54. Zibara H., Hooton R. D., Thomas M .D. A., Stanish K. 2008. Influence of the C/S and C/A ratios of hydration products on the chloride ion binding capacity of lime-SF and lime-MK mixtures. *Cem. Concrete Res.,* 28, 422-426.

CHAPTER TWO

A review of the use of sugarcane bagasse ash with a high LOI content to produce sustainable cement composites.
Maldonado-García M. A., Montes-García P., Valdez-Tamez P. L. 2017.
PRO119. Proceedings of the 2nd International Conference on Bio-based Building Materials. RILEM Publications S.A.R.L., Paris, France, 595-605. http://www.rilem.net.

A REVIEW OF THE USE OF SUGARCANE BAGASSE ASH WITH A HIGH LOI CONTENT TO PRODUCE SUSTAINABLE CEMENT COMPOSITES

M. A. Maldonado-García[1]*, P. Montes-García[1], P. L. Valdez-Tamez[2]

[1] Instituto Politécnico Nacional – CIIDIR Oaxaca, Hornos No. 1003, Col. Noche Buena, Santa Cruz Xoxocotlán, C.P. 71230, Oaxaca, México.

[2] Universidad Autónoma de Nuevo León – Instituto de Ingeniería Civil, Cd Universitaria s/n, San Nicolás de los Garza, C.P. 66451, Nuevo León, México.

*Corresponding author; mmaldonadog1500@alumno.ipn.mx

Abstract

In recent years, agricultural wastes have been employed as supplementary cementitious materials to produce sustainable cement composites. One of these wastes is the sugarcane bagasse ash (SCBA). The SCBA is available in large quantities in developing countries such as Brazil, India and Mexico, and its disposal is causing different environmental issues. The SCBA has high amounts of silicon, aluminum and iron oxides as major components. Several researchers report that the high amount of these oxides leads to the improvement of the mechanical and microstructural properties of cementing composites containing the SCBA. On the other hand, a high amount of unburned carbon, commonly expressed by the loss on ignition (LOI), could be also present in the SCBA due the inefficient burning process of the bagasse in the boiler in sugar mills. It has been reported that this high LOI content in the SCBA change the water requirement and the rheological properties of cement binders. This might adversely affect the mechanical, microstructural and durability properties of hardened cement composites prepared with this material as well. In order to decrease the LOI content of the SCBA the combination of sieving, grinding and recalcination have been proposed; however, these methods are highly demanding in energy and generate additional contaminants. Sieving is the less energy demanding procedure and appears to be an interesting approach to post-treat the existing SCBA in open damps. Based on the above, this paper presents a review on the effects of the use of SCBA with a high LOI content to manufacture cement composites.

Keywords:
Recalcination, cement composites, grinding, sieving, post-treatment

1 INTRODUCTION

Portland cement is used in cement composites (concrete, mortars and other cementitious materials) and is considered one of the most produced and significant building material for society´s infrastructures around the world [Hendriks 2004, CIF 2011]. Currently, concrete is produced in large quantities, between 2 and 2.8 billion of tons annually [Schneider 2011, Shi 2011], to satisfy the housing demand of the population and industrial activities. A demand scenario indicates that the Portland cement production could reach 3.69 to 4.40 billion of tons by 2050 [IEA 2009]. However, the cement production is a high energy-intensive process yielding an enormous negative effect on the environment. In this context, it is reported that the production of each ton of Portland cement emits approximately 0.8 to 1.0 tons of anthropogenic CO_2 into the atmosphere [Aprianti 2015, Habert 2013]. This represents between 3 and 5% of current global emissions [IEA 2009].

For this reason, several studies have been focused in the use of alternative materials, such as wastes generated from the industry and agriculture, which are used as supplementary cementitious materials of Portland cement composites [Aprianti 2015]. The disposal of these wastes is another serious problem worldwide. Waste materials form the industry such as fly ash, ground granulated blast furnace slag and silica fume have been successfully used in cement composites for many years [Madurwar 2013, Shafigh 2014, Demis 2014].

Agricultural waste materials have been employed in cement composites recently. The utilization of these wastes as a partial Portland cement replacement can provide the break-through needed to make a more environment friendly and sustainable construction industry [Madurwar 2013, Demis 2014, Aprianti 2015]. It has been reported that the agricultural wastes in large quantities are sugarcane bagasse ash, rice husk ash, palm oil fuel ash, wood waste ash, corn cob ash and bamboo leaf ash. This review focuses on the use

597

of sugarcane bagasse ash (SCBA) as cement replacement in cement composites.

The SCBA is a by-product generated from the combustion process of sugarcane bagasse in sugar mills. The production of SCBA is approximately 15 millions of tons annually and is causing serious disposal problems and environmental issues worldwide [Frías 2013]. The SCBA is mostly composed by silicon, aluminum and iron oxides. Several researches confirm that a high amount of these oxides in the chemical composition of the SCBA leads to the improvement of the mechanical and microstructural properties of cementing composites (when the SCBA replaces up to 30% of Portland cement). They also suggest the improvement of some durability properties of Portland cement based composites added with this material [Ganesan 2007, Cordeiro 2009a, Cordeiro 2009b, Morales 2009, Chusilp 2009a, Chusilp 2009b, Frías 2011, Bahurudeen 2015].

However, it is reported that a high amount of unburned carbon particles, generally presented in the form of cellular particles and commonly expressed by the loss on ignition (LOI), could be present in the SCBA [Chusilp 2009a, Somma 2012, Maldonado 2012, Bahurudeen 2015, Asrif 2016]. The high LOI content in the SCBA can be attributed to termo-mechanical conditions during the burning process of the bagasse in the boilers of sugar mills as well as the nature of the parent biomass [Batra 2008]. A high LOI content can be an obstacle for the use of the SCBA in cement composites due to the reduction of the fluidity during the mixing process [Jímenez 2013], and due to a slight effect in the compressive strength development of these composites as well [Chusilp 2009a].

Several researchers have focused on the implementation of some post-treatments to the SCBA in order to reduce the LOI content, such as sieving, grinding, recalcination or the combination of them. They suggest that these methods can increase the pozzolanic activity when the SCBA is subjected to specific conditions of grinding or recalcination [Cordeiro 2009a, Chusilp 2009, Somma 2012, Buhurudeen 2015]. Unfortunately, these methods are highly demanding in energy making necessary to use them as "practically as received" from sugar mills, i.e. a SCBA processed with a minimum energy demand post-treatment such as only sieving.

Based on the afore mentioned dilemma, a discussion about the effects of the use of SCBA with a high LOI content in cement composites is presented on this paper.

2 NATURE AND PYROLYSIS PROCESS OF THE SUGARCANE BAGASSE

The sugarcane bagasse is a fibrous residue obtained after the crushing and milling process of the sugarcane stalks to squeeze the juice out. It is reported that the sugarcane bagasse is made up of water, fiber bundles (which consist of cellulose, hemicelluloses, lignin, pectin, waxes and pentosane), vesels, parenchyma, epidermal cells and small amounts of soluble solids. Each of the mentioned compounds varies according with the soil type, harvesting methods, variety and maturity of the sugarcane. It has been reported that cellulose is a hydrophilic compound while hemicelluloses and lignin have hygroscopic and hydrophilic properties, respectively [Sanjuán 2001, Chiparus 2004, Verma 2012]. The nature of the cellulose and hemicellulose could elucidate the rheological performance of the SCBA when is used as cement replacement.

Some studies suggest that the pyrolysis of the sugarcane bagasse is divided in two steps. In the first step, a rapid mass loss occurs due the volatilization of the cellulose obtaining bio-oil. In the second step, a slower mass loss rate occurs due the lignin decomposition obtaining products with properties of char and bio-oil [Gani 2007, Varma 2016].

3 CHEMICAL COMPOSITION AND MORPHOLOGY OF THE SUGARCANE BAGASSE AFTER BURNING

After the burning process of the sugarcane bagasse, the residual ash is composed by approximately 85% of silicon, aluminum and iron oxides (Tab. 1). It also contains other compounds such as calcium, potassium, sodium and magnesium oxides as well as unburned carbon particles. From Tab.1, it can be seen that the SCBA may have different LOI contents, ranging from 0.40 to 24.15%. The different chemical compositions of the SCBA depend on the variety, maturity and harvesting methods of the sugarcane; likewise depend on the bagasse combustion environment and bagasse ash collection [Arif 2016].

Several researchers have shown that the SCBA has a morphology consisting in particles with a large variety of shapes and sizes [Batra 2008, Cordeiro 2009a, Chusilp 2009a, Maldonado 2012, Buhurudeen 2015]. This morphology is attributed to the variations of the temperature and air flow during the burning process of the bagasse. In general, the SCBA has prismatic, agglomerated, spherical and fibrous particles (unburned matter) (Fig. 1).

Researchers reported that the SCBA has a potential use as a beneficial cement replacement in cement composites; however, the physical and chemical variations limitates its use as cementing material [Frías 2011, Demis 2014]. In view of this, it is suggested that individual sources of SCBA should be evaluated in terms of physical and chemical characteristics in order to determinate its most effective utilization [Arif 2016].
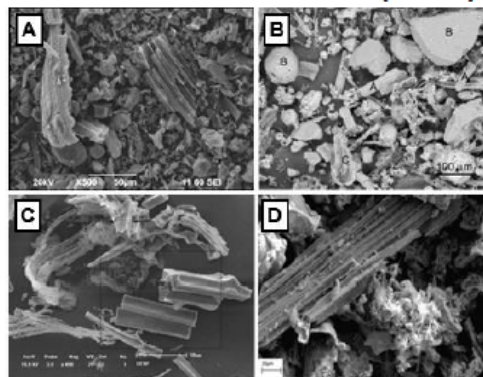

Fig. 1: Morphology of the SCBA. SEM images obtained from A) Maldonado 2012, B) Batra. 2008, C) Cordeiro 2009a and D) Chusilp 2009a.

Tab. 1: Summary of chemical compositions and LOI content of SCBAs from varied sources (%, in mass). S = sieving, G = grinding, R = recalcination, * = Selected chemical compositions from the mentioned paper.

Reference	SiO$_2$	Al$_2$O$_3$	Fe$_2$O$_3$	CaO	MgO	SO$_3$	K$_2$O	Na$_2$O	P$_2$O$_5$	LOI	Post-treatment
Martirena 1998	72.74	5.26	3.92	7.99	2.78	0.13	3.47	0.84	1.56	0.77	R
Ganesan 2007	64.15	9.05	5.52	8.14	2.85	---	1.35	0.92	---	4.90	R + G
Cordeiro 2008	78.34	8.55	3.61	2.15	---	---	3.46	0.12	---	0.42	G
Cordeiro 2009a, *	60.96	0.09	0.09	5.97	8.65	---	9.02	0.70	8.34	5.70	R
Chusilp 2009a	54.10	5.69	3.54	15.37	1.41	0.03	---	---	---	19.36	G
Morales 2009, *	58.61	7.32	9.45	12.56	2.04	0.53	3.22	0.92	2.09	2.73	G + S
Noor-ul 2011	87.40	3.60	4.90	2.56	0.69	0.11	0.47	0.15		8.25	R + G
Hernández 2010	51.66	9.92	2.32	2.59	1.44	---	2.10	1.23	0.90	24.15	S
Somma 2012	55.00	5.10	4.10	11.00	0.90	2.20	1.20	0.20	---	19.60	G
Maldonado 2012	56.37	14.61	5.04	2.36	1.43	---	3.29	1.57	0.85	10.53	S
Valencia 2012	70.05	8.50	3.10	2.80	0.50	---	---	---	---	8.50	---
Frías 2013	58.61	7.32	9.45	12.56	2.04	0.53	3.22	0.92	2.09	2.73	---
Montakartiwong 2013, *	67.10	5.70	2.50	2.90	0.50	---	---	---	---	20.4	G
Buhurudeen 2015, *	72.95	1.68	1.89	7.77	1.98	4.45	9.28	---	---	21.00	S, S + G
Rerkpiboon 2015	55.04	5.14	4.06	11.03	0.91	---	1.22	0.24	---	19.60	G
Arif 2016	78.49	7.27	3.48	1.28	1.28	1.55	1.14	0.69	---	7.15	---
Cordeiro 2016	80.80	5.10	1.60	3.10	---	1.50	6.30	---	0.80	0.40	G
Soares 2016	72.30	5.52	10.80	1.57	1.13	---	---	---	1.11	1.52	---

4 EFFECT OF THE CALCINATION ON THE PERFORMANCE OF SCBA IN CEMENT COMPOSITES

Some authors suggest that a proper calcination of the sugarcane bagasse is enough to obtain ashes with good quality to be used as replacement in cement composites. In general, it is recommended that the sugarcane bagasse must to be calcined at temperatures between 600 and 800ºC considering a heating rate of 10ºC/min [Morales 2009, Cordeiro 2010, Ribeiro 2014]. For example, [Cordeiro 2009a] evaluated the pozzolanic behavior of SCBA obtained under controlled calcination conditions. Sugarcane bagasse samples were burnt in an aired electric oven at 350ºC with a heating rate of 10ºC for 3 hours, and then at temperatures between 400 and 800ºC for another 3 hours. They found that the LOI content of the SCBA decreased with increasing the temperature of calcination. The authors found that the SCBA produced with air calcination at 600ºC for 3 hours with a rate of heating of 10ºC/minute present amorphous silica, low carbon content (5.70% by mass represented by the LOI content according with Tab. 1) and hence a good pozzolanic activity.

[Morales 2009] evaluated the microstructural features of SCBA obtained under controlled calcination conditions. For this purpose, the sugarcane bagasse was calcined at temperatures of 800 and 1000ºC (±5ºC) in an electric furnace for 20 minutes. The ashes were ground and sieved to <90µm after the calcination process. The authors concluded that the textures and morphologies of the SCBA calcined at both temperatures change in dependence of the Ca and Si content. They also concluded that the calcination process not only influence the mineralogical composition of the SCBA but also change the morphology and composition of their individual particles in dependence of the Ca and Si contents. Finally, the authors suggest that the SCBA, obtained from both calcination temperatures, have properties which indicate a high pozzolanic activity.

[Cordeiro 2010] evaluated the influence of ultrafine SCBA in the properties of high performance concretes. The SCBA was obtained by controlled burning and ultrafine grinding process. The burning process was in two steps. In the first step the bagasse was calcined at 350ºC and, in the second step the bagasse was calcined at temperatures between 400 and 800ºC considering a heating rate of 10ºC/min and a resident time of 3 hours. The authors suggest that a burning process at 600ºC in a muffle oven produce an amorphous SCBA with high specific surface area and with low LOI content; while the ultrafine grinding process during 120 minutes leads the production of a SCBA with pozzolanic activity of 100%. The results indicate that the SCBA used in this research improved the durability properties of the high-performance concretes without any change on the rheological and mechanical properties.

[Ribeiro 2014] evaluated the pozzolanic activity of the SCBA obtained under controlled calcination conditions when is used as a partial Portland cement replacement

599

in mortars. The sugarcane bagasse was calcined at 500, 600 and 700ºC in an oven considering a heating rate of 10ºC/min. The authors concluded that the particle size of the SCBA is higher as the calcination temperature increase; they also found that the specific gravity decrease due to the loss of the organic matter. The authors reported that the SCBA calcined at 600ºC has a higher amorphous matter than the SCBA calcined at 500 and 700ºC. Mortars prepared with 10% of SCBA as partial Portland cement replacement showed better mechanical properties compared with a control mortar for all temperatures examined.

5 INFLUENCE OF THE LOI CONTENT AND DIFFERENT POST-TREATMENTS ON THE POZZOLANICITY OF THE SCBA IN CEMENT COMPOSITES

Several post-treatments are used to reduce the high LOI content of the SCBA and in consequence to improve its pozzolanic activity in cement composites. It has been suggested that a minimum processing method must to be employed for these purposes, because the as received SCBA from sugar mills contains large quantities of unburned carbon particles which is the result of uncontrolled calcination procedures in the boilers [Cordeiro 2009b, Chusilp 2009a, Hernández 2010, Somma 2012, Buhurudeen 2015]. The outcome of the research indicate that the most common post-treatments used for the SCBA improvement are sieving, grinding, recalcination and the combination of them.

5.1 Sieving

Sieving is the main process used to remove coarse and fine fibrous particles in the SCBA received from sugar mills [Buhurudeen 2015]. Researchers conclude that a sieving process is sufficient to exceed the minimum strength activity index (75% of the control at 7 and 28 days) required in the ASTM C618 standard.

[Hernández 2010] evaluated the replacement of 10 and 20% of Portland cement by sieved SCBA (sieved through the 75μm ASTM mesh for five minutes) on the mechanical and durability properties of mortars with different curing times. The SCBA used in this research has the highest LOI content showed in the Tab. 1 (24.15%). The results show that a poor curing time had a negative effect on the compression strength of the mortars; however, the replacement of 10 and 20% of cement by sieved SCBA decreases in about 50% the chloride diffusion coefficients.

[Maldonado 2012] evaluated the compressive strength and microstructural properties of mortars (at long ages) containing 10 and 20% of SCBA with a LOI content of 10.53 (obtained at temperatures between 550 and 700ºC in the boiler from a sugar mill). The SCBA used on this research was sieved for only 5 minutes through the 75μm ASTM mesh (this post-treatment was selected in accordance with the reported by [Hernández 2010]). The results show that the compressive strength was higher at 28, 90 and 450 days in comparison with the control mortar; likewise, the microstructure of the mortars was denser due to the consumption of the calcium hydroxide during the pozzolanic reactivity of the SCBA. The author suggests that the durability of the mortars containing SCBA with a high LOI content could be increased. This is based on the microstructure refinement observed in the mortars which reduce the chloride diffusion coefficients

of the mortars. This statement is also based on the analysis of electrochemical test results obtained in an ongoing long-term study of the durability of reinforced mortars (containing SCBA with a high LOI content of 24.15%) exposed to wetting and drying cycles in a NaCl solution of 3% during 1000 days which was started by [Hernández 2010].

[Torres 2014] evaluated the pozzolanic activity of two sieved SCBAs obtained from the bottom of the multicyclone and precipitator of a boiler which were acquired at temperatures between 600 and 900ºC. The sieving process through the 106, 90 and 75μm meshes was applied to reduce the LOI content of the both ashes to 3.7 and 11%, respectively. The authors concluded that the pozzolanic activity indexes of the ashes were higher than the minimum from the required by the ASTM C618. However, according with the results from the Frattini test, an additional grinding process to the ashes is suggested.

[Buhurudeen 2015] suggest that the coarse particles and fine fibrous carbon particles in the SCBA could be completely removed by sieving. They found that the ash passing through the 300μm ASTM mesh is enough to have fine burnt particles rich in silica content. The authors found that a simple sieving process by the 300μm ASTM mesh increased the pozzolanic activity of the SCBA above the minimum requirement by the ASTM. However, the pozzolanic activity of the sieved ash could be improved by a grinding process reducing the particle size of the ash to the cement fineness (300m^2/kg).

[Arenas 2016] analyzed the influence of SCBA "practically as received" on the mechanical and durability properties of mortars mixtures. The used SCBA was only sieved thought the 75μm ASTM mesh during five minutes. They found that the addition of 10 and 20% of sieved SCBA decrease the compressive strengths of the mortars at early ages but after 90 days were similar or higher than the mortars without SCBA or fly ash additions. It was found that the electrical resistivity increased generally for all the mortars except for the mortar containing 10% of SCBA which surpassed the reference at 180 days. Finally, it was also found that the level of permeability decreased in all the mortars but it was especially observed in the mortar containing 20% of SCBA. The authors hypothesize that the unburned matter from the SCBA could bond chlorides.

[Maldonado 2016] evaluated the carbonation of reinforced mortars containing 10 and 20% of SCBA with a high LOI content. The SCBA used on this research was obtained by [Hernández 2010] and the reinforced mortars were exposed for 2000 days to wetting and drying cycles following the methodology described by [Maldonado 2012]. The results, obtained by the phenolphthalein method and by pH measurements of the alkaline reserve of the mortars, suggest that the high LOI content of the SCBA decrease the alkalinity of the mortars; however, the pH value remains above 10 which is the minimum value considered to activate the corrosion mechanism of the steel embedded in cement composites.

5.2 Grinding

Grinding is the main post-treatment used to control the particle size distribution and decrease the negative effect of the crystalline compounds on the pozzolanic reactivity of the SCBA [Cordeiro 2009b, Chusilp 2009b]. Several researchers suggest that grinding is

the most useful post-treatment to obtain a higher pozzolanic reactivity for the SCBA in comparison with sieving methods.

[Cordeiro 2008] found that the ground SCBA produced in a vibratory mill considering grinding times from 8 to 240 minutes increase the compressive strength of mortars due to an increase in the pozzolanic behavior of the sugarcane ash and to the improvement of the packing density in the mortars. The authors concluded that the pozzolanic activity of mortars containing ground SCBA increase significantly with longer grinding times.

[Chusilp 2009a] affirm that the grinding process reduce the particle size of the SCBA making the particles more dense. In that research SCBA with a high LOI content (Tab. 1) was used to study the development of the compressive strength and the sulfate resistance of mortars. The obtained SCBA was ground in a ball mill (until the particles retained by a 45µm mesh were less than 5% by weight), and subsequently the ground ash was put in an oven at 550°C for about 45 minutes to reduce the LOI content down to 5%. They made different mortar mixtures using SCBAs with 5, 10, 15, and 20% of LOI content. The authors concluded that the high LOI content of the SCBA is attributed to the carbon content of the unignited bagasse but this LOI had no adverse effects on the properties of mortars. Nonetheless, ground SCBA with a LOI content less than 10% was proved to be an excellent pozzolanic material.

[Somma 2012] studied the utilization of ground SCBA with a high LOI content to improve the mechanical properties and durability of recycled aggregated concrete. The SCBA was ground to improve its reactivity because the original collected ash showed a lower strength activity index than the suggested by the standards. After grinding, the SCBA had higher fineness and lower porosity in comparison with the original ash and the strength activity indexes at 7 and 28 days were higher than those required by the ASTM C 618. The results of the experiments indicate that the mechanical properties and durability of these concretes were improved when Portland cement was replaced by up to 20% of ground SCBA with a high LOI content.

[Montakarntiwong 2013] evaluated two different SCBAs with low and high LOI contents, respectively. The SCBAs were ground in a ball mill until the particles retained by a 45µm mesh were less than 5% by weight. They replaced the ordinary Portland cement with 20, 30 and 40% of SCBA by weight of the binder. The results indicate that the cement replacement by ground SCBA with low and high LOI content at 20 and 30% by weigh of binder, respectively, resulted in a compressive strength higher than the control mixture. However the concrete mixed with SCBA with a low LOI content had a slightly higher compressive strength than the concrete mixed with SCBA with a high LOI. The authors also found that most of the original SCBA (before the grinding process) with low and high LOI had the same particle shapes showing tubular shaped particles with highly irregular shapes and porous structure. These irregularities in shape remained even after the grinding process.

[Rerkpiboon 2015] evaluated the replacement of 10, 20, 30, 40 and 50% of Portland cement by ground SCBA with a LOI content of 19.60 (Tab.1) on the mechanical and durability properties of concretes. The

SCBA was ground using a ball mill until the particles retained by a 45µm mesh were only 0.42%. The results show that the cement replacement of 50% by ground SCBA did not have any effect on the modulus of elasticity of the concrete. It was also found that the replacement of 10 to 50% by ground SCBA increased the chloride resistance of the concrete. However the replacement of 20% of Portland cement by ground SCBA contributed to obtain the highest compressive strength.

[Cordeiro 2016] explored a selective grinding process to reduce the content of quartz in the SCBA. The proposed strategy was capable to remove the quartz and hence to increase the homogeneity and the pozzolanic activity of the SCBA. The authors suggest that selective grinding could result in a less costly ultrafine grinding due the quartz particles were about over fifteen times the strength of the cellular-based SCBA particles.

5.3 Recalcination

Recalcination is a process which helps to decrease the coarse unburnt particles in as received SCBA from sugar mills to increase its pozzolanic reactivity [Bahurudeen 2015].

[Martirena 1998] evaluated the SCBA as probable pozzolanic material. The SCBA was burned to remove undesirable substances such as carbon particles. The authors conclude that the main factors that affect the reactivity of the SCBA are the degree of the crystallinity of the silica and the presence of impurities such as carbon and unburned matter. The carbon and unburned matter could limit the reaction between the reactive silica with the calcium hydroxide to form stable compounds. These impurities take place due to high temperatures and incomplete combustion of the sugarcane bagasse in the boilers of sugar mills.

[Bahurudeen 2015] evaluated the effect of the burning process in the pozzolanic activity of the SCBA. They burnt bagasse ash samples, collected from a sugar mill, at temperatures of 600, 700, 800 and 900°C. The authors found that the pozzolanic activity indexes of burnt samples were higher than the obtained with the as received ash because the burning of the fibrous particles. However, an increase of the burning temperature beyond 700°C reduces the index value due the crystallization of the crystoballite.

5.4 Combination of different post-treatments

More research suggests that the combination of different post-treatments help to decrease the LOI content and improve the pozzolanic activity of the SCBA. For example, as a mentioned earlier, [Bahurudeen 2015] concluded that a sieving process through the 300µm ASTM mesh is enough to decrease LOI content of the SCBA; however, a grinding process could improve it as well. The most common combinations used are burning plus grinding and sieving plus grinding.

[Ganesan 2007] studied the effects of SCBA as a partial Portland cement replacement on physical and mechanical properties of hardened concrete. The SCBA was burnt under controlled temperature at 650°C for one hour and ground to 5.4µm mean grain size (after collecting from a sugar mill). The results indicate that the SCBA (with a LOI content of 4.90%, Tab.1) is an effective mineral admixture, and can replace up to 20% of Portland cement because of the resulting improvement of its pozzolanicity.

[Noor-ul 2011] also reported the impact of the use of SCBA as a partial Portland cement replacement on the physical and mechanical properties of hardened concrete. The SCBA was burned at 650°C for one hour and ground before being used. The burning process reduced the carbon content of the ash as the LOI content decreased from 8.28 to 4.5%. The processed SCBA was used in seven different proportions (ranging from 5 to 30%) in concrete mixtures. The results indicate that the SCBA is an effective mineral admixture and pozzolan, with an optimal replacement ratio of 20% cement, which reduces the chloride diffusion of the concrete by 50% without any adverse effects on the mechanical properties of concretes. This behavior is mainly attributed to the fines particles which have a large surface area to react and filling the micro and macropores and developing a discontinuous and tortuous pore structure in the concrete matrix.

[Buhurudeen 2015] studied the influence of different post-treatments such as sieving, grinding, burning and combination of these methods on the pozzolanic performance of the SCBA. They suggest that a minimum processing energy is needed to obtain a good pozzolanic activity and a low value of LOI for the SCBA. The authors obtained a pozzolanic activity index of 108% and 106% at 7 and 28 days for the SCBA subjected to sieving (material passing thought the 300μm mesh) and grinding. However, they obtained a pozzolanic activity index of 79% when the SCBA was only sieved, which is higher than the minimum required pozzolanic index value required by the ASTM C311 standard. The authors recommend a combination of sieving through the 300μm mesh to remove coarse and fine fibrous particles and grinding to cement fineness (300m^2/kg).

6 POZZOLANIC BEHAVIOUR OF THE AS RECEIVED SCBA IN CEMENT COMPOSITES

There are only few studies addressing the use of as received SCBA from sugar mills for Portland cement replacement. One of these studies [Valencia 2012] reported that the replacement of 10% of as received SCBA increased the compressive strength of mortars; however, its effects on the durability are not clear. These uncertainties can be attributed to the physical properties of the ash.

[Frías 2011] showed that the as received SCBA from sugar mills did not show a properly pozzolanic activity in comparison with the ash obtained under controlled laboratory conditions (obtained in an electrical furnace under two burning temperatures; 400°C during 20 minutes followed by 800°C during 60 minutes, with heating rate of 10°C/min). From this research a proper management for the sugarcane bagasse before their use as combustibles removing all the contaminant materials is suggested; moreover, the authors suggest a controlling calcination of the bagasse at temperatures around 800°C in order to obtain a SCBA with a similar pozzolanic behavior to that showed by the SCBA obtained in the laboratory.

[Arit 2016] reported the effects of the used of as received SCBA obtained with a high-efficiency co-generation boiler in a sugar mill. The authors concluded that this sugarcane ash does not contain significant amorphous silica which substantially reduces the pozzolanic reactivity of the ash in cement composites. Only pastes with addition of 5% of as received SCBA showed a proper pozzolanic reactivity. Results also indicate that up to 15% SCBA replacements achieve a pozzolanic activity index above to 75%. The authors suggest that this performance could be attributed more likely to a filler effect rather than true pozzolanic activity.

[Soares 2016] evaluated the pozzolanic behaviour of the SCBA by comparing it to amorphous and crystalline silica. Cement pastes with partial cement replacement by 20% of as received SCBA, 20% of quartz, and 0, 5, 10, 15 and 20% of silica fume were cast for this purpose. The results show that the as received SCBA has a low pozzolanic activity which is closer to crystalline SiO_2 (observed at the x-ray diffraction patterns between SCBA-pastes and quartz-pastes). Based on this finding, the authors suggest that the as received SCBA evaluated on this research should be used as an inert supplementary material.

7 DISCUSSION

In general, researchers suggest that a post-treatment such as sieving, grinding, recalcination or combination of them significantly influence the pozzolanic activity of the as received SCBA from the sugar mills. In some cases, the LOI content is reduced to less than 10% leading to beneficial effects when the ash is used as cement replacement in cement composites. [Chusilp 2009a] suggested that a SCBA with a LOI content lower than 10% by mass is a good pozzolanic material to partially replace, up to 20%, the Portland cement in concrete mixtures; they also reported that a high LOI content (more than 10% by mass) in the bagasse ash slightly affect the 28 and 90 days compressive strength of mortars. Another research [Somma et al. 2012] reported that the use of SCBA with a high LOI content (19.6%) is suitable to improve the mechanical properties and durability of recycled aggregate concrete; however in both studies the used SCBA was physically improved by a grinding process.

Additional research suggests that a sieving process is enough to remove some unburned carbon particles and unburned matter from the SCBA. In this case sieving contributes to enhance the pozzolanic activity of the as received SCBA from sugar mills when is used as partial cement replacement in cement composites even if the ash has a LOI content larger than 10% [Hernández 2010, Maldonado 2012, Bahurudeen 2015, Arenas 2016, Arif 2016]. As a summary, it can be stated that the sieving process is the lower energy demanding post-treatment in comparison with the grinding and recalcination processes and it appears to be a good environment friendly alternative for the use of the SCBA which is actually available in open damps.

On the other hand, some studies suggest that the unburned fibrous carbon particles of the SCBA are amorphous. This is because some carbon fibers are covered with a layer of Si and O and have a cell structure, with intercellular channels, containing pits in the cell walls [Batra 2008, Bahurudeen 2015]. Therefore, the potential use of as received SCBA as cement replacement could be a more environment friendly for a usual practice. However, research suggests that a low LOI content (less than 10%) does not assure an appropriate pozzolanic performance of the SCBA since the SiO_2 (the main compound in the SCBA) could be quite crystalline. For example [Soares 2016] used 20% of SCBA (as received from a sugar mill) with a low LOI content (1.52%) as partial cement

replacement in cement pastes; however, they found that the pozzolanic activity of the SCBA was similar to the pozzolanic activity obtained in cement pastes added with 20% of quartz. Another example is showed by [Arift 2016]. They found that the SCBA as received from a high-efficiency co-generation boiler (which has a LOI content of 7.15%, Tab. 1) does not show a proper pozzolanic activity in cement composites. This is because the ash has low amorphous silica content.

8 CONCLUSIONS

SCBA with a high LOI content must be subjected to a post-treatment in order to obtain an acceptable pozzolanic activity (more than the required by the strength activity index in the ASTM C618) and be used as a partial Portland cement replacement. Sieving appears to be a more environment friendly post-treatment process when compared to grinding and recalcination; however, long-term durability tests of composites prepared with this ash are needed to allow its use in large quantities.

The existing SCBA in open damps could have a high amount of unburned carbon due the poor controlled burning process of the bagasse in the boilers of sugar mills. Nonetheless, some unburned carbon particles could be amorphous increasing the reactivity of the ash. A detailed study about the amorphous phase of the unburned carbon particles of the SCBA is suggested.

It has been observed that the SCBA with high LOI content decrease the chloride diffusion coefficient of cement composites. There are a number of possible explanations about the interactions between the LOI content of the SCBA and chlorides. First, the unburned carbon could bond chlorides; second, the unburned carbon works only as a physical barrier for chlorides; and three, the unburned carbon particles are amorphous, as mentioned earlier, increasing the reactivity of the SCBA and hence improving the microstructure of the composites.

The use of SCBA with a high LOI content decreases the pH value of the alkaline reserve of cement composites. However, this value is higher than the critical pH value suggested in the literature to promote active corrosion of the steel embedded in the composites. A detailed study about the $Ca(OH)_2$ consumption during the pozzolanic reactions of the SCBA and its interaction with the high LOI content of the ash could be evaluated in further research.

9 ACKNOWLEDGMENTS

10 REFERENCES

[Arenas 2016] Arenas Piedrahita J.C.; Montes-García P.; Mendoza-Rangel J.M.; López-Calvo H.Z. et al.; Mechanical and durability properties of mortars prepared with untreated sugarcane bagasse ash and untreated fly ash. Construction and Building Materials 2016, 105, 69-81, ISSN: 0950-0618.

[Arif 2016] Arif Elisabeth; Clark Malcolm W.; Lake Neal; Sugar cane bagasse ash from a high efficient co-generation boiler: Applications in cement and mortar production. Construction and Building Materials 2016, 128, 287-297, ISSN: 0950-0618.

[Aprianti 2015] Aprianti Evi; Shafigh Payam; Bahri Syamsul; Farahani Javad Nodeh; Supplementary cementitious materials origin from agricultural wastes – A review. Construction and Building Materials 2015, 74, 176-787, ISSN: 0950-0618.

[Bahurudeen 2015] Bahurudeen A.; Santhanam Manu; Influence of different processing methods in the pozzolanic performance of sugarcane bagasse ash. Cement and Concrete Composites 2015, 56, 32-45, ISSN: 0958-9465.

[Batra 2008] Batra Vidya S.; Urbonaite Sigita; Svensson Gunnar; Characterization of unburned carbon in bagasse fly ash. Fuel 2008, 87, 2972-2976.

[CIF 2011] Cement Industry Federation (CIF). Sustainability Report 2011. www.cement.org.au

[Chiparus 2004] Chiparus Ovidio Iulius; Bagasse fiber for production of nonwoven materials (PhD Thesis). Lousiana State University and Agricultural and Mechanical College. USA. 2004.

[Chusilp 2009a] Chusilp N.; Jaturapitakkul C.; Kiattikomol K.; Effects of LOI of ground bagasse ash on the compressive strength and sulfate resistance of mortars. Construction and Building Materials 2009, 23, 3523-3531, ISSN: 0950-0618.

[Chusilp 2009b] Chusilp N,; Jaturapitakkul C.; Kiattikomol K.; Utilization of bagasse ash as a pozzolanic material in concrete. Construction and Building Materials 2009, 23, 3352-3358, ISSN: 0950-0618.

[Cordeiro 2016] Cordeiro G.C.; Tavares L.M.; Toledo Filho R.D.; Improved pozzolanic activity of sugar cane bagasse ash by selective grinding and classification. Cement and Concrete Research 2016, 89, 269-275, ISSN: 0008-8846.

[Cordeiro 2008] Codeiro G.C.; Toledo Fhilo R.D.; Tavares L.M.; Fairbairn E.M.R.; Pozzolanic activity and filler effect of sugar cane bagasse ash in Portland cement and lime mortars. Cement and Concrete Composites 2008, 30, 410-418, ISSN: 0958-9465.

[Cordeiro 2009a] Cordeiro G.C.; Toledo-Filho R.D.; Fairbairn E.M.R.; Effect of calcination temperature on the pozzolanic activity of sugar cane bagasse ash. Construction and Building Materials 2009, 23, 3301-3303, ISSN: 0950-0618.

[Cordeiro 2009b] Cordeiro G.C.; Toledo-Fhilo R.D.; Tavares L.M.; Fairbair E.M.R.; Ultrafine grinding of sugar cane bagasse ash for application as pozzolanic admixture in concrete. Cement and Concrete Research 2009, 39, 110-115, ISSN: 0008-8846.

[Cordeiro 2010] Cordeiro G.C.; Toledo Fhilo R.D.; Fairbairn E.M.R.; Ultrafine sugar cane bagasse ash: high potential pozzolanic material for tropical countries. IBRACON Structures and Materials Journal 2010, 3, 1, 50-67. ISSN: 1983-4195.

[Demis 2014] Demis S.; Tapali J.G.; Papadakis V.G.; An investigation of the effectiveness of the utilization of biomass ashes as pozzolanic materials. Construction

and Building Materials 2014, 68, 291-300, ISSN: 0950-0618.

[Frías 2013] Frías Rojas M.; Sánchez de Rojas Gómez M. I.; Eco-efficient concrete. Chapter 5: Artificial pozzolans in eco-efficient concrete. Woodhead Publishing Limited. 2013.

[Frías 2011] Frías M.; Villar E.; Svastano H.; Brazilian sugar cane bagasse ashes from the cogeneration industry as active pozzolans for cement manufacture. Cement and Concrete Composites 2011, 33, 490-496, ISSN: 0958-9465.

[Ganesan 2007] Ganesan K.; Rajagopal K.; Thangavel K.; Evaluation of bagasse ash as supplementary cementitious material. Cement and Concrete Composites 2007, 29, 515-524, ISSN: 0958-9465.

[Gani 2007] Gani Asri; Naruse Ichiro; Effect of cellulose and lignin content on pyrolysis and combustion characteristics for several types of biomass. Renewable Energy 2007, 32, 649-661, ISSN: 0960-1481.

[Haber 2013] Habert G; Eco-efficient concrete, Chapter 1:Environmental Impact of Portland cement production. First edition, Woodhead Publising Limited. 2013.

[Hernández 2010] Hernández Toledo Ur Iván; Efecto de una puzolana de desperdicion agrícola y el tiempo de curado en la corrosión del ferrocemento (MEng Thesis). Instituto Politécnico Nacional – CIIDIR Oaxaca. México, 2010. (In Spanish).

[Hendriks 2004] Hendriks C.A.; Worrell E.; de Jager D.; Blok K.; et al. Emission reduction of greenhouse gases from the cement industry. Greenhouse gas control technologies Conference paper-cement. 2004 www.ieagreen.org.uk.

[IEA 2017] IEA International Energy Agency. World Business Council for Sustainable Development, [on-line], Cement Technology Roadmap 2009, https://www.iea.org/publications/freepublications/publication/Cement.pdf [Accessed 10 January 2017]

[Jiménez 2013] Jiménez Quero V.G.; León-Martínez F.M.; Montes-García P.; Gaona-Tiburcio C. et al.; Influence of sugar-cane bagasse ash and fly ash on the rheological behaviour of cement pastes and mortar. Construction and Building Materials 2013, 40, 691-701, ISSN: 0950-0618.

[Madurwar 2013] Madurwar Mangesh V.; Ralegaonkar Rahul V.; Mandavgane Sachin A.; Application of agro-waste for sustainable construction materials: A review. Construction and Building Materials 2013, 38, 872-878, ISSN: 0950-0618.

[Maldonado 2012] Maldonado García Marco Antonio; Efecto de la adición de ceniza de bagazo de caña en la microestructura y durabilidad del ferrocemento (MEng Thesis). Instituto Politécnico Nacional – CIIDIR Oaxaca. México, 2012. (In Spanish).

[Maldonado 2016] Maldonado García M.A.; Montes García P.; Valdez Tamez P.L.; Estudio de la carbonatación de morteros adicionados con ceniza de bagazo de caña con alto contenido de PxC. VII Con greso Nacional ALCONPAT. Pachuca de Soto, Hidalgo, México. 302-310 (In spanish).

[Martirena 1998] Martirena Hernández J.F; Middendorf B.; Gehrke M.; Budelmann H.; Use of wastes of the sugar industry as pozzolana in lime-pozzolana binders: Study of the reaction. Cement and Concrete Research 1998, 28, 1525-1536, ISSN: 0008-8846.

[Montakarntiwong 2013] Montakarntiwong Kawee; Chusilp Nuntachai; Tangchirapat Weerachart; Jaturapitakkul Chai; Strengh and heat evolution of concretes containing bagasse ash from thermal power plants in sugar industry. Materials and Desing 2013, 49, 414-420, ISSN: 0264-1275.

[Morales 2009] Morales E.V.; Villar-Cociña E.; Frías M.; Santos S.F. et al.; Effects of calcining conditions on the microstructure of sugar cane waste ashes (SCWA): Influence in the pozzolanic activation. Cement and Concrete Composites 2009, 31, 22-28, ISSN: 0958-9465.

[Noor-ul 2011] Noor-ul Amin; Use of bagasse ash in concrete and its impact on the strength and chloride resistivity. Journal of Materials in Civil Engineering 2011, 717-720, ISSN: 0899-1561.

[Rerkpiboon 2015] Rerkpiboon Aukkadet; Tangchirapat Weerachart; Jaturapitakkul Chai; Strengh, chloride resistance, and expansion of concretes containing ground bagass ash. Construction and Building Materials 2015, 101, 983-989, ISSN: 0950-0618.

[Ribeiro 2014] Ribeiro Daniel Véras; Morelli Marcio Raymundo; Effect of calcination temperature on the pozzolanic activity of Brazilian sugar cane bagasse ash (SCBA). Materials Research 2014, 17,4, 974-981, ISSN: 1516-1439.

[Sanjuán 2001] Sanjuán R.; Anzaldo J.; Vargas J.; Turrado J. et al.; Morphological and chemical composition of pith and fibers from Mexican sugarcane bagasse. Holz als Rho-und Werkstoff 2001,59, 447-450

[Schneider 2011] Schneider M.; Romer M.; Tshudin M.; Bolio H; Sustainable cement production-present and future. Cement and Concrete Research 2011, 41, 642-650, ISSN: 0008-8846.

[Shafigh 2014] Shafigh Payam; Mahmud Hilmi Bin; Jumaat Mohd Zamin; Zargar Majid; Agricultural wastes as aggregated in concrete mixtures – A review. Conctruction and Building Materials 2014, 53, 110-117, ISSN: 0950-0618.

[Shi 2011] Shi Caijin; Fernández Jiménez A.; Palomo Angel; New cements for the 21st century: the pursuit of an alternative to Portland cement. Cement and Concrete Research 2011,41, 750-763, ISSN: 0008-8846.

[Soares 2016] Soares Marcela M.N.S.; García Dayana C.S.; Figueiredo Roberto B.; Aguilar María Teresa P. et al.; Comparing the pozzolanic behavior of sugar cane bagasse ash to amorphous and crystalline SiO$_2$. Cement and Concrete Composites 2016, 71, 20-25, ISSN: 0958-9465.

[Somma 2012] Somma Rattapon; Jaturapitakkul Chai; Rattanachu Pokpong; Chalee Wichian; Effect of ground bagasse ash on mechanical and durability properties of recycled aggregated concrete. Materials and Desing 2012, 36, 597-603, ISSN: 0264-1275.

[Torres 2014] Torres Agredo J.; Mejía de Gutiérrez R.; Escandon Giraldo C.E.; González Salcedo L.O.; Characterization of sugar cane bagasse ash as supplementary material for Portland cement. Ingeniería e Investigación 2014, 34, 5-10.

[Valencia 2012] Valencia G.; Mejía de Gutierrez R.; Barrera J.; Delvasto S.; Durability and corrosion study of reinforced blended mortars with tuff and sugar cane bagasse ash. Revista de la construcción 2012, 12, 1112-122. (In Spanish).

ICBBM& ECOGRAFI 2017

[Verma 2012] Verma D.; Gope P.C.; Maheshwari M.K.; Sharma R.K.; Bagasse fiber composites – A review. Journal of Materials and Environmental Science 2012, 3(6), 1079-1092. ISSN: 2028-2508.

[Varma 2016] Varma A.K., Mondal P.; Pyrolysis of sugarcane bagasse in semi bach reactor: Effects of process parameters on product yields and characterization of products. Ind. Crps Prod. (2016).

According to the literature review from this chapter, a sieving process was selected as treatment method for the SCBA used in this research. From now on, the term untreated sugarcane bagasse ash (UtSCBA) will be employed to refer to the sieved SCBA. The aims, hypotheses and the experimental design of the research are presented in the next paragraphs.

Aims of the research

The main objective of this thesis was to evaluate the effect of UtSCBA on the corrosion of reinforced cement-based mortars. For that purpose, five specific objectives were devised.

The specific objectives are:

1.- Evaluate the effect of the addition of UtSCBA on the microstructural and mechanical properties of cement-based mortars at long-term ages.

2.- Identify the corrosion initiation period of uncured reinforced mortar slabs added with UtSCBA when exposed to a simulated marine environment

3.- Analyse the corrosion risk of reinforced mortar slabs containing UtSCBA when exposed to a simulated marine environment.

4.- Estimate the corrosion damage of the reinforced mortar slabs containing UtSCBA when exposed to a simulated marine environment.

5.- Propose a corrosion mechanism of the mortar slabs added with UtSCBA after being exposed to a simulated marine environment.

Hypotheses

According to the specific objectives, the following hypotheses were considered in this research:

1.- The use of SCBA with a high loss on ignition content does not affect the microstructural, mechanical and durability properties of mortars.

2.- The addition of 10 and 20% of UtSCBA does not affect the microstructural and mechanical properties of mortars at long-term ages.

3.- The use of 10 and 20% of UtSCBA does not affect the corrosion initiation period of uncured reinforced mortars.

4.- The addition of 10 and 20% of UtSCBA does not affect the corrosion risk of reinforced mortars at long-term ages.

5.- The use of 10 and 20% of UtSCBA does not affect the corrosion damage of reinforced mortars at long-term ages.

The experimental design

The experimental design for the research consists in two factors with three levels each (3^2). The factors were the percentage of addition of UtSCBA and the increment of curing time. The chosen levels were 0, 10 and 20% of UtSCBA addition and 0, 7 and 28 days of curing time, respectively.

The percentages of addition of UtSCBA were chosen based on the literature review in which a cement replacement of up to 20% by pre-treated SCBA and UtSCBA does not affect the mechanical properties of mortars and concretes [Chusilp et al. 2009, Hernández 2010, Olibeira et al. 2010, Maldonado 2012, Valencia et al. 2012, Muangtong et al. 2013, Dhengare et al. 2015].

The different curing times were adopted from those proposed in the ASTM C 39 standard as these ages are considered important indicators of significant changes of the properties of cement-based composites.

CHAPTER THREE

The influence of untreated sugarcane bagasse ash on the microstructural and mechanical properties of mortars.

Maldonado-García M. A., Hernández-Toledo U. I. Montes-García P., Valdez-Tamez P. L. 2018.

Mater. Construcc. 68 [329], e148. https://doi.org/10.3989/mc.2018.13716.

The influence of untreated sugarcane bagasse ash on the microstructural and mechanical properties of mortars

M. A. Maldonado-García[a], U. I. Hernández-Toledo[a], P. Montes-García[a,✉], P. L. Valdez-Tamez[b]

a. Instituto Politécnico Nacional, CIIDIR-Oaxaca, (Oaxaca, México)
b. Universidad Autónoma de Nuevo León, FIC, (Nuevo León, México)
✉ pmontesgarcia@gmail.com, pmontes@ipn.mx

ABSTRACT: This study investigated the effects of the addition of untreated sugarcane bagasse ash (UtSCBA) on the microstructural and mechanical properties of mortars. The SCBA was sieved for only five minutes through a No. 200 ASTM mesh, and fully characterized by chemical composition analysis, laser ray diffraction, the physical absorption of gas, scanning electron microscopy (SEM) and X-ray diffraction (XRD) techniques. Mortar mixtures with 0, 10 and 20% UtSCBA as cement replacement and a constant 0.63 water/cementitious material ratio were prepared. Fresh properties of the mortars were obtained. The microstructural characteristics of the mortars at 1, 7, 28, 90 and 600 days were evaluated by SEM and XRD. The compressive strengths of the mortars at the same ages were then obtained. The results show that the addition of 10 and 20% UtSCBA caused a slight decrease in workability of the mortars but improved their microstructure, increasing the long-term compressive strength.

Keywords: Pozzolan, waste treatment, mortar, hydration products, compressive strength

RESUMEN: *Influencia de la ceniza de bagazo de caña sin tratamiento en la microestructura y propiedades mecánicas de morteros.* En esta investigación se evaluó el efecto de la adición de ceniza de bagazo de caña (CBC) en la microestructura de morteros. La CBC fue tamizada durante 5 minutos a través de la malla No. 200 ASTM y evaluada mediante pruebas de análisis químico, difracción láser, absorción física de gases, Microscopia Electrónica de Barrido (MEB) y Difracción de Rayos X (DRX). Se elaboraron mezclas de mortero con 0, 10 y 20% de CBC como sustituto parcial del cemento manteniendo una relación agua/materiales-cementantes de 0.63. Se realizaron pruebas en estado fresco y pruebas de caracterización microestructural a través de MEB y DRX y de resistencia a la compresión a edades de 1, 7, 28, 90 y 600 días. Los resultados muestran que la adición de 10 y 20% de CBC decrementa la trabajabilidad de los morteros, sin embargo, mejora su microestructura e incrementa su resistencia a la compresión a edades tardías.

Palabras clave: Puzolana, Tratamiento de residuos, Mortero, Productos de hidratación, Resistencia a la compresión

ORCID ID: M. A. Maldonado-García (http://orcid.org/0000-0002-9522-6779); U. I. Hernández-Toledo (http://orcid.org/0000-0001-9392-0487); P. Montes-García (http://orcid.org/0000-0003-3799-8372); P. L. Valdez-Tamez (http://orcid.org/0000-0002-1298-2051)

2 • M. A. Maldonado-García et al.

1. INTRODUCTION

Portland cement is used in concrete and is considered one of the most fundamental and widely produced materials for civic infrastructure projects around the world (1–4). Concrete is second to water in the total volume consumed per person, approximately three tons annually (3–4). However, cement production is a highly energy-intensive process. The manufacture of each ton of Portland cement emits approximately 0.8–1.0 ton of anthropogenic CO_2 (depending on the ratio of clinker to cement) into the atmosphere (1–2,5). This represents 3–5% of current global emissions (1–3), which contribute to consequential environmental damage.

As a remedial measure, pozzolanic materials are now used as a partial substitute for Portland cement in concrete. Numerous studies show that SCBA can be used as a pozzolanic material when it is burned at temperatures between 600 and 1000°C and subjected to post-treatment such as recalcination or grinding. Results indicate that such post-treatments change some of the physical characteristics and chemical composition of the SCBA, as well as improve the pozzolanic potential (6–12). A post-treatment leads to the formation of silica, alumina (7–9,13), and especially amorphous silica (6–7). These compounds react with calcium hydroxide (CH), released during the hydration of cement, to form additional cementitious compounds such as calcium silicate hydrate (C-S-H), thus improving the microstructural properties of concrete and mortar mixtures. This could lead to an improvement of some durability properties without having negatives effects on physical and mechanical properties (6–8,11,14–16).

As previously mentioned, most research has focused on the effect of post-treatments of the SCBA in order to improve its potential activity and mechanical properties when used as a pozzolan in mortar and concrete; nevertheless, such treatments demand high levels of energy and contribute, once again, to generating contaminants. SCBA is a by-product widely available in Mexico. According to Mexico's Union Nacional de Cañeros (National Union of Sugarcane Producers) (17), approximately 54 million tons of sugarcane are produced annually, from which some 15 million tons of bagasse are obtained. Akram et al. (18) reported that each ton of sugarcane produces approximately 0.62% of residual ash. This suggests that in Mexico approximately 0.34 million tons of SCBA are produced every year, which are mainly deposited in open garbage dumps, causing significant disposal problems and pollution.

Taking these last observations into consideration, it was decided that in this study the SCBA would be used practically as received from the sugar mill (subjected only to sieving, a low energy post-treatment) as a partial replacement for Portland cement. Our proposal was to evaluate the mechanical properties and the microstructure of mortars made with relatively untreated bagasse ash.

2. EXPERIMENTAL

2.1. Selection of a low-energy post-treatment method for the "as received" SCBA

The SCBA was collected from a sugar mill located in the community of Tezonapa, Veracruz, México. This ash is generated as a combustion by-product of sugarcane bagasse at temperatures between 550 and 700°C and recovered by sprinkling water during the sugar production. The collected ash was homogenized and dried for 24 hours in an electric oven at 105°C.

In order to select the SCBA to be used in subsequent phases of this research, its pozzolanic potential was estimated at 7, 14 and 28 days after the ash was subjected to two low-energy post-treatments. The first post-treatment consisted of sieving the SCBA for five minutes through No. 8 (2.36 mm), No. 100 (150 μm) and No. 200 (75 μm) ASTM sieves (SCBA8, SCBA100 and SCBA200). The fractions removed in the sieving process were 0, 20 y 30% for the No. 8 (2.36 mm), No. 100 (150 μm) and No. 200 (75 μm) sieves, respectively.

The second post-treatment consisted of sieving through the same sieves for the same period of time followed by two hours of grinding (SCBA8g, SCBA100g and SCBA200g). Sieving was carried out to reduce the particle size and to remove organic material, and posterior grinding was done solely to increase the specific surface area of the SCBA (7, 9,12,19–21). Ordinary Portland Cement CPO 40 Lafarge®, SCBA from each post-treatment (at 20% cement replacement), standard silica sand and distilled water were used to prepare mortar cubes in order to obtain the strength activity indexes (SAI) (ASTM C 311) of the six post-treated SCBAs. A mortar mixture (FA20) containing 20% Admix Tech® Class F Fly Ash (FA) was prepared as a reference; the FA meets the requirements described in the ASTM C 618 standard.

Originally, water/cement or cementitious materials and sand/cement ratios of 0.484 and 2.75 were used to prepare the mortars in accordance with the ASTM C 311. However, a water/cement ratio of 0.57 for the control mortar and a water/cementitious material ratio of 0.68 for mortars containing 20% SCBA were necessary to keep the sand/cementitious material ratio of 2.75 (ASTM C 311) and to fulfill the mortars' flow of 110±5% (ASTM C 1437). A water/cementitious material ratio of 0.56 was used for the mortar containing 20% FA to keep the same sand/cement ratio and as well fulfill the mortars' flow requirements. No superplasticizer was used in these experiments.

2.2. Selection of the SCBA used for preparation of the mortars

SAIs for sieved and ground SCBAs and for the FA estimated at 7, 14 and 28 days are presented in Figure 1. In accordance with the literature, the SAI value increases when the particle size of the SCBA decreases as a result of sieving or grinding; the SAI also increases with age as a consequence of the pozzolanic reaction (7–9,12,21).

Most mixtures had 28-day compressive strength values higher than 75% of the control mixture specified by the ASTM C 618 (this percentage was considered as a reference point for the analysis since the ASTM C 618 accounts for the various materials from natural resources requiring calcination to induce satisfactory properties). The only value smaller than 75% was for the mortar containing the material that passed the No. 8 sieve (SCBA8).

Poor performance of grinding SCBA after passing through the No. 8 and 100 sieves is supported by the fact that the wider sieves allow the passage of larger carbon particles, while a posterior grinding is not effective in increasing the SAI, as carbon particles are ground together along with particles rich in silica and alumina.

The mixture with 20% FA (FA20) yielded the highest SAIs at the studied ages (98, 95 and 104% at 7, 14 and 28 days respectively) followed by the mixture with the combination of sieved plus ground SCBA (SCBA200g) (90, 87 and 95 at 7, 14 and 28 days respectively), and then only sieved SCBA (SCBA200) (85, 91 and 92% at 7, 14 and 28 days respectively). As may be observed, the difference between SCBA200g and SCBA200 was not significant.

Based on the above information, it was decided to use only SCBA sieved through sieve No. 200 (75 µm) (SCBA200) for the remaining stages of the present research. The SAI at the three ages of the selected SCBA was more than 75%; therefore, this material can be considered a natural pozzolan, in accordance with the ASTM C 618.

2.3. Characterization of materials

From analyzing the results of the previous section, SCBA200, the material in which the post-treatment consisted of sieving it only through the No. 200 (75 µm) sieve for five minutes, was selected as the study subject for the following phase of this research. For brevity SCBA200 will be further designated only as UtSCBA (Untreated Sugarcane Bagasses Ash).

Blended Portland Cement 30R Holcim Apasco® (CPC) (approximately 5% ground granulated blast furnace slag), which is readily available in southwestern México, was chosen as the cementing material.

Chemical composition, particle size distribution (PSD), density (ASTM C 188) and specific surface area (SSA) of the CPC and UtSCBA were obtained. The PSDs were obtained by wet method (via isopropyl alcohol) using a laser analyzer Microtrac S3500®; shape particles and refractive indices of 1.70 and 1.54 for CPC and UtSCBA were considered respectively. The SSAs were obtained by physical adsorption of nitrogen using a Quantachrome Nova 2000e® analyzer; the BET method was used for the analysis. The morphology and mineralogical phases of the UtSCBA were analyzed by SEM and XRD, respectively. The morphology of the materials was observed using a scanning electron microscope
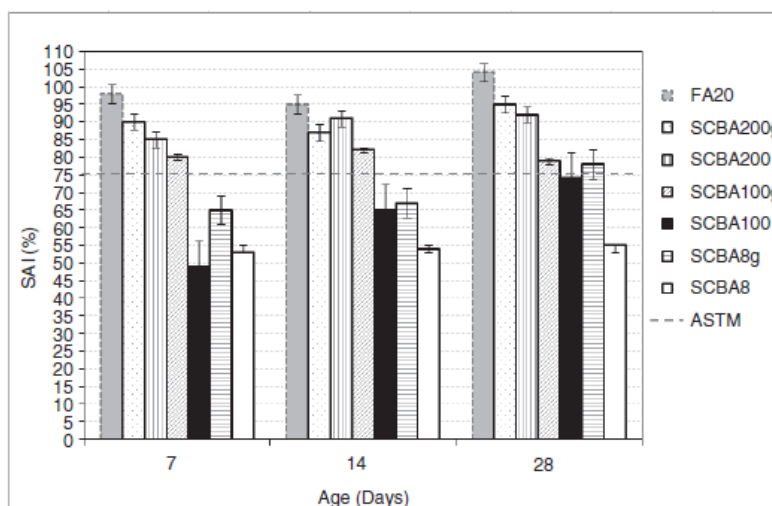

FIGURE 1. SAIs at 7, 14 and 28 days for samples with 20% sieved and ground SCBA.

4 • M. A. Maldonado-García et al.

JEOL JSM-6490LV® equipped with an X-ray scattering analyzer (EDS) from Oxford Instruments 7573®. Mineralogical phases were identified using a diffractometer Bruker D8 Advance®, which uses radiation of CuK and a wavelength of 1.5418Å to a passage of 0.05° and a time of incidence of 0.5 seconds per step, maintaining an interval 2θ from 10° to 70°.

2.4. Mixture proportioning and preparation of the mortars

UtSCBA, river sand (with a density of 2.7g/cm^3 and a fineness modulus of 2.45 (ASTM C 33), distilled water and a high-range water reducer (HRWR), Plastol 4000® (ml per kg of cementitious materials), were used to prepare the mortars. All mortars had a 0.63 water/cementitious material, a 1:3 cementitious material to sand ratio, and were prepared replacing 0, 10 and 20% of the weight of cement by UtSCBA (Control, UtSCBA10 and UtSCBA20 mixtures, respectively) (Table 1).

Flow table (ASTM C1437), temperature (ASTM C1064/C1064M), volumetric weight (ASTM C138/C138M) and air content (ASTM C231) tests of the mortars were carried out. Cylindrical specimens with a diameter of 75 mm and a height of 150 mm were prepared to study the microstructure and obtain the compressive strength. All specimens were cast in two layers and compacted using a vibrating table. Only the mixtures with an addition of UtSCBA required HRWR to maintain the workability. Specimens were cured in a 3% calcium hydroxide solution until the time of the test.

2.5. Mortar test methods

The morphology of gold-palladium-covered mortar samples at 1, 7, 28, 90 and 600 days were analyzed using a scanning electron microscope JEOL JSM-6490LV®. The mineralogical phases of mortar samples ground and sieved through a 150 µm mesh (ASTM) at 1, 7, 28, 90 and 600 days were identified by XRD using a diffractometer Bruker D8 Advance® and were analyzed by the software EVA version 11.0.0.3®. The compressive strengths (ASTM C 39/C39M) at 1, 7, 28, 56, 90, and 450 days were obtained by using a hydraulic press ELVEC E 659®. The compressive strength at 600 days was obtained from small mortar cubes (50 x 50 x 50 mm). These cubes were obtained from cylinders used during the microstructural evaluation. The results from the cubes were corrected by size and shape. For this purpose, the conversion factors for size and shape for normal-strength concrete proposed by Seong-Tae et al. (22) were implemented.

3. RESULTS AND DISCUSSION

3.1. Chemical and physical properties of the selected UtSCBA

Chemical analysis of the selected UtSCBA (Table 2) shows that the sum of major oxides ($SiO_2 + Al_2O_3 + Fe_2O_3 = 76\%$) is slightly larger than 70% of the overall material composition (ASTM C 618); this result along with the SAI estimate corroborates the pozzolanic activity of the UtSCBA despite the high loss on ignition (LOI) content.

The analysis of the physical characteristics shows that the UtSCBA has lower density, greater mean PSD and larger SSA than the CPC (Table 3).

Figure 2a shows the PSDs for CPC and UtSCBA. It can be observed that the UtSCBA has a PSD between 3.8 and 250 µm and CPC between 0.7 and 400 µm. The results indicate that UtSCBA has larger size particles when compared to CPC.

A detailed analysis of the PSD of these materials can be done analyzing their density distributions (Figure 2b). UtSCBA shows a monodisperse distribution, which can be associated with a sieved material (23). On the other hand, it can be observed that for the CPC the PSD shows two particle populations (bimodal) at 7 and 30 µm. This type of distribution

TABLE 1. Proportions of mortar mixtures (kg/m^3)

Mixture	Cement, kg	UtSCBA, kg	Water, kg	Sand, kg	HRWR, mL/kg of cementitious materials
Control	465.0	0	293.0	1395.0	0
UtSCBA10	418.5	46.5	293.0	1395.0	2.0
UtSCBA20	372.0	93.0	293.0	1395.0	6.5

HRWR: high range water reducer.

TABLE 2. Chemical composition of materials used in mortars (% by mass)

Material	SiO$_2$	Al$_2$O$_3$	Fe$_2$O$_3$	CaO	P$_2$O$_5$	Na$_2$O	K$_2$O	MgO	LOI
CPC	23.86	5.77	2.19	50.76	0.12	0.91	0.92	1.36	6.97
UtSCBA	56.37	14.61	5.04	2.36	0.85	1.57	3.29	1.43	10.53

LOI: Loss on ignition.

TABLE 3. Physical characteristics of materials

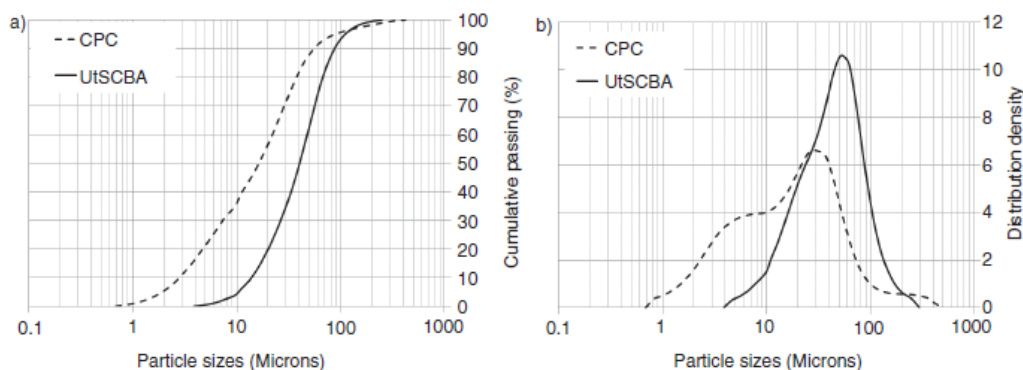| Material	Density (g/cm³)	D_{10} (μm)	D_{50} (μm)	D_{90} (μm)	BET specific surface area (m²/g)	Retained in the mesh 325 ASTM (%)
CPC	2.94	2.9	16.3	55.2	3.6	-
UtSCBA	2.19	13.9	40.3	87.3	42.3	60

FIGURE 2. Particle-size distribution of materials.

can be caused by two factors: the presence of particles from the different mineralogical components because a compound cement was used (13), and the result of grinding because fine particles tend to cluster (7).

The UtSCBA show grains of varied shapes and sizes in accordance with the calcination conditions (Figure 3) (12,24). There are agglomerated particles with high porosity, typical for organic materials, and prismatic particles with well-defined edges (9,25–26).The EDS microanalysis revealed that the agglomerated particles (A) are rich in Si, Al and C oxides and not so rich in Ca oxides (8). The prismatic particles (B) are constituted mostly by Si. Furthermore, spherical (C) and fibrous carbon particles (unburned carbon) (D) were observed. The spherical particles are rich in Ca and Si oxides as well as Al and Fe, and the fibrous particles contain mainly Si and Al. In this respect, recent studies (27) found that some fibrous carbon particles from SCBA may be covered by Si and O depending on the pyrolysis of the bagasse, affirming that the unburned carbon can present amorphicity.

In summary, the high LOI, lower density, greater PSD, larger SSA (in comparison with CPC), simultaneous appearance of amorphous and crystalline phases, and variability of the the UtSCBA's shapes and sizes can be attributed to the variations of temperature and air flow during the bagasse's calcination process in the sugar mill, in accordance with results observed by other authors (24).

The results of the XRD mineralogical analyses show that the CPC (Figure 4a) contains mainly di-calcium and tri-calcium silicate, tri-calcium aluminate and tetra-calcium aluminoferrite, and to a lesser extent calcium oxide, calcium carbonate and gypsum. The results of the XRD mineralogical analyses (Figure 4b) show that the UtSCBA exhibited amorphous and crystalline phases. The amorphous phase in the UtSCBA was observed as a diffuse halo in the interval 2θ from 10° to 35°. This halo, which is characteristic of pozzolanic materials, suggests the presence of amorphous substances such as silica (6,8,15,24,28–29). The crystalline phases of quartz and cristobalite in the UtSCBA were detected; both phases have been reported by others (6, 25, 29). Also gibbsite (Al_2O_3), hematite (Fe_2O_3) and calcium (Ca) phases were identified, and the residual carbon (C) phase in the UtSCBA, commonly attributed to the bagasse's LOIs (8,13), was detected at 2θ of 22.8° and 26.6°. However, the identification of carbon in the crystalline phase was little reliable due to the small quantity as well as the overlapping observed in the signal.

3.2. Properties in fresh state of mortars

Mortars prepared with UtSCBA presented workability problems which were overcome with a superplasticizer, as previously demonstrated in the section on the proportioning of the mortar mixture. The high LOI content, an indication of the high level of unburned carbon particles, can be blamed for this. Chandara et al. (30) mentioned that high levels of unburned carbon particles increase the requirement
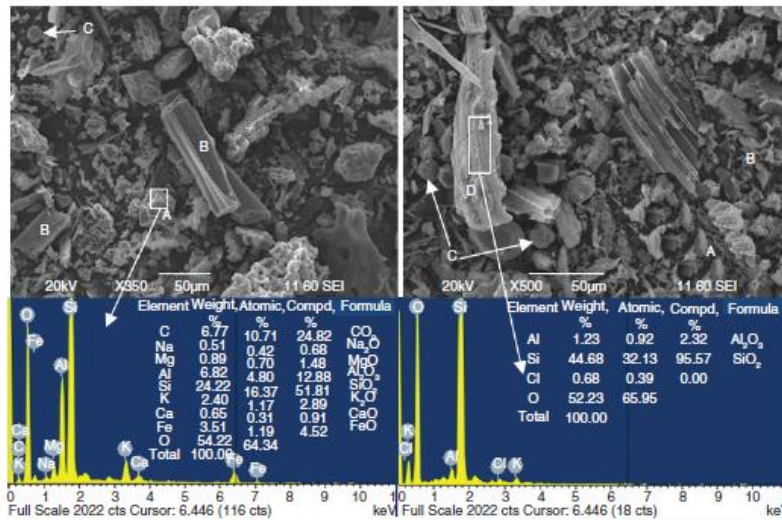
6 • M. A. Maldonado-García et al.

FIGURE 3.   SEM micrographs and elemental analysis of the UtSCBA used in the present study.
A is an agglomerated particle, B a prismatic, C a spherical, and D a fibrous.
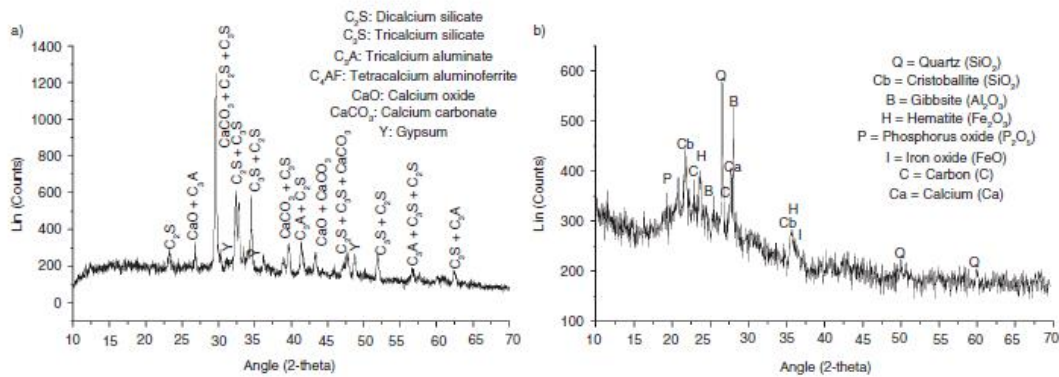

FIGURE 4.   XRD diagrams for the a) CPC and the b) UtSCBA used in the present study.

for water, and Jiménez-Quero et al. (31) reported that the variety of shapes of sieved UtSCBA particles can reduce the flow of the mortar mixtures since these particles can increase friction during the mixing process.

Mortar with 20% UtSCBA was less dense than the other mortars (Table 4). This was expected, as UtSCBA is a porous material with a lower density, greater mean PSD, and larger SSA than CPC.

3.3. Microstructure of mortars

The micrograph of the control mortar at day 1 shows a heterogeneous matrix. The phases of C-S-H and CH created from the Portland cement hydration were found to be in the majority of the cementitious products (32–33). At 1 and 7 days,

unhydrated particles of cement and particles with layers of hydration products were observed (Figures 5a and 5b) (32–34). Moreover, discontinuities in the interphase aggregate-cementitious paste were observed (Figure 5a) at day 1. At 28, 90 and 600 days the matrix of the mortars was denser (Figures 5c, 5d and 5e); nevertheless, porous zones with cementitious materials and cement particles were still observed.

Similarly to the control mortar, micrographs of mortars containing 10 and 20% UtSCBA taken at day 1 (Figures 6a and 7a) show some cement particles, unreacted particles of UtSCBA and some cementitious products on the surface of the UtSCBA particles. The EDS microanalyses (Figure 6a) show the different elements on the surface of a prismatic particle of UtSCBA. In UtSCBA mortars it

TABLE 4.   Fresh properties of mortars

Mixture	Flow (%)	Temperature (°C)	Volumetric weight (Kg/m³)	Air content (%)
Control	118	22.5	2100	2.80
UtSCBA10	104	20.3	2096	2.65
UtSCBA20	105	20.2	2072	3.4
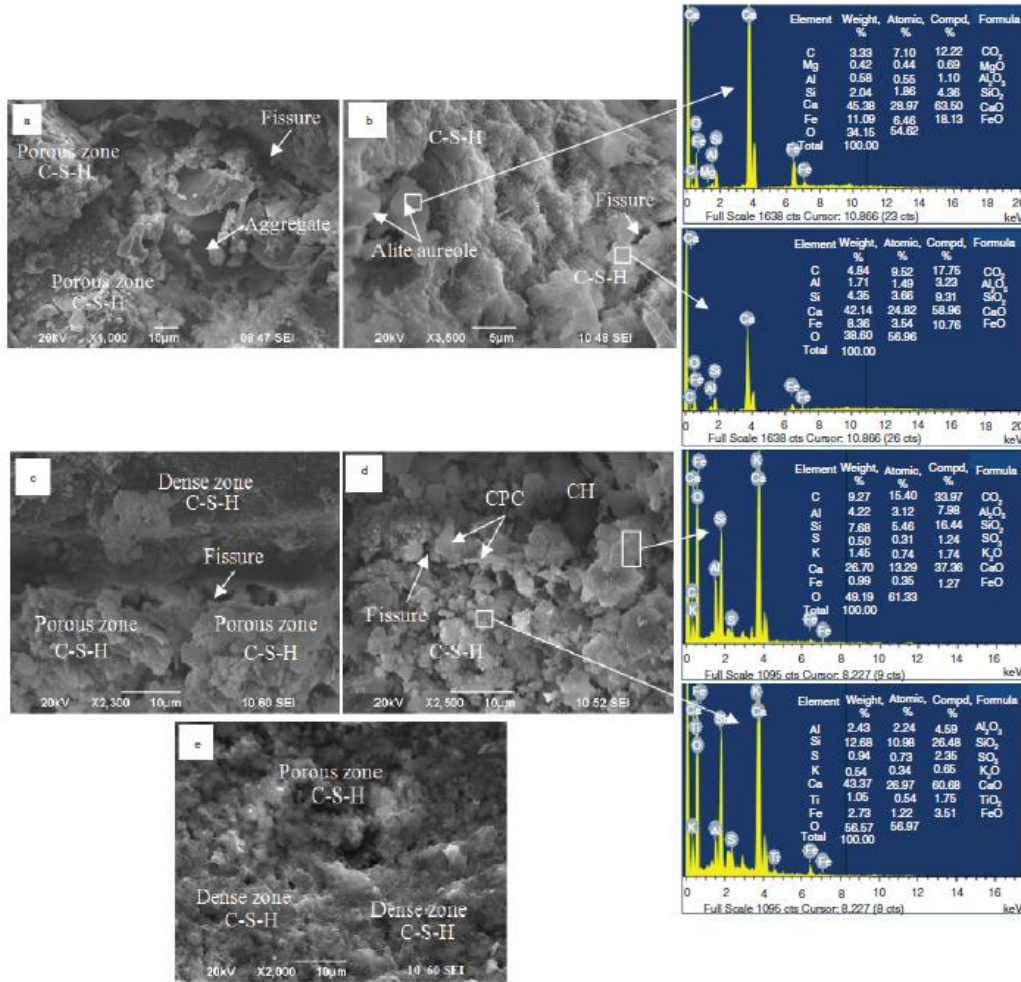
FIGURE 5.   SEM observations of control mortar at A) 1, B) 7, C) 28, D) 90 and E) 600 days of age.

was observed that as time passes, the cementitious matrixes were denser than the control mortar. The same effect was found by Govindarajen et al. (35) in cement pastes with 10% SCBA evaluated at 7 and 28 days, and in concrete when up to 30% SCBA was added and evaluated until 180 days of age (36).

The information mentioned above supports the occurrence of pozzolanic reactions as a consequence of the CH consumption and the formation of C-S-H and calcium-aluminum silicate hydrate (C-A-S-H) (Figures 6b, 6c, 6d, 6e, 7b, 7c, 7d and 7e) improving in this way compressive strength at later ages. However, at 90 days unreacted prismatic particles of UtSCBA were observed (Figure 6d) in the UtSCBA10 mortar; these particles were the largest in size and could improve the cementitious matrix

8 • M. A. Maldonado-García et al.
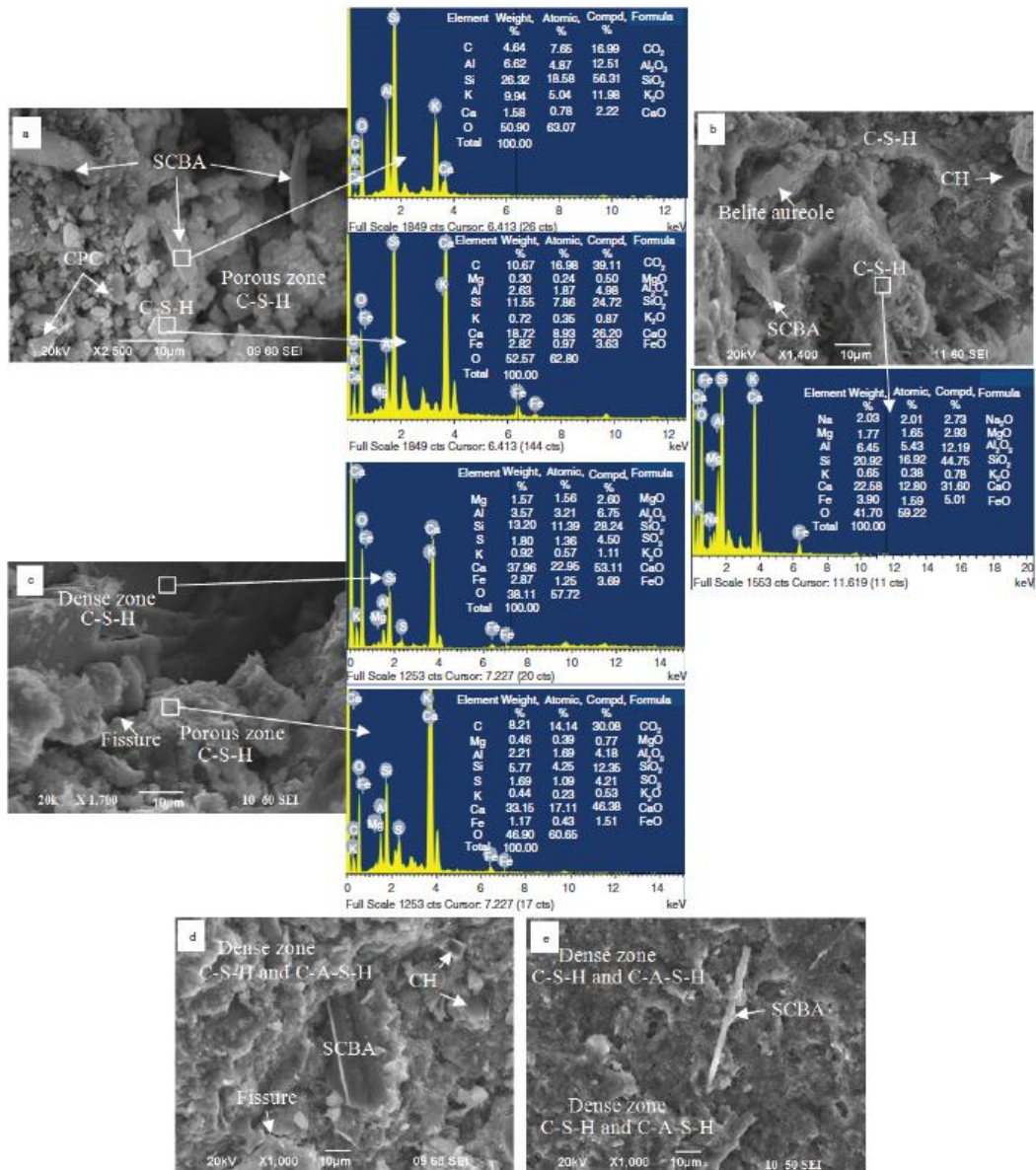
FIGURE 6. SEM observations of UtSCBA10 mortar at A) 1, B) 7, C) 28, D) 90 and E) 600 days of age.

at later stages. Finally, at 600 days it can be seen as a compacted matrix in both UtSCBA mortars when compared to earlier ages.

3.4. Mineralogical composition of mortars

The XRD patterns of the control mortar (Figure 8) show that the C-S-H ($4CaO.5SiO_2.5H_2O$) and CH ($Ca(OH)_2$) were the main mineralogical phases formed; both phases were produced during the Portland cement hydration. At day 1 the phase of calcium silicate ($CaSiO_3$), attributed to unhydrated particles in the cement, was detected; at later ages the intensity of the peaks of this phase decreased. At 28, 90 and 600 days a phase of C-S-H with different stoichiometry ($CaSiO_3.H_2O$) and the phase of C-A-S-H ($CaAl_2Si_3O_{10}.6H_2O$) were detected. The appearance of two or more phases of C-S-H is known and
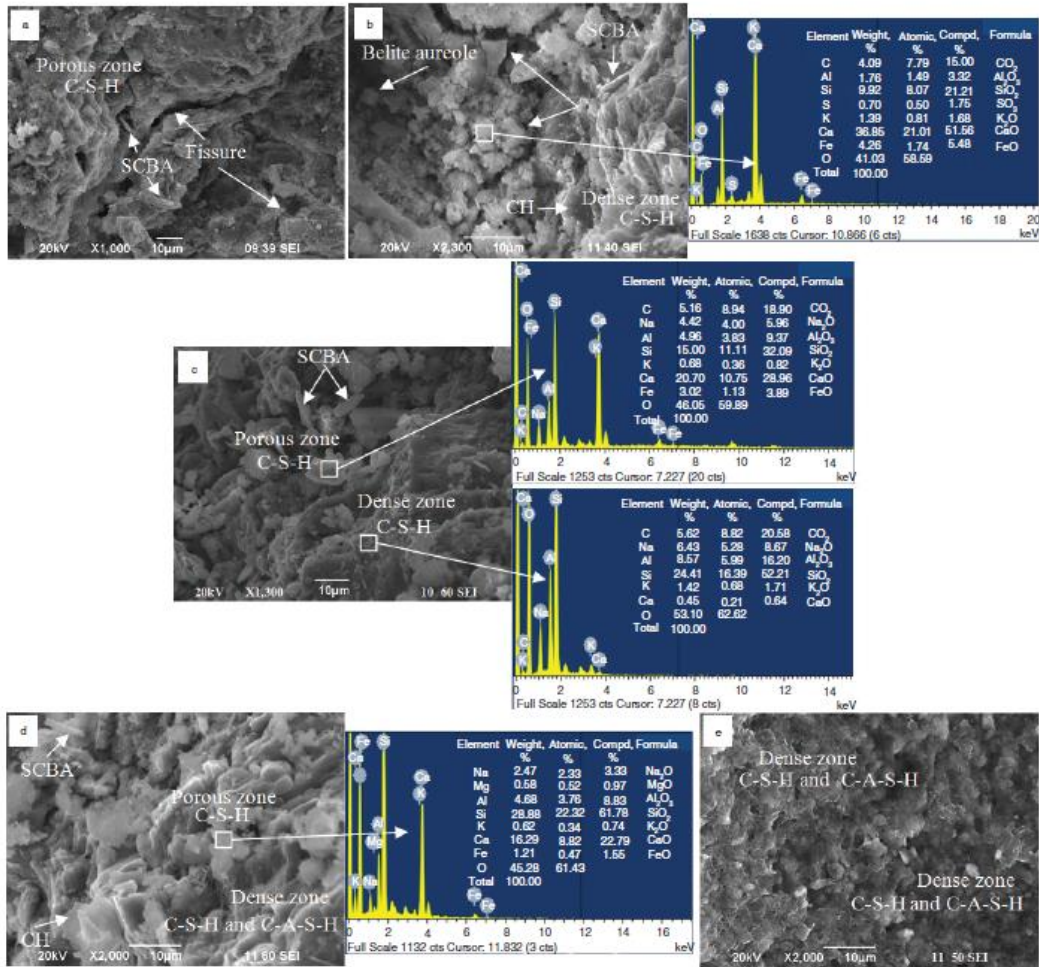
FIGURE 7. SEM observations of UtSCBA20 mortar at A) 1, B) 7, C) 28, D) 90, and E) 600 days of age.

reported by other authors (32, 37–38). The C-A-S-H is a product formed after activation of the aluminate and silicate phases in the presence of CH and could improve the microstructure and increase the durability of mortars (38). Other phases like quartz (SiO_2) and anorthite attributed to the sand, and Calcite ($CaCO_3$) attributed to the CPC, were also detected.

The XRD patterns of the UtSCBA10 and UtSCBA20 mortars (Figures 9 and 10) show the increase of the peak intensities of the C-S-H and C-A-S-H phases on the mortars as age progressed. Both products were created as the result of pozzolanic reactions between the UtSCBA, CH and water; this observation is supported by the decreased intensity of the CH phase and the increase of the C-S-H phase in comparison to the control mortar, as observed at 28, 90 and 600 days. The consumption of CH and the increase of the C-S-H in lime and cement pastes with the addition of SCBA at ages between 3 and 28 days has been reported (25,35).

In the present research, when 10% of cement is replaced by UtSCBA a pozzolanic reaction occurs and CH still remains in the matrix until the active material in the pozzolan is depleted. When 20% cement is replaced by UtSCBA, the CH is once again consumed but at a slower rate than for 10% UtSCBA. In this mixture there is a larger amount of silica present but also a larger amount of carbon, and carbon can be blamed for significantly inhibiting the pozzolanic reaction (25). When 20% UtSCBA is incorporated there is still a considerable amount of CH because only a very large replacement of cement by a pozzolan depletes the CH content. For example, when more than 50% FA is used to replace cement the CH is totally consumed (39).
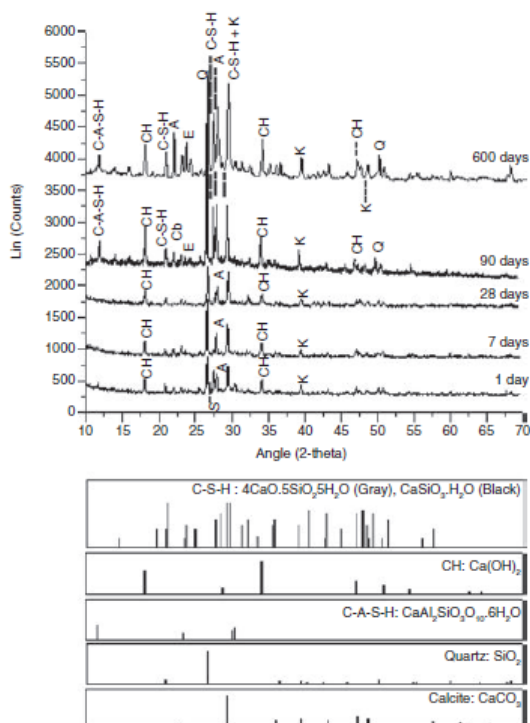
10 • M. A. Maldonado-García et al.

FIGURE 8. XRD patterns of control mortar at 1, 7, 28, 90 and 600 days of age. C-S-H: calcium silicate hydroxide; CH: calcium hydroxide; C-A-S-H: calcium aluminum silicate hydrate; Q: quartz, K: calcite; E: ettringite; A: anorthite; S: calcium silicate; and Cb: cristobalite.
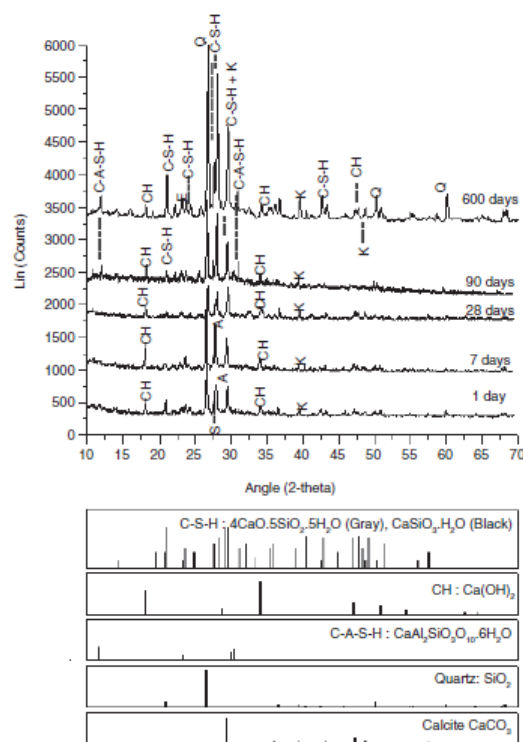

FIGURE 9. XRD patterns of UtSCBA10 mortar at 1, 7, 28, 90 and 600 days of age. C-S-H: calcium silicate hydroxide; CH: calcium hydroxide; C-A-S-H: calcium aluminum silicate hydrate; Q: quartz; K: calcite; E: ettringite; A: anorthite; and S: calcium silicate.

The above mentioned information and the physical characteristics of the UtSCBA explain the increase in the compressive strength of mortars with the addition of UtSCBA at later ages.

Moreover, the phase of cristobalite showed variations at different ages. These variations can be attributed to the disordered structures or its metastable state, which could improve pozzolanicity (40–41).

3.5. Compressive strength of mortars

Compressive strength of the mortar mixtures containing UtSCBA increased over time. The addition of 10 and 20% UtSCBA (UtSCBA10 and UtSCBA20) increased the strength at 28, 56, 90, 450 and 600 days when compared to the control mortar (Figure 11). However, the beneficial effect on the strength when adding UtSCBA was noted only after 28 days. The same effect was observed by other authors when ground SCBA was used in concrete mixtures (36).

Moreover, it was observed that when the content of UtSCBA increased from 10 to 20%, the compressive strength at 1, 7, 28, 56 and 90 days decreased between 7 and 12%. Chusilp et al. (11) reported this effect in mortars with ground bagasse ash and 10% LOI (similar to the LOI obtained in this research). In contrast, compressive strength results at 450 and 600 days show that when the content of UtSCBA increased from 10 to 20% in mortars mixtures, a slight increase in strength occurred. Results show that the addition of 20% UtSCBA increased the compressive strength by 10.6% and 11.2% at 450 and 600 days respectively compared with the compressive strength at 90 days, while the mortar with addition of 10% UtSCBA remains practically constant at 90, 450 and 600 days. In this respect, Chusilp et al. (16) reported a similar behavior using 10 and 20% ground SCBA (95% of the ash passing the No. 325 sieve and LOI of 8.16%) in concrete mixtures at 28 and 90 days, in which the compressive strength of the concrete with the addition of 20% SCBA was greater than that of the concrete with the addition of 10% SCBA.

The above mentioned could be attributed to the fact that after 90 days the UtSCBA20 mortar has

The influence of untreated sugarcane bagasse ash on the microstructural and mechanical properties of mortars • 11
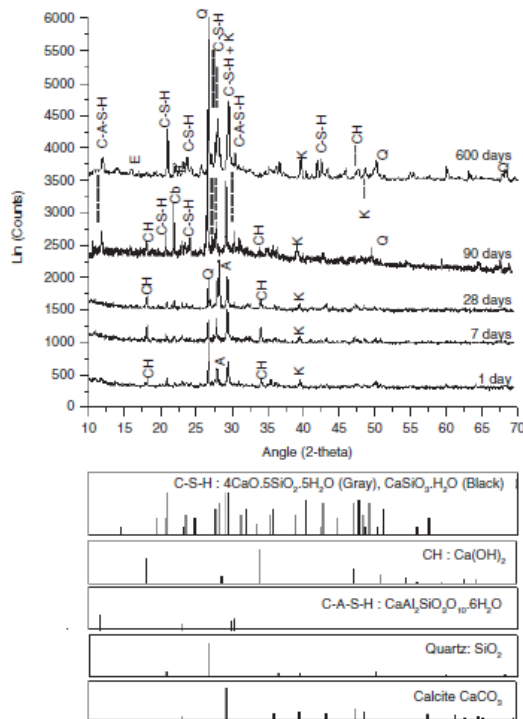

FIGURE 10. XRD patterns of UtSCBA20 mortar at 1, 7, 28, 90 and 600 days of age. C-S-H: calcium silicate hydroxide; CH: calcium hydroxide; C-A-S-H: calcium aluminum silicate hydrate; Q: quartz; K: calcite; E: ettringite; A: anorthite; and Cb: cristobalite.
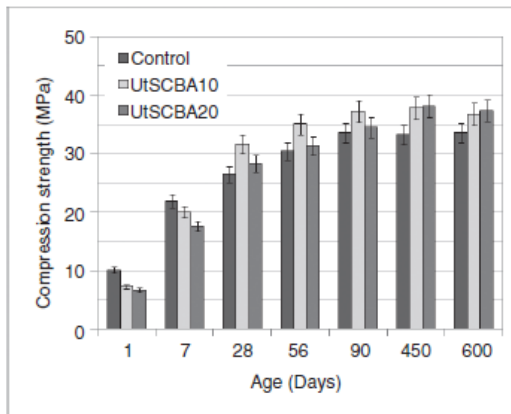

FIGURE 11. Compressive strength of mortars.

more unreacted UtSCBA, which improves the pozzolanic activity in comparison with the UtSCBA10 mortar. Likewise, the large fibrous-porous particles of UtSCBA (which are covered with a layer of Si and O), as well as the small particles, increase the specific surface area for the pozzolanic activity; consequently there is a gain in strength when 20% UtSCBA is added to the mortar.

The results indicate that, despite using a basically untreated SCBA as a cement replacement for preparing mortars, ash like this helps improve the long-term compressive strength and the microstructure of such mortars.

4. CONCLUSIONS

Based on the analysis of results, the following conclusions can be drawn:

- The SAIs results show that, for this research, the sieving of the "as received SCBA" through the No. 200 (75 μm) mesh (ASTM) is an optimal treatment with minimum energy requirements in comparison to other treatments such as grinding or sieving plus grinding. This treatment leads to a good pozzolanic performance of the "as received" SCBA due to the removal of large unburnt carbon particles and the reduction of particle size.
- Results of XRD show that the UtSCBA (sieved through the 75 μm ASTM mesh) is a good pozzolanic material due to the presence of amorphous phases observed in the interval 2θ from 10° to 35°. Likewise, the micrographs of the UtSCBA suggest that the fibrous carbon particles can react since they have a layer of Si and O on their surfaces.
- Compressive strength results show that the additions of 10 and 20% UtSCBA increase the strength of mortars at ages between 28 and 600 days. Furthermore, results show that the compressive strength of the mortar with 10% UtSCBA is greater than the mortar with 20% UtSCBA at ages of 1, 7, 28, 56 and 90 days. This was reversed at 450 and 600 days. This suggests that the optimum fraction of UtSCBA replacing cement in mortars is 10% by weight of cement.
- Results indicate that the addition of 10 and 20% UtSCBA significantly improved the microstructure of the mortars by the refinement of pore structure and a denser matrix in comparison to the control mortar, especially at 28, 90 and 600 days, despite the large particle-size distribution, porous particles and high LOI presented in the UtSCBA.
- Results in the compressive strength and microstructural evaluations at long-term ages show that the use of 10 and 20% UtSCBA as a replacement for cement might improve the durability of mortars. In this respect, long-term durability studies using UtSCBA have been addressed in ongoing research.

12 • M. A. Maldonado-García et al.

REFERENCES

1. Worrell, E.; Price, L.; Martín, N.; Hendriks, C.; Ozawa, M.L. (2001) Carbon dioxide emissions from the global cement industry. Annu. Rev. Energy Environ. 26, 303–329. https://doi.org/10.1146/annurev.energy.26.1.303
2. Hendriks, C.A.; Worrell, E.; de Jager, D.; Blok, K.; Riemer, P. (2004) Emission reduction of greenhouse gases from the cement industry. Greenhouse gas control technologies Conference paper-cement. www.ieagreen.org.uk
3. International Energy Agency (IEA). Carbon emissions reduction up to 2050. World Business Council for Sustainable Development. Cement Technology Roadmap 2009. https://www.iea.org/publications/freepublications/publication/Cement.pdf
4. Cement Industry Federation (CIF). Sustainability Report 2011. www.cement.org.au
5. Josa, A.; Aguado, A.; Cardim, A.; Byars, E. (2007) Comparative analysis of the cycle impact assessment of available cement inventories in the EU. Cem. Concr. Res. 37 [5], 781–788. https://doi.org/10.1016/j.cemconres.2007.02.004
6. Ganesan, K.; Rajagopal, K.; Thangavel, K. (2007) Evaluation of bagasse ash supplementary cementitious material. Cem. Concr. Comp. 29 [6], 515–524. https://doi.org/10.1016/j.cemconcomp.2007.03.001
7. Cordeiro, G.C.; Toledo-Filho, R.D.; Tavares, L.M.; Fairbairn, E.M.R. (2008) Pozzolanic activity and filler effect of sugar cane bagasse ash in Portland cement and lime mortars. Cem. Concr. Comp. 30 [5], 410–418. https://doi.org/10.1016/j.cemconcomp.2008.01.001
8. Morales, E.V.; Villar-Cociña, E.; Frías, M.; Santos, S.F.; Savastano, J.R.H. (2009) Effects of calcining conditions on the microstructure of sugar cane waste ashes (SCWA): Influence in the pozzolanic activation. Cem. Concr. Comp. 31 [1], 22–28. https://doi.org/10.1016/j.cemconcomp.2008.10.004
9. Cordeiro, G.C.; Toledo-Filho, R.D.; Fairbairn, E.M.R. (2009)a Effect of calcination temperature on the pozzolanic activity of sugar cane bagasse ash. Construct. Build. Mat. 23 [10], 3301–3303. https://doi.org/10.1016/j.conbuildmat.2009.02.013
10. Cordeiro, G.C.; Toledo-Fhilo, R.D.; Tavares, L.M.; Fairbair, E.M.R. (2009)b Ultrafine grinding of sugar cane bagasse ash for application as pozzolanic admixture in concrete. Cem. Concr. Res. 39 [2], 110–115. https://doi.org/10.1016/j.cemconres.2008.11.005
11. Chusilp, N.; Jaturapitakkul, C.; Kiattikomol, K. (2009)a Effects of LOI of ground bagasse ash on the compressive strength and sulfate resistance of mortars. Construct. Build. Mat. 23 [12], 3523–3531. https://doi.org/10.1016/j.conbuildmat.2009.06.046
12. Bahurudeen, A.; Santhanam, M. (2015) Influence of different processing methods on the pozzolanic performance of sugarcane bagasse ash. Cem. Concr. Comp. 56, 32–45. https://doi.org/10.1016/j.cemconcomp.2014.11.002
13. Frías, M.; Villar, E.; Svastano, H. (2011) Brazilian sugar cane bagasse ashes from the cogeneration industry as active pozzolans for cement manufacture. Cem. Concr. Comp. 33, 490–496. https://doi.org/10.1016/j.cemconcomp.2011.02.003
14. Dhengare S.; Amrodiya S.; Shelote M.; Asati A.; Bandwaf N.; Anand K.; Jichkar. (2015) Utilization of sugarcane bagasse ash as a supplementary cementitious material in concrete and mortar – a review. International Journal of Civil Engineering and Technology. 6 [4], 94–106. http://www.iaeme.com/ijciet/index.asp
15. Valencia, G.; Mejía de Gutierrez, R.; Barrera, J; Delvasto, S. (2012) Estudio de durabilidad y corrosión en morteros armados adicionados con toba volcánica y ceniza de bagazo de caña de azúcar. Revista de la Construcción. 12 [22], 112–122. https://doi.org/10.4067/S0718-915X2012000200010
16. Chusilp, N.; Jaturapitakkul, C.; Kiattikomol, K. (2009)b Utilization of bagasse ash as a pozzolanic material in concrete. Construct. Build. Mat. 23 [11], 3352–3358. https://doi.org/10.1016/j.conbuildmat.2009.06.030
17. Unión Nacional de Cañeros A. C. de México. (2016). Viewed on July 13th 2016, www.caneros.org.mx
18. Akram, T.; Memon, S.A.; Obaid, H. (2009) Production of low-cost self-compacting concrete using bagasse ash. Construct. Build. Mat. 23 [2], 703–712. https://doi.org/10.1016/j.conbuildmat.2008.02.012
19. Villar-Cociña, E.; Valencia-Morales, E.; Gonzáles-Rodriguez, R,; Hernández-Ruiz, J. (2003) Kinetics of the pozzolanic reaction between lime and sugar cane straw ash by electrical conductivity measurement: A kinetic-diffusive model. Cem. Concr. Res. 33 [4], 517–524. https://doi.org/10.1016/S0008-8846(02)00998-5
20. Frías, M.; Villar-Cociña, E.; Sanchez de Rojas, M.I.; Valencia-Morales, E. (2005) The effect that different pozzolanic activity methods has on the kinetic constants of the pozzolanic reaction in sugar cane straw-clay ash/lime systems: Application of a diffusive model. Cem. Concr. Res. 35 [11], 2137–2142. https://doi.org/10.1016/j.cemconres.2005.07.005
21. Bahurudeen, A.; Wani K.; Abdul B.M.; Santhanam, M. (2016) Assessment of pozzolanic performance of sugarcane bagasse ash. J. Mater. Civ. Eng. 28[2], 01–11. https://ascelibrary.org/doi/10.1061/%28ASCE%29MT.1943-5533.0001361
22. Seong-Tae Y.; Eun-Ik Y.; Joong-Cheol C. (2006) Effect of specimen sizes, specimen shapes, and placement directions on compressive strength of concrete. Nuclear Engineering and Design 236 [2], 115–127. https://doi.org/10.1016/j.nucengdes.2005.08.004
23. Germán, R M. (1994) Powder metallurgy Science. MPIF Princeton. USA, (1994).
24. Soares, M.M.N.S.; Poggiali, F.S.J.; Bezerra, A.C.S.; Figueiredo, R.B.; Aguilar, M.T.P.; Catlin, P.R. (2014) The effect of calcination conditions on the physical and chemical characteristics of sugar cane bagasse ash. REM: R. Esc. Minas, Ouro Petro. 67(1), 33–39. https://doi.org/10.1590/S0370-44672014000100005
25. Martirena, J.F.; Middendor, F.B; Gehrke, M; Budelmann, H. (1998) Use of wastes of the sugar industry in lime-pozzolana binders: Study of the reaction. Cem. Concr. Res. 28[11], 1525–1536. https://doi.org/10.1016/S0008-8846(98)00130-6
26. Somna, R.; Jaturapitakkul, C.; Rattanachu, P.; Chalee, W. (2012) Effect of ground bagasse ash on mechanical and durability properties of recycled aggregated concrete. Materials and Design. 36, 597–603. https://doi.org/10.1016/j.matdes.2011.11.065
27. Batra, V.S.; Urbonaite, S.; Svensson, G. (2008) Characterization of unburned carbon in bagasse fly ash. Fuel. 87 [13-14], 2972–2976. https://doi.org/10.1016/j.fuel.2008.04.010
28. Martirena, F.; Middenford, B.; Day, R.L.; Gehrke, M.; Roque, P.; Martinez, L. (2006) Rudimentary, low-tech incinerators as a means to produce reactive pozzolan out of sugar cane straw. Cem. Concr. Res. 36 [6], 1056–1061. https://doi.org/10.1016/j.cemconres.2006.03.016

The influence of untreated sugarcane bagasse ash on the microstructural and mechanical properties of mortars • 13

29. Cordeiro, G.C.; Toledo Filho, R.D.; Tavares, L.M.; Fairbairn, E.M.R. (2012) Experimental characterization of binary and ternary blended-cement concretes containing ultrafine residual rice husk and sugar cane bagasse ashes. *Construct. Build. Mat.* 29, 641–646. https://doi.org/10.1016/j.conbuildmat.2011.08.095

30. Chandara, C.; Sakai, E.;Azizli, K.A.M.; Ahmad, Z.A.; Hashim, S.F.A. (2010) The effect of unburned carbon in palm oil fuel ash on fluidity of cement pastes containing superplasticizer. *Construct. Build. Mat.* 24 [9], 1590–1593. https://doi.org/10.1016/j.conbuildmat.2010.02.036

31. Jímenez-Quero, V.G.; León-Martínez, F.M.; Montes-García, P.; Gaona-Tiburcio, C.; Chacón-Nava, J.G. (2013) Influence of sugar-cane bagasse ash and fly ash on the rheological behavior of cement pastes and mortars. *Construct. Build. Mat.* 40, 691–701. https://doi.org/10.1016/j.conbuildmat.2012.11.023

32. Diamond, S. (2004) The microstructure of cement paste and concrete--a visual primer. *Cem. Concr. Comp.* 26 [8], 919–933. https://doi.org/10.1016/j.cemconcomp.2004.02.028

33. Giraldo, M.A.; Tobón, J.I. (2006) Mineralogical evolution of Portland cement during hydration process. *Dyna.* 73 [148], 69–81. http://www.scielo.org.co/scielo.php?script=sci_arttext&pid=S0012-73532006000100007&lng=en&nrm=iso&tlng=es

34. Torres, J.; Mejía de Gutiérrez, R.; Castelló, R.; Vizcaino, C. (2008) Proceso de hidratación depastas de OPC adicionadas con caolín tratado térmicamente. *Revista Facultad de Ingeniería.* Universidad de Antioquia. 43, 77–85. http://www.scielo.org.co/pdf/rfiua/n43/n43a07.pdf

35. Govindarajan, D.; Jayalakshmi, G. (2011) XRD, FIRT and SEM studies on calcined sugarcane bagasse ash blended cement. *Archives of Physics Research.* 2 [4], 38–44. http://scholarsresearchlibrary.com/APR-vol2-iss4/APR-2011-2-4-38-44.pdf

36. Hussein, A.A.E.; Shafiq, N.; Nuruddin, M.F.; Memon, F.A. (2014) Compressive strength and microstructure of sugar cane bagasse ash concrete. *Research Journal of Applied Sciences, Engineering and Technology.* 7 [12], 2569–2577. https://www.researchgate.net/publication/287501413_Compressive_Strength_and_Microstructure_of_Sugar_Cane_Bagasse_Ash_Concrete

37. Richardson, I.G. (2008) The calcium silicate hydrates. *Cem. Concr. Res.* 38 [2], 137–158. https://doi.org/10.1016/j.cemconres.2007.11.005

38. Arizzi, A.; Cultrone, G. (2012) Aerial lime-based mortars blended with a pozzolanic additive and different admixtures: A mineralogical, textural and physical-mechanical study. *Construct. Build. Mat.* 31, 135–143. https://doi.org/10.1016/j.conbuildmat.2011.12.069

39. Sisomphon, K.; Franke, L. (2011) Evaluation of calcium hydroxide contents in pozzolanic cement pastes by a chemical extraction method. *Construct. Build. Mat.* 25 [1], 190–194. http://doi.org/10.1016/j.conbuildmat.2010.06.039

40. Valdez-Tamez, P.L.; Tushar, D.R.; Rivera-Villareal, R. (2004) Evaluación de la velocidad dehidratación en sistemas puzolanas naturales-portlandita. *Revista Ciencia UANL.* 8, 190–195. http://eprints.uanl.mx/1606/1/art_puzolanas.pdf.

41. Amethyst Galleries, Mineral Gallery. Encyclopedia. http://www.galleries.com/Cristobalite

CHAPTER FOUR

Effect of the addition of sugar-cane bagasse ash on the corrosion risk of uncured mortars.
Maldonado-García Marco A., Montes-García Pedro, Valdez-Tamez Pedro L. 2016.
Proceedings of the 11th fib International PhD Symposium in Civil Engineering. Tokyo, Japan, 77-84. www.fib-international.org.

Effect of the addition of sugar-cane bagasse ash on the corrosion risk of uncured mortars

Marco A. Maldonado-García[1], Pedro Montes-García[1] and Pedro L. Valdez-Tamez[2]

[1]Instituto Politécnico Nacional,
CIIDIR Oaxaca,
Hornos No. 1003, Col. Noche Buena, Sta. Cruz Xoxocotlán, Oaxaca, México, C.P. 71230.

[2]Universidad Autónoma de Nuevo León,
Facultad de Ingeniería Civil,
Cd Universitaria s/n, San Nicolás de los Garza, Nuevo León, México, C.P. 66451.

Abstract

In recent years a number of studies on Sugar-cane Bagasse Ash (SCBA) as a partial Portland cement replacement in concrete have been addressed. The research has focused on the pozzolanic activity and mechanical properties of mortars and concretes containing SCBA; however, the durability of such composites needs to be evaluated, especially when no-proper curing is applied. This research evaluates the effects of the SCBA on the corrosion risk of mortars with no curing. Cylinders and reinforced small-scale slabs with 0, 10 and 20% of SCBA as cement replacement, were cast. The effective chloride diffusion coefficients, D_{eff}, were estimated and the slabs were exposed to wetting-drying cycles in a 3% NaCl solution for 2000 days. Corrosion potentials were processed using the FFT to estimate the corrosion initiation period. Results show that the SCBA decreases the D_{eff} which in turn has the beneficial effect of diminishing the corrosion risk.

1 Introduction

Chloride ingress is considered to be the major cause of the degradation of reinforced concrete (Angst et al. 2009, Torres-Luque et al. 2014). Chlorides are transported through the cementitious matrix by mechanisms such as diffusion, in which the concrete is fully submerged and chlorides diffuse in response to concentration gradients, and absorption, in which concrete is relatively dry and capillary suction predominates (Chisholm 2001). It has been established that diffusion is the main ingress mechanism by which chloride ions penetrate through the concrete pore network, triggering the corrosion of steel reinforcement once the chloride content at the steel surface has reached a critical threshold value (Angst et al. 2009). Previous studies have confirmed that a denser cementitious matrix delays the time in which the critical threshold value is reached (Ki and Ha-won 2007, Angst et al. 2009, Gastaldini et al. 2010). The improvement of the density of the cementitious matrix can be done by using supplementary pozzolanic materials as a partial Portland cement replacement. The presence of these supplementary materials in concrete influences the amount, kind and volume of the hydrates formed, which in turn modify the porosity, permeability of the cementitious matrix and durability of the steel reinforcement (Gastaldini et al. 2010, Lothenbach et al. 2011, Aprianti et al 2015). Some of them used the sugar-cane bagasse ash (SCBA).

SCBA is obtained as a by-product generated from the combustion process of sugar-cane bagasse in sugar mills. It is reported that the production of SCBA is increasing to approximately 15 millions of tons annually (Frías y Sánchez 2013), leading to disposal problems and serious environmental issues worldwide (Aprianti et al 2015). In this context, numerous researchers have been focus on the use of the SCBA as a partial Portland cement replacement and confirms that up to 30% of addition improves the mechanical properties, decreases the chloride ion penetration, and decreases the total chloride diffusion in mortars and concretes (Ganesan et al. 2007, Noor-ul 2011, Valencia et al. 2012, Ríos-Parada 2013, Dhengare et al. 2015). These effects occur especially when the ash is subjected to pos-treatments like sieving, re-calcination and grinding.

Proc. of the 11th *fib* International PhD Symposium in Civil Engineering | 77
Aug 29 to 31, 2016, The University of Tokyo, Tokyo, Japan

Instituto Politécnico Nacional – CIIDIR Oaxaca   **40**

There are only few studies addressing the effects of SCBA on steel corrosion in mortars and concretes. Research found that the addition of SCBA delays the corrosion process of the embedded steel, due to the microstructural improvements in the cementitious matrix (Nuñez-Jaquez et al. 2012, Valencia et al. 2012, Ríos-Parada 2013). Other studies report that the use of pozzolanic materials and curing regimens of 28 and 90 days reduce the chloride penetration rates (Gastaldini et al. 2010). Nevertheless, under practical conditions long curing regimens when pozzolans are incorporated in concrete mixtures might result economically prohibitive.

The aim of this research is to evaluate the effects of the addition of SCBA as a Portland cement replacement on the corrosion risk of uncured small-scale reinforced mortar slabs. The slabs were exposed to a simulated marine environment for 2000 days. Corrosion potential measurements were taken daily and the results were analyzed as a discrete signal in the time domain and processed by the Fast Fourier Transform (FFT) in order to decrease the signal noise.

2   Experimental procedure

2.1   Materials

Blended Portland Cement CPC-30R Apasco® (with approximately 5% of blast furnace slag added) which is readily available in the Southeast of México and SCBA sieved through a No. 200 (75μm) ASTM mesh were used as cementitious materials. River sand with a fineness modulus of 2.45 and density of 2.7g/cm^3 and distilled water were used to prepare the mortars. A high-range water reducer (HRWR) Plastol 4000® was added to improve the workability of the mixtures. Galvanized hexagonal wire meshes with 1mm in diameter and 1/2in in aperture were used as reinforcement.

The SCBA was collected from a sugar mill located in the community of Tezonapa, Veracruz, México. This ash is generated as a combustion by-product at temperatures between 550 to 700 ^{0}C during sugar production and is recovered by sprinkling water in the exit of the boilers. Ash samples were collected randomly from a heap in the yard of the sugar mill and carried to the laboratory in bags. The collected ash was homogenized and dried over 24 hours in an electric oven at 105 ^{0}C. After that the SCBA was sieved through a No. 200 ASTM mesh for four minutes. Its chemical composition by I.C.P optical and gravimetric methods, density according with the ASTM C 188, median particle size (MPS) using a laser analyzer Microtrac S3500® (via isopropyl alcohol and considering a refractive index of 1.54), and the superficial area (SA) by physical adsorption of nitrogen using a Quantachrome Nova 2000e® analyzer were obtained. The morphology of the SCBA was analyzed using a scanning electron microscope JEOL JSM-6510LV. The strength activity index (SAI) of the SCBA was evaluated in mortars 50-mm cubes at 28 days (ASTM C109) in previous studies (Hernández 2009).

2.2   Mixture proportions, casting of mortar specimens and exposure conditions of reinforced slabs

Three mortar mixtures were prepared in previous studies (Hernández 2009) replacing 0, 10 and 20% of CPC by SCBA (mixtures SCBA-0, SCBA-10 and SCBA-20 respectively) (at temperatures between 23 to 26^{0}C). All mortars had a 0.63 water-to-cementitious materials ratio and a 1:3 cement-to-sand ratio. Segregation and bleeding of the mortars during the mixing and the flow table tests (ASTM C1437) were not observed. Only the mortars with SCBA additions required the HRWR additive because the ash produced an increase in the viscosity of the fresh mixture and this led to workability problems. The mixture proportions are summarized in Table 1. Cylindrical specimens of 100mm diameter and 200mm of height, and 250 x 200 x 30mm reinforced small-scale slabs were cast. The cylinders were used to obtain the water-soluble chloride content while the slabs were used to evaluate the corrosion risk, respectively. The slabs were reinforced with two galvanized hexagonal wire meshes placed in the centre of the thickness leaving 20mm of cover depth from each edge. A 14 caliber AWG cable was connected to the meshes in order to measure the corrosion potentials. The connection was coated with epoxy resin to prevent galvanized corrosion. All specimens were cast in two layers, compacted using a vibrating table and then placed in a curing room for 24 hours. Next, the forms were removed and the cylinders and slabs were kept in a safe place for 28 days of mature; not curing was applied to any of the mixtures during that time. After the maturity period the cylinders were exposed to chloride contamination in accordance with the NT BUILD 443 standard and the slabs were exposed to a simulated marine environment consisting in wetting and drying cycles of 12 hours each to simulate the tidal effect in a 3% NaCl solution. The NaCl solution from the simulated marine environment was changed periodically to keep the chloride concentration constant (ASTM C1543)

and a pumping system was used to soak the slabs during the day and to empty the solution at night. The slabs were placed 10cm above of the bottom of the container to prevent the awicking effect which could be caused by the remaining solution.

Table 1   Mortar mixture proportioning, kg per m³.

Mixture	CPC-30R, kg	SCBA, kg	River sand, kg	Water, kg	HRWR, ml/kg
SCBA-0	466	0	1398	294	0
SCBA-10	417	46	1390	292	9
SCBA-20	368	92	1381	290	17

2.3   Chloride diffusion

The water-soluble chloride content was determined in the cylindrical specimens after exposure to chloride contamination over 35 days, in accordance with the NT BUILD 443 standard. Powder samples were obtained every 2mm using a profile grinder Metabo® equipment. The chloride concentrations were determined by the combination of two methods; first, the extraction of the water-soluble chlorides in accordance with the ASTM D512 standard, and second, the determination of the concentration by chemical titration as suggested by the Volhard technique in the NT BUILD 208 standard. The Table Curve 2D version 5.01® software was used to determine the effective chloride diffusion coefficients D_{eff} based on the Crank's solution to Fick's second law.

2.4   Corrosion potential measurements

The corrosion potentials of the steel reinforcement in the slabs were monitored daily according with the ASTM C876 during 2000 days of exposure. The high frequency between readings and the long period of testing were required for the later processing of the data. The measurements were carried out during the wetting cycle using an Ag/AgCl half-cell and a high impedance digital voltmeter M. C. Miller Co. LC-4 (Fig. 1). The results were analysed as signals in the time domain and processed by the FFT in order to decrease the experimental error to have a better estimation of the corrosion initiation periods for each mortar mixture studied. The processing consisted of the application of a low-pass filter to the first derivative of the signals, and then the transformation to the frequency domain. Next, the filtered signals were returned to the time domain using the Inverse Fast Fourier Transform (IFFT).

Fig. 1   Setup for the corrosion potentials measurements during the wetting cycle of the slabs.

2.5   Visual inspection

The appearance of the surface of the slabs was monitored in regular basis by visual inspection. Corrosion cracks, rust stains and mortar deterioration caused by corrosion, if any, were recorded. Further, the internal damage caused by corrosion was evaluated breaking one slab of each mortar mixture after 2000 days of exposure to the chloride contaminated environment. For the later inspection, special

emphasis was made on the examination of the wire-mesh connection to know the reliability of the corrosion potential measurements.

3 Results and discussion

3.1 Physical and chemical properties of the SCBA

The densities, MPSs and SAs of the CPC and of the SCBA were 2.94 and 2.19 g/cm^2, 26.08 and 55.37 μm and 3.87 and 60.53 m^2/g. The results show that the SCBA has a lower density than the CPC but greater MPS and greater SA. The chemical analysis (Table 2) shows that the SCBA has a sum of major oxides (SiO$_2$+Al$_2$O$_3$+Fe$_2$O$_3$) of 63.9% and a loss of ignition value (LOI) of 24.15%. The sum of major oxides of the SCBA is less than 70% and its LOI value is largely exceeds the 10% value recommended by the ASTM C618 standard to classify the ash as a natural pozzolan; however, the SAI value obtained was 92%. This SAI value is significant larger than the 75% value required by the standard at 7 and 28 days. The SCBA has particles with a large variety of shapes and sizes which is attributed to the variations of the temperature and air flow during the burning process of the bagasse in the sugar mill. There are agglomerated particles with high porosity, prismatic particles with conoidal failures and fibrous particles which are attributed to be unburned bagasse (Fig. 2).

Table 2   Chemical composition of the CPC and SCBA, (%).

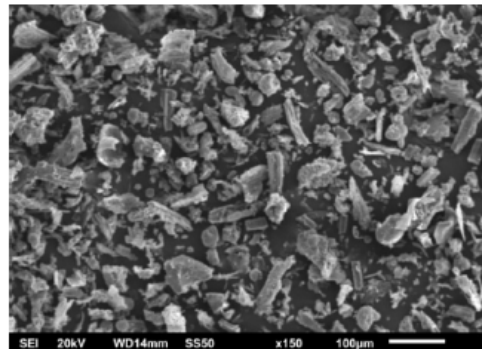|	SiO$_2$	Al$_2$O$_3$	Fe$_2$O$_3$	CaO	K$_2$O	MgO	Na$_2$O	P$_2$O$_5$	LOI
CPC	23.86	5.77	2.19	50.76	0.92	1.36	0.91	0.12	6.97
SCBA	51.66	9.92	2.32	2.59	2.10	1.44	1.23	0.90	24.15

Fig. 2   Morphology of the SCBA.

3.2 Effective chloride diffusion coefficients

The addition of 10 and 20% of SCBA in uncured mortars decreased the values of the D_{eff} in 41.5 and 35.6%, respectively, Fig. 3 (Left). Research shows that the addition of SCBA and long curing periods (28 and 90 days) lower the total chloride diffusion coefficients in mortars and concrete samples (Ganesan et al. 2007, Noor-ul 2011, Ríos-Parada 2013). There are a number of possible explanations of the results of this research. Chief among them is one, the filler effect of the ash; two, the pozzolanic reaction, as suggested by Dhengare et al. (2015); and three, the physical interactions between the carbon particles in the SCBA and chloride ions. A detailed examination of the chloride concentration profiles should help to elucidate which mechanism contributes the greatest to decrease the D_{eff} of the mortars containing SCBA.

Water-soluble chloride concentration profiles, Fig. 3 (Right), show that the addition of 10 and 20% of SCBA increased the water-soluble chloride content in superficial layers (1 to 7mm) when is compared to the control mixture. Beyond the 7mm depth, the chloride contents of the SCBA-10 and SCBA-20 mixtures are lower than in the control. Because no-curing was applied to the mortars a low content of Portlandite from the un-complete cement hydration was produced, and under this conditions, pozzolanic activity is unlikely to occur. In this proposed mechanism the agglomerated particles of SCBA could work as an adsorbent media due its large MPS and SA or as physical barrier.
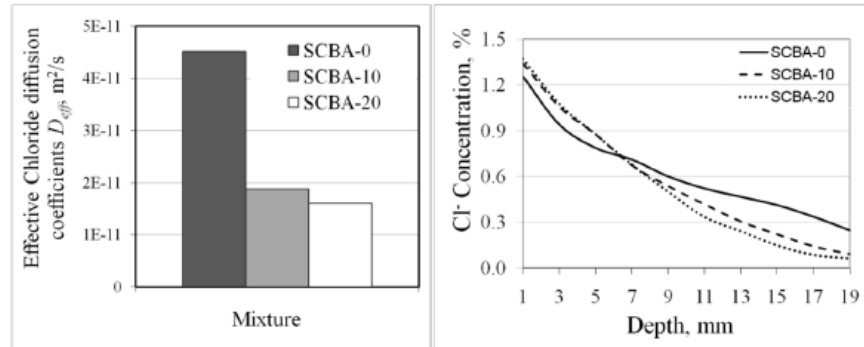
Fig. 3   Effective chloride diffusion coefficients (Left) and water-soluble chloride concentration profiles of uncured mortars (Right). Results are the average of three specimens.

3.3   Half-cell corrosion potentials measurements

Original corrosion potentials are show in Fig. 4. A large variability in corrosion probability during the 2000 days of evaluation is observed. After processing the signals using the FFT tool the noise caused by the experimental error was minimized. In Fig. 5, a clearer signal is presented with which an analysis of the potentials measurements is easier to perform. Results show that the corrosion potentials were between -450mV and -850mV. These are higher than those established by the ASTM C876 standard for half-cell potentials of uncoated steel reinforcement on concrete to be considered a high corrosion risk. However, these results are consistent with other authors who evaluated the corrosion risk on galvanized steel. These authors reported that half-cell readings between -550 to -1200mV indicate active corrosion (Farina y Duffó 2007, Tittarelli and Moriconi 2011).
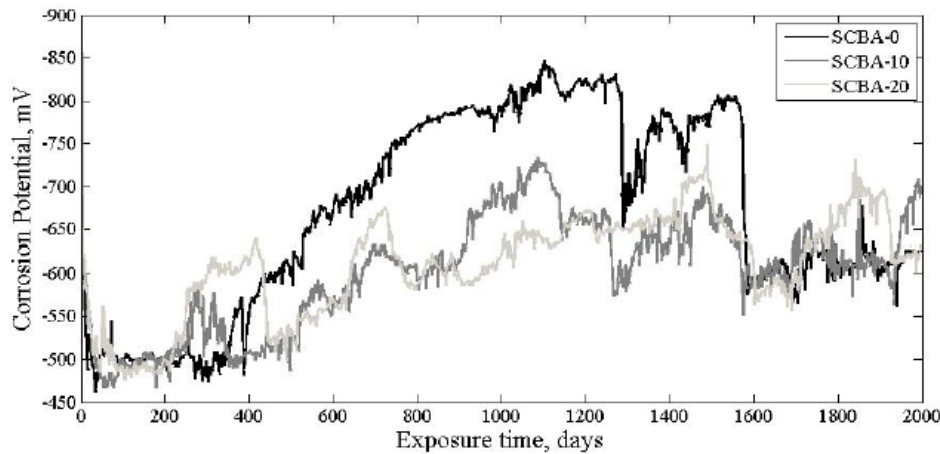

Fig. 4   Original corrosion potential measurements of uncured mortars (average of three slabs).
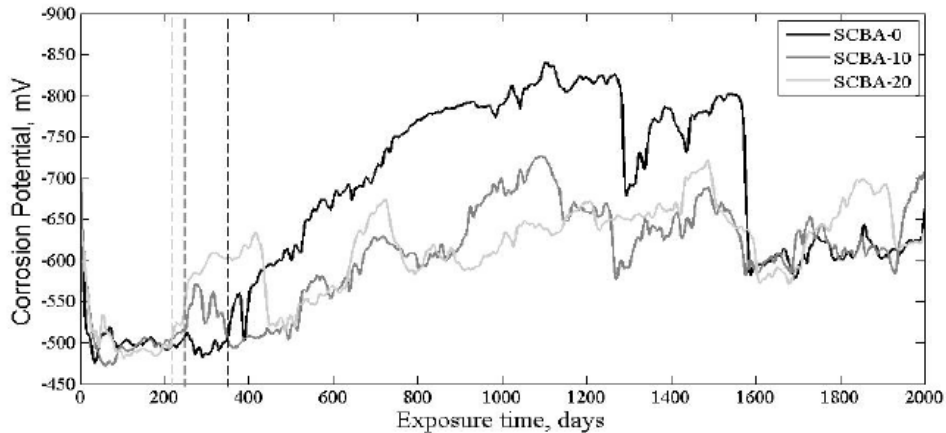
Fig. 5   Processed corrosion potential measurements by the FFT of uncured mortars (average of three slabs); initiation periods suggested for the SCBA-0, SCBA-10 and SCBA-20 reinforced mortars at 350, 240 and 220 days are indicated by the dotted lines.

Three different stages can be observed in Fig. 5. The proposed stages are based on large variations of corrosion potentials recorded over the entire testing period. The first stage, between 0 to 100 days, is considered to be a passivation period in which a greater variability of the measurements occurs due the formation of a passive film on the steel reinforcement. The second stage, between 100 to 350 days is considered to be the corrosion initiation period for galvanized steel reinforcement (Farina and Duffó 2007, Tittarelli and Moriconi 2011). During this stage, in which corrosion potentials between -400 to -550 mV were obtained, chlorides penetrate the cementitious matrix of the mortars until the chloride threshold is reached at the steel surface. The third stage, after 350 days, is considered to be a propagation period in which the galvanized steel corrodes. There is a possibility of a fourth stage for the SCBA-0 after 1600 days, in which it is thought that the zinc coating was completely depleted because corrosion.

Initiation periods of SCBA-10 and SCBA-20 mortars were expected to be in accordance with the D_{eff}, as discussed in the previous section; however, this was not observed. Results of the corrosion potential measurements show that the propagation period of the SCBA-0 mixture started approximately at 350 days, while the propagation periods for the SCBA-10 and SCBA-20 mixtures started approximately at 240 and 220 days, respectively (dotted lines in Fig. 5). However, more negative corrosion potentials for the SCBA-0 mortar were recorded during the propagation period (after approximately 440 days). This shows that the active corrosion process in the SCBA-10 and SCBA-20 mortars occur in more prolonged periods of time as compared with the SCBA-0 mortar. A recent study, using SCBA as a partial Portland cement replacement in mortar mixtures cured 28 days and reinforced with steel bars, shows a similar behaviour in which the corrosion potentials of the mortar without SCBA additions are less than the corrosion potentials of the mortars with SCBA; however they monitored only 375 days of exposure to aggressive agents (Valencia et al 2012).

A possible explanation for the shorter corrosion initiation period of the steel reinforcement embedded in mortars containing SCBA is based on the fact that the absorption of species predominates at the beginning of the experiment. The addition of SCBA to the mortars increases their water absorption which facilitates the penetration of chlorides as reported in section 3.2. On the other hand, curing effects of un-hydrated cement particles could occur after a long exposure time leading to the formation of more calcium silicate hydrate and more calcium hydroxide. Re-hydration of cement particles has beneficial effects to recover the microstructure, strength and durability of concrete due the reduction in connected pores (Chi-Sun et al. 2001, Henry et al. 2014). Also, the calcium hydroxide produced during re-hydration reacts with the pozzolan in presence of moisture. Ganesan et al. (2007) reported an increase of water absorption in concrete containing SCBA at 28 days of curing but at 90 days the absorption decreased with respect to a control mixture. After the structural changes caused by the re-hydration of cement and the pozzolanic reaction the diffusion of species predominates which is a result of the movement of the chloride through a much denser cementitious matrix.

The improvement of the mortar matrices containing SCBA is beneficial in two manners. First, the densification restrains the entrance of oxygen which is necessary for the corrosion reaction and sec-

ond, the present species in the pore solution are decreased; therefore, the corrosion potentials of the reinforcing in mortars with SCBA are less negative than those from the slabs without SCBA.

Fig. 6 shows a section of the slabs near to the connection between the galvanized wire meshes and the cables used for the corrosion potential tests. As it can be observed the connections were in good condition. This observations help to corroborate that the corrosion potentials measured during the testing period are reliable because they are the result of the corrosion of the steel reinforcement under evaluation, and not that caused by galvanic corrosion at the connection.

SCBA-0   SCBA-10   SCBA-20

Fig. 6   Aspect of the wire-mesh connection in autopsied slabs after 2000 days of exposure in the simulated marine environment (one slab for each mortar mixture).

4   Conclusions

In view of the discussed results, the following conclusions can be drawn:
1) The replacement of Portland cement by 10 and 20% of SCBA in mortars decreased the effective diffusion coefficient, D_{eff}, making them less permeable. This was achieved by a physical effect promoted by the formation of a barrier at early ages and by the microstructural improvement of the mortars at long ages.
2) The use of 10 and 20% of SCBA as a partial replacement of Portland cement causes the decrease in the corrosion initiation period of galvanized steel reinforcement embedded in un-cured mortar slabs exposed to a chloride contaminated environment.
3) The use of 10 and 20% of SCBA as a partial replacement of Portland cement decreases the risk of corrosion over time of galvanized steel reinforcement embedded in un-cured mortar slabs exposed to a chloride contaminated environment.

5   Recommendations

In view of the discussed results and conclusions, the following recommendations can be drawn:
1) The analysis of the corrosion process of the galvanized steel reinforcement embedded in un-cured mortar slabs exposed to a chloride contaminated environment using a quantitative method such as the linear polarization resistance is recommended.
2) The analysis of the corrosion products for the elucidation of the corrosion mechanism which led to the deterioration process of the steel reinforcement is also recommended.

Acknowledgments

References

Angst Ueli, Elsener Bernhard, Larsen Claus K. and Vennesland Øystein. 2009. "Critical chloride content in reinforced concrete – A review". Cement and Concrete Research 39:1122-1138.

11th *fib* International PhD Symposium in Civil Engineering

Aprianti Evi, Shafigh Payam, Bahri Syamsul and Nodeh Farahani Javad. 2015. "Supplementary cementitious materials origin from agricultural wastes – A review". Construction and Building Materials 74:176-187.

Chi-Sun Poon, Azhar Salman, Anson Mike and Yuk-Lung Wong. 2001. "Strength and durability recovery of fire-damaged concrete after post-fire-curing". Cement and Concrete Research 31;9:1307-1318.

Chisholm D.H. and Lee N.P. 2001. "Actual and effective diffusion coefficients of concrete under marine exposure conditions". Conference Paper No. 96. 20th Biennial Conference of the Concrete Institute of Australia.

Dhengare Sagar, Amrodiya Sourabh, Shelote Mohaninsh, Asati Ankush, Bandwaf Nikhil, Anand Khangan and Jichkar Rahul. 2015. "Utilization of sugarcane bagasse ash as a supplementary cementitious material in concrete and mortar – A review". International Journal of Civil Engineering and Technology 6;4:94-106.

Farina S.B. and Duffó G.S. 2007. "Corrosion of zinc in simulated carbonated concrete pore solutions". Electrochemical Data 52:5131-5339.

Frías Rojas M. and Sánchez de Rojas Gómez M. I. 2013. Eco-efficient concrete. Chapter 5: Artificial pozzolans in eco-efficient concrete. Woodhead Publishing Limited.

Ganesan K., Rajagopal K. and Thangavel K. 2007. "Evaluation of bagasse ash as supplementary cementitious material". Cement and Concrete Composites 29:515-524.

Gastaldini A.L.G., Isaia G.C., Saciloto A.P., Missau F. and Hoppe T.F. 2010. "Influence of curing time on the chloride penetration resistance of concrete containing rice husk ash: A technical and economical feasibility study". Cement and Concrete Composites 32:783-793.

Henry Michael, Darma Ivan Sandi and Sugiyam Takafumi. 2014. "Analysis of the effect of heating and re-curing on the microstructure of high-strength concrete using X-ray CT". Construction and Building Materials 67:37-46.

Hernández Toledo Ur Iván. 2010. "Efecto de una puzolana de desperdicio agrícola y el tiempo de curado en la corrosión del ferrocemento" Master Thesis, IPN-CIIDIR-Oaxaca, México.

Ki Yong Ann and Ha-Won Song. 2007. "Chloride threshold level for corrosion of steel in concrete". Corrosion Science 49:4113-4133.

Lothenbach Barbara, Scrivener Karen and Hooton R. D. 2011. "Supplementary cementitious materials". Cement and Concrete Research 41:1244-1256.

Noor-ul Amin. 2011. "Use of bagasse ash in concrete and its impact on the strength and chloride resistivity". Journal of Materials in Civil Engineering 717-720.

Nuñez-Jaquez R. E. Buelna-Rodríguea J. E. Barrios_Durstewitz C. P. Gaona-Tiburcio C. and Almeraya-Calderon F. 2012. "Corrosion of modified concrete with sugar cane bagasse ash" International Journal of Corrosion 2012:1-5.

Ríos-Parada Venustiano. 2013. "Análisis de las propiedades mecánicas, microestructurales y de durabilidad de concretos ternarios con ceniza de bagazo de caña" Master Thesis, IPN-CIIDIR_Oaxaca México.

Tittarelli F. and Moriconi G. 2011. "Comparison between surface and bulk hydrophobic treatment against corrosion of galvanized reinforcing steel in concrete". Cement and Concrete Research 41:609-614.

Torres-Luque M., Bastidas-Arteaga E., Schoefs F., Sánchez-Silva M. and Osma J.F. 2014. "Non-destructive methods for measuring chloride ingress into concrete: State-of-the-art and future challenges" Construction and Building Materials 68:68-81.

Valencia G., Mejía-Guitierrez R., Barreraj. and Delvasto S. 2012. "Durability and corrosion study of reinforced blended mortars with tuff and sugar cane bagasse ash". Revista de la Construcción 12;22:112-122.

CHAPTER FIVE

Long-term corrosion risk of thin cement composites containing untreated sugarcane bagasse ash.
Maldonado-García Marco Antonio, Hernández-Toledo Ur Iván, Montes-García Pedro, Valdez-Tamez Pedro Leobardo. 2018.
Accepted manuscript in the Journal of Materials in Civil Engineering.
Ms. No. MTENG-7260.

Long-term corrosion risk of thin cement composites containing untreated sugarcane bagasse ash

Marco Antonio Maldonado-García[1], Ur Iván Hernández-Toledo[2], Pedro Montes-García[3,*], Pedro Leobardo Valdez-Tamez[4].

[1] PhD candidate. Instituto Politécnico Nacional, CIIDIR-Oaxaca, Hornos No. 1003, Col. Noche Buena, Sta. Cruz Xoxocotlán C.P. 71230, Oaxaca, México. marco_mg.age@hotmail.com

[2] PhD candidate. Universidad Autónoma de Nuevo León, Facultad de Ingeniería Civil, Cd Universitaria S/N, San Nicolás de los Garza, C.P. 66451, Nuevo León, México. urivanmxx@gmail.com

[3] PhD. Instituto Politécnico Nacional, CIIDIR-Oaxaca, Hornos No. 1003, Col. Noche Buena, Sta. Cruz Xoxocotlán C.P. 71230, Oaxaca, México. pmontesgarcia@gmail.com, pmontes@ipn.mx

[4] PhD. Universidad Autónoma de Nuevo León, Facultad de Ingeniería Civil, Cd Universitaria S/N, San Nicolás de los Garza, C.P. 66451, Nuevo León, México. pedro.valdeztz@uanl.edu.mx

* **Corresponding author:** (951) 517 0619 ext. 82775. pmontesgarcia@gmail.com, pmontes@ipn.mx

Abstract: The corrosion risk in reinforced mortar slabs containing untreated sugarcane bagasse ash (UtSCBA) (0, 10 and 20% replacement of cement) was analyzed for 75 months. The mortars were prepared with a constant 0.63 water/cementitious-materials ratio. Cylinders and reinforced slabs were cast with the mortars. Two galvanized wire meshes were used as reinforcement for the slabs. Curing regimes of 0, 7 and 28 days were applied to the samples. The cylinders were used to obtain the compressive strength (CS) and the chloride diffusion coefficient (D_{eff}) of the mortars. To evaluate the corrosion risk, the slabs were exposed to wet-dry cycles of 12 hours each in a 3% NaCl solution. Corrosion potential measurements and linear polarization resistance tests were taken every 28 days for that purpose. It was found that the addition of 10% and 20% UtSCBA reduces the workability of the mortar binders and leads to a slight decrease in the CS of hardened mortars. However, it significantly reduced the D_{eff} of the mortars by 50% and 65% ($p \ll 0.05$), respectively, and also decreased the corrosion risk of mortar slabs over time.

Keywords: Pozzolan, mortar, curing-time, corrosion, long-term performance.

ORCID ID: Marco Antonio Maldonado-García (http://orcid.org/0000-0002-9522-6779); Ur Iván Hernández-Toledo (http://orcid.org/0000-0001-9392-0487); Pedro Montes-García (http://orcid.org/0000-0003-3799-8372); Pedro Leobardo Valdez-Tamez (http://orcid.org/0000-0002-1298-2051).

INTRODUCTION

Steel bars are normally passivated when embedded in concrete; however, when passivity is lost, corrosion can occur. This process takes place due to the penetration of harmful chemical substances, including chloride ions, from the surrounding environment (Liu et al. 2016; Michel et al. 2016). Chlorides penetrate through the concrete pore network, reaching a maximum threshold value at which the passive layer of the steel is destroyed, allowing steel corrosion to occur (Angst et al. 2009; Shi et al. 2012; Torres-Luque et al. 2014). The corrosion products from this process reduce the durability and life-cycle performance of the reinforced concrete (Torres-Luque et al. 2014).

A number of researchers affirm that a denser cementitious matrix (CM) decreases chloride ingress into the reinforced concrete (RC). As a result, the time in which the chloride threshold value is reached increases accordingly (Angst et al. 2009; Gastaldini et al. 2010 Song et al. 2008). A denser CM can be obtained with the use of supplementary cementitious materials (SCM) as a partial Portland cement replacement. These materials influence the amount and kind of hydrates formed, such as C-S-H, which in turn reduce the porosity and permeability of the CM (Aprianti et al. 2015; Gastaldini et al. 2010; Lothenbach et al. 2011). Different SCMs are used around the world; some of them are by-products from manufacturing and agro-industry. Disposing of these materials is a problem, causing several environmental issues (Aprianti et al. 2015). An example of SCM is fly ash (FA), a by-product obtained from coal combustion that has been extensively studied for many years; it is a well-recognized pozzolanic material which reduces the corrosion risk of RC due to improvement of its microstructure and hence the reduction of its permeability to chloride ions (Choi et al. 2006; Liu et al. 2016; Simčič et al. 2015). However, the use of any specific type of SCM is limited by its availability, the cost of production (Gastaldini et al. 2010), and the environmental impact.

Considering the above, agro-industry waste materials appear to be a more suitable, environmentally-friendly alternative for a sustainable construction industry (Aprianti et al. 2015). One of these materials is sugarcane bagasse ash (SCBA). SCBA is a by-product from the combustion of sugarcane bagasse in sugar mills and is available in large quantities in developing countries such as Brazil, India, Thailand and Mexico. In Mexico, the National Union of Sugarcane Producers (UNC 2017) reports that the production of sugarcane reached approximately 54 million tons in 2016/2017; from this, about 15 million tons of bagasse were

obtained. According to Akram et al. 2009, each ton of sugarcane produces approximately 0.62% residual ash. This suggests that in Mexico about 0.34 million tons of SCBA are produced annually after processing. This ash is generally deposited in open dumps causing soil contamination even when it is used as fertilizer due to its lack of nutrients and high silica content (Soares et al. 2014). The improper disposal of the SCBA also pollutes the air (Dhengare et al. 2015,) because of the fine particles in the ash, and pollutes water in nearby rivers and groundwater (Katare et al. 2017) due to the transport of SCBA particles by rainwater.

Numerous researchers affirm that a post-treatment, such as re-calcination or grinding, increases the pozzolanic activity of the SCBA (when used in mortar and concrete mixtures) due to the change of its physical and/or chemical characteristics (Chusilp et al. 2009a; Chusilp et al. 2009b; Cordeiro et al. 2010; Cordeiro et al. 2012; Morales et al. 2009). However, these post-treatments are highly demanding in energy, time consuming, and contribute to the generation of contaminants. To overcome these problems, the use of "practically as received" SCBA from sugar mills with only a sieving post-treatment can be implemented (Maldonado-García et al. 2017). Recent research reports that a simple post-treatment of sieving with a No. 50 (300μm) ASTM mesh increases the pozzolanic activity of the SCBA just above the minimum strength activity index recommended by the ASTM C 618 standard (Bahurudeen and Santhanam 2015). However, the authors recommend an additional grinding process for greater pozzolanic activity of the SCBA. A sieving post-treatment through different meshes, followed by a grinding process, has been also suggested by other researchers to increase the pozzolanic activity of SCBA (Torres et al. 2014).

On the other hand, previous studies have shown that the SCBA sieved through a No. 200 (75μm) ASTM mesh for five minutes (UtSCBA)

increases the CS and the electrical resistivity of mortars (Arena-Piedrahita et al. 2016). The authors used the term UtSCBA to describe the used SCBA subjected to that low-energy post-treatment which could be considered as "as received SCBA" from sugar mills because only large unburned bagasse particles were removed from the ash. The addition of UtSCBA also improves the microstructure of mortars over a long period of time (Maldonado-García et al. 2018), does not affect the mechanical properties, and improves the microstructure of ternary concretes containing FA (Ríos-Parada et al. 2017).

Few studies have focused on the use of SCBA in mortar and concrete mixtures to combat steel corrosion. Nuñez-Jaquez et al. 2012 report a beneficial effect of the use of SCBA against steel corrosion due to reduction of pore size in the cement paste, which minimizes the ingress of chloride ions into the concrete. On the other hand, Valencia et al. 2012 report that because of the presence of capillary pores in the mortars (attributed to the chemical and physical properties of SCBA), SCBA does not decrease steel corrosion in mortars exposed to chloride ions. However, these studies were carried out considering only a few months of electrochemical testing in samples exposed to saturated or wet-dry conditions. Under such conditions, it is estimated that the corrosion propagation period may continue for 20 years at low corrosion rates (in order of $1\mu A/cm^2$) (Austin and Lyons 2004). In both studies, maximum corrosion rates of $1\mu A/cm^2$ were reported, leading to some uncertainties.

Considering the previous statements, a long-term evaluation of the use of SCBA against corrosion in concrete is needed. The present research evaluates the effect of the addition of UtSCBA on the corrosion risk of small-scale reinforced mortar slabs exposed to a simulated marine environment for 75 months. The effect of different curing periods on the corrosion risk was also evaluated.

MATERIALS

Materials description

Blended Portland cement 30-R Holcim Apasco® (CPC) (with approximately 5% ground granulated blast furnace slag) available in the southwest region of Mexico, UtSCBA (SCBA sieved though a 75µm mesh for five minutes), and class F fly ash (FA) Admix Tech® (which meets the requirements established by the ASTM C 618 standard) were used as cementitious materials for the mortar binders. The UtSCBA was collected randomly from a heap in the yard of a sugar mill located in the community of Tezonapa, Veracruz, Mexico. This ash is generated as a combustion by-product of sugarcane bagasse at temperatures between 550 and 700ºC during sugar production and is recovered by spraying water over it. The collected ash was carried to the laboratory in bags, then homogenized and dried for 24 hours in an electric oven at 105ºC. Subsequently, the ash was sieved through a No. 200 ASTM mesh for five minutes. This methodology was chosen in accordance with the findings in previous research in order to obtain optimum pozzolanic performance of the UtSCBA with a minimum low-energy post-treatment (Maldonado-García et al. 2018). Fig. 1 shows the as received SCBA from the sugar mill and the sieved SCBA. It can be observed that a sieving process through the 75µm ASTM mesh for five minutes is enough to remove large unburned particles from the SCBA.

River sand (with a fineness modulus of 2.45 and density of 2.7g/cm³) and distilled water were also used to prepare the mortar binders. A polycarboxylate-based high-range water reducer (HRWR) Plastol 4000® was used to maintain the workability of the mortars containing UtSCBA. Finally, two galvanized hexagonal wire meshes 0.68 mm in diameter and 12.7 mm

in aperture were used as reinforcement for the mortar slabs. The galvanized meshes were chosen as reinforcement because of the geometry of the slabs. Moreover, long corrosion initiation periods as well as an increase in the

amount of chlorides needed to induce corrosion had to be considered for the experiments in this research, due to the zinc coating of the reinforcement (Rivera-Corral et al. 2017).
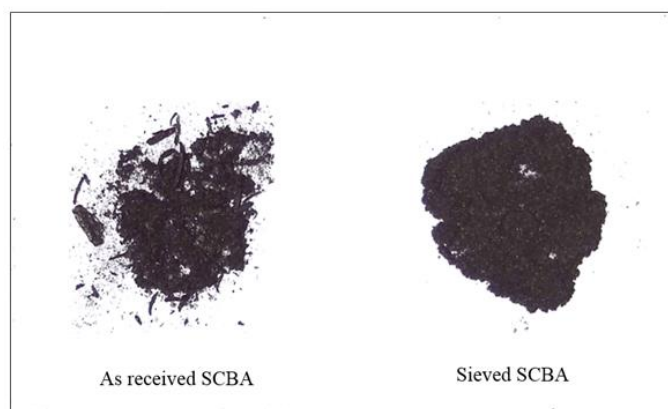

Fig. 1. The as received SCBA from the sugar mill and sieved SCBA

Chemical and mineralogical analysis of the cementitious materials

The chemical analysis of the cementitious materials (by I.C.P optical and gravimetric methods) is shown in Table 1. The UtSCBA fulfills the sum of major oxides (SiO_2 + Al_2O_3 + Fe_2O_3 = 76%) required by the ASTM C 618 standard, but, it has a slightly larger loss on ignition content (LOI). However, this ash is the subject of long-term ongoing research in which the effect of UtSCBA on the rheological behavior of fresh pastes and mortars, as well as the microstructure and mechanical properties of mortars containing it, have already been reported (Jímenez-Quero et al. 2013; Maldonado-García et al. 2018). Fig. 2a shows the X-ray diffraction (XRD) pattern of the UtSCBA, where the

presence of a hump observed in the interval 2-theta from 18° to 35° suggests low crystallinity in this material. This implies the presence of amorphous phases (Cordeiro et al. 2012; Ganesan et al. 2007; Martirena et al. 2006; Morales et al. 2009; Valencia et al. 2012). Crystalline phases of quartz, cristobalite, gibbsite, hematite and calcium were detected. As well the residual carbon phase, commonly attributed to the LOI of the ash, was detected (Frias et al. 2011; Morales et al. 2009). On the other hand, the XRD pattern in Fig. 2b indicates that FA is mainly composed of the crystalline phases of quartz and mullite with an amorphous component on the interval 2-theta from 18° to 30°.

Table 1. Chemical compositions of the materials used for the mortars (% by mass)

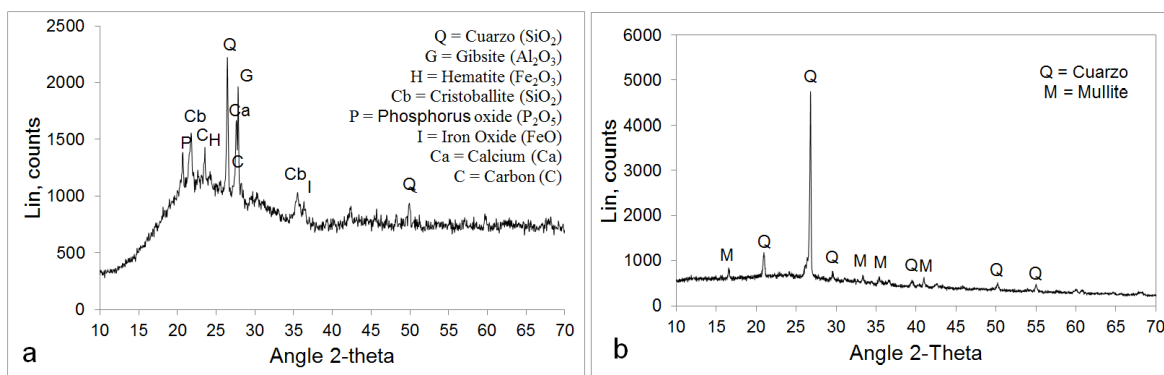| Material	SiO_2	Al_2O_3	Fe_2O_3	CaO	MgO	Na_2O	K_2O	P_2O_5	LOI
CPC	23.86	5.77	2.19	50.76	1.36	0.91	0.92	0.12	6.97
UtSCBA	56.37	14.61	5.04	2.36	1.43	1.57	3.29	0.85	10.53
FA	58.02	23.28	4.44	5.47	1.37	0.62	0.95	0.33	3.69

Note: LOI = loss on ignition

Fig. 2. XRD diffraction pattern of the a) UtSCBA and b) FA

Physical and morphological properties of the cementitious materials

UtSCBA has a lower density, greater median-particle size and larger specific surface area (SSA) than FA and CPC (Table 2). The larger SSA of UtSCBA can be attributed to its cellular origin (Cordeiro et al. 2010). Fig. 3a shows that the UtSCBA has grains with a large variability of shapes and sizes. The agglomerated particles are mainly constituted by Si and C, while the prismatic particles with well-defined edges are rich in Si (Maldonado-García et al. 2018).

Furthermore, fibrous carbon particles were also observed in the UtSCBA. The appearance of the fibrous carbon particles offers a possible explanation for the larger SSA of the UtSCBA. However, some studies report that these particles may be covered by Si and O and could also present amorphicity (Batra et al. 2008). In contrast, the FA is mostly composed of cenospheres (spherical solid particles) and plerospheres (particles packed with smaller spheres) (Fig. 3b) (Ramachandram 2001).

Table 2. Physical properties of the materials used for the mortars

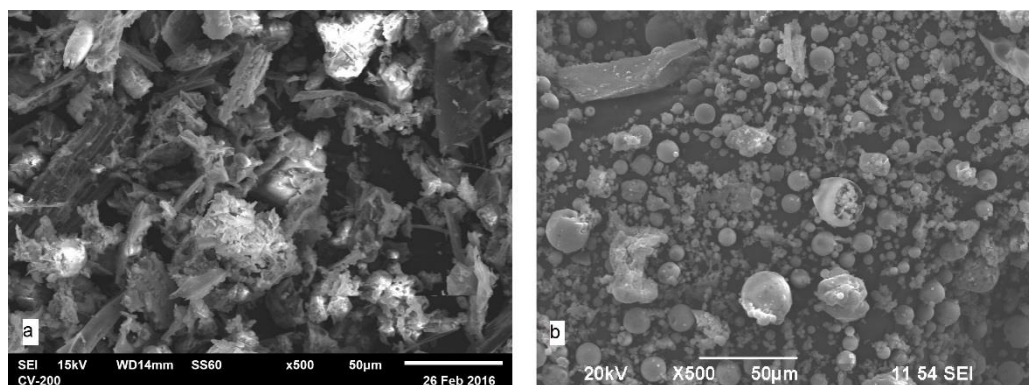| Material	Density (ASTM C188) (g/cm^3)	Particle-size distribution (Laser ray diffraction)			Specific surface area (BET) (m^2/g)
		D_{10} (µm)	D_{50} (µm)	D_{90} (µm)	
CPC	2.94	3.48	18.93	53.63	3.6
UtSCBA	2.19	14.22	36.85	78.11	60.53
FA	2.27	5.04	22.76	79.07	3.26

Fig. 3. SEM micrographs of the a) UtSCBA and b) FA

Mixture proportions and casting of the mortar specimens

Three mortar mixtures containing 0, 10 and 20% UtSCBA (control, UtSCBA10 and UtSCBA20, respectively) as a partial Portland cement replacement were prepared. The three UtSCBA levels were chosen based on previous research (Maldonado-García et al. 2018). An additional mixture containing only 20% fly ash as a cement replacement was also prepared as a reference. All mortars had 0.63 water-cementitious materials and 1:3 cementititous materials-sand ratios. Only the mortars containing UtSCBA required the HRWR additive since the ash produced an increase in the viscosity of the fresh mixtures, leading to workability reduction. The mortar mixture proportions are shown in Table 3.

Flow (ASTM C 1437), volumetric weight (ASTM C 138) and air content (ASTM C 231) tests of the fresh mixtures were carried out. A total of 191 cylinders 75 mm in diameter and 150 mm in height and 30 cylinders 100 mm in diameter and 200 mm in height were cast with the mortars in order to evaluate the CS and the D_{eff}. Subsequently, 10 small-scale reinforced mortar slabs 250 x 200 x 30 mm in size were cast in order to evaluate the corrosion risk. The slabs were reinforced with two galvanized hexagonal wire meshes placed in the center of the thickness, leaving 20 mm of cover depth from each edge. A caliber 14 AWG copper cable was connected to the meshes to measure the corrosion potentials and current intensities. The connection between the wire meshes and the copper cable was coated with an epoxy resin to prevent galvanic corrosion at the connection. The cylinders and the slabs were cast in two layers and compacted using a vibrating table for five seconds.

All the specimens were demolded after 24 hours and placed in a $Ca(OH)_2$-saturated solution for curing purposes during 0, 7 and 28 days. These curing times were adopted from those proposed in the ASTM C 39 standard as these ages are important indicators of significant changes in Portland cement-based composites. Likewise, those curing times were chosen to evaluate the effect of curing sensitivity on the performance of mortars containing UtSCBA against corrosion. Accordingly, the magnitude of the curing effects upon compressive strength and chloride penetration resistance depends on the mineral addition as well as the amount of substitution, the water/binder ratio, and the curing time used (Gastaldini et al. 2010). The additional mixture containing 20% fly ash was cured for only 28 days.

The cylinders used for the CS were then stored in the laboratory until the test periods of 28 and 90 days were reached. Accordingly, only the cylinders with 28 days of curing and 28 days of maturity were tested under wet conditions as ASTM C 39 standard suggests. Therefore, the CS results of the cylinders tested under dry conditions were corrected (a decrease of 20% of the obtained gross value) in accord with the findings by Yurtdas et al. 2004. The cylinders for the D_{eff} tests and the slabs used to evaluate the corrosion risk were stored in the laboratory only until the 28-day limit was reached.

Table 3. Mixture proportions of mortars (kg/m^3)

Mixture	CPC (kg)	UtSCBA (kg)	FA (kg)	Water (kg)	Sand (kg)	HRWR (ml/kg of cementitious materials)
Control	466.0	0	0	293.6	1398.0	0
UtSCBA10	419.4	46.6	0	293.6	1398.0	9.0
UtSCBA20	368.3	92.2	0	293.6	1398.0	17.5
FA20	368.3	0	92.2	293.6	1398.0	0

Note: HRWR = High-Range Water Reducer

Exposure conditions of the reinforced slabs

After the maturity period, the mortar slabs were placed in a container and wet-dry cycles of 12 hours each in a 3% NaCl solution were applied to simulate a marine environment and create a tidal effect (Fig. 4). A pumping system was used to fill the container with the NaCl solution during the day and a manual valve to empty the solution at night. To keep the chloride concentration constant, the NaCl solution was changed periodically according to the ASTM C 1543 standard. The slabs were placed 150 mm above the bottom of the container to prevent a wicking effect which the remaining solution could potentially cause during the drying cycles. Because of the sensitivity of the electrochemical tests to environmental changes (Verma et al. 2013), the temperature of the experimental room was recorded during the test period using a HOBO® data logger device.

Fig. 4. The simulated marine environment for the reinforced mortar slabs

Test methods

The CSs of the mortars were obtained according to the ASTM C 39/39M standard. The tests were carried out in a hydraulic testing machine ELVEC E-659® using unbonded neoprene pads in metal-retaining bases. According to ASTM C 1231 standard, the neoprene pads deform in initial loading to conform to the contour of the specimens' ends, allowing CS testing in specimens with low resistance. This configuration was useful for the CS tests in the cylinders with a short curing period evaluated in this research.

The total chloride content of the mortars was determined after 28 days of maturity. The cylinders were exposed to chloride contamination over 35 days in accordance with the NT BUILD 443 standard. Powder samples were obtained from the cylinders every 2 mm using a Metabo® profile grinder. The chloride concentration of each powder was determined by chemical titration as suggested by the Volhard technique in the NT BUILD 208 standard. Table Curve 2D version 5.01® software was used to find the D_{eff} of the mortars based on Crank´s solution to Fick´s second law.

The corrosion risk of the mortar slabs was monitored by corrosion potential (E_{corr}) measurements and linear polarization resistance (LPR) tests taken every 28 days during the wetting cycles throughout the 75-month period. The E_{corr}, based on the ASTM C 876 standard, was measured using a Ag/AgCl half-cell and a high-impedance digital voltmeter M.C. Miller Co LC-4®. The LPR tests, based on the ASTM G59 standard, were taken using a potentiostat Gamry® series G 300. An Ag/AgCl half-cell and an external galvanized mesh were used to perform the tests as reference and counter electrodes, respectively. The working electrode was polarized to ±20mV vs E_{ref} at a scan rate of 0.075 mV/s, while a density of 7.87gr/cm^2 and an equivalent weight of 27.92gr/equivalent were considered for the LPR tests. Corrosion intensities were obtained from the LPR tests using Echem Analyst ™ version 5.1.3 software.

A reaction´s Tafel constant of 0.12volts/decade was used to estimate the corrosion densities.

At the end of the exposure time each slab was divided into 12 small square sections using an electric diamond cutting machine. The square sections were then transversely opened by hammer and chisel to expose the steel reinforcement and inspect its surface condition. The visual examination of the opened slabs was carried out following the recommendations provided by the ASTM C 856 standard.

RESULTS AND DISCUSSION

Fresh properties of mortars binders

Results for fresh properties of the mortars are presented in Table 4. Mortars containing UtSCBA had workability problems, which were overcome using the HRWR. In the end, all the mortars achieved a flow value of 110±5 mm, fulfilling the ASTM C 1329 requirements. The high LOI in the UtSCBA (10.53%), which is an indication of an elevated level of unburned bagasse particles, can be blamed for these problems. Researches report that a high LOI content (larger than 10%) decreases the major oxides (SiO_2, Al_2O_3 and Fe_2O) in the SCBA and increases the water requirement of fresh cement-based mixtures (Arenas-Piedrahita et al. 2016; Chusilp et al. 2009b; Somma et al. 2012). In addition to the LOI, the large variability of the UtSCBA's shapes and sizes could also reduce the flow of the fresh mixtures. An explanation for the above is given by Jímenez-Quero et al. 2013, who found that the different shapes and sizes of the SCBA particles increase the friction between the particles during the mixing process of mortars.

A reduction of the volumetric weight and an increase of the air content of the fresh mortars were obtained when the cement replacement increased from 0 to 10 and 20%. This effect was caused by the lower densities of the UtSCBA and FA.

Table 4. Fresh properties of mortars mixtures

Mixture	Flow (%)	Volumetric weight (kg/m^3)	Air content (%)
Control	110.3	2123	2.20
UtSCBA10	113.8	2085	3.27
UtSCBA20	107.9	2070	3.83
FA20	107.5	2070	2.20

Compressive strength of mortars

Table 5 shows the CS of the mortars for the different curing times. At 28 days, the control and the UtSCBA10 and UtSCBA20 mortars showed a CS increment as the curing time increased from 0 to 7 days. However, when the curing time increased from 7 to 28 days a significant CS increment was only observed for the UtSCBA10 and UtSCBA20 mortars. On the other hand, comparing the results from each curing period, a CS decrement was obtained in the mortars as the UtSCBA content increased. This could be attributed to the high LOI content of the UtSCBA. The detrimental effect of the high LOI content (larger than 10%) of the SCBA on lowering the CS in mortars has been reported by Chusilp et al. 2009a. A similar result was reported by Montakarntiwong et al. 2013 in concrete mixtures containing SCBA with a high LOI content.

At 90 days, a CS increment was obtained in the control and in the UtSCBA10 and UtSCBA20 mortars as the curing time increased. However, as observed at 28 days, a CS decrement occurred as the UtSCBA content increased. A slight drop in the CS between 28 and 90 days was observed for the control and the UtSCBA10 and UtSCBA20 mortars when no curing was applied (0 days). This suggests that the CS of the mortars is more sensitive to poor curing as the UtSCBA content increases. CS sensitivity increasing with an increase of SCM has been reported by Ramezanianpour and

Malhotra 1995, who proposed that this sensitivity could be attributed to inherent cementitious properties and the pozzolanic reactivity of the materials. Nonetheless, a parametric statistical analysis indicates that there are not significant differences ($p \gg 0.05$) between the CS results from 28 and 90 days. This indicates no regression in the CS from 28 to 90 days. Previous research on the same mortars tested at 450 and 600 days does not show a deleterious effect of the addition of UtSCBA on the CS (Maldonado-García et al. 2018). Furthermore, other studies do not report a negative effect on the CS in concrete mixtures containing ground SCBA after 10 years (Cordeiro et al. 2018).

Based on the results of the CS at 28 and 90 days (Table 5), 7 days of curing could be enough for a proper CS performance of the mortars containing UtSCBA. This might be useful since an extended curing period is impractical. Nonetheless, an extended curing period such as 28 days is recommended to evaluate the pozzolanic performance of SCMs.

Finally, the FA20 mortar had a lower CS when compared with the control and UtSCBA10 and UtSCBA20 mortars with 28 days of curing. The CS decrement in the FA20 mortar with respect to the control mortar could be attributed to a low pozzolanic reactivity rate of the FA as suggested in other studies (Gastaldini et al. 2010; Ramezanianpour and Malhotra 1995). Otherwise, the CS decrement in the FA20 mortar when compared to the UtSCBA10 and UtSCBA20 mortars suggests that the UtSCBA has a higher amount of amorphous compounds, as observed in the XRD patterns.

Table 5. Compressive strength of the mortars. Standard deviation is indicated in parentheses

Mixture	Curing time (days)	Compressive strength (MPa)	
		28 days	90 days
Control	0	24.8 (1.18)	24.3 (1.29)
	7	29.1 (0.79)	31.6 (0.59)
	28	30.5 (0.69)	36.3 (1.07)
UtSCBA10	0	21.5 (0.80)	20.2 (0.90)
	7	28.3 (0.41)	29.7 (0.84)
	28	31.6 (0.64)	36.4 (0.53)
UtSCBA20	0	18.7 (0.74)	17.4 (0.82)
	7	24.9 (0.41)	24.8 (0.64)
	28	27.0 (0.70)	31.6 (0.29)
FA20	28	23.9 (0.57)	30.8 (1.99)

Chloride diffusion of mortars

The chloride concentration profiles of the mortars are shown in Fig. 5. In the control mortar, the chloride penetration was reduced as the curing time increased. Following the above, at lower depths as the curing time increases the chloride concentration levels of the control mortar fell 0.67 by mass of concrete, a value assumed as a critical chloride threshold for corrosion initiation for galvanized steel embedded in concrete (Darwin et al. 2009). However, the effect of increasing the curing time was only marginally observed in the UtSCBA10 and UtSCBA20 mortars. In these mortars, the chloride concentration was reduced below the chloride threshold practically at the same depth, between 7 and 9 mm. This was very similar to

the depth observed in the FA20 mortar with 28 days of curing.

A more detailed analysis of the results indicates that the chloride concentration of the control and the UtSCBA10 and UtSCBA20 mortars with 0 days of curing was similar between 1 and 3 mm of depth. After that, the chloride concentration of the control mortar became higher, reaching the chloride threshold at a greater depth than in the UtSCBA10 and UtSCBA20 mortars. When 7 days of curing were applied, the control mortar had a lower chloride concentration between 1 and 5 mm of depth than the UtSCBA10 and UtSCBA20 mortars. At greater depths, the chloride concentration values in the control mortar were higher than in the mortars containing UtSCBA. With 28 days of curing, the chloride concentration of the control mortar remained lower between 1 and 7 mm of depth, but was higher than in the UtSCBA10 and UtSCBA20 mortars below 7 mm. A similar result was observed when comparing the control and the FA20 mortars with 28 days of curing. Researchers report that some SCM, such as FA, can increase the surface chloride concentration in concrete (between 0 and 4 mm depth) due to pore network refinement, but also reduces the D_{eff} (Song et al. 2008). In the case of the mortars containing UtSCBA, the increase of the chloride concentration at superficial depths might be attributed to several reasons; one of these is the filler effect (Ganesan et al. 2007), but the UtSCBA used in this research has a large particle-size distribution. Another reason is the pozzolanic reactions of the SCBA (Dhengare et al. 2015); however, the magnitude of the curing effects upon the CS suggest another cause. Analysis of the data suggests physical interactions by electrostatic forces between positively charged particles of the UtSCBA, such as the unburned particles, and the negatively charged chloride ions. With this

proposed mechanism, unburned and agglomerated particles of the UtSCBA work as a physical barrier and as an absorbent media for chlorides due to their large media particle size and large surface area.

The results presented in Fig. 6 show a decrease of approximately 50% and 65% in the D_{eff} in the mortars when 10% and 20% UtSCBA are used, respectively. These decrements are clearly observed when comparing mortars with the same curing time and they were significantly different (p<<0.005) based on the statistical analysis. Those D_{eff} reductions are in agreement with the findings in the literature when SCBA is used as cement replacement in concrete mixtures (Ganesan et al 2007). The D_{eff} decrement in the mortars containing UtSCBA supports the occurrence of the previously proposed physical interactions between unburned particles of UtSCBA and chloride ions. This is also supported by the rehydration of anhydrous cement particles, if any, in the mortars. However, the rehydration process, as well as the pozzolanic reactions between resulting $Ca(OH)_2$ from rehydration of cement particles and the UtSCBA, could take several months (Neville 2000; Sajedi and Razak 2011). From this, a non-significant difference (p>>0.05) in the D_{eff} was observed when comparing 7 and 28 days of curing in each mortar mixture. This might indicate that 7 days of curing is enough for the mortars in spite of the increments in the CS of the mortars when comparing 7 and 28 days of curing.

Finally, the addition of 20% of FA also reduces the D_{eff} in the mortars with 28 days of curing. In this case, a decrement of 50% was obtained with respect to the control mortar with the same curing period. Furthermore, the D_{eff} in the FA20 mortar is comparable with the D_{eff} in the UtSCBA10 mortar with 28 days of curing.
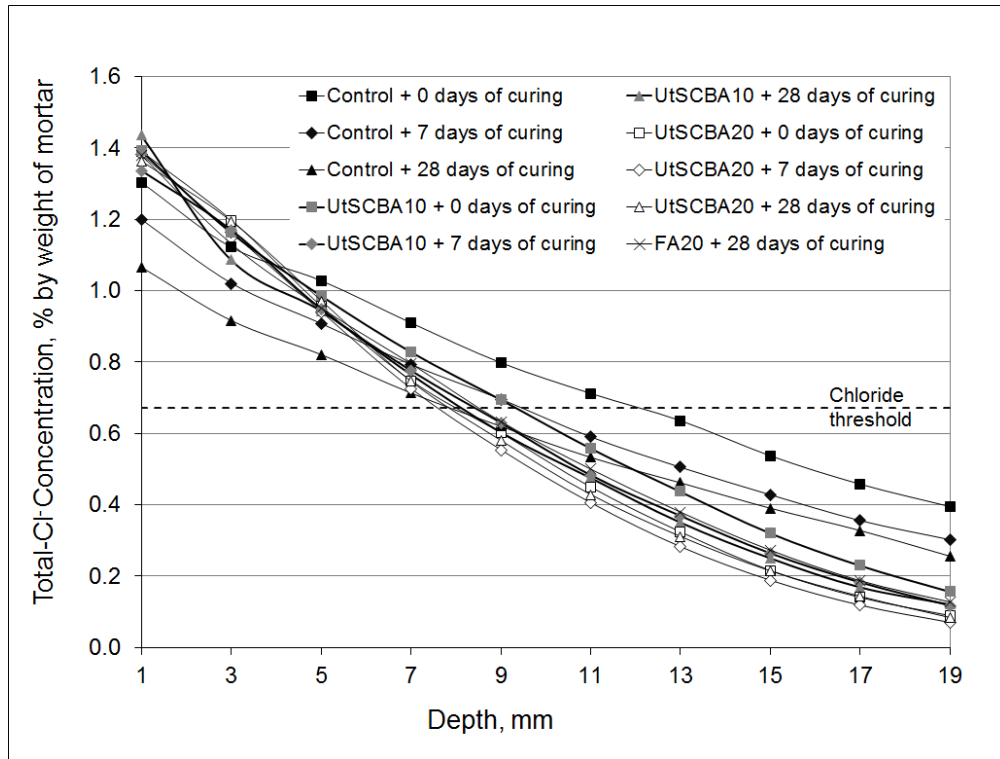
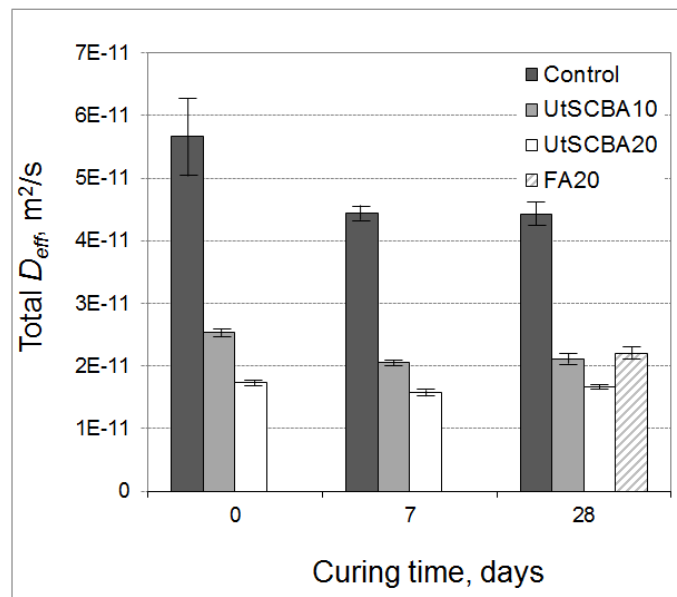**Fig. 5.** Chloride concentration profiles of the mortars

Fig. 6. Chloride diffusion coefficients of the mortars

Corrosion potential of the reinforced mortar slabs

The corrosion potentials (E_{corr}) of the reinforced mortar slabs are shown in Fig. 7. The Ag/AgCl half-cell potential limits were set based on the findings for CSE half-cell limits of the η-phase for galvanized reinforcement bars in chloride-contaminated concrete reported by

Sistonen 2008. The conversion factors between reference electrodes established by the ASTM G3-14 were used for this purpose.

The results in Fig.7a show fluctuations in the E_{corr} readings with sudden drops. The fluctuations match with the periods in which the temperature of the testing room increased (i.e. during the summer). This is in accordance with reports in the literature about the sensitivity of E_{corr} readings to temperature variations (Deus et al. 2012). However, the increase of the E_{corr} readings to more negative values as the temperature increases was only observed before and at the beginning of the drops. After that, the drops may also be associated with changes in the composition of the galvanized meshes in terms of the redox process of the zinc and iron. This finding agrees with that reported in the literature, which mentions an increase in the E_{corr} readings of galvanized steel to more negative values during an extended period before the drops occurs; also, each drop occurs after nearly total consumption of the different corrosion potential limits according to the amount of iron and zinc (Sistonen 2009).

Results also show that the addition of 10 and 20% UtSCBA reduced the corrosion risk of the mortar slabs with 0 days of curing (Fig. 7a). It can be observed that the E_{corr} in the control slab remained in the low corrosion risk condition during the first 64 weeks. Next, the E_{corr} readings increased gradually from the low to the severe corrosion risk condition in a period of 48 weeks. After that, the E_{corr} readings remained in the severe corrosion risk condition for 112 weeks. Finally, the E_{corr} readings decreased to the intermediate corrosion risk condition zone. The UtSCBA10 showed less negative E_{corr} values than those obtained in the control slab. In this case, the E_{corr} readings increased only to the high corrosion risk condition for a short period. Only the UtSCBA20 slab maintained an intermediate corrosion risk over time, showing potentials less negative than those presented by the control and

the UtSCBA10 slabs. In the present study the E_{corr} readings in the control and UtSCBA10 slabs with 0 days of curing remained in the intermediate corrosion risk zone after the fluctuations. This suggests that the zinc coating of the galvanized meshes was completely depleted in large areas of the meshes and therefore the exposed steel began to corrode; this coincides with its propagation period. Furthermore, the fluctuations in the UtSCBA20 slab could be more associated with the changes in the temperature of the testing room because they show values similar to a normal distribution. In this case, the difference between the lowest and the highest corrosion potentials in the fluctuations was less (between 50 and 70 percent) than in the control and UtSCBA10 slabs.

Results in Fig. 7b show that the control and the UtSCBA10 mortar slabs with 7 days of curing remained in a condition of high to severe corrosion risk, showing fluctuations with sudden drops as in the slabs with 0 days of curing. Once again, this suggests that the galvanized coating was completely depleted in large areas from the galvanized meshes in those slabs. Despite the control and the UtSCBA10 slabs showing similar E_{corr} values over time, a beneficial effect on lowering the corrosion risk was found by the use of UtSCBA, which is actually considered a waste material. Only the UtSCBA20 slab showed an intermediate corrosion risk over time without the mentioned fluctuations in the Ec_{corr} readings. In this case, the proposed physical interactions between particles of the UtSCBA and chloride ions may have occurred as described in the last section; in addition, the pozzolanic reactions between the amorphous compounds of the ash, $Ca(OH)_2$ and moisture may have reduced the corrosion of the galvanized meshes. Physical interactions also work as a barrier against the ingress of moisture, oxygen, CO_2 and other aggressive agents (Malhotra 1994).

Fig. 7c shows a better scenario for decreasing the corrosion risk by increasing up to 28 days the initial curing time in the reinforced mortar slabs. In this case, no significant differences were observed when comparing the E_{corr} readings of the control and the UtSCBA10 and UtSCBA20 mortar slabs. A detailed analysis shows that the E_{corr} readings in the UtSCBA10 and UtSCBA20 slabs were slightly more negative (not more than -100mV) than those values observed in the control slab. This suggests that UtSCBA increases the E_{corr} readings in mortars, as observed when comparing the control and the FA20 slabs with 28 days of curing. Roman et al. 2014 report that the slight increases in the E_{corr} readings in concrete with added pozzolans (or pozzolanic cement) can be attributed to the lower content of C_3A, which reacts with chloride ions, decreasing the corrosion activity of the steel bars. Nevertheless, all the reinforced mortar slabs showed an intermediate corrosion risk, even with the slight increment observed in the E_{corr} readings by the used of the UtSCBA and FA. Based on the above, the small difference in the E_{corr} reading observed in Fig. 7c does not conclude a negative effect on lowering the corrosion risk of the reinforced mortar slabs by using UtSCBA.

As the last paragraphs describe, the corrosion risk of the reinforced slabs generally decreases with an increase of UtSCBA content. The results are consistent with the D_{eff} decrements observed for the mortar with added UtSCBA shown in the last section. As expected, the increment of the initial curing time in the reinforced slabs was positive on decreasing the corrosion risk. This is mainly attributed to the pore refinement of the cementitious matrix of the mortars containing UtSCBA, as reported in previous studies (Maldonado-García et al. 2018). Physical interactions between UtSCBA particles and chloride ions may occur; thus, chemical bonding in the mortars containing UtSCBA must be evaluated.
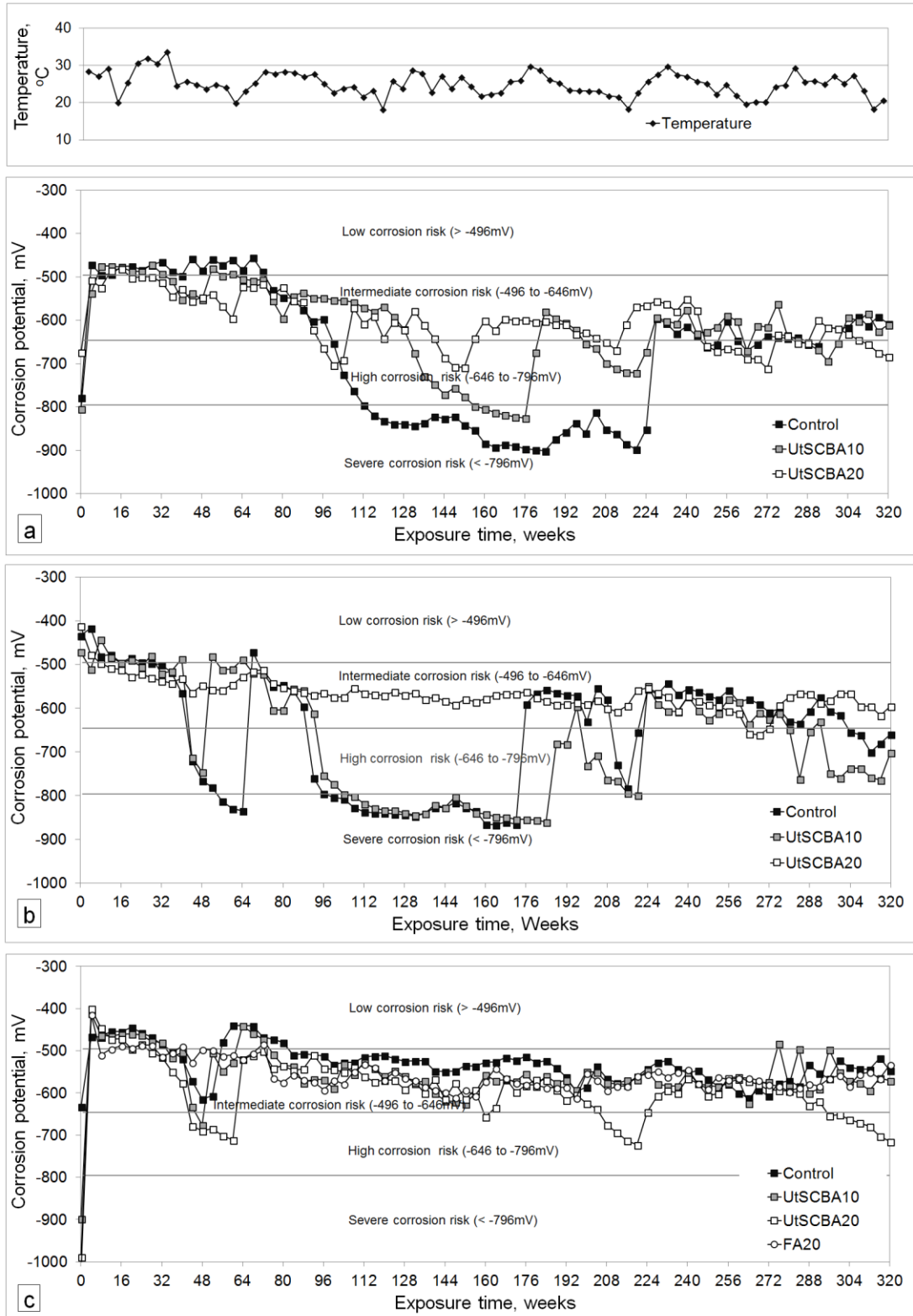
Fig. 7. Corrosion potential measurements of the reinforced mortar slabs with a) 0, b) 7 and c) 28 days of curing

Current densities of the reinforced mortar slabs

Current densities (I_{corr}) of the reinforced mortar slabs are shown in Fig. 8. The fluctuations in the I_{corr} readings linked with the changes in the temperature of the testing room were less evident than in the corrosion potential measurements. Results show that the addition of 10 and 20% UtSCBA reduced the I_{corr} of the mortar slabs with 0 days of curing (Fig. 8a). In this case, the control slab showed a high corrosion-rate condition (above $1 \mu m/cm^2$) after 96 weeks. The UtSCBA10 slab was in the same condition after 128 weeks. However, the I_{corr} values in the UtSCBA10 slab were lower than those observed in the control slab over time. The UtSCBA20 slab showed comparable I_{corr} values to those observed by the UtSCBA10 slab over time even when the UtSCBA10 was in the high corrosion-rate condition after 96 weeks. The results in Fig.8a suggest a beneficial effect of reducing corrosion activity in reinforced mortar slabs by using UtSCBA. This effect can be attributed to the pozzolanic reactions of the UtSCBA during the wetting cycles. The pozzolanic reactions of the UtSCBA could also have occurred even when the slabs were not cured initially, due to the long testing time in which the slabs were exposed to water (during the wetting cycles). During that time the rehydration of anhydrous cement particles occurs by a gradual reduction in the size of the cement particles (Neville 2000), creating additional $Ca(OH)_2$ necessary for the pozzolanic reactions of the UtSCBA. The beneficial effect of slowing steel corrosion in concrete by using SCM has been well documented in the literature (Broomfield 1997; Choi et al. 2006; Neville 2000).

Results in Fig. 8b show the I_{corr} values of the reinforced mortar slabs with 7 days of curing. In this case, the control slab showed higher I_{corr} values, which increased rapidly, than those obtained in the UtSCA10 and UtSCBA20 slabs

during the first 144 weeks. After that the I_{corr} of the control slab kept decreasing below the I_{corr} values in the UtSCBA10 and UtSCBA20 slabs. In contrast, the I_{corr} values in the UtSCBA10 and UtSCBA20 slabs increased slowly during the first 96 weeks; after that they remained practically constant over time. The previous statements also suggest a positive effect of the addition of 10 and 20% UtSCBA in lowering the corrosion activity of the reinforced mortar slabs. As mentioned previously, the pozzolanic reactions between the UtSCBA, the $Ca(OH)_2$ and water could be blamed for this. Nevertheless, results suggest lower corrosion activity in the slab containing 10% UtSCBA instead of 20% UtSCBA.

Fig 8c shows the I_{corr} values of the reinforced mortar slabs with 28 days of curing. In this case, a very noticeable peak from increasing the current densities in the control and the UtSCBA10 and UtSCBA20 slabs is observed between the weeks 24 to 64. This peak was not observed in Fig. 8a and was not well defined in Fig. 8b. This apparently shows that the increment of the initial curing time did not have a positive effect on lowering the corrosion activity of the reinforced mortar slabs. Furthermore, this contrasts with what was expected based on the D_{eff}, in which the chloride diffusion in the control mortar became lower as the curing time increased. Nevertheless, the same effect is also observed in the E_{corr} readings (Fig. 7). An explanation for the above can be found in the literature: a totally dry concrete cannot corrode; however, if the dry concrete is exposed to water saturation the embedded steel corrodes rapidly. Conversely, totally saturated concrete can have a slow corrosion because of oxygen starvation, but if oxygen gains access to the steel the corrosion rate will be very high (Broomfield 1997). In the present research, the slabs with 0 days of curing were in a dry condition before starting the corrosion monitoring. After that, they were exposed to

water saturation (with chlorides) for 12 hours followed by drying in atmospheric conditions during another 12 hours, and this was repeated for 75 months. Under these conditions, a slow but continuous corrosion of the galvanized meshes took place. On the other hand, the slabs with 28 days of curing were completely saturated before their exposure to the wet-dry cycles. Subsequently, oxygen penetrated into the mortar during the drying cycles, corroding the galvanized meshes rapidly during a certain period. However, the zinc corrosion products resulting from the dissolution of the galvanized coating (less voluminous than the iron corrosion products by about 150 to 250%) migrated into the mortar matrix in a three-dimensional planar filling small pores and microcracks, creating an apparent densification of the cementitious matrix adjacent to the reinforcing steel (Yeomas 1998). As reported in previous research (Maldonado-García et al. 2018), mortars with longer curing times have a denser CM; therefore, small spaces in the CM of the slabs can be easily filled by the zinc corrosion products, which in turn reduces corrosion activity in the galvanized meshes.

After the discussion in the previous paragraph, similar I_{corr} values in the control and the UtSCBA10 mortar slabs were observed over time. As expected, the 28 days of initial curing had a positive effect on lowering the corrosion activity in those slabs. The UtSCBA20 slab shows the higher corrosion activity when compared with the control and the UtSCBA10 slabs in Fig. 8c.

The FA20 mortar slab with 28 days of curing showed the lowest corrosion densities over time. This is attributed to the pozzolanic reactions of the FA and its small media-particle size.

Furthermore, the current density peak reported in the control and UtSCBA10 and UtSCBA20 slabs between the weeks 24 to 64 was not observed in the FA20 slab. This could be attributed to the cementing efficiency and the pozzolanic reaction of the FA. In this mechanism, the FA had little cementing efficiency at early ages and worked like a filler, but at later ages, the pozzolanic activity took place (Hemalatha and Ramaswamy 2017).

In this research, the results from the CS show a lower pozzolanic performance of the FA20 mortar at 28 and 90 days when compared with the control and the UtSCBA10 and UtSCBA20 mortars with the same curing period. However, the D_{eff} of the FA20 mortar is lower (by about 50%) than in the control and comparable with the results from the UtSCBA10 mortar (which is also reduced by about 50%). In the case of the reinforced mortar slabs containing UtSCBA, the mentioned peak could be also related to physical interactions between the unburned particles of the UtSCBA and chloride ions, as mentioned in previous sections. However, these physical interactions may be reversed after longer periods of time during the exposure of the slabs to the wet-dry cycles.

As discussed in the last paragraphs, the addition of 10 and 20% UtSCBA decreased the corrosion activity of the reinforced mortar slabs. The increment of the initial curing time also had a positive effect on lowering the corrosion activity of the slabs. This coincides with that reported in the corrosion potential measurements (Fig. 7). In accord with the current density results, the addition of 10% UtSCBA could be enough to reduce corrosion in the mortar slabs.
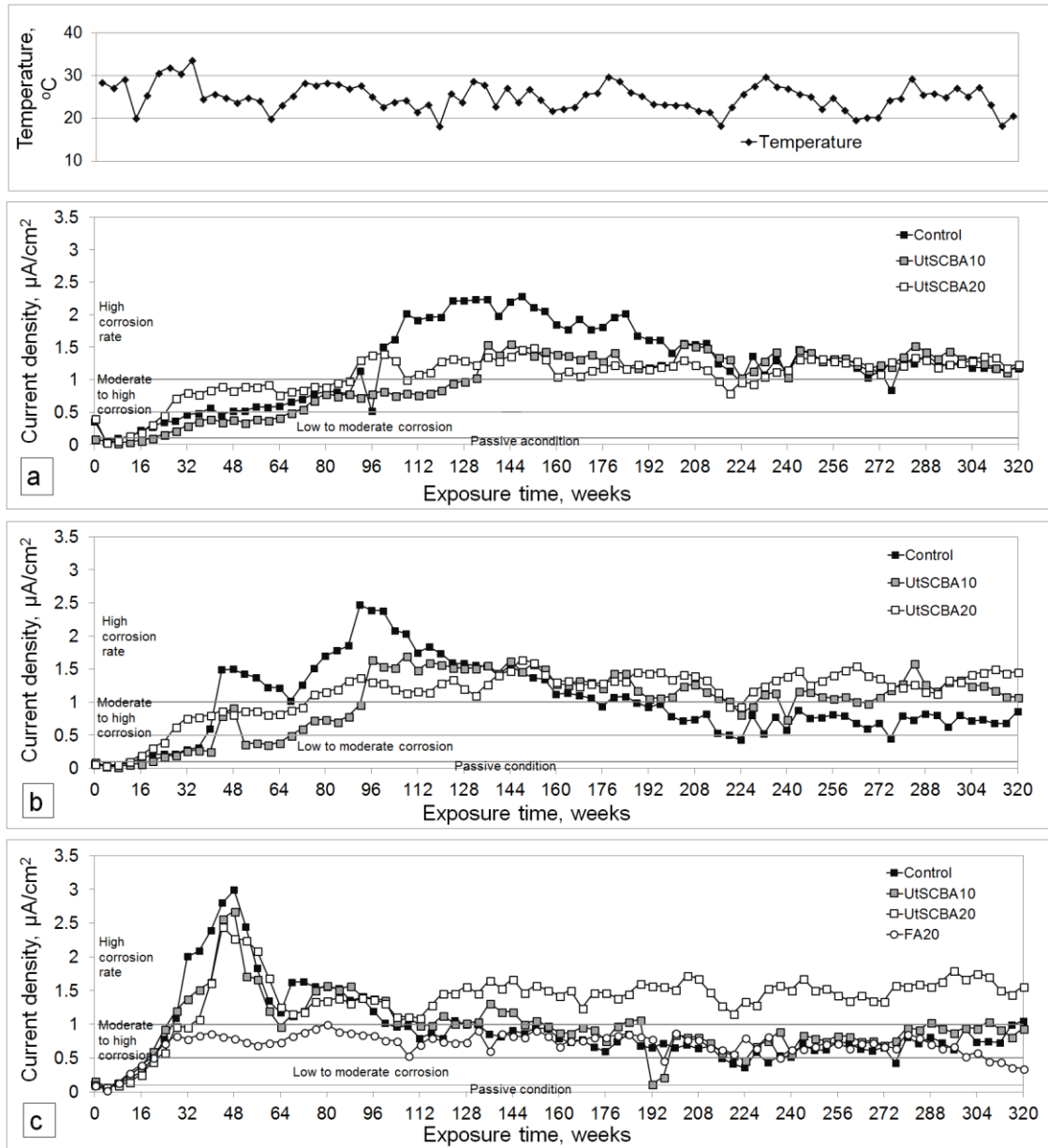
Fig. 8. Current densities of the reinforced mortar slabs with a) 0, b) 7 and c) 28 days of curing

Visual examination of the reinforced mortar slabs

Fig. 9. shows a photographic record of the galvanized steel reinforcement embedded in the different mortar slabs after breakage. It can be observed that the control slabs exhibit large areas with white rust, indicating that the zinc coating of the galvanized meshes has been depleted (Figs. 9a, 9b and 9c). The control slab with 0 days of curing also shows a large surface area with iron corrosion products, which are dark ochre in color due to oxygen starvation (Fig. 9a). The control slabs with 7 and 28 days of curing also show some areas with iron corrosion products (Figs. 9b and 9c). In accord with the images, the control slab with 28 days of curing shows slightly less corrosion products than that

observed in the control slab with 7 days of curing.

On the other hand, the UtSCBA10 slabs show that the galvanizing layer over the steel remains in large areas (Figs. 9d, 9e and 9f). Few corrosion products from iron were observed in these slabs. This confirms less corrosion damage in the UtSCBA10 slabs than in the control slabs as suggested by the electrochemical testing. From this it can be observed that the zinc coating was less depleted as the initial curing time increased in the slabs. Fig. 9d shows that the UtSCBA10 slab with 0 days of curing has small areas with iron corrosion products, which is similar to the iron corrosion products observed in the control slabs. The UtSCBA10 slab with 7 days of curing (Fig. 9e) shows slightly less corrosion damage than the UtSCBA10 slab with 0 days of curing (Fig. 9d). In this case, a small amount of iron corrosion products was also observed. The UtSCBA10 slab with 28 days of curing shows the lowest corrosion damage (Fig. 9f), as smaller corrosion areas than for the 0 and 7 days of curing periods were observed.

The UtSCBA20 slabs (Figs. 9g, 9h and 9i) show larger areas in which the galvanizing layer has been depleted when compared to the UtSCBA10 slabs and also show some areas in which the iron was corroded. However, the corrosion damage observed in the UtSCBA20 slabs is less than that observed in the control slabs. These findings match those reported in the electrochemical result section. In this case, the effect of the initial curing time is difficult to observe because the slabs show a very similar quantity of corrosion products on the galvanized meshes' surface. The UtSCBA20 slab with 0 days of curing shows some areas with white rust and some areas with iron corrosion products in dark or light ochre color (Fig. 9g). A similar set-up is observed in the UtSCBA20 slabs with 7 and 28 days of curing (Fig. 9h and 9i). However, the UtSCBA20 with 28 days of curing shows apparently less corrosion damage than the UtSCBA20 with 0 and 7 days of curing. A further microstructural evaluation of the slabs will help clarify the effect of the initial curing time. Finally, the FA20 slab with 28 days of curing (Fig. 9j) shows corrosion damage which is comparable to that observed in the UtSCBA20 slabs.
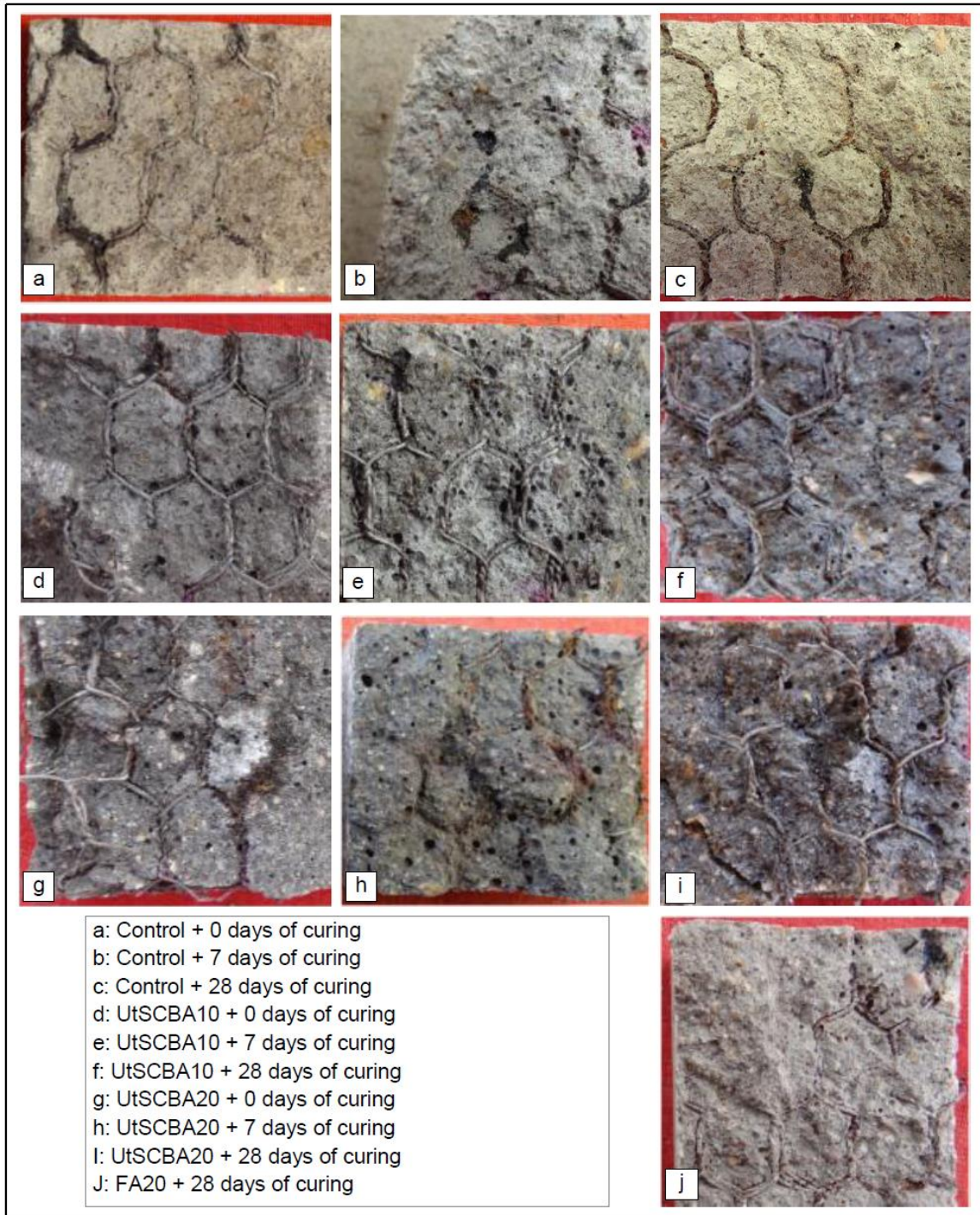
Fig. 9. Images from the visual examination of the reinforced mortar slabs taken after 75 months of testing

CONCLUSIONS

UtSCBA (sieved through 75µm ASTM mesh for five minutes) reduces the workability of mortar mixtures because of the varied sizes and shapes of its particles as well as its high LOI content.

According to the CS results, mortars containing UtSCBA appear more sensitive to

poor curing than the control mortar. The sensitivity increases with the increasing amounts of UtSCBA. On the other hand, a non-significant difference ($p \gg 0.05$) was obtained in the CS results of all mortars when comparing 28 and 90 days of age.

The use of 10 and 20% UtSCBA as cement replacement increases the chloride concentration of mortars at superficial depths (between 1 and 7mm). After that, the chloride concentration of the mortars containing UtSCBA is reduced to below the chloride concentration of the control mortar. This was observed for the three different curing times. However, an increase of 10 and 20% UtSCBA reduces the D_{eff} of the mortars more than 50% and 65%, respectively, which is significantly different ($p \ll 0.05$). The greatest decrease in the D_{eff} ($p \ll 0.05$) was found when the curing period was increased from 0 to 7 days, but only a slight difference ($p \gg 0.05$) was observed when the curing period was extended to 28 days.

The E_{corr} results show that the increase of UtSCBA content reduces the corrosion risk of the reinforced mortar slabs over time even when the mortar slabs are not initially cured. But as well, the decrease in the corrosion risk of the slabs is more evident with an increased initial curing time.

The I_{corr} results show that the use of 10% UtSCBA reduces the long-term corrosion activity of the mortar slabs; however, a lower decrement in the corrosion activity was found when using 20% of UtSCBA.

The visual examination shows that the addition of 10 and 20% UtSCBA was beneficial in reducing the corrosion damage of the mortar slabs, which agrees with that reported in the electrochemical testing. However, in ongoing research a further microstructural evaluation will help to clarify the effect of the increase of UtSCBA from 10 to 20% in lowering the corrosion resistance of the slabs.

According with the results, the addition of 10% UtSCBA as a partial Portland cement replacement performs as a better option than 20% UtSCBA in decreasing the risk of corrosion in reinforced mortars. Further, 7 days of curing could be enough for a proper performance of the mortars containing UtSCBA.

ACKNOWLEDGMENTS

REFERENCES

Akram T., Memon S.A., and Obaid H. (2009). "Production of low-cost self-compacting concrete using bagasse ash." *Constr. Build. Mater.,* 23(2), 703–12.

Angst U., Elsener B., Larsen C.K., and Vennesland Ø. (2009). "Critical chloride content in reinforced concrete – A review." *Cem. Concrete. Res.*, 39(12), 1122 1138.

Aprianti E., Shafigh P., Bahri S., and Nodeh F. J. (2015). "Supplementary cementitious materials' origin from agricultural wastes – A review." *Constr. Build. Mater.,* 74, 176-187.

Arenas-Piedrahita J.C., Montes-García P., Mendoza-Rangel J.M., López-Calvo H.Z., Valdez-Tamez P.L., and Martínez-Reyes J. (2016). "Mechanical and durability properties of mortars prepared with untreated sugarcane bagasse ash and untreated fly ash." *Constr. Build. Mater.,* 105, 69-81.

Austin S. A., Lyons R., and Ing M. (2004). "Electrochemical behavior of steel-reinforced concrete during accelerated corrosion testing." *Corrosion.,* 60(2), 203-212.

Bahurudeen A., and Santhanam M. (2015). "Influence of different processing methods in the pozzolanic performance of sugarcane bagasse ash." *Cem. Concrete. Comp.,* 56, 32-45.

Batra V.S., Urbonaite S., and Svensson G. (2008). "Characterization of unburned carbon in bagasse fly ash." *Fuel.,* 87(13-14), 2972-2976.

Broomfield J.P. (1997). *Corrosion of steel in concrete*, E & FN Spon, London.

Choi Y.S., Kim J. G., and Lee K.M., (2006). "Corrosion behavior of steel bar embedded in fly ash concrete." *Corros. Sci.,* 48(7), 1733-1745.

Chusilp N., Jaturapitakkul C., and Kiattikomol K. (2009a). "Effects of LOI of ground bagasse ash on the compressive strength and sulfate resistance of mortars." *Constr. Build. Mater.*, 23(12), 3523-3531.

Chusilp N., Jaturapitakkul C., and Kiattikomol K. (2009b). "Utilization of bagasse ash as a pozzolanic material in concrete." *Constr. Build. Mater.*, 23(11), 3352-3358.

Cordeiro G. C., Toledo-Fhilo R. D., and Fairbairn E. M. R. (2010). "Ultrafine sugarcane bagasse ash: high potential pozzolanic material for tropical countries." *IBRACON Estrut. Mater.,* 3(1), 50-67.

Cordeiro G. C., Toledo Filho R. D., Fairbairn E. M. R. (2012). "Experimental characterization of binary and ternary blended-cement concretes containing ultrafine residual rice husk and sugarcane bagasse ashes." *Constr. Build. Mater.,* 29, 641-646.

Cordeiro G. C., Paiva O. A., Toledo Fhilo R. D. Fairbairn E. M. R., and Tavares L. M. (2018). "Long-term compressive behaviour of concretes with sugarcane bagasse ash as a supplementary cementitious material". *J. Test. Eval.,* 46(2), 564-573.

Darwin D., Browning J., O´Reilly M., Xing L., and Ji J. (2009). "Critical chloride corrosion threshold of galvanized reinforcing bars." *ACI Materials Journal.,* 106(2), 176-183.

Deus J. M., Freire L., Montemor M. F., and Nóvoa X.R (2012). "The corrosion potential of stainless steel rebars in concrete: Temperature effect." *Corros. Sci.,* 65, 556-560.

Dhengare S., Amrodiya S., Shelote M., Asati A., Bandwaf N., Anand K., and Jichkar R. (2015). "Utilization of sugarcane bagasse ash as a supplementary cementitious material in concrete and mortar – A review." *International Journal of Civil Engineering and Technology.,* 6(4), 94-106.

Frias M., Villar E., and Svastano H. (2011). "Brazilian sugarcane bagasse ashes from the cogeneration industry as active pozzolans for cement manufacture." *Cem. Concrete Comp.,* 33(4), 490-496.

Ganesan K., Rajagopal K., Thangavel K. (2007). "Evaluation of bagasse ash as supplementary cementitious material." *Cem. Concrete Comp.,* 29(6), 515-524.

Gastaldini A. L. G., Isaia G. C., Saciloto A. P., Missau F., and Hoppe T. F. (2010). "Influence of curing time on the chloride penetration resistance of concrete containing rice husk ash: A technical and economical feasibility study." *Cem. Concrete Comp,.* 32(10), 783-793.

Hamalatha T. and Ramaswamy A. (2017). "A review on fly ash characteristics – Towards promoting high volume utilization in developing sustainable concrete". *J. Clean. Prod.*, 147, 546-559.

Jímenez-Quero V. G., León-Martínez F. M., Montes-García P., Gaona-Tiburcio C., and Chacón-Nava J.G. (2013). "Influence of sugarcane bagasse ash and fly ash on the rheological behavior of cement pastes and mortars." *Constr. Build. Mater.,* 40, 691-701.

Katare V. D., Madurwar M. V. (2017). "Experimental characterization of sugarcane biomass ash – A review" *Constr. Build. Mater.,* 152, 1-15.

Liu J., Qiu Q., Chen X., Wang X., Xing F., Han N., and He Y. (2016). "Degradation of fly ash concrete under the coupled effect of carbonation and chloride aerosol ingress." *Corros. Sci.,* 112, 364-372.

Lothenbach B., Scrivener K., and Hooton R. D. (2011). "Supplementary cementitious materials." *Cem. Concrete Res.,* 41(12), 1244-1256.

Maldonado-García M. A., Hernández-Toledo U. I., Montes-García P., and Valdez-Tamez P. L. (2018). "The influence of untreated sugarcane bagasse ash on the microstructural and mechanical properties of mortars." *Mater. Construcc.,* 68(329), e148.

Maldonado-García M. A., Montes-García P., and Valdez-Tamez P. L. (2017). "A review of the use of sugarcane bagasse ash with a high LOI content to produce sustainable cement composites." *PRO119: Proceedings of the 2nd International Conference on Bio-based Building Materials.*, RILEM Publications S.A.R.L., Paris, France, 595-605.

Malhotra V.M. (1994). *Fly ash in concrete,* CANMET publications. Ontario.

Martirena, F., Middenford B., Day R. L., Gehrke M., Roque P., Martinez L., and Betancourt S. (2006). "Rudimentary, low-tech incinerators as a means to produce reactive pozzolan out of sugarcane straw." *Cem. Concr. Res*., 36(6), 1056-1061.

Michel A., Otieno M., Stang H., and Geiker M. R. (2016). "Propagation of steel in concrete: Experimental and numerical investigations." *Cem. Concrete Com.,* 70, 171-182.

Montakarntiwong K., Nuntachi C., Weerachat T., and Chai J. (2013). "Strength and head evolution of concretes containing bagasse ash from thermal power plants in sugar industry." *Mater. Design.,*. 49, 414-420.

Morales E. V., Villar-Cociña E., Frías M., Santos S. F., and Savastano Jr. H. (2009). "Effects of calcining conditions on the microstructure of sugarcane waste ashes (SCWA): influence in the pozzolanic activation." *Cem. Concrete Comp.,* 31(1), 22-28.

Neville A. (2000). *Properties of Concrete,* Prentice Hall, London.

Nuñez-Jaquez R. E., Buelna-Rodríguez J.E., Barrios-Durstewitz C.P., Gaona-Tiburcio C., and Almeraya-Calderón F. (2012). "Corrosion of modified concrete with sugarcane bagasse ash." *International Journal of Corrosion.,* 2012, 1-6.

Ramachandram V. S. (2001). *Handbook of analytical techniques in concrete science and technology. Principles, techniques and applications*, Noye Publicatios, Park Ridge, Yersey, USA.

Ramezanianpour A. A., and Malhotra V.M. (1995). "Effect of curing on the compressive strength, resistance to chloride-ion penetration and porosity of concretes incorporating slag, fly ash or silica fume." *Cem. Concrete Comp.,* 17(2), 125-133.

Ríos-Parada V., Jíménez-Quero V. G., Valdez-Tamez P. L., and Montes-García P. (2017). "Characterization and use of an untreated Mexican sugarcane bagasse ash as supplementary material for the preparation of ternary concretes" *Const. Build. Mater.,* 157, 83-95.

Rivera-Corral J. O., Fajardo G., Arliguie G., Orozco-Cruz R., Deby F., and Valdez P. (2017). "Corrosion behaviour of steel reinforcement bars embedded in concrete exposed to chlorides: Effect of surface finish." *Constr. Build. Mater.,* 147, 815-826.

Román J., Vera R., Bagnara M., Carvajal A. M., and Aperador W. (2014). "Effect of chloride ions on the galvanized steel embedded in concrete prepared with cements of different composition." *Int. J. Electrochem. Sci*., 9, 580-592.

Sajedi F., Razak H. A. (2011). "Effects of curing regimens and cement fineness on the compressive strength of ordinary cement mortars." *Constr. Build. Mater.,* 25(4), 2036-2045.

Shi X., Xie N., Fortune K., and Gong J. (2012). "Durability of steel-reinforced concrete in chloride environments: An overview." *Constr. Build. Mater.,* 30, 125-138.

Simčič T., Pejovnik S., De Schutter G., and Bokan B. V. (2015). "Chloride ion penetration into fly ash concrete during wetting-drying cycles." *Constr. Build. Mater.,* 93, 1216-1223.

Sistonen E. (2009). *Service life of hot-dip galvanized reinforcement bars in carbonated and chloride-contaminated concrete.* PhD dissertation, Helsinki University of Technology.

Sistonen E., Cwirzen A., Puttonen J. (2008). Corrosion mechanism of hot-dip galvanised reinforcement bar in cracked concrete. *Corros. Sci.,* 50, 3416-3428

Soares M. M. N. S., Poggiali F. S. J., Bezerra A. C. S., Figueiredo R. B., Aguilar M. T. P., Cetlin P. R. (2014). "The effect of the calcination conditions on the physical and chemical characteristics of sugar cane bagasse ash." *R. Esc. Minas.,* 67, 33-39.

Somna R., Jaturapitakkul C., Rattanachu P., Chalee W. (2012). "Effect of ground bagasse ash on mechanical and durability properties of recycled aggregated concrete." *Mater. Design.,* 36, 597-603.

Song H. W., Lee C. H., Ann K. Y. (2008). "Factors influencing chloride transport in concrete structures exposed to marine environments." *Cem. Concrete Comp.,* 30(2), 113-121.

Torres Agredo J., Mejía de Gutiérrez R., Escandon Giraldo C. E., González Salcedo L. O. (2014). "Characterization of sugarcane bagasse ash as supplementary material for Portland cement." *Ing. Inv.,* 34(1), 5-10.

Torres-Luque M., Bastidas-Arteaga E., Schoefs F., Sánchez-Silva M., and Osma J. F. (2014). "Non-destructive methods for measuring chloride ingress into concrete: State-of-the-art and future challenges." *Constr. Build. Mater.,* 68, 68-81.

UNC (Unión Nacional de Cañeros A. C. de México). (2017). www.caneros.org.mx_(October 04, 2017).

Valencia G., Mejía de Gutierrez R., Barrera J., and Delvastos S. (2012). "Estudio de durabilidad y corrosión en morteros armados adicionados con toba volcánica y ceniza de bagazo de caña de azúcar." *Rev. Constr.,* 12(2), 112-122. (In Spanish).

Verma S. K., Bhadauria S. S., and Akhtar S. (2013). "Review of nondestructive testing methods for condition monitoring of concrete structures." *Journal of Construction Engineering.,* 2013, 1-12.

Yeomas S. R. (1998). "Corrosion of the zinc alloy coating in galvanized reinforced concrete." *Corrosion.,* 653, 1-10.

Yurtdas I., Burlion N., Skoczylas F. (2004). "Experimental characterization of the dry effect on uniaxial mechanical behavior of mortar." *Mater. Struct.,* 37, 170-176.

CHAPTER SIX

Corrosion evaluation of reinforced sugarcane bagasse ash mortar slabs by ultrasonic guided waves.

Maldonado-García Marco Antonio, Montes-García Pedro, Valdez-Tamez Pedro Leobardo.

2018.

Manuscript in preparation

Corrosion evaluation of reinforced sugarcane bagasse ash mortar slabs using ultrasonic guided waves

Marco Antonio Maldonado-García.[1], Pedro Montes-García[2,*], Pedro Leobardo Valdez-Tamez[3]

[1] PhD candidate. Instituto Politécnico Nacional, CIIDIR Oaxaca, Hornos 1003, Col. Noche Buena, Sta. Cruz Xoxocotlán, C.P. 61230, Oaxaca, México.

[2] PhD. Instituto Politécnico Nacional, CIIDIR Oaxaca, Hornos 1003, Col. Noche Buena, Sta. Cruz Xoxocotlán, C.P. 61230, Oaxaca, México.

[3] PhD. Universidad Autónoma de Nuevo León, Facultad de Ingeniería Civil, Cd Universitaria s/n, San Nicolás de los Garza, C.P. 66451, Nuevo León, México.

* Corresponding author: (951) 517 0619 ext. 82775. pmontesgarcia@gmail.com, pmontes@ipn.mx

Abstract: In this research, the effect of untreated sugarcane bagasse ash (UtSCBA) in corrosion of thin reinforced mortar slabs exposed to wet-dry cycles in a 3% NaCl solution during 75 months was evaluated. The slabs were cast with 0, 10 and 20% of UtSCBA as a partial Portland cement replacement. Curing regimes of 0, 7 and 28 days were applied to the slabs as well. Two galvanized wire meshes with 0.68mm in diameter were used as reinforcement for the slabs. The corrosion of the slabs was evaluated by corrosion potentials and current density mapping and by ultrasonic guide waves (UGW). The ultrasonic pulse velocity (UPV), amplitude and energy were obtained from the UGW signals. Electrochemical measurements showed less corrosion risk in the mortar slabs containing UtSCBA. Results from UPS do not show significant differences in the slabs; however, the analysis of the amplitude and energy suggest less corrosion in the slabs containing UtSCBA. As expected, the increase of the curing time was beneficial. Correlations between corrosion potentials and amplitude and energy shows the capability of UGW to evaluate the corrosion damage in cement composites added with UtSCBA as supplementary cementitious material.

Keywords: Supplementary materials, reinforced mortar, non-destructive testing, durability.

ORCID ID: Marco Antonio Maldonado-García (http://orcid.org/0000-0002-9522-6779); Pedro Montes-García (http://orcid.org/0000-0003-3799-8372); Pedro Leobardo Valdez-Tamez (http://orcid.org/0000-0002-1298-2051).

INTRODUCTION

Corrosion is a serious problem in reinforced concrete (RC). This problem leads to high repair cost or to the final collapse of the RC structures in extreme circumstances. Corrosion can occur due to the presence of harmful chemical substances, such as chlorides, in the surrounding environment in which RC is exposed. Chlorides penetrate through the cementitious matrix of RC reaching a maximum value at which the passive firm of steel is broken, allowing corrosion [Angst et al. 2009, Shi et al. 2012].

Researchers around the world have been used different supplementary cementitious materials (SCM) to improve the microstructure and reduce corrosion in RC [Lothenbach et al. 2011, Aprianti et al. 2015]. One of these materials is sugarcane bagasse ash (SCBA). SCBA is a byproduct from sugar mills which contain silica, aluminum and iron oxides as main compounds. Researchers affirm that this ash improves the

microstructural and mechanical properties of concrete and could help to combat corrosion in RC [Ganesan et al. 2007, Nuñez-Jaquez et al. 2012, Maldonado-García et al. 2018, Cordeiro et al. 2018].

Corrosion in RC can be monitored by a wide range of non-destructive techniques including electrochemistry detection and ultrasound wave testing [Verma et al. 2013]. Electrochemical methods such as half-cell corrosion potentials and linear polarization tests have been commonly used to evaluate the corrosion process of RC. However, these techniques are sensitive to the surface state changes of the concrete [Verma et al. 2013]. Compared with the electrochemistry-based methods, the ultrasound wave propagation method provides supplementary tools for a more accurate non-invasive and non-destructive monitoring because of its physical approaches [Sharma et al. 2010, Lei et al. 2013]. On this context, the ultrasound guide waves (UGW) appears to be an alternative to evaluate corrosion in RC due to its high sensitivity at a single frequency [Ervin and Reis 2008, Li et al. 2014].

There are three different methods in which the UGW can be applied: transmission-reception, pulse-echo and impact-echo. From these, the transmission-reception method is divided in direct, semi-direct and indirect modes [McCann and Forde 2001, Martínez-Martínez 2008]. Each method can be used in diverse RC evaluations. The ultrasonic pulse velocity (UPV) is the most common parameter obtained from the UGW signals to evaluate the RC, this is by measuring the time in which the ultrasonic pulse travels through a known path length [Verma et al. 2013]. However, a number of researchers report that other parameters such as amplitude, energy and frequency from the UGW signals can be used to evaluate the RC quality [Gaydecki et al. 1992, Yeih and Huang 1998, Liang and Su 2001, Kořenská et al 2006, Sagar et al. 2012, Khan and Bartoli 2015, Fröjd and Ulriksen

2016]. In summary, those researchers concluded that the UGW signals has a remarkably sensitivity to evaluate the RC and affirm that signal attenuation, loss of energy and frequency decrement in the UGW imply defects in the RC caused by external factors (such as loading) or internal factors (such as rebar corrosion). Traditionally, the compressional ultrasonic waves (P-waves) have been used to evaluate the RC. Nevertheless, the shear waves (S-waves) can be also used for that purpose because they are less sensitive to confinement and boundary conditions than P-waves [Lee et al. 2016]. This implies that S-waves have the potential for better in situ or specific evaluations. Following the above, several researches have focused on the evaluation of RC by using the UGW. However, it appears there are not studies addressing corrosion monitoring in RC containing SCM employing the UGW.

Considering the previous statements, the corrosion of small-scale reinforced mortar slabs containing untreated sugarcane bagasse ash (UtSCBA) as cement replacement, exposed to a simulated marine environment for 75 months, was evaluated in this research by the UGW technique. The P and S waves were used for that purpose.

EXPERIMENTAL PROCEDURE

Description of the reinforced mortar slabs

A total of 9 reinforced mortar slabs (250 x 200 x 30mm) were evaluated in this research. The slabs were cast with 0, 10 and 20% of sugarcane bagasse ash sieved by the 75µm ASTM mesh for five minutes as partial Portland cement replacement (CPC-30R Apasco®), called as untreated sugarcane bagasse ash (UtSCBA) in previous researches [Arena-Piedrahita 2016, Maldonado-García et al. 2018]. Three slabs were cast from each mortar binder and were named as Control, UtSCBA10 and UtSCBA20, respectively. The mortar binders

had 0.63 water/cementitious material and 1:3 cementitious material/sand rations. A polycarboxylate-based high-range water reducer Plastol 4000® was added to the mortar binders containing 10 and 20% of UtSCBA to achieve the 110±5 mortar flow. Two galvanized hexagonal wire meshes with 12.7mm in aperture and 0.68mm in diameter were used as reinforced for the slabs. The meshes were placed in the middle of the thickness, leaving 20mm of cover from each edge (Fig. 1).
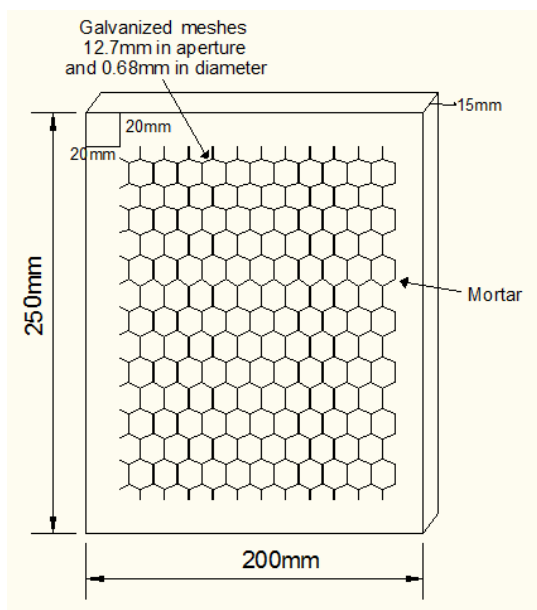

Fig. 1. Schematic view of the reinforced mortar slabs design

Exposure conditions of the reinforced slabs

After casting, curing regimes of 0, 7 and 28 days were applied to all the specimens. Once the maturity period was reached (28 days), the slabs were exposed to wetting-drying cycles of 12 hours each in a 3% NaCl solution to simulate a tidal effect during 75 months (Fig.2). The solution was changed periodically as suggested by the ASTM C1543 standard. At the end of the exposure time corrosion potentials, current density and UGW tests were carry out.

Fig. 2. Exposure conditions of the reinforced mortar slabs

Corrosion potentials and corrosion current density tests.

The corrosion potentials were obtained according with the ASTM C 876 standard. An Ag/AgCl half-cell and a high-impedance digital voltmeter M. C. Miller Co LC-4® were used for that purpose. A total of 172 corrosion potential measurements were taken from each slab at every 12.7mm which coincides with the aperture of the galvanized meshes. The slabs were divided in 12 sections (A-L) and the mean corrosion potential for each section was obtained.
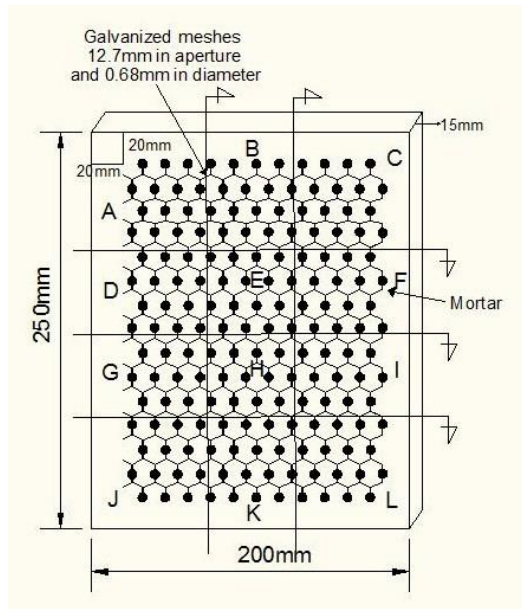
Fig. 3. Distribution of the corrosion potentials in the discrete reinforced mortar slabs (A-L)

The current densities were obtained from linear polarization tests following the procedures in the ASTM G 59 standard. A potentiostat Gamry® series G 300 and an arranged guard ring, 50mm in diameter and 5mm in thickness, coupled to an Ag/AgCl half-cell were used for the tests (Fig. 4a). The working electrode was polarized to $\pm 20mV$ vs E_{ref}. A total of 12 points (A-L) were tested for the current densities as show in Fig. 4b. The diameter of the guard ring was chosen accordingly to the used transducers in the UGW tests.
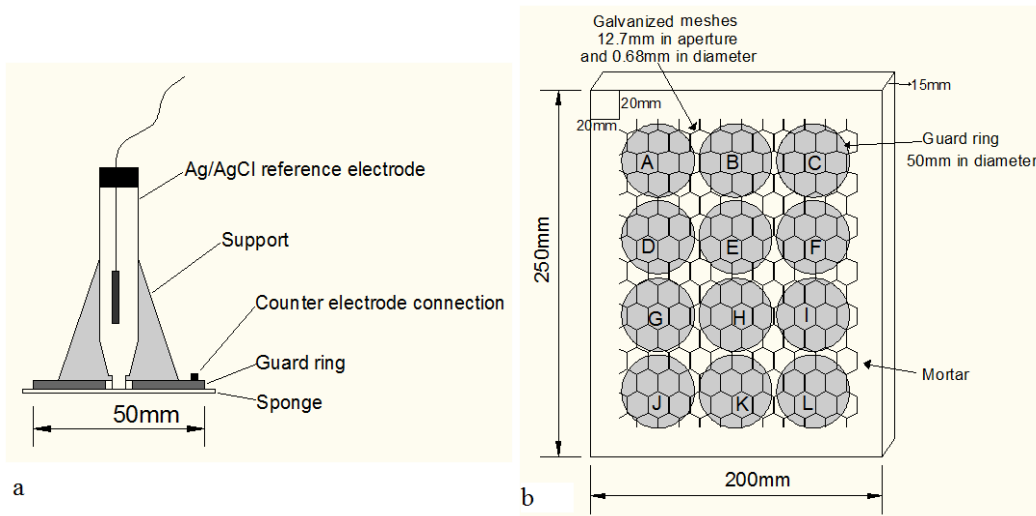

Fig. 4. Corrosion current density tests a) arranged guard ring and b) tested points (A-L)

Ultrasonic measurements

The ultrasonic testing of the reinforced mortar slabs was done in saturated conditions. A pair of P-wave transducers with a frequency of 50 kHz (X1021 Panametrics®) and a pair of S-wave transducers with a frequency of 0.1 MHz (V1548 Panametrics®) were used for the ultrasonic testing. The frequency of the transducers was chosen because a conventional ultrasonic testing does not extend 500 kHz in and

RC evaluations [Gaydecki et al. 1992, Yeih and Huang 1998, Lee et al. 2016]. From this, 50 kHz appears to be the most suitable frequency for concrete evaluation [ACI 228.2R-98, Oh 2012]. The transducers were coupled at both sides of the slab´s surface using a medium-grade petroleum-based grease. A total of twelve spots (from sections A to section L in Fig. 3) in A-scan mode were taken for each slab. A high voltage pulser-receiver Olympus 5058PR® and a TDS 3014C

digital phosphor oscilloscope Tektronix® were used for the signal generation and acquisition, respectively (Fig. 5). A rep-date of 50Hz, a damping of 200Ω and a voltage of 200V were used for the UGW signals generation. No filters were used during the ultrasonic measurements. The UGW signals were recorded for a further processing using the Matlab® software.

Fig. 5. The used equipment for ultrasonic measurements in the reinforced mortar slabs

Ultrasonic parameters

The UPV, amplitude and waveform energy were obtained from the recorded UGW signals (P and S waves). For this purpose, the UGW signals were corrected by attenuation and gain (40 and 60dB for P-waves and 19 and 60dB for S-waves). The UPVs were calculated by measuring the wave arrival time of the recorded UGW signals. The maximum peak amplitude was obtained from the absolute values of the UGW signals. Both, the UPVs and the attenuations were acquired in the time-domain. Whereas, the waveform energy (in absolute value) of the UGW signals was calculated in the frequency-domain using the Fast Fourier Transform.

Visual examination

After the ultrasonic testing, the slabs were broken into 12 small square sections (in accordance with the distribution of the 12 testing sections showed in Fig. 3 using an electric diamond cutting machine. Next, the sections were transversely opened by hammer and chisel to observe the corrosion of the slabs in the steel/mortar interface. The visual examination of the slabs was done following the recommendations of the ASTM C 856 standard.

RESULTS AND DISCUSSION
Corrosion potentials and corrosion current densities

The average results from the corrosion potential measurements and current densities tests of the reinforced mortar slabs are shown in Figs. 6 and 7, respectively. The average corrosion potentials from each section (A-L) in the slabs (Fig. 6) range between -488 to -654mV which is a high value because of the zinc coating of the galvanized meshes [Sistonen 2008]. According with this reference, an intermediate corrosion risk is suggested for the reinforced mortar slabs. Results also show low variability in the corrosion potentials which suggest a dense cementitious matrix in each slab. In general, a non-significant difference on the corrosion potentials was observed when comparing the control slab against the UtSCBA10 and UtSCBA20 slabs with 0 days of curing (Fig. 6a). Based on this, it can be concluded that the addition of 10 and 20% of UtSCBA do not have a negative effect on increasing the corrosion risk of the uncured reinforced mortar slabs. A similar effect by the addition of UtSCBA was noted when applying 7 days of curing in the slabs (Fig. 6b). With 28 days of curing, a significant decrement in the corrosion potentials between the control and the UtSCBA10 slabs was obtained, nonetheless, the UtSCBA20 slab shows similar corrosion potentials when comparing to the control (Fig. 6c). On the other hand, it can be observed that the corrosion potentials of the slabs decreased when the curing time increased from 0 to 7 (Fig. 6b) and from 0 to 28 days (Fig. 6c). According with the above, a positive effect on decreasing the corrosion risk in the slabs by the increment of the initial curing

time could be noted since a difference of 100mV in the corrosion potentials might be significant [Sistonen 2008].
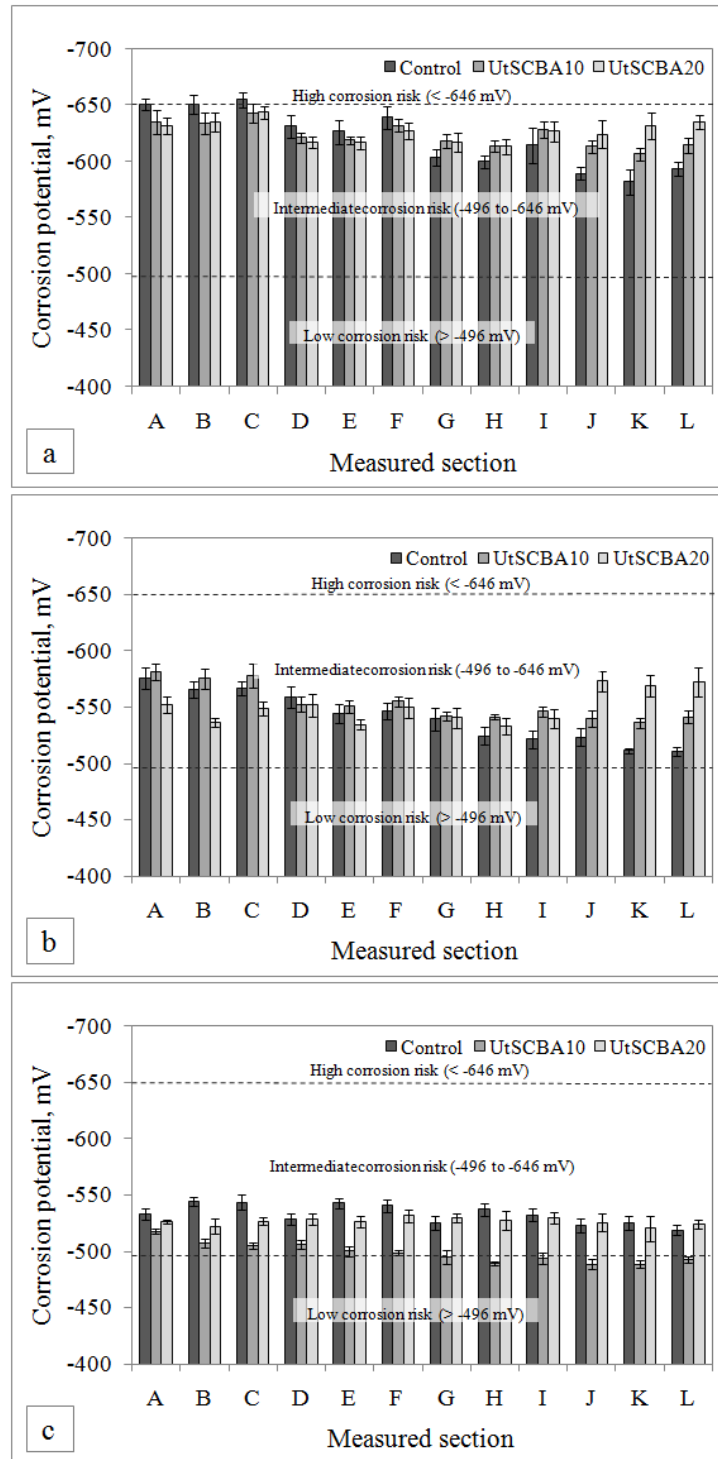

Fig. 6. Corrosion potential measurements of the reinforced mortar slabs. The corrosion potential limits showed in dotted lines correspond to the η-phase of galvanized steel. a) 0, b) 7 and c) 28 days of curing

The average corrosion current densities of the reinforced mortar slabs are show in Fig. 7. The variability of the current densities from each slab may indicate a non-uniform corrosion activity in the galvanized meshes. Apparently, the results show that the addition of 10 and 20% of UtSCBA increased the corrosion current density in the slabs which may suggest a detrimental effect. This same tendency was observed for the three different curing times. However, according to the data all the slabs might have a comparable corrosion activity (around $1\mu A/cm^2$) after 75 months of exposure in the simulated marine environment. According with the above, a comparison of the corrosion activity between the slabs could be trickly since the galvanized meshes could have pits on its criss-crossed areas and linear polarization devices cannot differentiate between general and pitting corrosion [Broomfield 1997]. Furthermore, a comparison between the corrosion current density results and the ultrasonic parameters could not be reliable in this case.
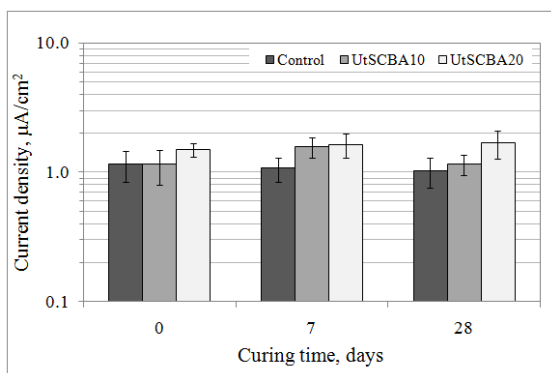

Fig. 7. Corrosion current density of the reinforced mortar slabs

Evaluation of the reinforced mortar slabs by P-waves

Ultrasonic pulse velocity

The average results of the UPV of P-waves (Vp) in the reinforced mortar slabs are shown in Fig. 8. Results do not show a significant difference between the Vp in the control and in the UtSCBA10 and UtSCBA20 mortar slabs when 0, 7 and 28 days of curing are applied. Because all Vp values in the reinforced mortar slabs ranges between 3500 to 4500m/s, typical Vp values for concrete [Lee et al. 2016], a non-significant difference was found when comparing the results from the three different curing times. The thickness of the slabs could be a problem when analyzing the UPV by direct transmission mode. Researches advice that the longitudinal waves travelling along thin sections, such as plates, becomes dispersive and the velocity is a relationship of different frequency components [Jones and Fǎcǎoaru 1969].
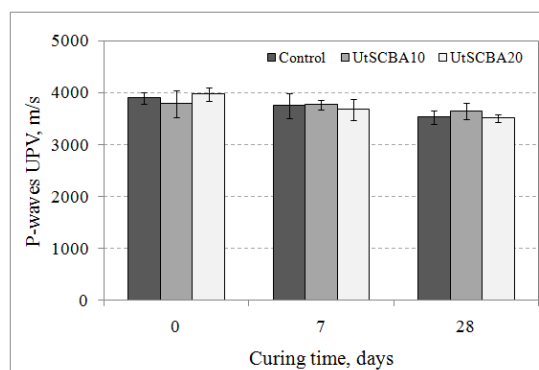

Fig. 8. Ultrasonic pulse velocity of the reinforced mortar slabs by P-waves

Amplitude

The average of the maximum amplitude by P-waves of the reinforced mortar slabs are shown in Fig. 9. Results show comparable amplitudes by P-waves in the control and the UtSCBA10 mortar slabs when 0 days of curing is applied. Nonetheless, the UtSCBA20 slab had greater amplitude than the control and the UtSCBA10 slabs. It was found that the amplitude in the UGW signals from the control and the UtSCBA10 and UtSCBA20 slabs began to rise as the initial curing time increases from 0 to 7 days. The above agrees with the corrosion potentials in which less corrosion risk for the slabs with 7 days of curing where reported. In

fact, the presence of porous zones is common when a mortar is not properly cured [Maldonado-García et al. 2018], leading to a higher corrosion risk than initially cured mortars. According with the above, the amplitude of UGW signals might be a capable method for corrosion damage evaluation as mentioned by other researchers [Yeih and Huang 1998, Fröjd and Ulriksen 2016]. It was also found that the amplitude of the UGW signals increased as the content of UtSCBA increases from 0 to 10 and 20% when 7 days of curing are applied. This could be attributed to the pore refinement of the mortar matrixes containing UtSCBA [Maldonado-García et al. 2018]. With 28 days of curing, the amplitude of the control and the UtSCBA10 slabs remain practically constant when compared with the slabs with 7 days of curing and as observed in the VPU by P-waves. This might indicate that 7 days of curing could be enough for proper performance of the reinforced mortar slabs containing 0 and 10% of UtSCBA against corrosion.
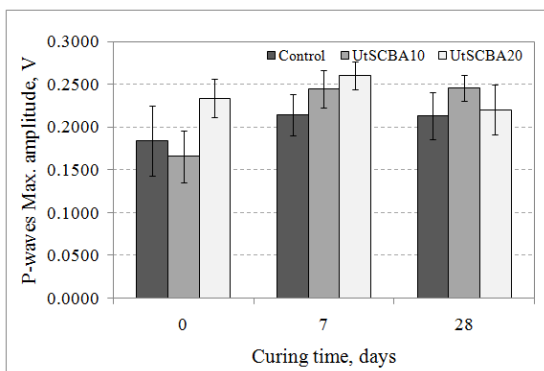
UtSCBA increased in the slabs. This agrees with the reported in the amplitude by P-waves. When 28 days of curing are applied, the control and the UtSCBA10 showed practically the same waveform energy than the slabs with 7 days of curing, respectively. Nonetheless, the energy in the UtSCBA20 slab with 28 days of curing was greatly higher when comparing with the slab with 7 days of curing. On the other hand, results also show a significant increment in the energy of the signals as the curing time increases from 0 to 7 and from 0 to 28 days in the control and the UtSCBA10 and UtSCBA20 slabs, respectively. This suggests more heterogeneities caused by corrosion in the slabs with 0 days of curing as indicated by the amplitude of the UGW signals by P-waves. It is well known that the reduction in energy of UGW signals is attributed to several factors such as pores and cracks, the boundaries between grains and the inhomogeneities of the materials [Valdeon et al 1996]. According with this, the results suggest that in fact the slabs with 0 day of curing have more corrosion damage than the slabs with 7 and 28 days of curing.

Fig. 9. Maximum amplitude of the reinforced mortar slabs by P-waves

Waveform energy

The waveform energy by P-waves of the reinforced mortar slabs are shown in Fig. 10. Results show comparable waveform energies in the control and the UtSCBA10 slabs with 0 days of curing, however, the energy of the UtSCBA20 slab became higher. With 7 days of curing, the waveform energy was greater as the addition of
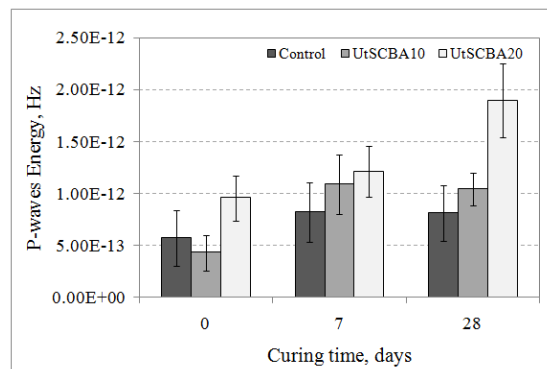

Fig. 10. Waveform energy of the reinforced mortar slabs by P-waves

Evaluation of the reinforced mortar slabs by S-waves

Ultrasonic pulse velocity

Fig. 11 shows the average UPV of the reinforced mortar slabs by S-waves (*Vs*). As in the case of the *Vp*, the *Vs* values of the control and the UtSCBA10 and UtSCBA20 slabs does

not show a significant difference when 0 days of curing is applied. However, very noticeable decrements in the *Vs* in the control and the UtSCBA10 and UtSCBA20 slabs were obtained (1460, 1561 and 1707 m/s, respectively) as the initial curing time increases from 0 to 7 days. Those significant decrements were not observed when analyzing the *Vp* values. It is known that S-waves does not propagate in fluids [Onajite 2014] and this suggest that mortar slabs with 0 days of curing could be filled with zinc and iron corrosion products creating an apparent solid media for S-waves. Subsequently, the *Vs* values of the slabs with 0 days of curing might be overestimated due to such corrosion products. Nonetheless, the *Vs* values of the slabs with 7 days of curing were not significantly different when comparing between them which indicates a non-negative effect when 10 and 20% of UtSCBA is used as cement replacement against corrosion. With 28 days of curing, the *Vs* values of the control and the UtSCBA10 slabs remains practically constant respect to the *Vs* values from the slabs with 7 days of curing; only the UtSCBA20 slab show a significant difference increasing the *Vs* value. In this case, less corrosion is suggested because of a denser cementitious matrix.

by P-waves, the amplitude attenuation by S-waves shows comparable values when comparing the control and the UtSCBA10 slabs with 0 days of curing. Nevertheless, the amplitude of the UtSCBA20 slab became higher than the control and the UtSCBA10 slabs. As expected, the amplitude of the UGW signals from the control and the slabs containing UtSCBA become higher as the initial curing time increases from 0 to 7 days. However, this increment was less noticeable in the UtSCBA20 slab. Even though a positive effect on increasing the amplitude of the signals by the increment of the initial curing time from 0 to 7 days, a decrement in the amplitude of the signals was observed when the curing time increases from 7 to 28 days.
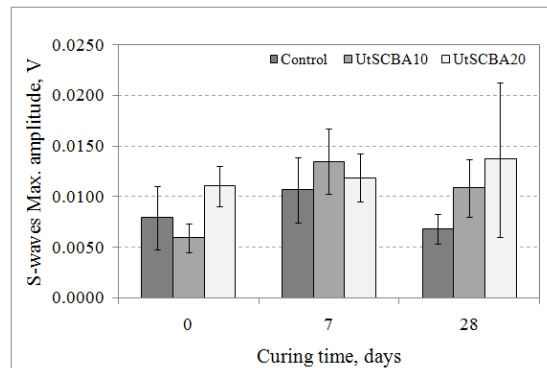
Fig. 12. Maximum amplitude of the reinforced mortar slabs by S-waves

Waveform energy

The energy values of the UGW signals by S-waves are shown in Fig. 13. Results show greater variability when comparing with the results from energy by P-waves. This creates some uncertainties concerning to the use of S-waves to evaluate corrosion in reinforced cement composites. Even the large variability in the results from S-waves energy, results agrees with the reported in the amplitude section by S-waves. According with the above, 7 days of curing could be enough for the reinforced mortar slabs.
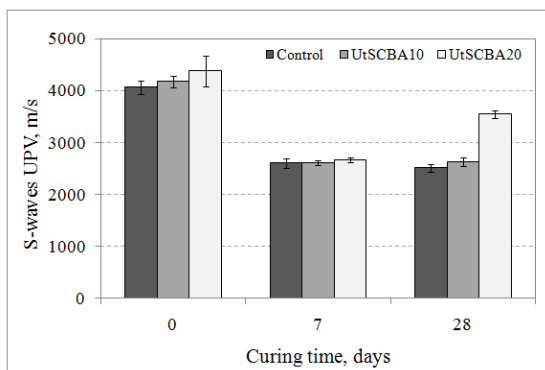

Fig. 11. Ultrasonic pulse velocity of the reinforced mortar slabs by S-waves

Amplitude

Fig. 12 shows the average amplitude of the reinforced mortar slabs by S-waves. As showed

Fig. 13. Waveform energy of the reinforced mortar slabs by S-waves

After analyzing the ultrasonic parameters by P and S waves, it was found that P-waves were more reliable for evaluation of the small-scale re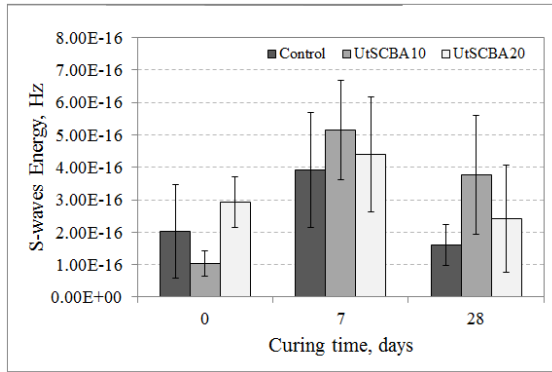inforced mortar slabs after exposing to the simulated marine environment for a long period. Even when S-waves can give important conclusions, it was affected by thickness of the slabs and also by internal humidity. Based on the above, correlations between corrosion potentials and the ultrasonic parameters obtained from P-waves are proposed in the next section.

Correlation between corrosion potentials vs P-waves ultrasonic parameters

According with the discussed in the electrochemical testing, only the corrosion potentials could be consistent to compare with the ultrasonic parameters from the UGW. Furthermore, the analysis of the UGW signals points to the use of P-waves parameters for that purpose. Based on the above, correlations between the corrosion potentials and the UPV, amplitude and energy from P-waves were obtained by linear regression analysis (Fig. 14). The correlations were proposed based in the fact that corrosion potentials measure the electrical potential between the steel reinforcement and a reference electrode which is in contact to the concrete´s surface. Certainly, the concrete quality might increase or decrease the corrosion potential. On the other hand, ultrasonic waves are affected by concrete quality and corrosion

products and could be sensitive to interface conditions between the concrete and steel reinforcement [Zaki et al. 2015, Sarma et al 2010].

Fig. 14a shows the correlations between the corrosion potentials and UPV by P-waves. It can be observed the positive effect of the curing time increase on lowering the corrosion potential of the control, UtSCBA10 and UtSCBA20 reinforced mortar slabs. Nonetheless, an effect of the addition of UtSCBA has been difficult to observe with the UPV when comparing the slabs with the same curing time. Practically, no correlations were found between the corrosion potentials and the UPV in all slabs. This is attributed to the thickness of the slabs which could be not enough to measure the UPV since longitudinal waves becomes disperse in thin concrete sections [Jones and Făcăoaru 1969].

The corrosion potentials and amplitude show most prospective correlations (Fig. 14b). It can be observed that the amplitude of the UWG signals became to increase, in the control and the UtSCBA10 and UtSCBA20 mortar slabs, as the corrosion potentials were less negative because the increment of the curing time from 0 to 7 and from o to 28 days. Also, the amplitude of the UGW signals began to rise as the addition of UtSCBA increased when comparing the mortar slabs for each curing time. Those effects suggest less corrosion in the mortar slabs containing UtSCBA. In fact, researches report that the amplitude in an UGW signal is lower as the corrosion increases in reinforced concrete [Li et al. 2014, Zaki et al. 2015]. It was also found that the correlation between the corrosion potentials and the amplitude was stronger as the addition of UtSCBA decreased. This tendency was observed when comparing the mortar slabs with the same curing time. Following the above, a relationship between the amplitude decrement and reinforced corrosion in the mortar slabs could exist because the direct path of the transducers and the arrangement of the galvanized meshes allow

swept a large volume of the mortar matrix, which could be enough to detect mortar deterioration due to corrosion [Yeih and Huang 1998].

Fig. 14c shows the correlations between corrosion potentials and energy from the UGW signals. In can be seen that the energy from the control and the UtSCBA10 and UtSCBA20 mortars slabs became higher as the corrosion potential was less negative. Likewise, the correlation between corrosion potentials and energy were stronger as the addition of UtSCBA in the mortar slabs was lower. Those tendencies agree with the reported correlations between corrosion potentials and amplitude (Fig. 14b). According with the above, there is a relationship between the amplitude and energy of the UGW signals with mortar deterioration due to corrosion of the galvanized meshes. Researchers report that energy from UGW signals becomes lower as the amplitude decrease due to reinforced corrosion concrete [Li et al. 2014, Zaki et al. 2015].

Visual examination

The photographic record of the internal visual inspection of the reinforced mortar slabs is show in Fig. 15. With 0 days of curing, the control slab shows large areas in which the zinc coating of the galvanized meshes was depleted, allowing steel corrosion (Fig. 15a). As the addition of UtSCBA increase, the galvanized meshes show less corrosion damage of the zinc coating (Figs, 15b and 15c) despite to the observed pores surrounding the galvanized meshes. Those pores might be attributed by casting problems in the galvanized steel/cementitious matrix interface due to the configuration of the meshes and the use of UtSCBA which increased the air content of the mortars [Maldonado-García et al. 2018].

When 7 days of curing are applied, the zinc coating of the galvanized meshes in the control slab is depleting (Fig. 15d). The UtSCBA10 slab show less corrosion of the zinc coating when comparing with the control (Fig. 15e). Nevertheless, the UtSCBA20 slab shows some areas with iron corrosion products which are ochre in color (Fig. 15f). This match to localized corrosion areas in the galvanized meshes embedded in the mortar slabs.

With 28 days of curing. The control slab shows areas in which the zinc coating of the galvanized meshes was depleted but also areas with iron corrosion products which differ in color depending of oxygen availability (Fig. 15g). The UtSCBA10 slab show less corrosion in the galvanized meshes (Fig. 15h) which is comparable with the observed in the UtSCBA10 slab with 7 days of curing. Finally, a similar set-up was observed in the UtSCBA20 slab (Fig. 15i).
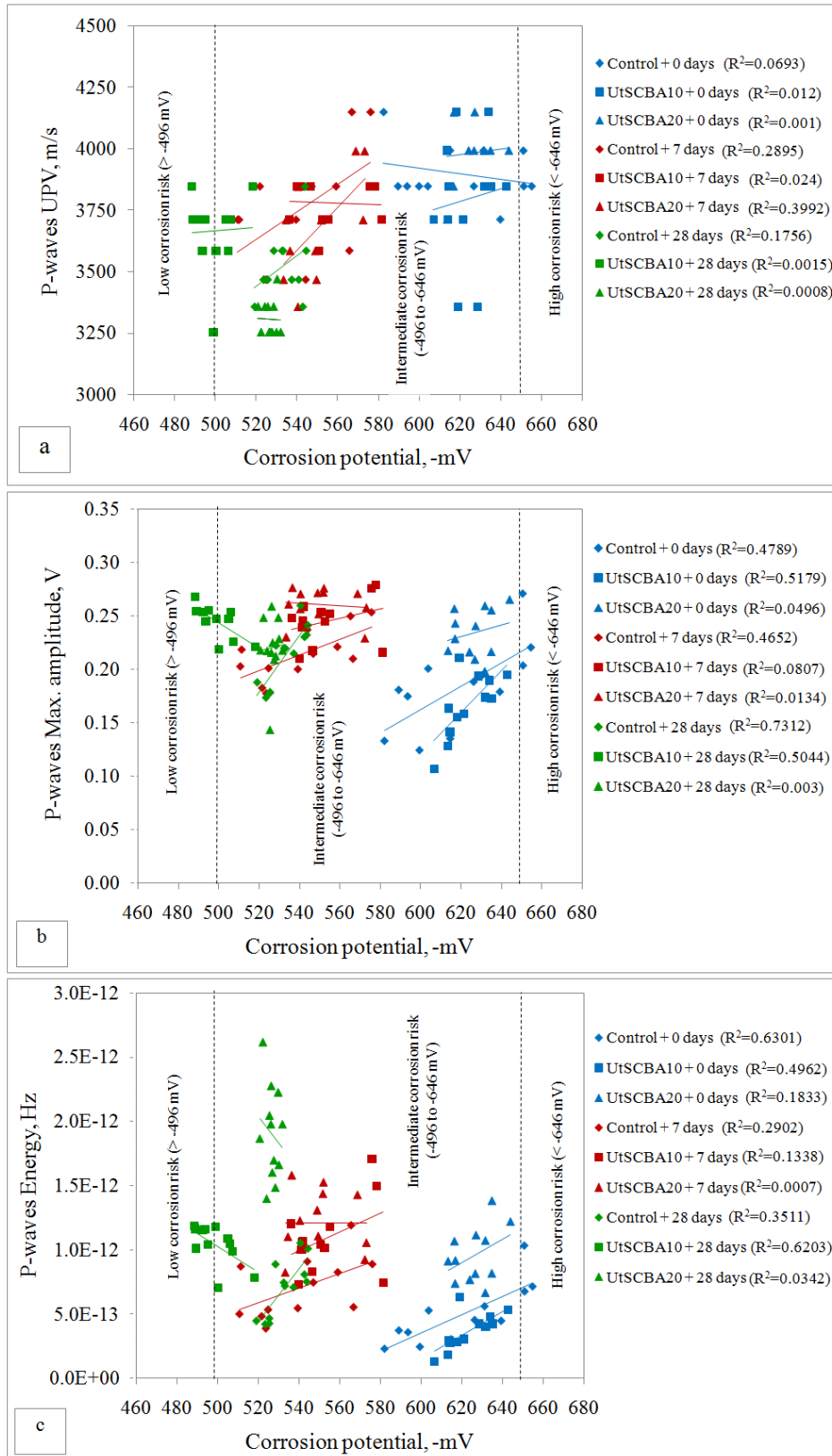
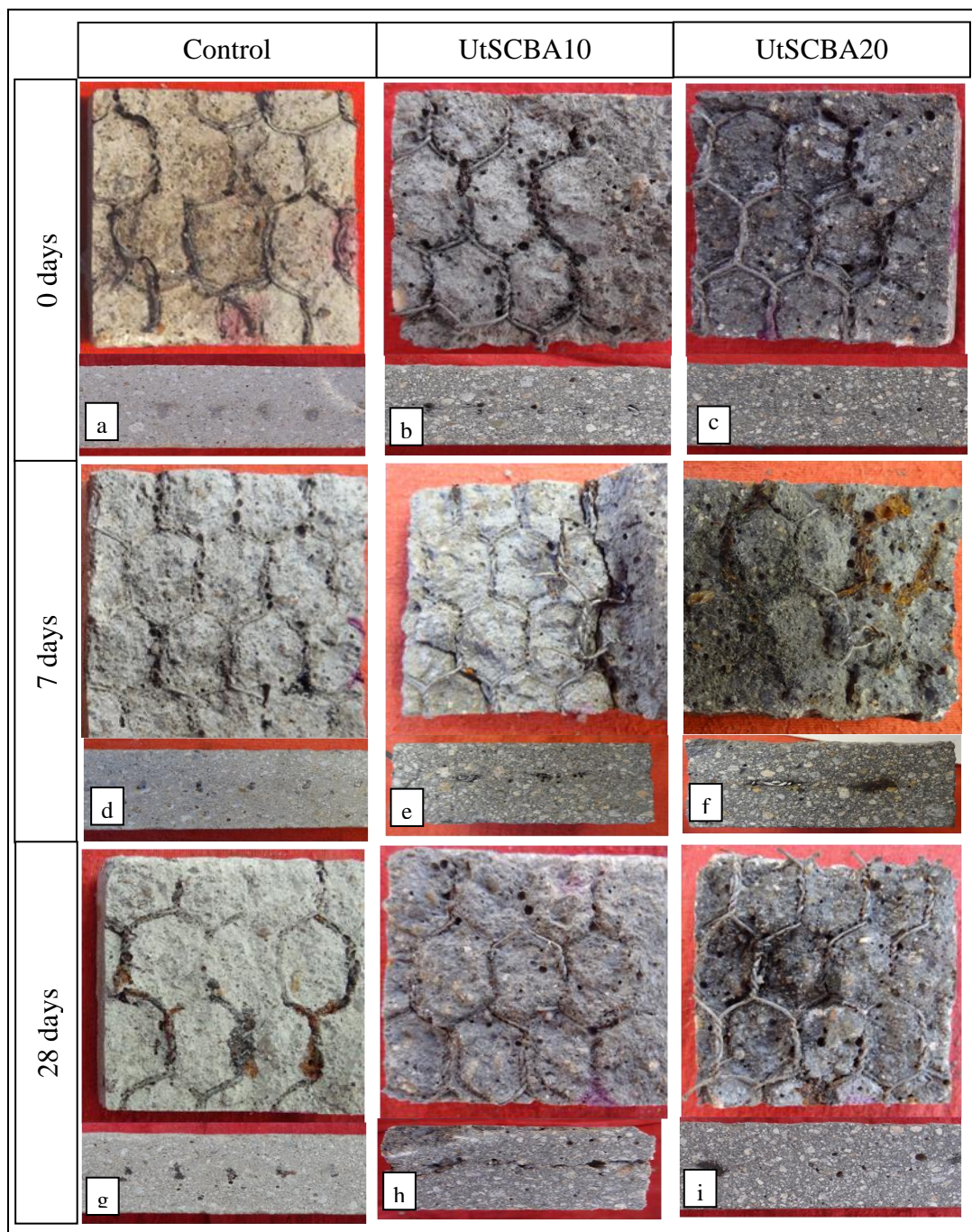Fig. 14. Correlation between corrosion potentials and a) UPV, b) max. amplitude and c) waveform energy

Fig. 15. Visual inspection of the reinforced mortar slab (a selected area from each mortar slab).

Analysis of correlations between corrosion potentials and ultrasonic parameters with physical evidence.

The correlations between amplitude and energy from UGW signals and the corrosion potentials (found in the control slabs with 0, 7 and 28 days of curing) agree with the observed in the visual examination. Those correlations were weaker as the addition of UtSCBA increased in the mortar slabs (for the three different curing times) which coincides with less corrosion evidence. To explain the above, it is necessary consider the direct path of the ultrasonic P-waves (used for the correlations) which travels through a large volume of mortar in the galvanized steel/cementitious matrix interface allowing detection of corrosion damage in the mortar matrix. In this way, as the galvanized steel corrodes, the adjacent mortar could have small cracks which disperse the UGW signals thought the slab. Since the addition of UtSCBA improves the cementitious matrix of mortars [Maldonado-García et al. 2018], less corrosion in the mortar slabs is allowed and hence fewer energy dispersion of the UGW. However, a further microstructural evaluation in the galvanized steel/cementitious matrix interface could help to clarify the evidence of micro-cracks by corrosion.

CONCLUSIONS

Based on the analysis of results, the following conclusions can be drawn:

Corrosion potentials show that the addition of 10 and 20% of UtSCBA do not increased the corrosion risk of the reinforced mortars. This was observed when analyzing the result from the three different curing times. Furthermore, the increment of the curing time decreased the corrosion risk of all mortars.

Current densities indicate that the control and the UtSCBA10 and UtSCBA20 reinforced mortars slabs might have comparable corrosion activity, around $1\mu A/cm^2$, after the exposure to the simulated marine environment. This is attributed to pitting corrosion in the criss-crossed areas of the galvanized meshes observed during the autopsy of the slabs.

Results from the UGW testing by P-waves do not show significant differences in the UPV´s when comparing the control and the UtSCBA10 and UtSCBA20 mortar slabs. This was observed for the three different curing regimens. The maximum amplitude of P-waves and energy of P-waves do not suggest a negative effect on increasing the corrosion damage of the slabs when 10 and 20% of UtSCBA is used. Furthermore, the increment of the curing time has a positive effect on decreasing the corrosion damage of all slabs. This agrees with the observed in corrosion potentials section and images from the autopsy of the slabs.

Results from the UGW testing by S-waves do not show a negative effect in the UPV´s when using 10 and 20% of UtSCBA in the slabs. However, a huge decrement was observed in all slabs as the curing time increased from 0 to 7 days. This is attributed to moisture of the slabs. On the other hand, results from the maximum amplitude and energy of the UGW shows large variability and hence a conclusion about the corrosion damage of the slabs using the S-waves could be tricky.

According to the previous statements, the results from the UGW testing suggest that P-waves are more reliable for the evaluation of corrosion in the reinforced small-scale mortar slabs instead to S-waves which are affected by the thickness of the slabs. This might be helpful to evaluate the effect of the addition of supplementary cementitious materials, such as the UtSCBA, as partial Portland cement replacement against corrosion.

REFERENCES

ACI 228.2R-98, Nondestructive Test Methods for Evaluation of Concrete inStructures ACI, American Concrete Institute Report, Farmington Hills,Michigan, 1998, p. 62

Arenas-Piedrahita J. C., Montes-García P., Mendoza-Rangel J. M., López-Calvo H. Z., Valdez-Tamez P. L., Martínez-Reyes J. 2016. Mechanical and durability properties of mortars prepared with untreated sugarcane bagasse ash and untreated fly ash. Construction and Building Materials 105, 69-81.

Angst U., Elsener M., Larsen C. K., Vennerland Ø. 2009. Critical chloride content in reinforced concrete – A review. Cement and Concrete research 39(12), 1122-1138.

Aprianti E., Sha figh P., Bahri S., Nodeh F. J. 2015. Supplementary cementitious materials origin from agricultural wastes – a review. Construction and Building Materials 74, 176-187.

Broomfield John P. 1997. Corrosion of steel in concrete. E &FN Spon.

Cordeiro G. C., Paiva O. A., Toledo Fhilo R. D. Fairbairn E. M. R., Tavares L. M. 2018. Long-term compressive behaviour of concretes with sugarcane bagasse ash as a supplementary cementitious material. *J. Test. Eval.*, 46(2), 564-573.

Ervin Benjamin L., Reis Henrique. 2008. Longitudinal guided waves for monitoring corrosión in reinforced mortar. Measurement Science and Technology 19, 1-19.

Fröjd P.,Ulriksen P. 2016. Amplitude and phase measurements of continuous diffuse fields for structural health monitoring of concrete structures. NDT&E International 77, 35-41.

Ganesan K., Rajagopal K., Thangavel K. 2007. Evaluation of bagasse ash as supplementary cementitious material. Cement and Concrete Composites 29(6), 515-524.

Gaydecki P. A., Burdekin F. M., Damaj W., John D. G., Payne P. A. 1992. The propagation and attenuation of medium-frequency ultrasonic waves in concrete: a signal analytical approach. Measurement Science and technology 3, 126-134.

Jones R., Făcăoaru I. 1969. Recommendations for testing concrete by the ultrasonic pulse method. Matériaux et Constructions 2[4], 275-284.

Khan Fuad, Bartoli Ivan. 2015. Detection of delamination in concrete slabs combining infrared thermography and impact echo techniques: a comparative experimental study. Proc. SPIE 9437, Structural Health Monitoring and Inspection of Advanced Materials, Aerospace, and Civil Infrastructure 943701, 1- 11.

Kořenská Marta, Chobola Zdeněk, Sokolář Radomír, Mikulková Petra, Martinek Jan. 2006. Frequency inspection as an assessment tool for the frost resistance of fired roof tiles. Ceramics-Silikáty 50(3) 185-192.

Lee Young Hark, Oh Taekeun. 2016. The measurement of P-, S-, and R-wave velocities to evaluate the condition of reinforced and prestressed concrete slabs. Advances in Materials Science and Engineering 2016, 1-14.

Li Dongsheng, Zhang Shuaifang, Yang Wei, Zhang Wenyao. 2014. Corrosion monitoring and evaluation of reinforced concrete structures utilizing the ultrasonic wave technique. International Journal of Distributed Sensor Networks 2014, 1-9.

Liang Ming-Te, Su Po-Jen. 2001. Detection of the corrosion damage of rebar in concrete using impact-echo method. Cement and Concrete Research 31(10), 1427-1436.

Lothenbach B., Scrivener K., Hooton R. D. 2011. Supplementary cementitious materials. Cement and Concrete Research 41(12), 1244-1256.

Maldonado-García M. A. Hernández-Toledo U. I., Montes-García P., Valdez-Tamez P. L. 2018. The influence of untreated sugarcane bagasse ash on the microstructural and mechanical properties of mortars. Materiales de Construcción 68(329), el48.

Martínez-Martínez Javier. 2008. Influencia de la alteración sobre las propiedades mecánicas de calizas, dolomías y mármoles. Evaluación mediante estimadores no destructivos (ultrasonidos). Doctoral thesis. Universidad de Alicante.

McCann D. M., Forde M. C. 2001. Review of NDT methods in the assessment of concrete and masonry structures. NDT&E International 34, 71-84.

Nuñez-Jaquez R. E., Buelna-Rodríguez J.E., Barrios-Durstewitz C.P., Gaona-Tiburcio C., and

Almeraya-Calderón F. 2012. Corrosion of modified concrete with sugarcane bagasse ash. International Journal of Corrosion 2012, 1-6.

Oh T. 2012. Defect characterization in concrete elements using vibration analysis and imaging. PhD dissertation. University of Illinois.

Onajite E. 2014. Understanding seismic wave propagation. Seismic data Analysis Techniques in Hydrocarbon Exploration, Chapter book No. 2, 17-32.

Sagar D., Hamid R., Khalim A. R. 2012. Algorithm for automatic data interpretation software for concrete slab in impact echo method. Materials and Structures 45, 727-746.

Sharma Shruti, Mukherjee, Abhijit. 2010. Longitudinal guided waves for monitoring chloride corrosion in reinforcing bars in concrete. Structural Health Monitoring 9(6), 555-567.

Shi X., Xie N., Fortune K.,Gong J. 2012. Durability of stee-reinforcement concrete in chloride environments: An overview. Construction and Building Materials 3, 125-138.

Sistonen E. 2008. Corrosion mechanism of hot-dip galvanized reinforcement bar in crecked concrete. Corrosion Science 50, 3416-3428.

Valdeon Luis, H. de Freitas M., King M. S. 1996. Assessment of the quality of buiding stones using processing procedures. Journal of Engineering Geology 29, 299-308.

Verma Sanjeev Kumar, Bhadauria Sudhir Singh, Akhtar Sallem. 2013. Review of nondetructive testing methods for condition monitoring corrosion structures. Hidawi Publishing Corporation 2013, 1-11.

Yeih W., Huang R. 1998. Detection of the corrosion damage in reinforced concrete members by ultrasonic testing. Cement and Concrete Research 28(7), 1071-1083.

Zaki A., Chai H. K., Aggelis D. G., Alver N. 2015. Non-destructive evaluation for concrete monitoring in concrete: A review and capability of acoustic emission technique. Sensors 15, 19069-19101.

CHAPTER SEVEN

Elucidation of the role of untreated sugarcane bagasse ash on the chloride-induced corrosion of reinforced mortars.

Maldonado-García Marco Antonio, Montes-García Pedro, Valdez-Tamez Pedro Leobardo.
Rodríguez-Ramírez Juan. 2018.
Manuscript in preparation

Elucidation of the role of untreated sugarcane bagasse ash on the chloride-induced corrosion of reinforced mortars

Marco Antonio Maldonado-García[1], Pedro Montes-García[2*], Pedro Leobardo Valdez-Tamez[3], Juan Rodríguez-Ramírez[2]

[1] PhD candidate. Instituto Politécnico Nacional, CIIDIR Oaxaca, Hornos 1003, Col. Noche Buena, Sta. Cruz Xoxocotlán, C.P. 61230, Oaxaca, México.

[2] PhD. Instituto Politécnico Nacional, CIIDIR Oaxaca, Hornos 1003, Col. Noche Buena, Sta. Cruz Xoxocotlán, C.P. 61230, Oaxaca, México.

[3] PhD. Universidad Autónoma de Nuevo León, Facultad de Ingeniería Civil, Cd Universitaria s/n, San Nicolás de los Garza, C.P. 66451, Nuevo León, México.

* **Corresponding author:** (951) 517 0619 ext. 82775. pmontesgarcia@gmail.com, pmontes@ipn.mx

Abstract

The corrosion of small-scale mortar slabs containing 10 and 20% of untreated sugarcane bagasse ash (UtSCBA) as cement replacement was analysed by analytical techniques. Two wire galvanized meshes were used as reinforcement for the slabs. Curing regimes of 0, 7 and 28 days were applied to the slabs as well. The slabs were exposed to wetting-drying cycles of 12 hour each in a 3% NaCl solution for 75 months. The corrosion products in the reinforced galvanized steel of mortars were observed by autopsy of the slabs and by SEM after the exposure to the wetting-drying cycles. Likewise, the mineralogical compounds near to the steel/mortar interface were analysed by DRX and TG/DTG. The results show that the UtSCBA does not increase corrosion in the slabs. A mechanism in which the UtSCBA inhibits corrosion steel has been proposed based on the experimental testing.

Keywords: Agricultural waste, microstructure, corrosion products, durability.

ORCID ID: Marco Antonio Maldonado-García (http://orcid.org/0000-0002-9522-6779); Pedro Montes-García (http://orcid.org/0000-0003-3799-8372); Pedro Leobardo Valdez-Tamez (http://orcid.org/0000-0002-1298-2051); Juan Rodríguez-Ramírez (http://orcid.org/0000-0002-0866-9230).

INTRODUCTION

Chloride-induced corrosion is considered one of the main deterioration mechanisms in reinforced concrete (RC), which leads to the reduction in strength, durability and serviceability of the structures [Angs et al. 2009, Shi et al. 2012, Michel et al. 2016]. The most common sources for concrete chloride contamination are the exposure to marine environments and the use of de-icing salts [Angs et al. 2009]. Chloride-induced corrosion is strongly related with the concrete microstructure because the presence of pores in the cementitious matrix allows not only the chloride ion diffusion but also the water and oxygen entrance necessary for steel corrosion in RC.

In order to minimize the chloride-induced corrosion in RC, the concrete microstructure can be enhanced by the addition of supplementary cementitious materials (SCM) such as fly ash, silica fume and ground granulated blast furnace slag. However, the use of a specific SCM is upon its availability in each country [Gastaldini et al. 2010]. This leads to the searching of alternative SCMs such as agricultural wastes. In this context, the sugarcane bagasse ash (SCBA) appears to be a proper option because of its positive effects on rheological, microstructural, mechanical and some durability properties of

cement-based composites [Ganesan et al. 2007, Cordeiro et al. 2009a, Chusilp et al. 2009a, Chusilp et al. 2009b, Jiménez-Quero et al. 2013, Cordeiro et al. 2018, Zareei et al. 2018].

Originally, the SCBA is obtained as byproduct from the combustion of the sugarcane bagasse in sugar mills. It contains silica, aluminum and iron oxides as main compounds. Nonetheless, researchers affirm that the SCBA needs a minimum post-treatment for a proper pozzolanic performance in cement-based composites [Bahuruden and Santhanam et al. 2015]. A number of researchers have been using different processing methodologies consisting in recalcination, grinding and sieving or combination of these methods [Ganesan et al. 2007, Cordeiro et al. 2009a, Cordeiro et al. 2009b, Chusilp et al. 2009b, Morales et al. 2009, Cordeiro et al. 2017]. From this, sieving appears to be the post-treatment with the less energy demand.

A long-term research where SCBA was sieved by the 75µm ASTM mesh during 5 months reported that such post-treatment is enough for proper pozzolanic activity of the SCBA. The results also indicate that the addition of this ash improves the microstructural, mechanical and some durability properties of cement-based composites [Arenas-Piedrahita et al. 2016, Ríos-Parada et al. 2017, Maldonado-García et al. 2018]. The authors named this ash as untreated sugarcane baggase ash (UtSCBA) because of the minimum energy demand required by the implemented post-treatment. The SCBA processed by this methodology could be also considered as "practically as received" ash from sugar mills and research on the effect of this UtSCBA on the corrosion of reinforced cement-based composites is needed.

The aim of this research is evaluated the effect of UtSCBA on the corrosion of reinforced mortars after exposing to a simulated marine environment for a long period. Furthermore, the mechanism in which the UtSCBA improves the performance of mortars against steel corrosion is proposed.

EXPERIMENTAL

Experimental design

To evaluate the effect of the UtSCBA on the corrosion of reinforced mortars, the percentage of addition of UtSCBA and the curing time were considered as factors. Following the above, 0, 10 and 20% of UtSCBA were added as cement replacement in the mortar binders, whereas, 0, 7 and 28 days of curing in a $Ca(OH)_2$-saturated solution were applied to the mortar specimens after casting and demolding. The curing times were chosen from those proposed in the ASTM C 39 standard. A detailed information about the materials used for the mortar binders and specimens are presented in the following sections.

Description of the materials used to the reinforced mortar slabs

Blended Portland cement (CPC) 30-R Holcim Apasco® (with approximately 5% of ground granulated blast furnace slag addition, GGBFS), UtSCBA (a sugarcane bagasse ash sieved through the 75µm ASTM mesh for five minutes), fly ash (FA) admix tech® (used for the mortar mixture for comparison purposes), river sand with a density of 2.7g/cm³ and a fineness modulus of 2.45, distilled water and a policarboxilate-based high-range water reducer Plastol 4000® were used to prepare the mortar binders. The chemical composition (analysed by I.C.P and gravimetric methods) of the CPC, UtSCBA and FA are presented in Table 1. The UtSCBA was collected from a sugar mill located in the community of Tezonapa, Veracruz, Mexico. This ash is generated as a combustion by-product of sugarcane bagasse (burned at temperatures between 550 and 700ºC) during the sugar production.

Table 1. Chemical composition of the cementitious materials used for the reinforced mortar slabs (% by mass)

Material	SiO_2	Al_2O_3	Fe_2O_3	CaO	MgO	Na_2O	K_2O	P_2O_5	LOI
CPC	23.86	5.77	2.19	50.76	1.36	0.91	0.92	0.12	6.97
UtSCBA	56.37	14.61	5.04	2.36	1.43	1.57	3.29	0.85	10.53
FA	58.02	23.28	4.44	5.47	1.37	0.62	0.95	0.33	3.69

LOI = loss on ignition

Two galvanized hexagonal wire meshes 0.68mm in diameter and 12.7mm in aperture were used as reinforcement for each slab. Prior to exposure, a small section of meshes was analysed using an optical microscope Carl ZEISS® Axio Scope.A1 and a scanning electron microscope microscope JEOL JSM-6510LV® equipped with an energy dispersive X-ray analyser (EDS) from Oxford Instruments 7573®. Cross section samples of the wire mesh were mounted in a polymer resin and then roughened using a set of sandpapers (No. 80, 240, 320, 600, 1000 and 2000). Subsequently, the samples were polished using an abrasive diamond paste (6µm) in a rotating disk. Finally, the samples were cleaned using acetone before the observation.

Fig. 1 shows heterogeneities in the meshes´s surface (Figs. 1a and 1b) and that the thickness of the zinc coating is not uniform, showing thickness values from 40.13 to 59.12µm (Figs 1c and 1d). The thickness of the zinc coating is less than the established by the ASTM A767 standard (95µm) because the diameter of the meshes. Furthermore, denser but non-homogeneous areas could be identified in the cross section of the zinc coating as reported by Sistonen et al 2008. Fig. 1e shows a micrograph in the cross section of the meshes in which the steel and the zinc coating are observed. According with the EDS analysis (Fig. 1f) and the EDS spots (Table2), the zinc coating of the galvanized meshes may by formed by a δ and γ zinc-iron alloy phases. These phases contain around 90% and 75% of zinc, respectively [Yeomas 2004]. The iron-zinc layers in galvanized steel are product from reactions between steel and zinc during the galvanizing process of steel with a layer of pure zinc at the outer surface [Yeomas 2004, Sistonen 2009].
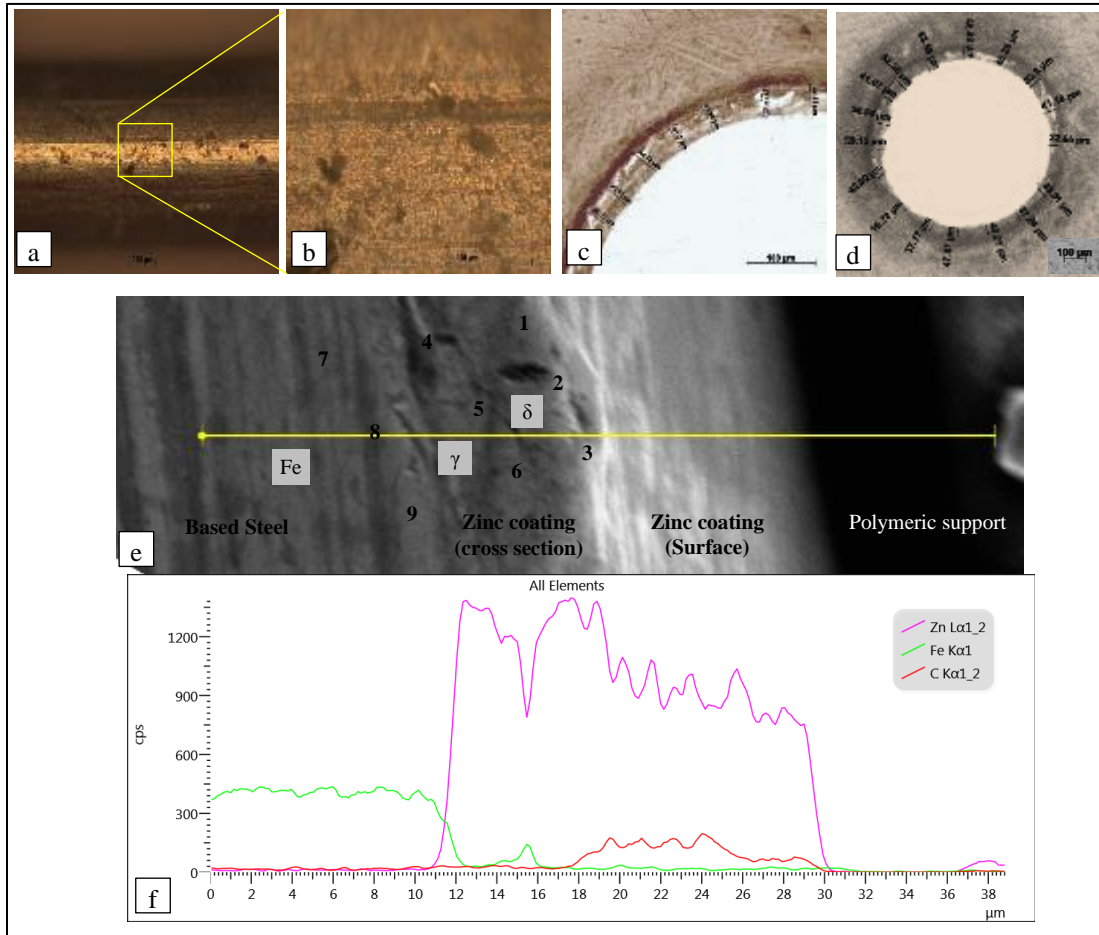
Fig. 1. Microscopical images of the galvanized meshes a) longitudinal section with 10x, b) amplification of the longitudinal section to 50x, c) and d) cross sections with 10x and 20x, respectively, e) SEM micrograph in a selected cross section and f) elemental analysis from the selected cross section observed in 1e.

Table 2. EDS spot analysis of Fig. 1e.

Spot	Zn, %	Fe, %	O, %	C, %
1	84.2	2.0	0	13.7
2	67.5	4.9	2.7	25.0
3	84.4	1.9	2.3	11.4
4	65.5	12.6	10.9	11.0
5	82.9	4.5	1.0	11.6
6	82.7	3.5	1.5	12.2
7	0	90.8	0	9.2
8	0	90.6	0	9.4
9	0	89.9	0	10.1

Mixture proportions and casting of specimens

Three mortar binders containing 0, 10 and 20% of UtSCBA as a partial Portland cement replacement (control, UtSCBA10 and UtSCBA20, respectively) were prepared. All mortars had a 0.63 water/cementitious materials and a 1:3 cementitious material/sand ratios. The mortar binder proportions are shown in Table 3. A high-range water-reducer additive was used in the mortar binders containing UtSCBA since the ash produced and increased the viscosity of the fresh mixtures. A total of 9 small-scale 250 x 200 x 30 mm reinforced mortar slabs were cast to evaluate the corrosion phenomenon. All slabs were demolded after 24 hours and cured in a $Ca(OH)_2$ saturated solution. Three curing regimes, 0, 7 and 28 days, were chosen to evaluate the effect of curing sensitivity on the performance of mortars containing UtSCBA

against corrosion. The slabs were reinforced with two galvanized hexagonal wire meshes placed in the centre of the thickness, leaving 20mm of cover from each edge. A 14 caliber

AWG copper cable was connected to the galvanized meshes for the electrochemical tests monitoring (Fig. 2).

Table 3. Mixture proportions of mortars in kg/m^3

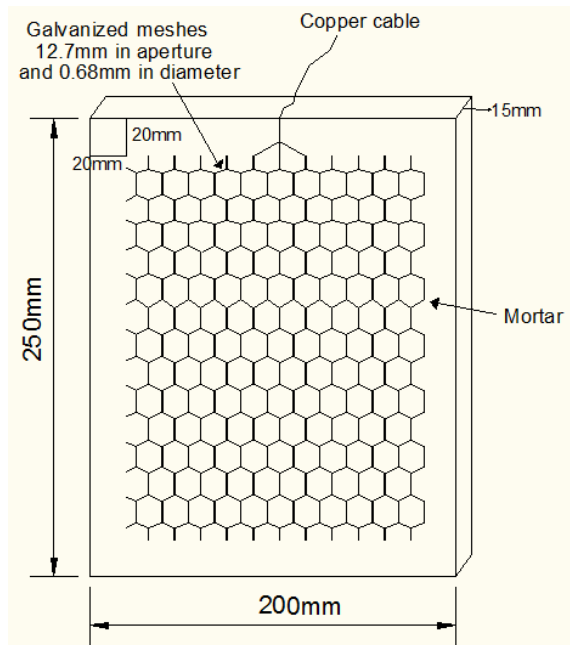| Mixture	CPC (kg)	UtSCBA (kg)	FA (kg)	Water (kg)	Sand (kg)	HRWR
Control	466.0	0	0	293.6	1398.0	0
UtSCBA10	419.4	46.6	0	293.6	1398.0	9.0
UtSCBA20	368.3	92.2	0	296.3	1398.0	17.5

HRWR = high-range water-reducer

Fig. 2 Schematic view of the reinforced mortar slabs

Exposure condition of the reinforced mortar slabs

The reinforced mortar slabs were exposed to wetting and drying cycles of 12 hours each in a 3% NaCl solution for 75 months, creating a tidal effect (Fig. 3). A pumping system was used to fill the container with the NaCl solution in which the mortar slabs were placed during the day while manually was emptied using a valve at night. The slabs were place 150mm above of the bottom of the container to prevent the wicking

effect by the remaining solution when the container was emptied.

Fig. 3. Exposure conditions of the reinforced mortar slabs

METHODS

Visual examination of the reinforced mortar slabs

The reinforced mortar slabs were visually examined every 6 months to detect any corrosion damage caused during its exposure to the wetting and drying cycles. Photographs of the slabs, taken at the end of the experiments, are presented in Fig. 3 to have a general overview. Practically, the slabs do not show any damage, such as cracks and delamination or corrosion stains in the mortar´s surface, induced by corrosion.

Autopsy of the reinforced mortar slabs

After 75 months of exposure to the chloride environment the reinforced mortar slabs were transversely cut in 12 small sections using an electrical diamond cutting machine. Immediately after cutting, carbonation test were carried spraying phenolphthalein indicator on the transversal sections of the reinforced mortar slabs. The phenolphthalein tests were performed following the recommendations by the RILEM CPC-18 standard.

Evaluation of the steel/mortar interface of the reinforced slabs

Sample preparation

The small sections were opened by hammer and chisel to observe the surface of the galvanized meshes and the steel/mortar interface. After that, the sections were covered with a plastic paraffin film and kept in hermetic bags to protect it against moisture and air for a short time until the date of the test. Subsequently, some of the small sections were removed from the bags and from the plastic paraffin to elaborate the samples for the analytical testing. Two sets of samples were prepared for the analytical testing. The first set was used for the scanning electron microscopy (SEM) observations; and the second set for the X-ray diffraction (XRD) and thermal analysis (DTA/TGA/DTG) analysis. For the first set, the mortars samples (10 x 10mm in size and 5mm of thickness), with a small piece of corroded galvanized mesh, were cut using an electrical diamond cutting machine. After that, the samples were placed in a desiccator for a short time until the observations were done. The second set of samples were obtained from mortar fragments (adjacent to the steel/mortar interface) of the reinforced mortar slabs. The mortar fragments were ground using a porcelain mortar and then sieved though a 200µm ASTM mesh.

Scanning electron microscopy

For this test, the samples were covered with gold-palladium using a Denton Vacuum Desk V® sputtering. The SEM images were taken using a scanning electron microscope JEOL JSM-6510LV® equipped with an energy dispersive X-ray analyser (EDS) from Oxford Instruments 7573®. The images were obtained in the SE mode with an acceleration voltage between 15 and 20kV.

X-ray diffraction

Powder XRD diffraction test were carried out using a diffractometer Bruker D8 advance® which uses a radiation of CuK and a wavelength of 1.5418Å. A passage of $0.05°$ and an incident time of 0.5 seconds per step were considered for the test maintaining an interval 2-theta from 7.5 to $80°$. The EVA version 11.0.0.3® software was used for the mineral phases identification from the XRD patterns.

Thermal analysis

The thermal analysis (DTA/TGA) were run in a Perkin Elmer – Simultaneous Thermal Analyzer 6000®. The samples were heated from 25 to $995°C$ with a $10°C$ per minute heating rate using an alumina container in an nitrogen inert atmosphere. The derived thermogravimetric curve (DTG) was also obtained for the samples.

Basics to propose a corrosion mechanism of reinforced mortar slabs added with UtSCBA.

Diffusion, convection, migration, permeation and absortion may be considered as main transport mechanisms for chloride ion in durability estimation of cement-based composites [Bahurudeen et al. 2015, Zareei et al. 2018]. Those mechanism for chloride ion transport might be affected by the porosity, chloride binding capacity of the cementitious matrix and saturation of the concrete pore network [Malheiro et al. 2011]. The use of supplementary cementitious materials as cement

replacement could change those characteristics of the cementitious matrix in cement-based composites [Lothenbach et al. 2011, Aprianti et al. 2015] which in turn to modify the chloride-ion transport mechanisms against corrosion of reinforced cement-based composites.

From electrochemical point of view, corrosion potential in cement-based composites depends of the entrance of environmental harmful substances (such as chloride ions) by the mentioned mechanism in the last paragraph, and the characteristics of the reinforcement steel (which differs accordingly to the alloy of the metal) [Angs et al. 2009]. In this research, chloride ion diffusion by immersion was considered to evaluate the performance of UtSCBA against corrosion in reinforced mortar slabs. According to results from previous researches, the UtSCBA improves the microstructural and mechanical properties of mortars [Maldonado-García et al. 2018] and reduced the chloride ion diffusion and the corrosion risk of reinforced mortars [Maldonado-García et al. 20XX]. Following the above, is expected that addition of UtSCBA as cement replacement in reinforced mortars increase the time in which a maximum chloride threshold value (0.67% by mass of concrete) [Darwing et al. 2009] is reached at the galvanized steel surface necessary for the dissolution of its passive layer. Therefore, the corrosion initiation period might be prolongated. Furthermore, during diffusion some of the chloride ions could be bound chemically or physically since ingress of chloride ions in cement-based composites is not only physical controlled phenomenon by mass transfer [Ipavec et al 2014]. In the case of physical bonding, is proposed that the unburned particles of the UtSCBA works as a physical barrier or as an absorbent media for chloride ions by electrostatic forces. This is because the large particle size and large surface area of this particles reported in a previous research

[Maldonado-García et al. 2018]. As a result of this process, the initiation of the propagation period for corrosion in the reinforced mortars is delayed.

Additionally, the corrosion propagation period of the reinforced slabs is prolongated by the use of galvanized steel. This is because corrosion of galvanized steel in concrete is a multi-stage process which depends to the dissolution of the different iron-zinc alloy phases (η, ζ, δ and γ as most reported phases after galvanizing process) which conform the zinc coating. Corrosion of galvanized steel in concrete also depends of the properties of concrete and the severity of the environment in which the concrete is exposed [Yeomas 1998, Sistonen 2008, Tittarelli and Bellezze 2010]. In concrete the zinc of the galvanized steel reacts with hydroxyl ions from the pore solution to form zinc oxide and hydrogen gas. After that, a reaction between the zinc oxide and calcium ions occurs to create stable calcium hydroxyzincate (CHZ) that passivates (in a pH value below to 13.3) the pure zinc layer (η phase) [Darwin et al. 2009]. The corrosion process of the η phase starts once the zinc of the CHZ passive layer is dissolved as a consequent of different factors such as the attack of chloride ions or the carbonation of the cementitious matrix. Therefore, the dissolution of internal zinc-iron (ζ, δ and γ) occurs eventually [Yeomas 1998]. Finally, the steel also corrodes after dissolution of the different zinc-iron phases in zinc coating. However, the zinc coating in galvanized steel delay the initiation period of corrosion in reinforced concrete because its higher chloride ion content tolerance (0.67%) and it remains passivate at lower pH values (up to 9.5) [Sistonen 2009] when compared to black steel. Furthermore, the consumption of the different zinc-iron phases takes an extra time delaying the corrosion initiation period and zinc cathodically protects regions in which the iron is exposed [Darwing et al. 2009].

RESULTS AND DISSCUSION

Visual examination of the reinforced mortar slabs

Photographs from the last visual examination of the reinforced mortar slabs are show in Fig. 4. Practically, the slabs do not show any corrosion damage after the long-term exposure to the wetting and drying cycles. The thickness of the galvanized meshes versus the cover depth of the mortar matrix could be blamed for this. Furthermore, researchers reported that the zinc corrosion products from the coating of galvanized steel are less voluminous than iron corrosion products (about 150 to 250%) and could fill small pores and microcracks creating an apparent densification of the cementitious matrix up to 0.5mm from the steel/cementitious matrix interface [Yeomas 1998]. According to the above, no corrosion damage might be expected in the slabs in spite of any corrosion activity in the reinforcement steel.

Autopsy of the mortar slabs

Figs. 5 to 7 show a photographic record taken of the autopsied mortar slabs. The control slab with 0 days of curing shows that the zinc coting of the galvanized meshes has been depleted in large areas (Fig. 5a). A detail for this is presented in Fig. 5-a1 in which localized iron corrosion products, which are dark ochre in colour due to oxygen starvation, could be identified as pitting damage. These corrosion products are mainly localized in the criss-cross sections of the meshes. Something similar was observed in the UtSCBA10 and UtSCBA20 slabs with 0 days of curing (Figs. 5b, 5-b1, 5c and 5-c1). Despite not significant differences in corrosion damage of the galvanized steel in the control and the UtSCBA10 and UtSCBA20 slabs, it can be inferred that the addition of 10 and 20% of UtSCBA as a partial cement replacement does not have a negative effect on increasing corrosion. A detailed examination by scanning electron microscopy could help to differentiate the corrosion products formed in those slabs.

When 7 days of curing are applied (Fig. 6), the control mortar slab show less corrosion damage of the galvanized steel reinforcement (Fig. 6a and 6-a1) when compared with the slab with 0 days of curing. In this case, less areas with localized iron corrosion products were observed. Something similar was observed for the UtSCBA10 slab (Fig. 6b and 6-b1). Once again, a study by scanning electron microscopy may help to compare the corrosion products of these slabs. The UtSCBA20 slabs show corrosion products which could be associated with uniform attack (Fig. 6c). In this case, iron corrosion products in some criss-cross areas of the galvanized meshes, which are ochre in colour, were observed (Fig. 6-c1).

With 28 days of curing (Fig. 7), the control slab shows general overall corrosion in the galvanized meshes (Fig. 7a). In this case, iron corrosion products which are ochre in colour (some of the in dark colour) are observed (Fig. 7-c1). This slab shows larger corroded areas when compared to the control slabs with 0 and 7 days of curing. However, the control slabs with 0 and 7 days show pitting damage. Compared to uniform corrosion, pitting could be considered one of the most destructive forms of corrosion [Fontana 1986]. The UtSCBA10 and UtSCBA20 slabs show less corrosion damage of the galvanized steel when comparing to the control mortar (Figs 7b and 7c). General corrosion was also observed in these slabs (Figs. 7-b1 and 7-c1, respectively).
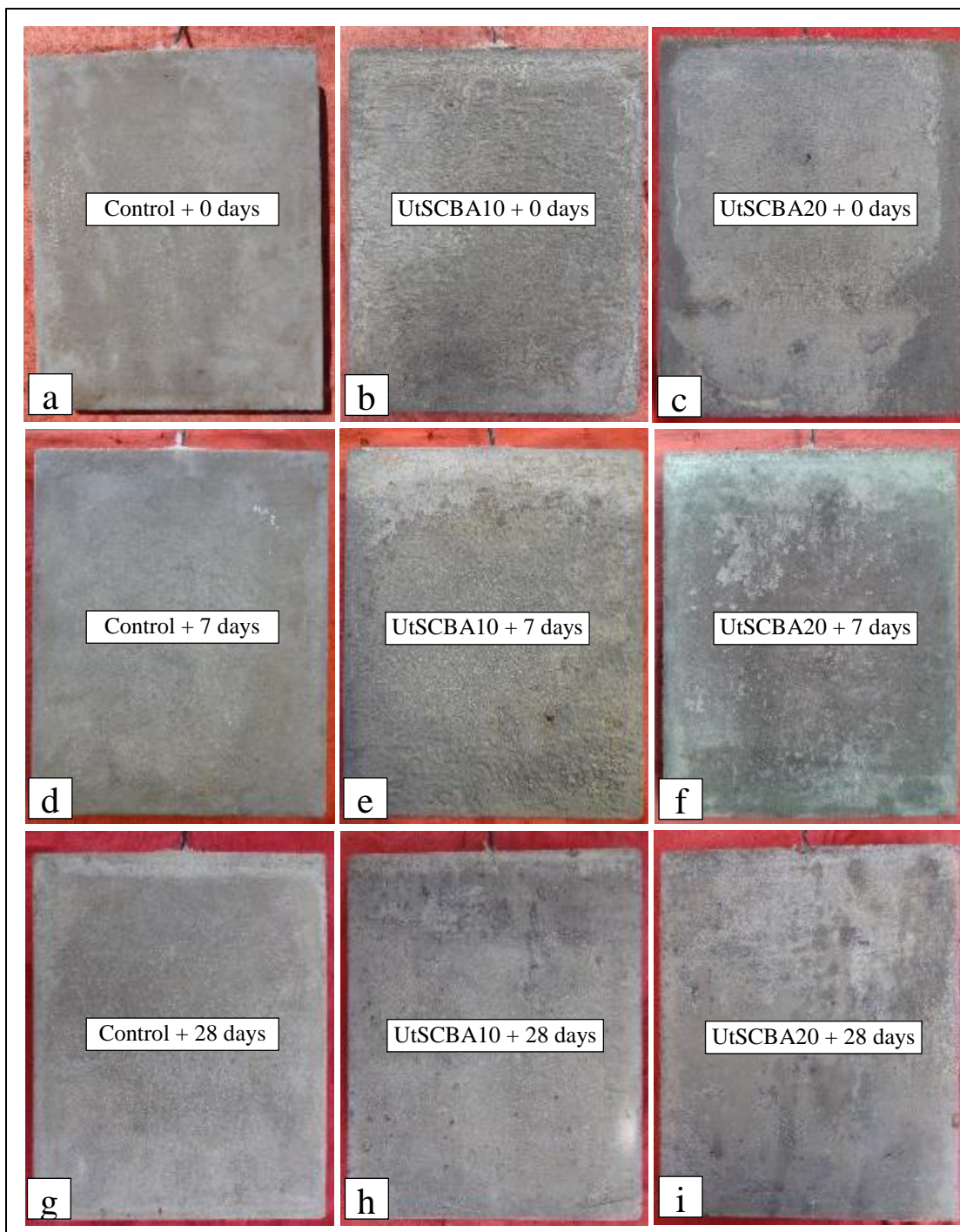
Fig. 4. Visual examination of the reinforced mortar slabs after its exposure to the wetting and drying cycles
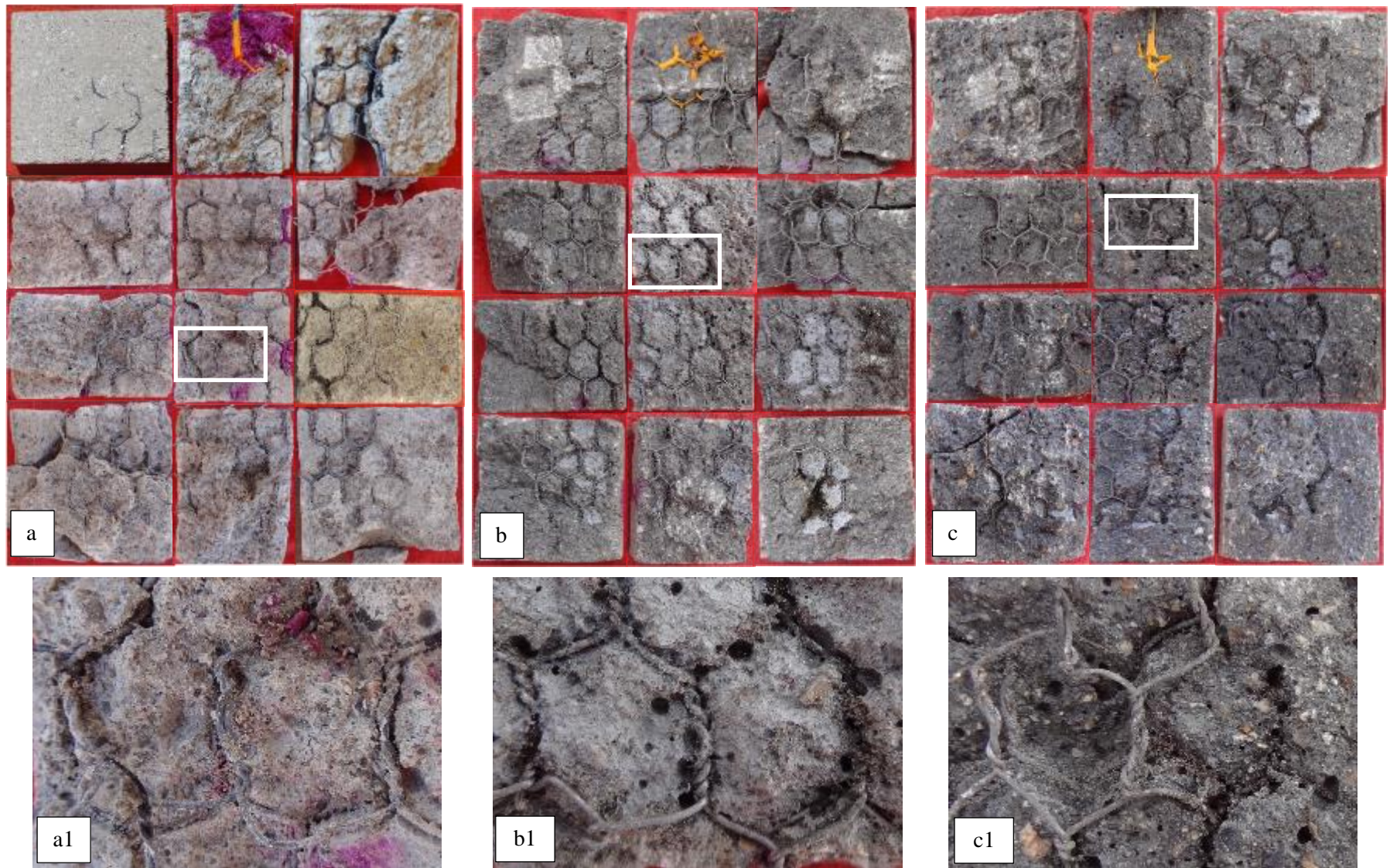
Fig. 5 Autopsied Reinforced mortar slabs with 0 days of curing a) control, b) UtSCBA10 and c) UtSCBA20
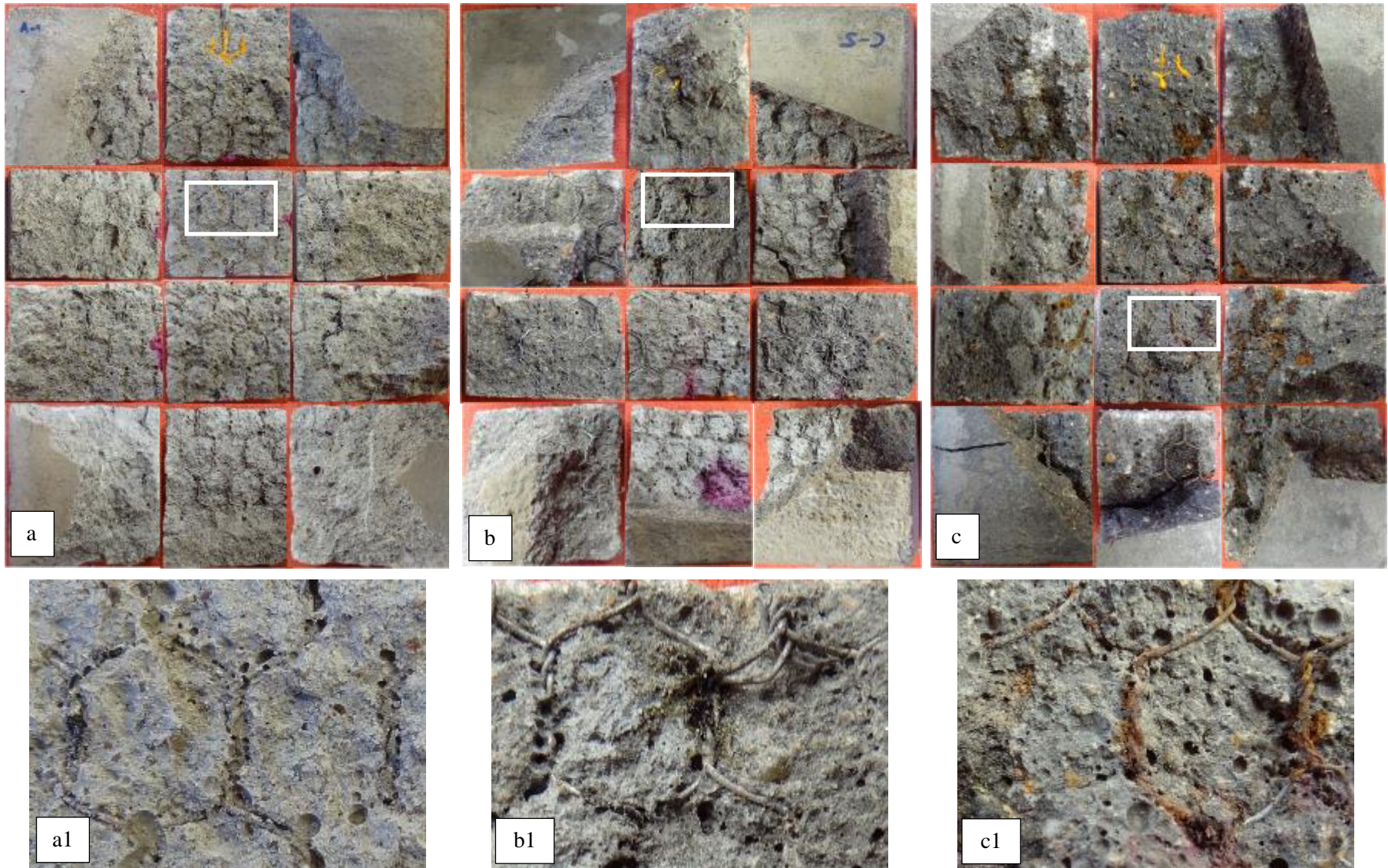
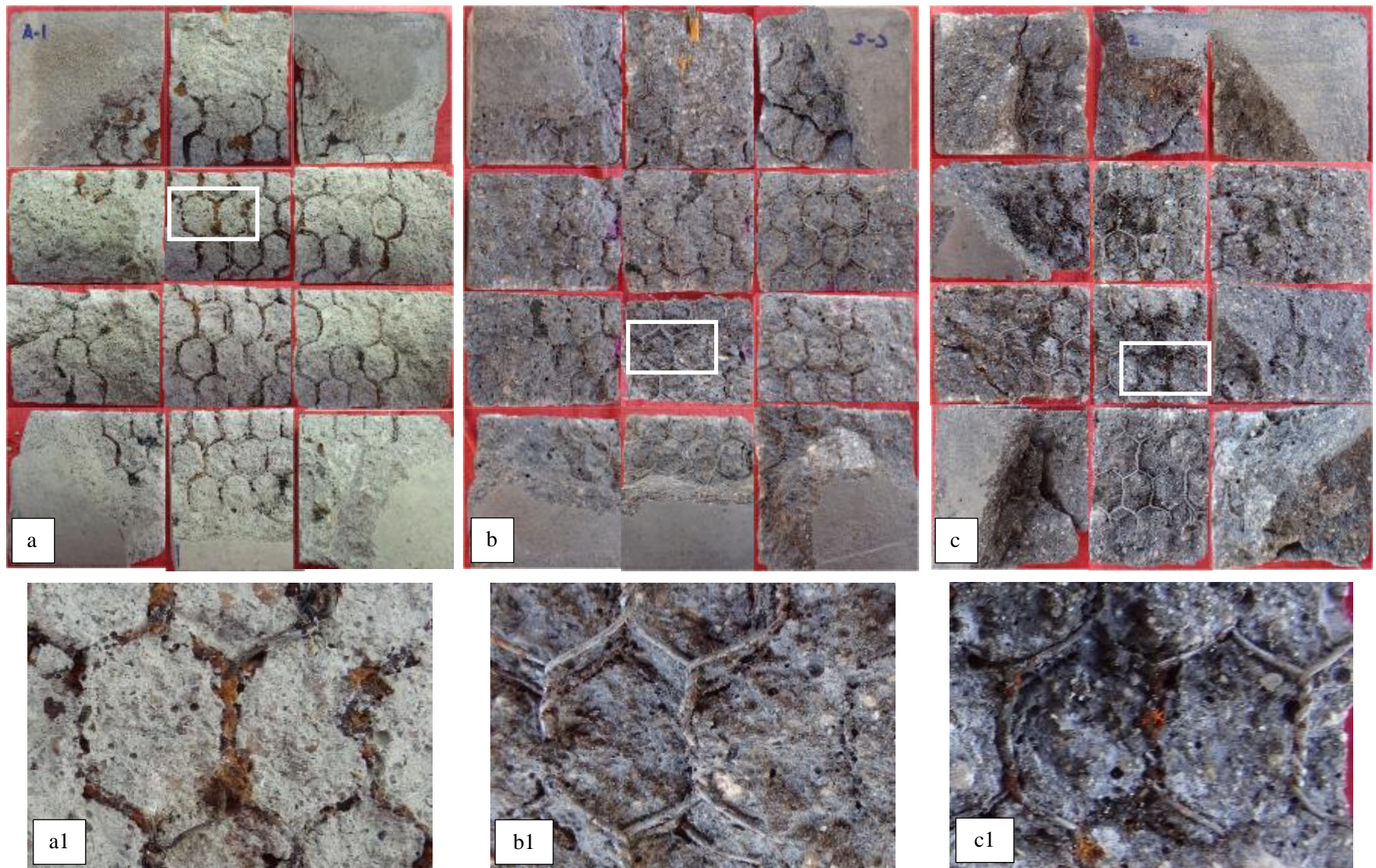Fig. 6 Autopsied Reinforced mortar slabs with 7 days of curing a) control, b) UtSCBA10 and c) UtSCBA20

Fig. 7 Autopsied Reinforced mortar slabs with 28 days of curing a) control, b) UtSCBA10 and c) UtSCBA20

Carbonation tests

A slight attenuation in the phenolphthalein indicator after spraying was observed as the addition of UtSCBA increases in the reinforced mortar slabs (Fig. 8). However, this could be attributed to the colour of the mortar matrixes which becomes darker when the UtSCBA is used. In this case, the phenolphthalein tests lead to some uncertainties.

Scanning electron microscopy

Figs 9 to 11 shows the SEM micrographs taken in representative locations at the galvanized steel/mortar matrix interface of the reinforced mortar slabs after exposure. Fig. 9 shows the microstructure of the interface of the reinforced mortar slabs with 0 days of curing. The micrographs of the control slab show large areas with different corrosion products around the steel´s surface (Fig. 9a). Iron corrosion products identified as magnetite (Fe_3O_4) with dense layer structure and visible cracks, lepidocrocite (γ-FeOOH) showing fine plates in "flowery" structures and goethite (α-FeOOH) with similar structure than the lepidocrocite (showing well-defined edges) can be observed around the galvanized meshes´s surface (Fig. 9-a1). The appearance of these iron corrosion products has been reported by other researchers [Duffó et al. 2004, Duffó et al. 2012]. It is noted that some of these iron corrosion products are formed by hydroxyl groups. The UtSCBA10 slab show a less corrosion products on the galvanized steel surface when compared to the observed in the control slab (Fig. 9b). In this case the magnetite was identified as donut-shaped bulges (Fig. 9-b1) [Duffó et al. 2012]. The UtSCBA20 slab shows corrosion products with less volume when compared to the observed in the control and the UtSCBA10 slabs (Fig. 9c). In this case, magnetite in dense layers with some cracks and lepidocrocite were identified (Fig. 9-c1).

In general, the reinforced mortar slabs with 7 days of curing (Fig. 10) show less amount of corrosion products in the galvanized steel surface than the observed in the slabs with 0 days of curing. In this case, the control slab shows small deposits of calcium hydroxyzincate which works as protective layer against corrosion (Fig. 10a) [Roventi et al. 2014]. However, areas with magnetite and lepidocrocite appears in the galvanized steel surface as iron corrosion products. The UtSCBA10 slab shows less iron corrosion products in the galvanized steel surface (Fig 10b) than the control slab. Here, only the magnetite was identified combined with the calcium hydroxyzincate and ZnO. Similar corrosion products on the galvanized steel surface are observed in the UtSCBA20 slab (Fig 10c).

With 28 days of curing the control slab also shows areas with calcium hydroxyzincate, magnetite and lepidocrocite as corrosion products in the galvanized steel surface (Fig. 11a). The UtSCBA10 slab shows the calcium hydroxyzincate in the galvanized steel which works as a passive layer (Fig 11b). The UtSCBA20 slab shows large areas conformed with calcium hydroxyzincate; but also, some areas with magnetite (Fig. 11c). Despite of this, the galvanized meshes has insignificant damage. From this, it can suggest that the mortars added with 10 and 20% of UtSCBA has better performance against corrosion than the mortar without SCBA addition.

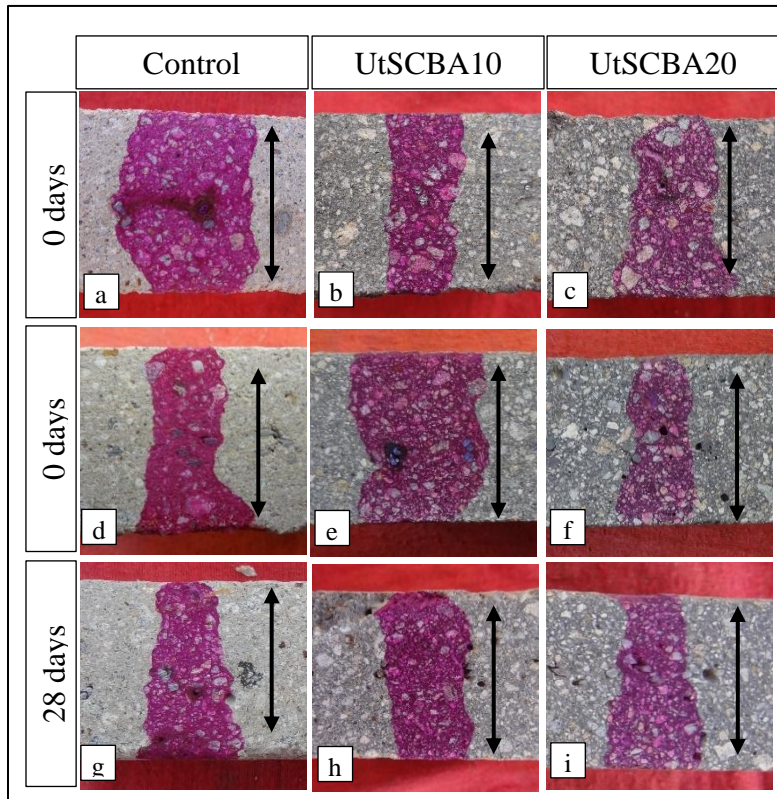Fig. 8. Images from the phenolphthalein tests in the reinforced mortar slabs. ↕ = measured front

Fig. 9. Micrographs of the mortar matrix/galvanized steel interface of the reinforced mortar slabs with 0 days of curing. a) Control, b) UtSCBA10 and c) UtSCBA20

Fig. 10. Micrographs of the mortar matrix/galvanized steel interface of the reinforced mortar slabs with 7 days of curing. a) Control, b) UtSCBA10 and c) UtSCBA20
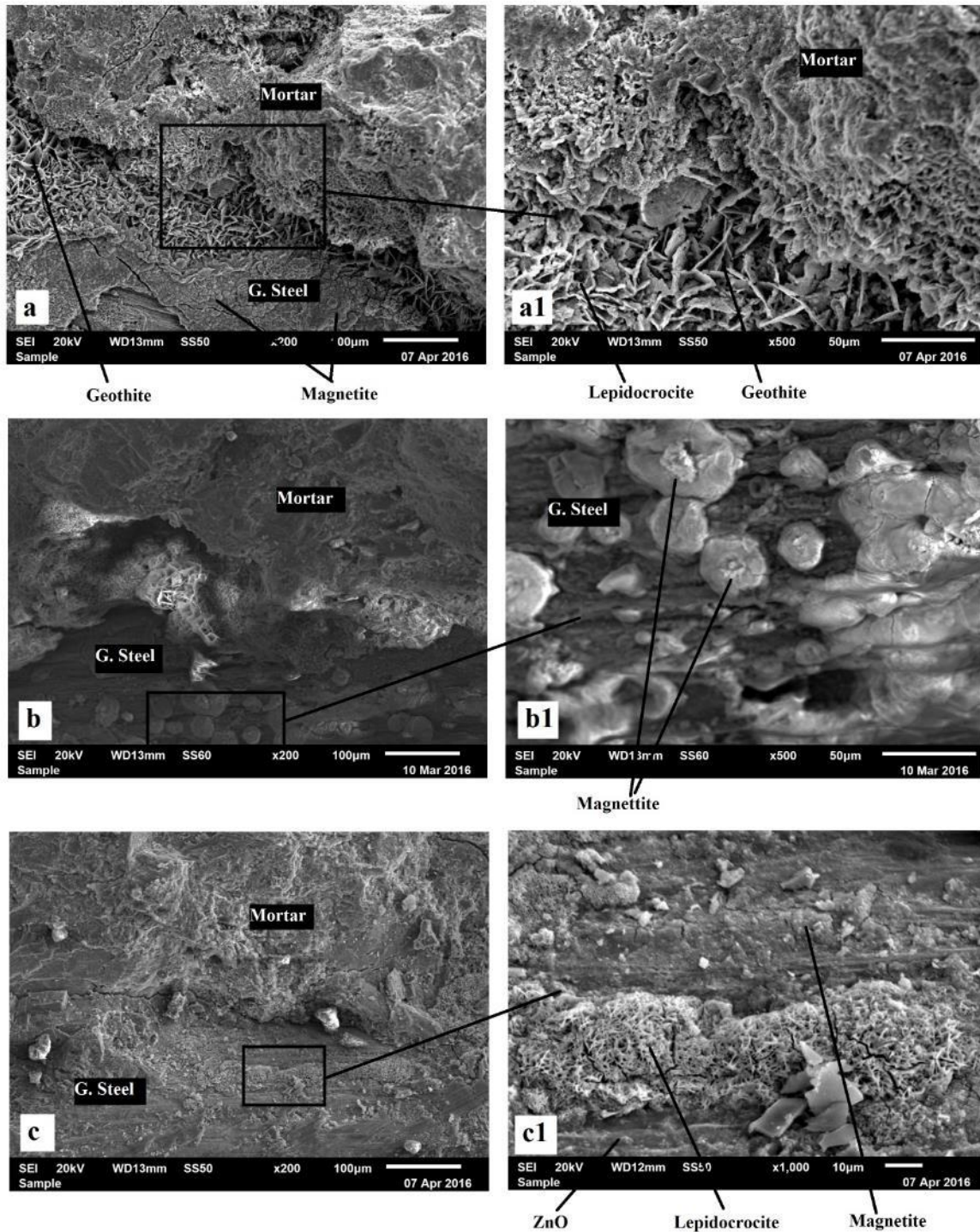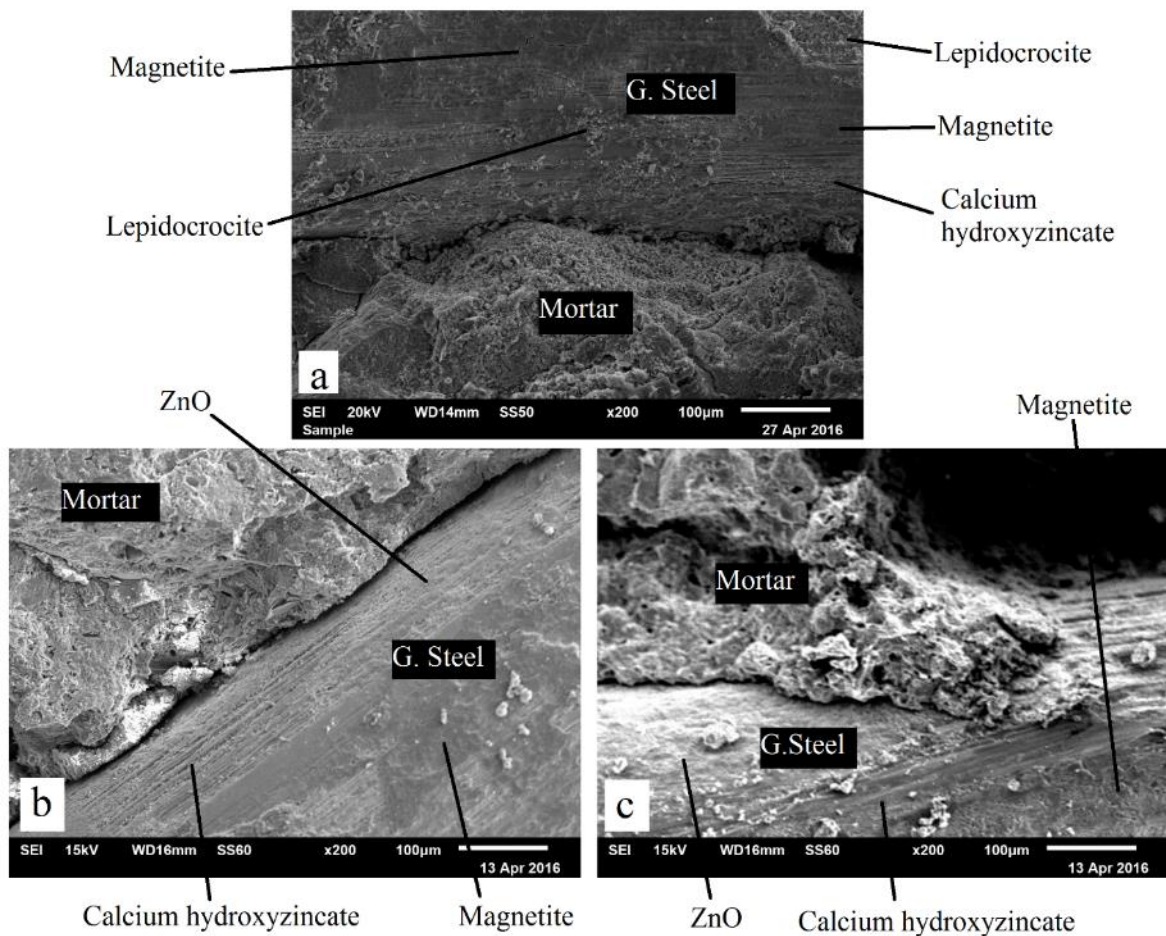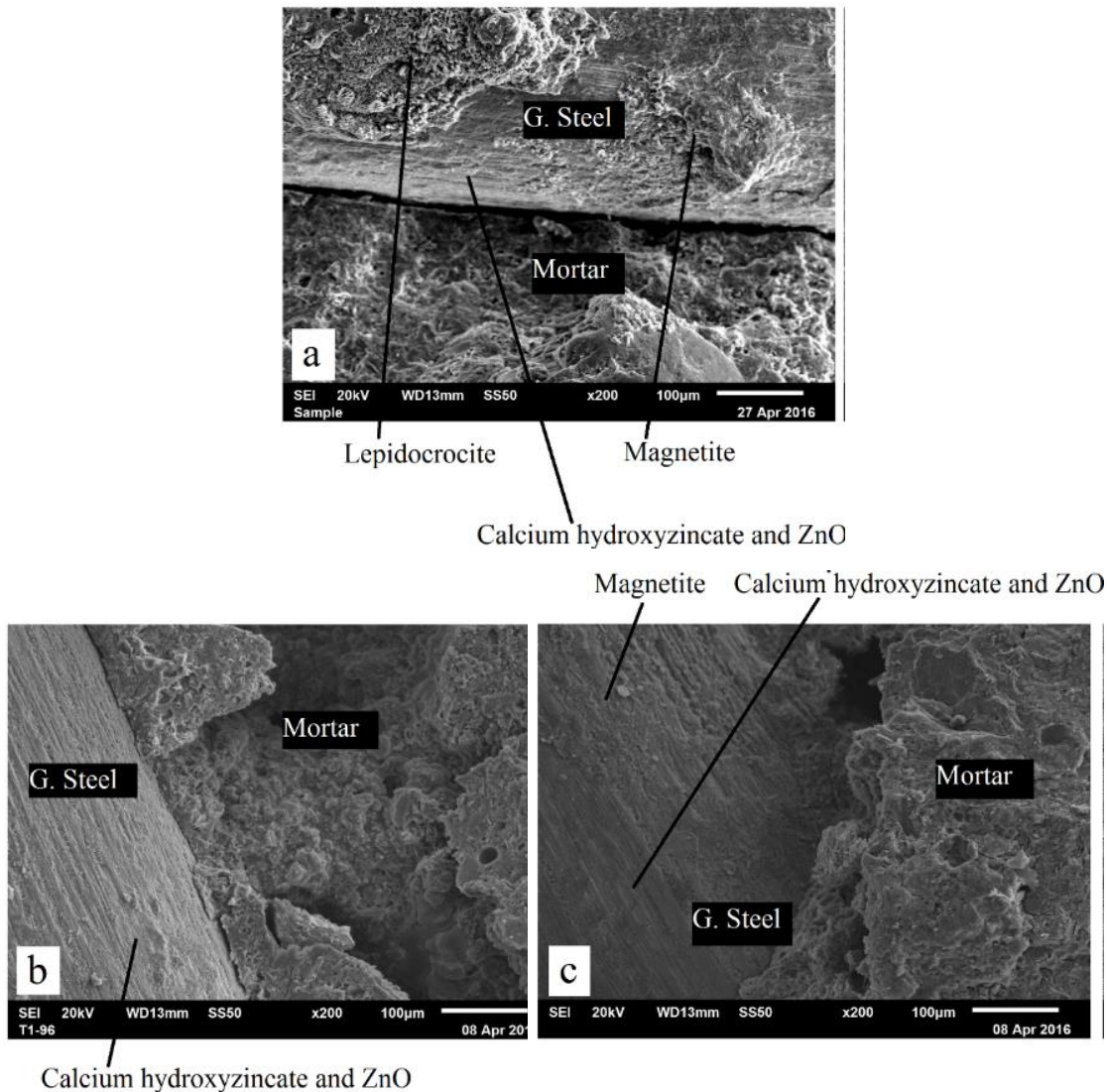
Fig. 11. Micrographs of the mortar matrix/galvanized steel interface of the reinforced mortar slabs with 28 days of curing. a) Control, b) UtSCBA10 and c) UtSCBA20

X-ray diffraction

Results from the X-ray diffraction tests are shown in Fig. 12. According to the results, the calcium silicate hydrate CSH ($CaSiO_3.H_2O$; $4CaO.5SiO_2.5H_2O$) and the calcium-aluminum silicate CAS ($Al_2Ca(SiO_4)_2$; $CaAl_2Si_2O_8$) were the main mineralogical phases formed in the reinforced mortar slabs. These were created from the cement hydration and the pozzolanic reactions between the UtSCBA the $Ca(OH)_2$ (created during cement hydration) and moisture.

The phase of calcite ($CaCO_3$) could be attributed to any intermediate hydration product or to the burning process of the CPC [Arizzi et al. 2012, Ríos-Parada et al. 2017]. The mineralogical phases of ettringite ($Ca_6Al_2(SO_4)_3(OH)_{12}.25H_2O$), sodium chloride (NaCl) and quartz (Q) detected in the XRD patterns are attributed to the use of CPC, the NaCl solution of the simulate marine environment in which the slabs were exposed, and the sand used to prepare the mortars,

respectively. A detailed analysis of the XRD patterns in Fig. 12 show the presence of the Friedel´s salt phase $(Ca_2Al(OH)_6Cl-2H_2O)$ which suggest that some chloride ions are chemically bound [Shi et al. 2012, Shi et al 2017]. Finally, the zinc oxide (ZnO) phase is attributed to the corrosion of the zinc coating of the galvanized meshes used as reinforcement in the slabs. Despite the slight thickness of the zinc coating in the galvanized meshes (40.13 to 59.12µm), the ZnO phase was detected in the XRD patterns. This could be attributed to the zinc corrosion products migrated into the mortar matrix in a three-dimensional planar filling microcracks and small pores [Yeomas 1998].

Fig. 12a shows the XRD patterns of the mortar slabs with 0 days of curing. The results show that the phases of CSH and CAS increased in intensity with the increment of UtSCBA addition. In contrast, the ettringite phase decreased in intensity in the UtSCBA10 and UtSCBA20 mortar slabs with respect to the control slab. This is attributed to the less CPC content in the slabs containing UtSCBA. It is noted that the intensity of the NaCl phase also decreased in the UtSCBA10 and UtSCBA20 mortar slabs. This suggest that the addition of UtSCBA improves the microstructure of mortar slabs by the refinement of the pore structure due to pozzolanic reactions which may occur during the rehydration process of cement when the mortar slabs are soaked in the simulate marine environment. It is reported that rehydration of cement occurs by gradual reduction in size of cement particles [Neville 2000] and hence more $Ca(OH)_2$ is available for the mentioned pozzolanic reactions with the UtSCBA. The mentioned reactions have been reported in long-term testing in a previous research [Maldonado-García et al. 2018]. The intensity of the Friedel´s salt phase also decreased in the UtSCBA10 and UtSCBA20 mortar slabs. Finally, the intensity of the ZnO phase in the control and the UtSCBA10 and UtSCBA20 mortar slabs was similar and

hence a conclusion about the corrosion condition of the galvanized meshes based on the intensity development from this phase could be tricky.

With 7 days of curing (Fig. 12b), the CSH and CAS phases also increased in the UtSCBA10 and UtSCBA20 mortar slabs when comparing with the control slab. The ettringite phase practically remains constant in the control and the UtSCBA10 and UtSCBA20 mortar slabs. In this case, the intensity of the Friedel´s salt peaks in the control slab was a little higher when comparing to the intensity of the peaks from this phase in the UtSCBA10 slab. Results also show that the intensity of the Friedel´s salt peaks of the UtSCBA10 and UtSCBA20 mortar slabs were practically comparable.

When 28 days of curing are applied (Fig. 12c) the CSH and CAS phases remain increasing as the addition of UtSCBA increased in the mortar slabs. Once again, the intensity of the ettringite peaks are similar in the control and the UtSCBA10 and UtSCBA20 mortar slabs. Here, the intensity of the Friedel´s salt peaks decreased as the addition of UtSCBA increased which may indicates less content of chemically bound chlorides.

Thermal analysis

The results from the TG/DTG analysis are shown in Fig. 13. Five different endothermic peaks are observed in the DTG curves. The first endothermic peak (A) corresponds to the water loss from the CSH [Gabrovšek et al. 2006]. The second peak (B) is attributed to the ettringite [Gabrovšek et al. 2006, Ramachandran 2001]. The third peak (C) refers to the decomposition of complex hydrated calcium-aluminate and calcium-silicates compounds [Schwiete et al. 1968, Sersale et al. 1980, Ramachandran 2001, Gabrovšek et al. 2006]. This peak can be also convoluted with the decomposition peak of the Friedel´s salt [Shi et al. 2017]. The fourth peak (D) corresponds to the weight loss of structural OH^- groups or carbonated phases [Gabrovšek et

al. 2006]. The hydroxyl groups could be linked with iron corrosion products from the galvanized meshes in the slabs since these groups refers to cathodic reactions and the formation of hydroxides [Broomfield 1997]. Finally, the fifth peak (E) could be associated to chlorides chemically bound by CSH [Ramachandran 2001].

Fig. 13a shows the TG/DTG curves of the mortar slabs with 0 days of curing. The results show a slight difference in the endothermic peak of water loss from CHS (A) when comparing the control and the UtSCBA10 and UtSCBA20 slabs. In this figure, the second peak (B) shows that the weight loss of ettringite in the control slab was greater than in the UtSCBA10 and UtSCBA20 slabs. This aggress with the reported in the XRD patterns of the mortar slabs with 0 days of curing (Fig 12a). Results also show greater weight loss in the C peak of the control slab when compared to the UtSCBA10 and UtSCBA20 slabs. This peak refers to the weight loss of hydrated calcium-aluminate and calcium-silicates compounds, but also Friedel´s salt. The minor intensity of the Friedel´s salt phase in the XRD patterns (Fig. 12a) as the addition of UtSCBA increased is in accordance with the increment in weight loss of the C peak from the DTG curve. The above also aggress with the observed in the E peak which is related to chemically bound chlorides. The D peak shows a slight difference in weight loss when comparing the control and the UtSCBA10 mortar slabs. However, the UtSCBA20 slab show less weight loss than the control and UtSCBA10 slabs. This suggest less iron corrosion products in the cementitious matrixes of the slabs containing 20% of UtSCBA. This in accordance with the less corrosion risk reported in the UtSCBA20 slab with 0 days of curing by the long-term electrochemical testing in a previous research [Maldonado-García et al. 20XX].

When 7 days of curing were applied (Fig, 13b), greater weight loss in the A peak was observed as the addition of UtSCBA increased in the mortar slabs. This coincide with the increment in intensity of the CSH phase reported in the XRD patterns (Fig. 12b). In this case, the control slab also shows greater weight loss of ettringite than the UtSCBA10 and UtSCBA20 slabs which is observed in the B peak. The control slab with 7 days of curing also shows major weight loss in the C peak when comparing with the UtSCBA10 and UtSCAB20 slabs with the same curing period, as this was reported previously. However, the difference in weight loss in the E peak was minor. Results also show that the weight loss in the D peak was minor as the addition of UtSCBA increased in the slabs with 7 days of curing. This difference was more evident than in the slabs with 0 days of curing and aim to less iron corrosion products in the cementitious matrix of the UtSCBA10 and UtSCBA20 slabs.

With 28 days of curing (Fig. 13c), the A peak of the control and the UtSCBA10 mortar slabs were similar in terms of weight loss. However, the A peak in the UtSCBA20 slab was minor than in the control and the UtSCBA10 slabs. An explanation for the above could be found in the fact that a large amount of unburned matter is present in the UtSCBA20 mortar and those particles can be blamed for inhibiting pozzolanic reactions which in turn to create less CSH [Martirena et al. 1998]. Results also show less weight loss of ettringite in the B peak as the addition of UtSCBA increased in the slabs. Likewise, the C peak shows minor weight loss as the addition of UtSCBA increased from 0 to 10 and 20%. This suggests less content of chlorides chemically bound in the UtSCBA10 and UtSCBA20 slabs as observed in the E peak. Those results coincide with the decrement of the Friedel´s salt intensity reported in the XRD patterns (Fig. 12c) of mortars containing 10 and 20% of UtSCBA.

Fig. 12. XRD patterns of the reinforced mortar slabs after exposure to the simulated marine environment for 75 months a) 0, b) 7 and c) 28 days of curing. CSH = calcium silicate hydroxide, Cc = calcite, Q = Quarts, CAS calcium-aluminum silicate hydrate, Fs =Friedel salt, Zn = zinc oxide, E = Ettringite Sc = sodium chloride and Cr = cristobalite. Figs. a1, b1 and c1 are amplifications for visual effects of their corresponding XRD patterns
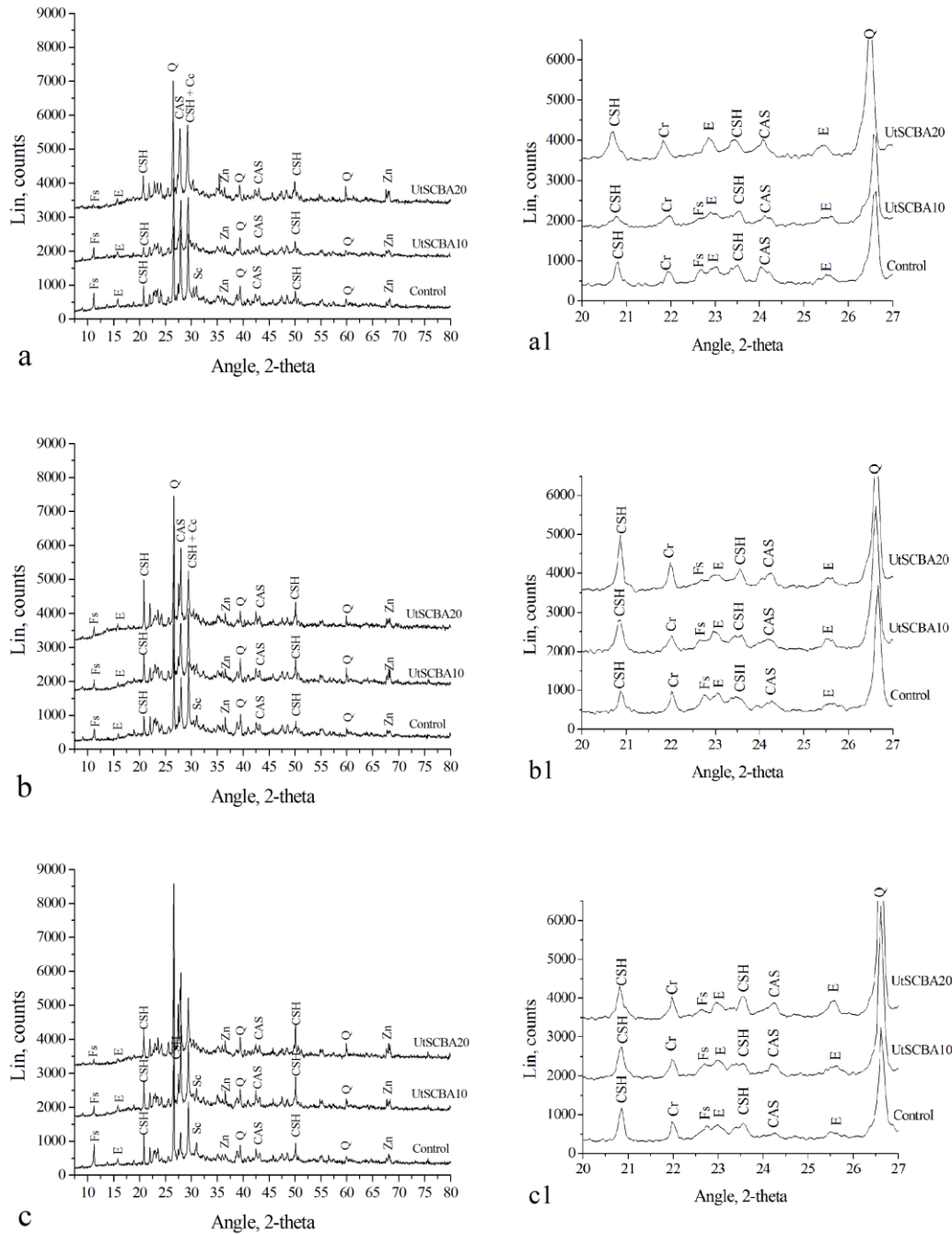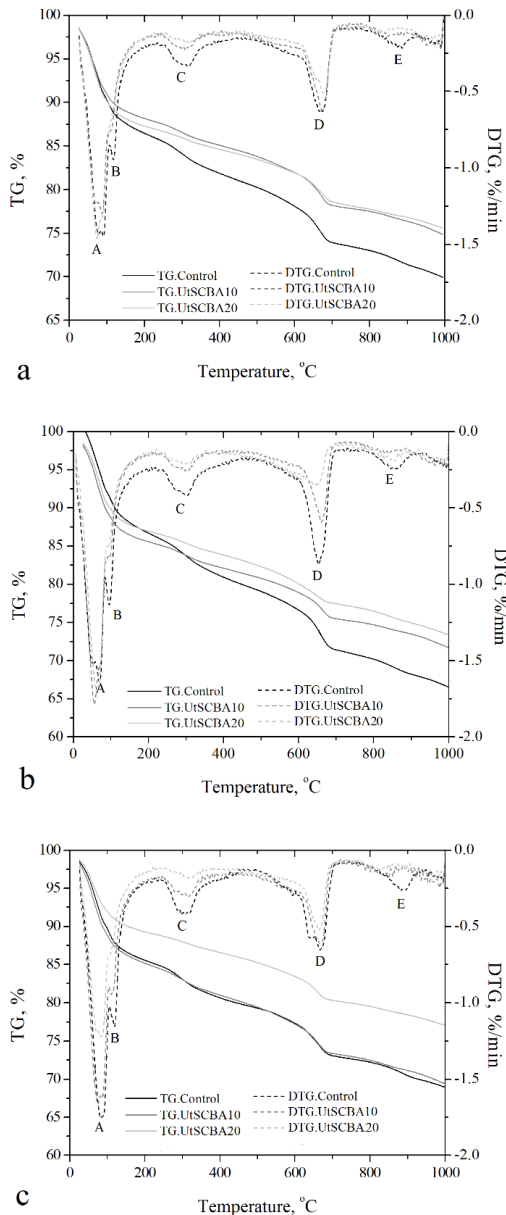
Fig. 13. TG/DTG curves of the reinforced mortar slabs after exposure to the simulate marine environment for 75 months a) 0, b) 7 and c) 28 days of curing. A = water loss from calcium silicate hydroxide (CSH) and moisture, B = ettringite, C = hydrated calcium-aluminate and calcium-silicates compounds and Friedel´s salt, D = structural OH⁻ groups or carbonated phases and E = chloride ions chemically bound

Proposed corrosion mechanism

Corrosion in the control slabs starts when a critical chloride threshold value (approximately 0.67% by mass of mortar according to Darwing et al. 2009) was reached by diffusion at the galvanized steel surface breaking its zinc passive film. The time in which that critical threshold value was reached in the steel/mortar interface of the slabs was longer as the curing time increases from 0 to 7 and from 0 to 28 days as suggested as suggested by the autopsy examination and SEM. This agrees with the reported in a previous research in which the chloride ion diffusion coefficient was reduced in about 25% for both cases [Maldonado-García et al. 20XX]. This is attributed to microstructural enhancement of the mortar matrixes as the curing time increases instead rehydration of cement particles in the mortars during the exposure to the simulated marine environment. The results from DRX and TG/DTG suggested that the control mortars with 0, 7 and 28 days of curing had practically the same amount of Friedes´s salt. According the this and the chloride ion diffusion coefficients [Maldonado-García et al. 20XX], the increment of curing time has a positive effect on increasing chloride binding which in turn to reduce corrosion in the slabs.

The addition of UtSCBA does not have a negative effect on increasing corrosion in the reinforced mortar slabs. This is attributed to the pozzolanic reaction of the ash which continue during the long-term period of testing creating additional CSH and CAS compounds as reported in a previous research [Maldonado-García et al. 2018]. This is because the amorphous matter (77.5%) in the UtSCBA [Maza 2017]. Then chloride ions could not easily penetrate through a denser mortar matrix and hence the time in which a critical chloride threshold value is reached in the galvanized steel surface is increased. In this case, the addition of 10 and 20% of UtSCBA reduced the chloride diffusion

coefficients in about 50 and 65% [Maldonado-García et al. 20XX]. During that process, some chloride ions are chemically bound creating Friedel´s salt. However, the amount of Friedel´s salt in the mortars containing UtSCBA was minor than in the control mortars. This points that some chloride ions are physically bound in the mortars by the unburned matter from the UtSCBA which could works as a physical barrier and as an absorbent media because its different shapes and larger mean particle size [Maldonado-García et al. 2018]. However, the physical bonding could be for certain period allowing diffusion of chlorides at greater ages.

Once a critical chloride threshold value is reached at the galvanized steel surface embedded in the slabs containing UtSCBA, the CHZ passive layer is broken allowing corrosion of the η, ζ, δ and γ phases of the zinc coating. At this steep the zinc cathodically protect the iron steel until large areas are damaged. According with the proposed by Yeomas 1998, the corrosion products from the zinc coating of the galvanized meshes could migrate in a three-dimensional planar filling microcracks and small pores allowing an apparent densification of the cementitious matrix, as a result chloride ions could not migrate easily through a denser cementitious matrix added with UtSCBA. After a certain period, the corrosion products of zinc migrated to the mortar´s surface by the effect of the wetting/drying cycles allowing the entrance of more chloride ions through the mortar matrix and hence corrosion of the iron. Finally, as observed in the autopsied slabs the increment of the curing time was also beneficial in the slabs containing 10 and 20% of UtSCBA in lowering corrosion.

A schematic representation of the role of UtSCBA against reinforced steel corrosion in the mortar slabs is presented in Fig. 14. In Fig. 14a chlorides migrate in a mortar without UtSCBA (control mortar) and corrosion of the zinc and iron occur in the galvanized steel as explained at the beginning of this section. The zinc corrosion products migrate to the mortar´s surface filling some pores. Fig. 14b show a mortar with UtSCBA with a denser cementitious matrix than the control mortar because of pozzolanic reactions over time [Maldonado-García et al. 2018], some chlorides are absorbed physically by the unburned matter from the ash. In Fig. 14c, corrosion occurs after more chlorides enter the mortar matrix, a longer initiation period than in the control mortar occurs in this step. Finally, zinc corrosion products migrate through the mortar matrix with UtSCBA filling small pores. Here, the unburned matter could also work as a physical barrier for zinc corrosion products by electrostatic forces which also contributes to block chloride ions penetration.
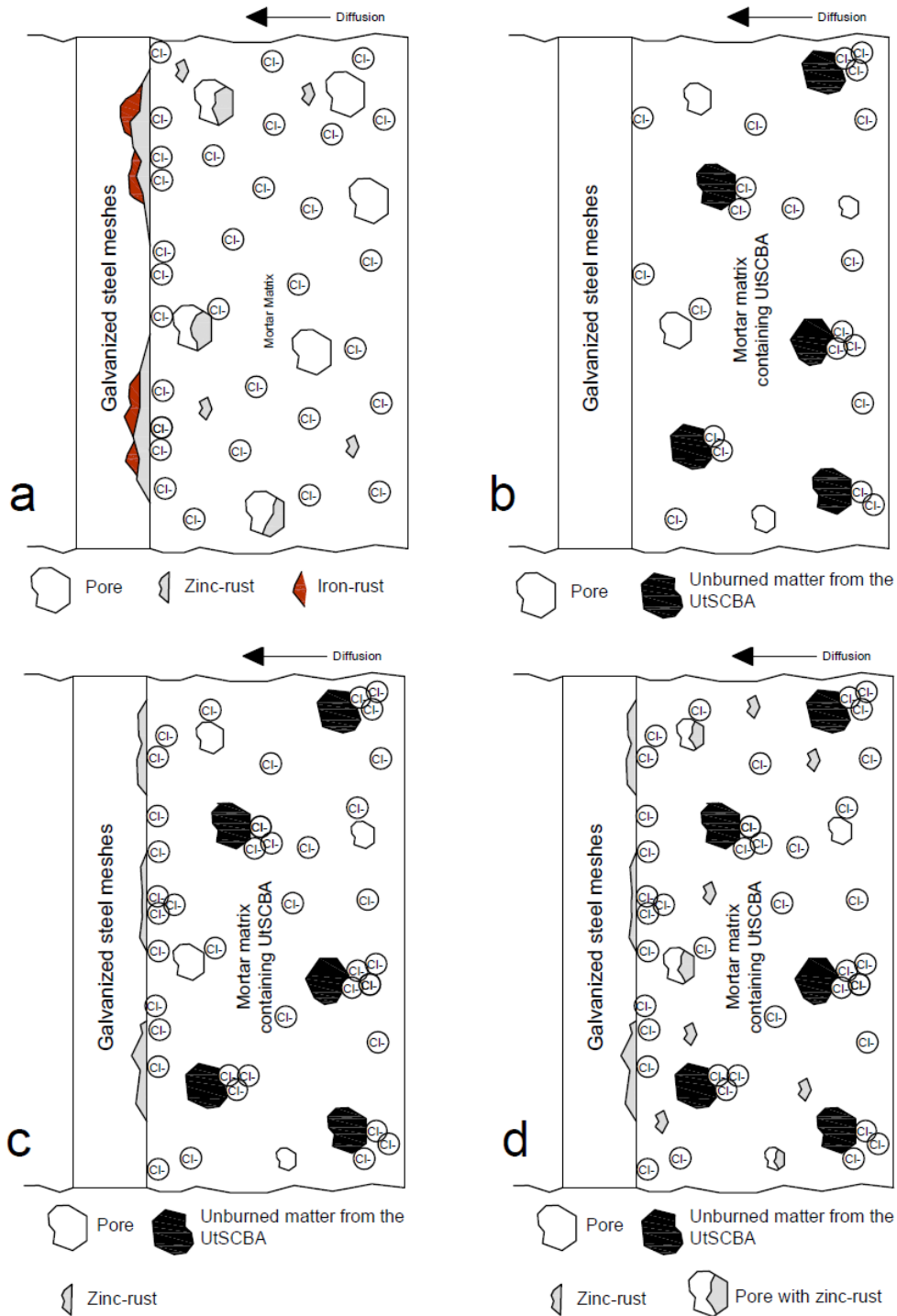
Fig. 14. Schematic representation of the role of UtSCBA in the corrosion mechanism of reinforced mortar slabs. a) chloride diffusion and corrosion in mortar without UtSCBA, b) chloride diffusion in mortar with UtSCBA, c) corrosion in mortar containing UtSCBA and d) zinc corrosion products filling small pores in the mortar with UtSCBA

Conclusions

According to the visual examination, no corrosion damage was observed in the slabs after exposure to the wetting and drying cycles. This is attributed to the thickness of the galvanized meshes.

The autopsy of the slabs shows that the addition of 10 and 20% of UtSCBA ash does not have a negative effect on increasing corrosion in reinforced mortar slabs. General overall corrosion and pitting on the criss-cross section of the galvanized meshes were observed in some slabs.

The SEM images shows less corrosion products in the galvanized steel surface as the addition of UtSCBA increased. This was also observed as the initial curing time increases from 0 to 7 and 28 days in the mortars.

The XRD patterns shows a reduction in the intensity of the Friedel´s salt peaks by the use of 10 and 20% of UtSCBA in the mortars. This suggest physical interactions between chloride ions and cementitious phases in the mortars containing UtSCBA.

The TG/DTG results agrees with the XRD patterns showing less weight loss in the endothermic peaks which correspond to chlorides chemically bound in mortars containing UtSCBA.

From results, the addition of 10% of UtSCBA appears as the most suitable option when comparing with the results using 20% of UtSCBA addition. Furthermore, 7 days of curing could be enough for proper performance of the UtSCBA in mortars against corrosion.

As a result from the long-term experimental testing, the role of UtSCBA (which contain a high LOI content) in the corrosion mechanism in reinforced galvanized steel mortar slabs can be described as a multi-part process. First, the amorphous phase of the UtSCBA is quite able for pozzolanic reactions with the $Ca(OH)_2$ from cement hydration and moisture. This improves the microstructural properties of the mortars which in turn densifies the cementitious matrix. Second, chloride ion diffusion is reduced in the mortars with UtSCBA because the improvement of the cementitious matrix by pozzolanic reactions. Third, the unburned matter of the UtSCBA could work as a physical barrier or as an absorbent media for chlorides reducing the rate in which chlorides migrate through the cementitious matrix.

Acknowledgments

References

Angst U., Elsener B., Larsen C.K., Vennesland Ø. 2009. Critical chloride content in reinforced concrete – A review. *Cem. Concrete. Res.*, 39(12), 1122 1138.

Aprianti E., Shafigh P., Bahri S., Farahani J. N. 2015. Supplementary cementitious materials origin from agricultural wastes – A review. *Constr. Build. Mater.*, 74, 176-187.

Arenas-Piedrahita J.C., Montes-García P., Mendoza-Rangel J.M., López-Calvo H.Z., Valdez-Tamez P.L., Martínez-Reyes J. 2016. Mechanical and durability properties of mortars prepared with untreated sugarcane bagasse ash and untreated fly ash. *Constr. Build. Mater.,* 105, 69-81.

Arizzi, A.; Cultrone, G. (2012) Aerial lime-based mortars blended with a pozzolanic additive and different admixtures: A mineralogical, textural and

physical-mechanical study. *Construct. Build. Mat*. 31, 135–143.

Bahurudeen A., Santhanam M. 2015. Influence of different processing methods in the pozzolanic performance of sugarcane bagasse ash. *Cem. Concrete. Comp.,* 56, 32-45.

Bahurudeen A., Kanraj D., Gokul Dev V., Santhanam M. 2015. Performance evaluation of sugarcane bagasse ash blended cement in concrete. *Cem. Concrete Comp.,* 59, 77-88.

Broomfield J. P. 1997. Corrosion of steel in concrete: Understanding, investigation and repair (1st edition). Published by E & FN Spon.

Chusilp N., Jaturapitakkul C., Kiattikomol K. 2009a. Utilization of bagasse ash as a pozzolanic material in concrete. *Constr. Build. Mater*., 23(11), 3352-3358.

Chusilp N., Jaturapitakkul C., Kiattikomol K. 2009b. Effects of LOI of ground bagasse ash on the compressive strength and sulfate resistance of mortars. *Constr. Build. Mater*., 23(12), 3523-3531.

Cordeiro G. C., Kurtis K. E. 2017. Effect of mechanical processing on sugar cane bagasse ash pozzolanicity. *Cem. Concrete. Res*., 97, 41-49.

Cordeiro G. C., Paiva O. A., Toledo Fhilo R. D. Fairbairn E. M. R., Tavares L. M. 2018. Long-term compressive behaviour of concretes with sugarcane bagasse ash as a supplementary cementitious material. *J. Test. Eval.*, 46(2), 564-573.

Cordeiro G.C., Toledo-Fhilo R.D., Tavares L.M., Fairbair E.M.R. 2009a Ultrafine grinding of sugar cane bagasse ash for application as pozzolanic admixture in concrete. *Cem. Concrete. Res.,* 39, 110-115.

Cordeiro G.C., Toledo-Filho R.D., Fairbairn E.M.R. 2009b Effect of calcination temperature on the pozzolanic activity of sugar cane bagasse ash. *Constr. Build. Mater*., 23, 3301-3303.

Darwin D. Browning J., O´Reilli M., Xing L., Ji J. 2009- Critical chloride corrosion threshold of galvanized reinforcing bars. *ACI Materials Journal* 106(2), 176-183.

Duffó G. S., Morris W., Raspini I., Saragovi C. 2004. A study of steel rebars embedded in concrete during 65 years. *Corros. Sci*., 46, 2143-2157.

Duffó G. S., Reinoso M., Ramos C. P., Farina S. B. 2012. Characterization of Steel rebars embedded in 70-year old concrete structure. *Cem. Concrete. Res*., 42, 111-117.

Fontana M. G. 1986. Corrosion engineering. Third edition. Mc Graw Hill.

Gabrovšek R., Vuk T., Kaučič V. 2006. Evaluation of the hydration of Portland cement containing various carbonates by means of thermal analysis. *Acta Chim Slov* 53, 159-165.

Ganesan K., Rajagopal K., Thangavel K. (2007). "Evaluation of bagasse ash as supplementary cementitious material." *Cem. Concrete Comp.,* 29(6), 515-524.

Gastaldini A. L. G., Isaia G. C., Saciloto A. P., Missau F., Hoppe T. F. 2010. Influence of curing time on the chloride penetration resistance of concrete containing rice husk ash: A technical and economical feasibility study. *Cem. Concrete Comp,*. 32(10), 783-793.

Ipavec A., Vuk T., Gabrovšek R., Kaučič V. 2013. Chloride binding into hydrated blended cements: The influence of limestone and alkalinity. *Cem. Concrete. Res*.,48, 74-85.

Jímenez-Quero V. G., León-Martínez F. M., Montes-García P., Gaona-Tiburcio C., Chacón-Nava J.G. 2013. Influence of sugarcane bagasse ash and fly ash on the rheological behavior of cement pastes and mortars. *Constr. Build. Mater.,* 40, 691-701.

Lothenbach B., Scrivener K., Hooton R. D. 2011. Supplementary cementitious materials. *Cem. Concrete. Res*., 41, 1244–1256.

Maldonado-García M. A., Hernández-Toledo U. I., Montes-García P., and Valdez-Tamez P. L. 2018. The influence of untreated sugarcane bagasse ash on the microstructural and mechanical properties of mortars. *Mater. Construcc.,* 68(329), e148.

Maldonado-García M. A., Hernández-Toledo U. I., Montes-García P., Valdez-Tamez P. L. 20XX Long-term corrosion risk of thin cement composites containing untreated sugar cane bagasse ash. Accepted in the *Journal of Materials in Civil Engineering*.

Malheiro R., Meira G., Lima M., Perazzo N. 2011. Influence of mortar redering on chloride penetration into concrete structures. *Cem. Concrete Comp.* 33, 233-239.

Martirena, J.F.; Middendor, F.B; Gehrke, M; Budelmann, H. (1998) Use of wastes of the sugar industry in lime-pozzolana binders: Study of the reaction. *Cem. Concrete. Res*., 28[11], 1525–1536.

Maza-Ignacio O. T. 2017. Efecto de la incorporación de residuos industriales en la

resistencia y durabilidad de ladrillos de arcilla. Master Thesis. Insituto Politécnico Nacional of México. (in spanish).

Michel A., Otieno M., Stang H., Geiker M. R. 2016. Propagation of steel in concrete: Experimental and numerical investigations. *Cem. Concrete Com.,* 70, 171-182.

Morales E. V., Villar-Cociña E., Frías M., Santos S. F., Savastano Jr. H. 2009. Effects of calcining conditions on the microstructure of sugarcane waste ashes (SCWA): influence in the pozzolanic activation. *Cem. Concrete Comp.,* 31(1), 22-28.

Neville. 2000. Properties of Concrete. Prentice Hall, London.

Ramachandran V. S. and Beaudoin James J. 2001. Handbook of analytical techniques in concrete science and technology: Principles, techniques and applications. William Andrew Publising/Noyes Publications.

Ríos-Parada V., Jiménez-Quero V. G., Valdez-Tamez P. L., Montes-García P. 2017. Characterization and use of an untreated Mexican sugarcane bagasse ash as supplementary material for the preparation of ternary concretes. *Constr. Build. Mater.,* 157, 83-95

Roventi G., Bellezze T., Giuliani G., Conti C. 2014. Corrosion resistance of galvanized steel reinforcements in carbonated concrete: effect of wet-dry cycles in tap water and in chloride solution on the passivating layer. *Cem. Concrete. Res.,* 65, 76-84

Schwiete E.H., Ludwig U. 1968. Crystal structure and properties of cement hydration products (hydrated calcium aluminates and ferrites), Proceeding of the 5th Int. Symposium on the Chemistry of Cement, Tokyo, 1968, Vol.2, p37-36.

Sersale R., Sabatelli V., Valenti G. L. 1980. Influence of some retarders on the hydration, at early ages, of tricalcium aluminate, Proceeding of the 7th International Congress on the Chemistry of Cement 4, p546. Paris.

Shi X., Xie N., Fortune K., Gong J. 2012. Durability of steel-reinforced concrete in chloride environments: An overview. *Constr. Build. Mater.,* 30, 125-138.

Shi Z., Geiker M. R., Lothenbach B., De Weerdt K., Ferreiro G. S., Enermark-Rasmussen K., Skibsted J. 2017. Friedel´s salt profiles from thermogravimetric analysis and thermodynamic modelling of Portland cement-based mortars exposed to sodium chloride solution. *Cem. Concrete Comp.,* 78, 73-83.

Sistonen E. 2009. Service life on hot-dip galvanised reinforcement bars in carbonated and chloride-contaminated concrete. Ph. D. Thesis dissertation. Helsinki University of Technology.

Sistonen E., Cwirzen A., Puttonen J. 2008. Corrosion mechanism of hot-dip galvanized reinforcement bar in cracked concrete. *Corros. Sci.,* 50, 3416-3428.

Tittarelli F., Bellezze T. 2010. Investigation of the major reduction reaction occurring during the passivation of galvanized steel bars. *Corros. Sci.,* 52, 978-983

Yeomas S. R. 1998. Corrosion of the zinc alloy coating in galvanized reinforced concrete. *Corrosion.,* 653, 1-10.

Yeomas S. R. 2004. Galvanized steel reinforcement in concrete: An overview. ELSEVIER.

Zareei A. S., Ameri F., Bahrami N. 2018. Microstructure, strength, and durability of eco-friendly concretes containing sugarcane bagasse ash. *Constr. Build. Mater.,* 184, 258-268.

CHAPTER EIGHT

General discussion

This thesis aimed the durability of UtSCBA-cement based composites. The focus is about the effect of 10 and 20% of UtSCBA as cement replacement against corrosion in reinforced mortars. The effect of the initial curing time, 0, 7 and 28 days on the corrosion risk in those reinforced mortars is also addressed. Previous research results using the UtSCBA affirm that this ash could be used in mortars without negative effects on its microstructural and mechanical properties [Hernández-Toledo 2010, Maldonado-García 2012, Arenas-Piedrahita et al. 2016]. In this thesis, a long-term evaluation on the microstructure, compressive strength and chloride-induced corrosion of mortars containing UtSCBA has been investigated. Further, the effect of the addition of UtSCBA and curing time on the corrosion of reinforced mortars at long-term ages is also investigated.

The effect of different post-treatments on the pozzolanic activity of the sugarcane bagasse ash

The sugarcane bagasse ash (SCBA) is mainly composed by silicon, aluminium and iron oxides. However, researches report that the SCBA needs a post-treatment, such as re-calcination, grinding and long-term sieving or the combination of these methods, in order to enhance its pozzolanic properties when is used as a partial Portland cement replacement in composites. The improvement of the pozzolanic activity of SCBA using these post-treatments is attributed to physical or chemical changes and the reduction of the amount of unburned matter in the ash (commonly expressed as loss on ignition content LOI) [Ganesan et al. 2007, Morales et al. 2009, Chusilp et al. 2019a, Cordeiro et al. 2010, Bahurudeen et al. 2016, Cordeiro et al. 2017, Cordeiro et al. 2018]. According to the literature, sieving appears as the post-treatment with the less energy consumption for the improvement of the pozzolanic activity of SCBA. A study reports that a simple post-treatment consisting in sieving using the 300 µm ASTM mesh increases the pozzolanic activity of SCBA just above to the minimum strength activity index value (SAI) stablished by the ASTM C 618 [Bahuruden and Santhanam 2015]. However, the authors recommend an additional grinding post-treatment for greater results. Other researchers also report a sieving process through different meshes followed by grinding for proper performance of the SCBA [Torres-Agredo et al. 2014].

Results from this research show that a sieving process through the 75 µm ASTM mesh for five minutes is enough to induce acceptable pozzolanizity to the SCBA instead a sieving process by the 300 µm ASTM mesh as suggested by Bahurudeen and Santhanam 2015. It is obvious that coarse fibrous unburned particles can be removed by sieving. However, the size and quantity of these particles can vary from different ashes depending to the calcination conditions and collecting methods in the sugar mills. Concerning the collecting methods, a filter as the reported by Bahurudeen an Santhanam 2015 might trap some fibrous particles when the filter is getting full. Collecting the ash by sprinkling water as mentioned on this research could trap particles with different sizes and forms allowing trapping fine fibrous unburned particles. Results from this research shows lower SAI than the specified on the

ASTM when the SCBA was throught the 2.36 mm and 150 µm meshes. This was caused by the high content of non-reactive particles. When the SCBA was sieved by the 75 µm ASTM mesh the SAI was greater than the suggested by the standard. The results from this process were comparable with those results obtained when sieving (by the 75 µm ASTM mesh) plus grinding is applied.

The effect of UtSCBA on the microstructure of mortars

The addition of 10 and 20% of UtSCBA makes the microstructure of mortars more complex at long-term ages (up to 600 days) due to pozzolanic reactions. These pozzolanic reactions occur between the silicon, aluminium and iron oxides from the ash with the calcium hydroxide from the cement hydration and in the presence of moisture. The changes in the microstructure of the mortars was observed despite the large particle-size distribution, the large superficial area and the high loss on ignition content (LOI) of the UtSCBA. An improvement of the microstructural properties of mortars is suggested from the results because the amorphous phase of the ash. A recent study reports that this UtSCBA has 77.5% of amorphous matter (including silica, alumina and iron) [Maza-Ignacio 2017]. This microstructural enhancement could improve the mechanical and durability properties of the mortars, as suggested by other researchers when they used treated sugarcane bagasse ash as cement replacement in cement-based composites [Chusilp et al. 2009a, Dhengare et al. 2015, Cordeiro et al. 2018, Rajasekar et al. 2018, Zarrei et al. 2018]. Additionally, research also reports microstructural improvement at ages between 7 and 120 days when using the UtSCBA in combination with fly ash in ternary concretes [Ríos-Parada et al. 2017].

Effect of UtSCBA on the compressive strength of mortars

The addition of 10 and 20% of UtSCBA increased the compressive strength (CS) of mortars at ages between 28 and 600 days. The increment of CS in the mortars added with UtSCBA is attributed to the changes of its microstructural properties (in spite of its high LOI content). These changes are mainly attributed to pozzolanic reactions of the ash rather than a filler effect. Other studies including the use of UtSCBA as cement replacement confirm that this ash increases the CS of mortars and ternary concretes containing fly ash at ages up to 180 and 120 days [Arenas-Piedrahita et al. 2016, Ríos-Parada et al. 2017]. The authors also suggest that the pozzolanic reactions contributed to the enhancement of the CS. Another research also reports the positive effect in the CS when using ground sugarcane bagasse ash as cement replacement in concrete (10, 15 and 20%) at long-term ages (1 and 10 years) due to the packing density optimization of cementitious matrix [Cordeiro et al. 2018]. However, in that research the bagasse ash was ground during 120 min to obtain a median particle size smaller than 10 µm, leading to a high demanding energy post-treatment.

According to the results from this research, mortars with UtSCBA appear more sensitive to poor curing (at 28 and 90 days) when compared to a mortar without UtSCBA. This sensitiveness increases with the UtSCBA increment in the mortars. This could be attributed to the a less amount of cementitious compounds at these ages because the addition of the ash. Further studies about the effect of curing time in the CS at longer ages must be addressed. Moreover, a similar behaviour related to the effect of the initial curing time in mortars was reported in other studies when using ground sugarcane bagasse ash with 10% of LOI content [Chusilp et al. 2009b].

In conclusion, the addition of UtSCBA increased the CS of mortars in comparison to a control mortar despite to its high LOI content. Other researchers do not report negative effects on CS in cement-based composites when a sugarcane bagasse ash with a high LOI content (>10%) is used as cement replacement (10 to 20% of cement replacement) [Chusilp et al 2009b, Somna et al. 2012, Montakarntiwong et al. 2013].

Effect of UtSCBA on chloride ion diffusion of mortars

The addition of 10 and 20% of UtSCBA decreased the 28-day chloride ion diffusion coefficient in mortars, in about 50 and 65% when compared to a control due to the microstructural changes of the mortar matrix. The increment of curing time also had a positive effect on decreasing the chloride ion content of the mortars. A research, using the same ash reports that the UtSCBA decreased the chloride ion diffusion in about 63 and 85% at 28 and 90 days in ternary concretes added with fly ash [Ríos-Parada 2013]. Other studies also report a positive effect of sugarcane bagasse ash as cement replacement on decreasing chloride ion diffusion in cement-based composites (in about 50% when using 10 to 20% of bagasse ash) [Ganesan et al. 2007, Noor-ul 2011, Somna et al. 2012]. Those results agree with the improvement of the cementitious matrix and mechanical properties reported in the precious sections.

A research report that the surface of the C-S-H appears to be positively charged due to the absorption of cations $Ca^{2}+$ and Na+ in the alkaline pore solution which leads to the formation of an electrical diffuse doble layer to absorbe the negatively charged chloride ions [Singh and Khan 2014]. Following the above, a greater amount of physically absorbed chloride ions may exist as the addition of UtSCBA increase which creates more C-S-H due to pozzolanic reactions. As a result, the chemical binding of chlorides is lower in the mortars containing UtSCBA. Furthermore, a hypothesis about physical interactions by electrostatic forces between chlorides (negatively charged) and the unburned matter from the UtSCBA (positively charged) is proposed. From this, the unburned particles from the UtSCBA could work as a physical barrier or as an absorbent media for chloride ions because its large media particle size and large surface area.

Effect of UtSCBA on the corrosion of reinforced mortars

The addition of 10 and 20% of UtSCBA does not have a negative effect on increasing the corrosion risk of reinforced mortars at long-term ages. This is attributed to the changes of the cementitious matrix of the mortars by pozzolanic reactions of the UtSCBA which in turn reduce the chloride ion ingress. This was observed even when the reinforced mortars were not initially cured. This is because a re-hydration effect of anhydrous cement particles could occur at long-term ages, during the wetting and drying cycles in which the reinforced mortars were exposed, creating additional calcium hydroxide for pozzolanic reactions of the UtSCBA. The re-hydration of cement particles at long-term ages was also observed in the mortars without UtSCBA. This process can occur at long-term ages (after several months) when cement-based composites are exposed to water [Neville 2000].

Other researches evaluated the corrosion risk of cement-based composites added with sugarcane bagasse ash but only for few months, leading to some uncertainties about the corrosion process of those composites [Nuñez-Jaquez et al. 2012, Valencia et al. 2012]. The limited information from electrochemical testing reported in those studies (2-6 months) prevented the authors to draw meaningful a more comprehensive conclusions about the corrosion mechanism because pozzolanic reactions of the sugarcane bagasse ash could continue at longer ages.

Effect of UtSCBA on the corrosion mechanism of reinforced mortars

In this research, only chloride diffusion was considered to describe a corrosion mechanism due to the small cover depth in the reinforced mortars (1.5 cm). In the proposed mechanism the UtSCBA reduced chloride ion diffusion and delayed the corrosion initiation period. The microstructural improvement of the cementitious matrix due to pozzolanic reactions of the ash may account for this, but also the physical absorption of chlorides mostly by electrostatic forces of the C-S-H and the unburned particles from the ash. On the other hand, zinc corrosion products from the galvanized steel used as reinforcement in the mortars can migrate easily through the mortar matrix filling small pores because its smaller size in comparison to iron corrosion products [Yeomas 1998]. The migration of the zinc corrosion products to the specimen´s surface could be blocked by the unburned matter particles from the UtSCBA creating a temporal physical barrier for chlorides. This phenomenon could be possible since the dissolution of the zinc coating could occur by different dissolution mechanisms according to its uniformity and the presence of different zinc-iron layers created during the galvanizing process [Sistonen et al. 2008].

Concluding remarks

In this research, the performance of practically "as received" SCBA (UtSCBA) was evaluated at long-term ages. Microstructural, mechanical and durability properties were discussed. It was found that the addition of 10 and 20% of UtSCBA made the microstructure of mortars more complex, which in turn increased the compressive strength and reduced chloride ion diffusion. While chloride ion diffusion was reduced by the addition of UtSCBA, corrosion in reinforced mortars was decreased at long-term ages.

The results from this research provide a break-through needed in the search of a more environmentally friendly construction materials by the use of practically "as received" agricultural waste material from sugar mills. The use of UtSCBA as a partial Portland cement replacement prevents environmental issues due to its improper disposal and is suitable option for the formulation of durable cement-based composites.

References

1. Arenas-Piedrahita J.C., Montes-García P., Mendoza-Rangel J.M., López-Calvo H.Z., Valdez-Tamez P.L., and Martínez-Reyes J. 2016. Mechanical and durability properties of mortars prepared with untreated sugarcane bagasse ash and untreated fly ash. *Constr. Build. Mater.,* 105, 69-81.
2. Bahurudeen A., Santhanam M. 2015. Influence of different processing methods in the pozzolanic performance of sugarcane bagasse ash. *Cem. Concrete. Comp.,* 56, 32-45.
3. Bahurudeen A., Wani K., Basit A. A., Santhanam M. 2016. Assesment of pozzolanic performance of sugarcane bagasse ash. *J. Mater. Civ. Eng*., 28(2), 04015095.
4. Chusilp N., Jaturapitakkul C., Kiattikomol K. 2009a. Utilization of bagasse ash as a pozzolanic material in concrete. *Constr. Build. Mater*., 23, 3352-3358.
5. Chusilp N., Jaturapitakkul C., Kiattikomol K. 2009b. Effects of LOI of ground bagasse ash on the compressive strength and sulfate resistance of mortars. *Constr. Build. Mater*., 23, 3523-3531.
6. Cordeiro G. C., Toledo-Fhilo R. D., Fairbairn E. M. R. 2010. Ultrafine sugarcane bagasse ash: high potential pozzolanic material for tropical countries. *IBRACON Estrut. Mater.,* 3(1), 50-67.
7. Cordeiro G. C., Kurtis K. E. 2017. Effect of mechanical processing on sugar cane bagasse ash pozzolanicity. *Cem. Concrete. Res*., 97, 41-49.
8. Cordeiro G. C., Paiva O. A., Toledo F. R. D., Fairbairn E. M. R., and Tavares L. M. 2018. Long-term compressive behavior of concretes with sugarcane bagasse ash as a supplementary cementitious material. *J. Test. Eval*. 46[2], 176-183.

9. Cordeiro G. C., Paiva O. A., Toledo F. R. D., Fairbairn E. M. R. Tavares L. M. 2018. Long-term compressive behaviour of concretes with sugarcane bagasse ash as a supplementary cementitious material. *J. Test Eval*., 46(2), 564-573.

10. Dhengare S., Amrodiya S., Shelote M., Asati A., Bandwaf N., Anand K., and Jichkar. 2015. Utilization of sugarcane bagasse ash as a supplementary cementitious material in concrete and mortar – a review. *International Journal of Civil Engineering and Technology*. 6 [4], 94–106.

11. Ganesan K., Rajagopal K., Thangavel K. 2007. Evaluation of bagasse ash as supplementary cementitious material. *Cem. Concrete Comp.,* 29(6), 515-524

12. Hernández Toledo Ur Iván. 2010. Efecto de una puzolana de desperdicio agrícola y el tiempo de curado en la corrosión del Ferrocemento. Master thesis. IPN-CIIDIR-Oaxaca, México.

13. Ipavec A., Vuk T., Gabrovšek R., Kaučič V. 2013. Chloride binding into hydrated blended cements: The influence of limestone and alkalinity. *Cem. Concrete. Res*., 48, 74-85.

14. Maldonado García Marco Antonio. 2012. Efecto de la adición de ceniza de bagazo de caña en la microestructura y durabilidad del ferrocemento, Master thesis, IPN-CIIDIR-Oaxaca, México. (In spanish).

15. Maza-Ignacio O. T. 2017. Efecto de la incorporación de residuos industriales en la resistencia y durabilidad de ladrillos de arcilla. Master thesis. Instituto Politécnico Nacional of Mexico. (in spanish).

16. Morales E. V., Villar-Cociña E., Frías M., Santos S. F., Savastano Jr. H. 2009. Effects of calcining conditions on the microstructure of sugarcane waste ashes (SCWA): influence in the pozzolanic activation. *Cem. Concrete Comp.,* 31(1), 22-28.

17. Montakarntiwong K., Chusilp N., Tangchirapat W., Jaturapitakkul C. 2013. Strength and heat evolution of concretes containing bagasse ash from thermal power plants in sugar industry. *Materials and Desing*. 49, 414-420.

18. Neville A. 2000. Properties of Concrete. Prentice Hall. London.

19. Noor-ul A. 2011. Use of bagasse ash in concrete and its impact on the strength and chloride resistivity. *Journal of Materials in Civil Engineering* 41, 1244-1256.

20. Nuñez-Jaquez R. E., Buelna-Rodríguez J.E., Barrios-Durstewitz C.P., Gaona-Tiburcio C., Almeraya-Calderón F. 2012. Corrosion of modified concrete with sugarcane bagasse ash. *International Journal of Corrosion.,* 2012, 1-6.

21. Rajasekar A., Arunachalam K., Kottaisamy M., Sraswathy V. 2018. Durability characteristics of Ultra High Strength Concrete with treated sugarcane bagasse ash. *Constr. Build. Mater.,*171, 350-356.

22. Ríos-Parada Venustiano. 2013. Análisis de las propiedades mecánicas, microestructurales y de durabilidad de concretos ternarios con ceniza de bagazo de caña. Master Thesis. Instituto Politécnico Nacional of México. (In spanish).

23. Ríos-Parada V. Jiménez-Quero V. G., Valdez-Tamez P. L. Montes-García P. 2017. Characterization and use of an untreated Mexican sugarcane bagasse ash as

supplementary material for the preparation of ternary concretes. *Constr. Build. Mater.,* 157, 83-95.

24. Singh F., Khan A. K. 2014. Role of supplementary cementitious material in concrete system as chloride binding. The Masterbuilder. www.masterbuilder.co.in

25. Sistonen E., Cwirzen A., Puttonen J. 2008. Corrosion mechanism of hot-dip galvanized reinforcement bar in cracked concrete. *Corros. Sci.,*50, 3416-3428.

26. Somna R., Jaturapitakkul C., Rattanachu P., Chalee W. 2012. Effect of ground bagasse ash on mechanical and durability properties of recycled aggregate concrete. *Materials and Design* 36, 597-603.

27. Torres-Agredo J., Mejía de Gutiérrez R., Escandon-Giraldo C. E. González-Salcedo L. O. 2014. Characterization of sugarcane bagasse ash as a supplementary material for Portland cement. *Ing. Inv*., 34(1), 5-10.

28. Valencia G., Mejía de Gutierrez R., Barrera J., Delvastos S. 2012. Estudio de durabilidad y corrosión en morteros armados adicionados con toba volcánica y ceniza de bagazo de caña de azúcar. *Rev. Constr.,* 12(2), 112-122. (In Spanish).

29. Yeomas S. R. 1998. Corrosion of the zinc alloy coating in galvanized reinforced concrete. *Corrosion* 163, 1-10.

30. Zarrei S. A., Ameri F., Bahrami N. 2018. Microstructure, strength, and durability of eco-friendly concretes containing sugarcane bagasse ash. *Constr. Build. Mater.,* 184, 258-268.

FURTHER RESEARCH

In addition to the advances presented in this thesis, a longer evaluation period of the corrosion risk in the reinforced mortars is suggested to clarify the effect of the increase of UtSCBA from 10 to 20%. Particularly when 7 and 28 days of curing are applied. The internal visual examination does not show enough corrosion damage in the reinforced mortars containing 10 and 20% of UtSCBA with 7 and 28 days of curing. This points out that the addition of 20% of UtSCBA in mortars could have comparable or better performance on reducing corrosion than the addition of 10% of UtSCBA.

The availability of large amount of data from electrochemical testing in the reinforced mortars could allow a detailed analysis using different mathematical tools in the frequency domain such as harmonics, the fast Fourier transform, the short-time Fourier transform, and the wavelet transform. The analysis of the electrochemical data in the frequency domain could help to identify important features during the corrosion process of the reinforced mortars added with UtSCBA. Some of these features are the effect of seasonal changes, the analysis of weight loss in the steel reinforcement, the identification of the corrosion initiation period for zinc and iron of the galvanized steel, the identification of the periods in which the different zinc-iron layers of the galvanized steel´s coating are consumed, and the identification of different stages in which corrosion activity increase due to variation of chloride ion content in the steel/mortar interface attributed to the effect of the wetting and drying cycles. The analysis of those features might support the structure to propose a model for corrosion propagation in the reinforced mortars added with UtSCBA. On that way, there are some studies which reports the capability of using mathematical tools to evaluate the corrosion damage in reinforced-cement based composites. Vedalakshmi et al. 2009 reports that harmonics have a good correlation with weight loss of reinforcement steel in cement-based composites and current densities. Another research carried by Montes-García et al. 2010 reports that the wavelet transform is capable for a detailed evaluation of the corrosion potentials in cement-based composites.

Another factor to consider when proposing a model for corrosion propagation in the reinforced mortars added with UtSCBA is the chloride binding capacity. The chloride binding reduces the amount of free or water-soluble chloride ions which in turn to reduce chloride diffusion and hence the chlorides accumulated in the reinforced steel surface [Li et al. 2014]. This phenomenon occurs because the ingress of chloride ions into cement-based composites is not only physically controlled by mass transfer; but also, chemical interactions between cementitious compounds (positively charged) and chloride ions (negatively charged) [Ipavec et al. 2013]. When SCM are added in cement-based composites, the chloride binding capacity could change because of different reasons: i) physical absorption of chlorides by the C-S-H from cement hydration [Ipavec et al. 2013] but also from the

pozzolanic reactions of the SCM and ii) the development of cementitious compounds with low C/S and C/A ratios [Zibara et al. 2008, Yuan et al. 2009].

Other factors such as electrical resistivity, porosity and absorption of mortars added with UtSCBA at long-term ages might be considered when proposing the model for corrosion propagation of the reinforced mortars. In that model, different stages must appear during the propagation period [Li 2004, Steel-Construction 2015] since reinforced steel corrosion is not a linear phenomenon as suggested in the Tuutti´s model [Tuutti 1982]. Furthermore, the different stages must appear in the model because the consumption of the different zinc-iron layers from the coating of galvanized steel which occur by different dissolution mechanisms [Sistonen et al. 2008]. In this step, the analysis of the electrochemical data by mathematical tools in the frequency domain could be accurate. Likewise, this may be helpful to predict the corrosion of reinforced concrete.

References

1. Li C. Q. 2004. Reliability based service life prediction of corrosion affected concrete structures. *J. Struct. Eng.* 130, 1570-1577.
2. Li J., Shao W. 2014. The effect of chloride binding on the predicted service life of RC pipe piles exposed to marine environments. *Ocean Engineering* 88, 55-62.
3. Ipavec A., Vuk T., Gabrovšek R., Kaučič V. 2013. Chloride binding into hydrated blended cements: The influence of limestone and alkalinity. *Cem. Concrete. Res*., 48, 74-85.
4. Montes-García P., Castellanos F., Vásquez-Feijoo J. A. 2010. Assessing corrosion risk in reinforced concrete using wavelets. *Corros Sci* 52, 555-561.
5. Sistonen E., Cwirzen A., Puttonen J. 2008. Corrosion mechanism of hot-dip galvanized reinforcement bar in cracked concrete. *Corros. Sci.,*50, 3416-3428.
6. Steel construction-info- 2015. Wethering Steel. The free enciclopedy for UK steel construction information. Viewed 16 June 2015.
7. Tuutti K. 1982. Corrosion of steel in concrete. Swedish Cement and Concrete Research Institute. Stockholm.
8. Vedalakshmi R., Manoharan S. P., Song H. W., Palaniswamy N. 2009. Application of harmonic analysis in measuring the corrosion rate of rebar in concrete. *Corros Sci* 51(11), 2777-2789.
9. Yuan Q., Shi C., De Schutter G., Audenaert K., Deng D. 2009. Chloride binding of cement-based materials subjected to external chloride environment − A review. *Constr. Build. Mater.,*23, 1-13.
10. Zibara H., Hooton R. D., Thomas M. D. A., Stanish K. 2008. Influence of the C/S and C/A ratios of hydration products on the chloride ion binding capacity of lime-DF and lime-MK mixtures. *Cem. Concrete Res*., 38, 422-426.

CURRICULUM VITAE

Name: Marco Antonio Maldonado García
Bachelor of engineering: Civil Engineer. Instituto Tecnológico de Oaxaca, México
Master in Science: Conservación y Aprovechamiento de Recursos Naturales. Instituto Politécnico Nacional, México.
PhD. Candidate. Conservación y Aprovechamiento de Recursos Naturales. Instituto Politécnico Nacional, México.

Indexed papers

Maldonado-García M. A., Hernández-Toledo U. I., Montes-García P., Valdez-Tamez P. L. "The influence of untreated sugarcane bagasse ash on the microstructural and mechanical properties of mortars". *Materiales de Construcción* 68[319]. El48. February 2018.

Maldonado-García Marco Antonio, Hernández-Toledo Ur Iván, Montes-García Pedro, Valdez-Tamez Pedro Leobardo. 2018. "Long-term corrosion risk of thin cement composites containing untreated sugarcane bagasse ash" Accepted in the *Journal of Materials in Civil* Engineering. September 2018.

Franco-Lujan Víctor Alberto, Maldonado-García Marco Antonio, Montes-García Pedro, Mendoza-Rangel José Manuel. "Chloride-induced reinforcing steel corrosion in ternary concretes containing fly ash and untreated sugarcane bagasse ash" Accepted in *Construction and Building Materials*. November 2018.

Maldonado-García Marco Antonio, Montes-García Pedro, Valdez-Tamez Pedro Leobardo. "Corrosion evaluation of reinforced untreated sugarcane bagasse ash mortar slabs by ultrasonic guided waves" Draft to be sent to *Construction and Building Materials*.

Maldonado-García Marco Antonio, Montes-García Pedro, Valdez-Tamez Pedro Leobardo, Rodríguez-Ramírez Juan. "Elucidation of the role of untreated sugarcane bagasse ash on the chloride-induced corrosion of reinforced mortars". Draft to be sent to *Cement and Concrete Composites*.

Franco-Lujan Víctor Alberto, Maldonado-García Marco Antonio, Montes-García Pedro, Mendoza-Rangel José Manuel. "Long-term performance evaluation of ternary concretes containing fly ash and untreated sugarcane bagasse ash by ultrasonic parameters". Draft to be sent to *Materiales de Construcción*.

International conferences

Maldonado-García M. A., Montes-García P., Valdez-Tamez P. L. "Corrosion de morteros adicionados concentza de bagazo de caña reforzados con acero galvanizado". II Congreso Internacional de Ciencias de la Ingeniería. Facultad de Ingeniería Mochis, Universidad Autónoma de Sinaloa. Sinaloa, México. 18-20 November, 2015.

Maldonado-García Marco A., Montes-García P., Valdez-Tamez P. L. "Effect of the addition of sugar-cane bagasse ash on the corrosion risk of uncured mortars. 11th fib International PhD Symposium in Civil Engineering. The University of Tokyo. Tokyo, Japan. 29-31 August, 2016.

Maldonado-García M. A., Montes-García P., Valdez-Tamez P. L. "A review of the use of sugarcane bagasse ash with a high LOI content to produce sustainable cement composites". 2nd International Conference on Bio-based Building Materials. Polytech Clermont-Ferrand. Clermont-Ferrand, France. 21-23 June, 2017.

National conferences

Maldonado-García Marco Antonio, Ríos-Parada Venustiano, Montes-García Pedro, Valdez-Tamez Pedro Leobardo. "Distribución de tamaños de partículas de materiales cementantes mediante difracción de rayos láser: análisis y consideraciones para la interpretación de resultados experimentales". VII Congreso Nacional de Ciencia e Ingeniería en Materiales. Benemérita Universidad Autónoma de Puebla. Puebla, México. 2-4 March, 2016.

Maldonado-García M. A., Montes-García P., Valdez-Tamez P. L. "Estudio de la carbonatación de morteros adicionados con ceniza de bagazo de caña con alto contenido de PXC". VII Congreso Nacional ALCONPAT – México. Universidad Autónoma del Estado de Hidalgo. Hidalgo, México. 6-9 November 2016.

Institutional conferences

Maldonado-García Marco Antonio. "Determinación de la DTP por difracción de rayos láser aplicado a materiales cementantes". CIIDIR Oaxaca. Oaxaca, México. 29 October, 2015.

Maldonado-García Marco Antonio. "Análisis cualitativo y cuantitativo de fases minerales por medio de difracción de rayos X". CIIDIR Oaxaca. Oaxaca, México. 08 December, 2015.

Maldonado-García Marco Antonio. "Potenciales de corrosión y resistencia a la polarización lineal como técnicas para evaluar la corrosión del acero de refuerzo en concreto". CIIDIR Oaxaca. Oaxaca, México. 12 December, 2017.

Maldonado-García Marco Antonio, Montes-García Pedro, Valdez-Tamez Pedro Leobardo. "Evaluación del deterioro por corrosión de morteros con ceniza de bagazo de caña utilizando ondas-ultrasónicas". XI Jornadas Politécnicas en Ciencia y Tecnología 2018. CIIDIR Oaxaca. Oaxaca, México. 17-18 May, 2018.

Maldonado-García Marco Antonio. "Análisis de materiales cementantes utilizando difracción de rayos X". CIIDIR Oaxaca, México. 26 September, 2018.

Radio Interview

Maldonado-García Marco Antonio. "Ceniza de bagazo de caña para la elaboración de morteros a base de cemento ecológicos" CORTV-Radio Oaxaca, México. September 2018.

Participation on institutional research proyects (BEIFI program)

Reología de pastas y morteros preparados con cementos activados alcalinamente utilizando como materiales base ceniza de bagazo de caña y ceniza volante. SIP-20150472. Instituto Politécnico Nacional-CIIDIR Oaxaca, México. 2015.

Estudio de las propiedades de morteros compositos activados alcalinamente utilizando velocidad de pulso ultrasónico. SIP-20160756. Instituto Politécnico Nacional-CIIDIR Oaxaca, México. 2016.

Efecto de la corrosion en las propiedades de tensión de acero embebido en concreto de altas prestaciones agrietado que contiene inhibidor a base de nitrito de calcio. SIP-20170716, Instituto Politécnico Nacional-CIIDIR Oaxaca, México. 2017.

Efecto de ICBNC en la corrosion de concreto reforzado de altas prestaciones agrietado. SIP-20180032, Instituto Politécnico Nacional-CIIDIR Oaxaca México. 2018.

Research stay

Facultad de Ingeniería Civil. Universidad Autónoma de Nuevo León. From february 08th to june 24th. 2016.